ELECTROCHEMICAL DEVELOPMENT AND CHARACTERIZATION OF MUTUAL ALLOYS OF IRON GROUP ELEMENTS
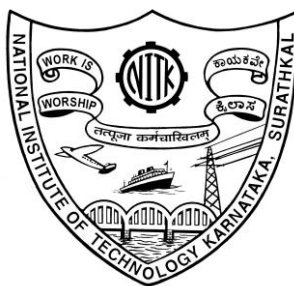
THESIS

Submitted in partial fulfillment of the requirements for the degree of
DOCTOR OF PHILOSOPHY

by

PAVITHRA G.P.

(Registration No: 081022CY08F01)

DEPARTMENT OF CHEMISTRY

NATIONAL INSTITUTE OF TECHNOLOGY

KARNATAKA, SURATHKAL, MANGALORE - 575 025

FEBRUARY – 2013

ELECTROCHEMICAL DEVELOPMENT AND CHARACTERIZATION OF MUTUAL ALLOYS OF IRON GROUP ELEMENTS
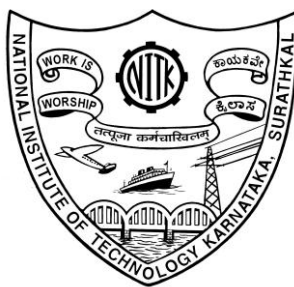
THESIS

Submitted in partial fulfillment of the requirements for the degree of

DOCTOR OF PHILOSOPHY

by

PAVITHRA G.P.
(Registration No: 081022CY08F01)

DEPARTMENT OF CHEMISTRY

NATIONAL INSTITUTE OF TECHNOLOGY

KARNATAKA, SURATHKAL, MANGALORE - 575 025

FEBRUARY – 2013

<div style="border: 1px solid black; padding: 20px;">

DECLARATION

by the Ph.D. Research Scholar

I hereby ***declare*** that the Research Thesis entitled "**Electrochemical development and characterization of mutual alloys of iron group elements**" which is being submitted to the *National Institute of Technology Karnataka, Surathkal* in partial fulfilment of the requirements for the award of the Degree of *Doctor of Philosophy* in *Chemistry* is a ***bonafide report of the research work carried out by me.*** The matter contained in this Research Thesis has not been submitted to any University or Institution for the award of any degree.

Pavithra G.P.

(Reg. No: **081022CY08F01**)

Department of Chemistry

Place: NITK, Surathkal

Date: 11/02/2013

</div>

CERTIFICATE

This is to *certify* that the Research Thesis entitled "**Electrochemical development and characterization of mutual alloys of iron group elements**" submitted by **Pavithra G.P.** (Register Number: **081022CY08F01**) as the record of the research work carried out by her, is *accepted as the Research Thesis submission* in partial fulfilment of the requirements for the award of degree of **Doctor of Philosophy.**

Prof. A. Chitharanjan Hegde

Research Guide

Date: 11/02/2013

Chairman-DRPC

Date: 11/02/2013

DEDICATED TO MY

TEACHERS

NOT FOR WHAT THEY TAUGHT; BUT FOR INVOKING MY THOUGHT

PARENTS

NOT FOR GIVING EDUCATION; BUT FOR GIVING ENCOURAGEMENT

HUSBAND

NOT FOR WALKING BESIDES ME; BUT FOR REMOVING THE THORNS FROM MY PATH

Acknowledgements

My deepest gratitude goes to my family for their support throughout my life; this research work is simply impossible without them. I am eternally grateful to my father Prabhu Kumar G.R. and mother Deviramma G.M. for their encouragement and great support. My husband, Prashanth Kumar K.R., has been a critical performer in realizing my goal. I have no suitable words that can fully describe his unflagging, everlasting love and commitment to me.

I acknowledge my faithful God, who has sat enthroned over the flood, never leaving or forsaking me and always leading me along good paths. You have made my life more bountiful joys. May your name be exalted, honored, and glorified.

Finally, I remain thankful to all those who helped me directly/indirectly in carrying out this work.

<div align="right">

Thank you,

PAVITHRA G.P.

</div>

ABSTRACT

This thesis titled **'Electrochemical development and characterization of mutual alloys of iron group elements'** details a comprehensive approach for electrodepositon mutual alloys of Fe-group metals by a relatively inexpensive, but advanced method called composition modulated multilayer alloy (CMMA) coating method. The coating has been accomplished galvanostatically on copper using Single Bath Technique (SBT). The essential feature of this method is their tailored micro/nano structured layers with alternatively changing composition is responsible for improved corrosion resistance of the coatings. The project involves optimization of three new binary baths of mutual alloys Fe-group metals and their multilayer coatings using direct current (DC) and pulsed current, respectively. The plating conditions and operating parameters have been optimized for best magnetic and corrosion performance of monolayer (non-nanostructured, or bulk) alloy coatings. As an attempt to increase the corrosion resistance of the monolayer coatings of Fe-group metals, namely Fe-Ni, Co-Ni and Fe-Co and multilayer coatings, represented as CMMA (Fe-Ni), (Co-Ni) and (Fe-Co) have been accomplished using square current waves having dual and triple pulses from respective baths (optimized). Multilayer coatings with different configurations have been developed with different combination of current densities, called cyclic cathode current densities (CCCD's) and number of layers. All depositions were carried out galvanostatically on copper from the respective baths for 10 minutes. Boric acid (BA), ascorbic acid (AA) and sulphanilic acid (SA) were used, as common additives to impart better appearance.

The corrosion behaviors of the coatings were evaluated in 1M HCl, as representative aggressive corrosion medium by electrochemical AC and DC techniques. The surface morphology, composition and phase structure of the coatings were characterized by SEM, EDX and XRD methods respectively. The experimental results revealed that CMMA coatings developed using dual and triple current pulses exhibit better (by several fold) corrosion resistance compared to monolayer alloys, developed from same bath for same time. The significant improvement in corrosion performance of CMMA coatings was attributed to small compositional difference in alternate layers, due to change in deposition current density. The formation of layers and their corrosion mechanism have been identified by SEM analysis. The improved corrosion protection of multilayer coatings was found to be the combined effect of compositional modulation of the individual layers and increased number of interfaces due to layering. The experimental data were analyzed, and results were discussed with Tables and Figures.

Key words: Nanocrystalline alloys, Magnetic and corrosion behavior, Multilayer coating, Dual and triple current pulse.

Table of Contents   Page No

NOMENCLATURE

AC	Alternate current
c.d.	Current density
CCCD's	Cyclic cathode current densities
CCE	Cathode current efficiency
C_{dl}	Capacitance double layer
CMMA/CMA	Composition modulated multilayer alloy
i_{corr}	Corrosion current
E_{corr}	Corrosion potential
CR	Corrosion rate
CV	Cyclic voltammetry
CVD	Chemical vapour deposition
DBT	Dual bath technique
DC	Direct current
EDX	Energy dispersive X-ray spectroscopy
EDL	Electrical double layer
EIS	Electrochemical Impedance Spectroscopy
GMR	Giant magneto resistance
HCD	High current density
i_p	Partial current density
OCP	Open circuit potential
PVD	Physical vapour deposition
SCE	Saturated calomel electrode
SBT	Single bath technique
SEM	Scanning electron microscopy
VSM	Vibrating sample magnetometer
XRD	X-ray diffraction

CHAPTER-1

INTRODUCTION

1.1 Electroplating technology

The development of novel materials and the assessment of their potential application constitute a major fraction of today's scientific research efforts. Here scientists and engineers have tried to develop new materials, and to tailor their properties to meet the desired functional properties. In this direction, the field of electroplating technology is entering a period of unprecedented intellectual challenge and productivity. Electrochemistry has, over recent decades, evolved from an art to exact science. This development is seen as responsible for the ever- increasing number and widening types of applications of this branch of practical science and technology. Electroplating, or alternatively electrodeposition is a term embracing the surface treatment and finishing of metals and non-metals, in which metallic coating is formed from an aqueous or non-aqueous solution by means of electrochemical reaction. Hence coating a substrate with metal or an alloy using an external source of current is referred as electrodeposition. The substrate to be coated serves as cathode (negative pole) where metal ions from the electrolyte are reduced and deposited elementally at the surface. The metal to be coated or inert material of good electrical conductivity (like graphite, lead, platinum) is used as anode. The fundamentals of electrodeposition are based on the laws introduced by Michael Faraday in 1833 and Walter Nernst in 1898 (Schlesinger and Paunovic 2000). Since then, metal and alloy deposition have developed continuously. Electroplating provide decorative and corrosion-resistant coatings and being used for various applications in industries.

In recent years the topics of materials science discloses how the principles of materials science can be used to explain various structures of electrodeposits and how these structures influence properties. Modern electroplating technology is highly

advanced and has been developed to cover a wide range of applications. In addition to the traditional use for surface finishing, plating technology has now been developed to fabricate high performance coatings. This rapid progress made the electroplating as one of the today's leading-edge technologies.

The ultimate goal of research in the electroplating technology is to investigate how to produce plated films with desirable mechanical, physical, and chemical properties that meet particular application's requirements (Watanabe 2004). In the past, a large number of papers and books have been published in the field of electroplating technologies, and their primary emphasis has been placed on electrochemical studies. At the same time, various attempts have been made to establish a unified theory that allows one to control both the microstructure and properties. Attempts to establish such a theory have been unsuccessful due to the complexities in achieving controlled experimental conditions.

Generally during electroplating while fixing one parameter others change uncontrollably, i.e., all the experimental parameters cannot be fixed at the same time. Furthermore, not all the chemical reactions occurring during electrodeposition processes are well understood. Because of these experimental difficulties and uncertainties, a reliable theoretical work that attempts to find a link to electroplating technologies has been largely hindered. Thus extensive electroplating research has led to the conclusion that all the physical properties of electroplated coatings must originate from their microstructure. It was found that the micro structural details provided more relevant information than the knowledge of the chemical reactions occurring during electrodeposition. The microstructures of the coatings are governed principally by the current density (c.d.), the driving force for electroplating and bath chemistry. Some of the technological areas in which means and methods of electrochemical deposition constitute an essential component are all aspects of electronics-both macro and micro, optics, optoelectronics, and sensors of most types to name only a few. In addition, a number of key industries, such as the automobile industry adopt the methods even when other

methods, such as evaporation, sputtering, chemical vapor deposition (CVD), and the like, are an option. That is so for reasons of economy and/or convenience (Paunovic and Schlesinger 2006).

Basically electroplating deals with the synthesis of solid films from dissolved species by alteration of their oxidation states using electricity. Electroplating technique is a versatile tool for developing a metal, or an alloy on the surface of a substrate for improved properties. It finds extensive applications in the field of electronics, protective coating industries and many other surface engineering fields. There are many books dealing with a variety of sub-topics such as surface preparation prior to deposition; reactions taking place in an atomistic level; thermodynamics and kinetics of electrodeposition; mechanisms of crystal growth; effect of bath chemistry and operating conditions; possibility of the deposition of specific metals, alloys and their structure-property relations, etc. (Brenner 1963, Kanani 2006).

1.2 History of electroplating

History of electroplating goes back to 1805, initiated by an Italian chemist Luigi V. Brugnatelli (Schlesinger and Paunovic 2000). Later in 1839, the scientists of Britain and Russia had independently devised the copper deposition technique for printing press plates, similar to Brugnatelli's method. By 1840, this discovery was adapted and refined by Henry and George Elkington of England for gold and silver plating. With the increased knowledge in the subject of electrochemistry, and its importance in understanding the processes of electroplating, other types of non-decorative metal deposition techniques have been developed. By the 1850's electroplating methods of bright nickel, brass, tin, and zinc were commercialized and were applied for engineering and specific commercial purposes. Electrochemical deposition for integrated circuits (IC's) can be achieved through either electroless or electrodeposition. Ting et al. (1987), Shacham-Diamand and Paunovic (1995) have demonstrated the feasibility of using selective electroless metal disposition for integrated circuit (IC) fabrication.

A turning point to this approach was associated with the announcement by IBM in 1997 of replacing vapor-deposited aluminum by electrodeposited copper wiring in ultra-large-scale integration (ULSI) silicon chips. Electrodeposition of Cu for IC fabrication was used successfully since 1997 for the production of interconnection lines down to 0.20 mm width. Another area of large research activity in electroplating is related to computer technology. It is electrodeposition of magnetic alloys for thin-film recording heads and magnetic storage media (Stefec 1973). The new magnetic materials needed to have properties superior to those of electrodeposited Ni-Fe (Perm alloy). The third example of new technology with increasing interest is electrodeposition of multilayer coatings (Raub 1967, Paunovic and Schlesinger 2006). This enabled the production of coatings having nanometer-scale structural and compositional variations. Schlesinger et al. (1995) reported giant magneto resistance (GMR) in electrodeposited Ni/Cu and Co/Cu multilayers. They are coatings of advanced electrical/electronic properties with a number of applications in the areas of surface engineering, corrosion protection, sensors as well as nanometer-scale electronic circuit systems (Alper et al. 1997, Landolt 2002).

Today, electroplating technology is responding in revolutionary and evolutionary ways to meet the modern requirement. It has become an exact science with the impressive progress and deeper understanding of the underlying principles of electrodeposition. Sophisticated power sources and plating baths formulae have been developed and are being employed for various applications. Those provide much greater control over the working characteristics of the deposition process than conventional method. Layer thickness, performance of electroplated finishes is among the attributes that have been brought under strict control. New developments enable greater plating speed, better throwing power (the ability to produce a relatively uniform coating upon a cathode of irregular shape), as well as reliable plated finishes.

1.3 Principles of electroplating

1.3.1 Theory of electroplating

By convention, the substrate or the base metal on which deposition is carried out is always the cathode. Similarly, the anode is always the electrode at which oxidation (e.g., metal dissolution or oxygen evolution) takes place. Electroplating using direct current (DC) can be represented schematically as in Fig. 1.1, where two electrodes immersed in solution are connected a DC source.
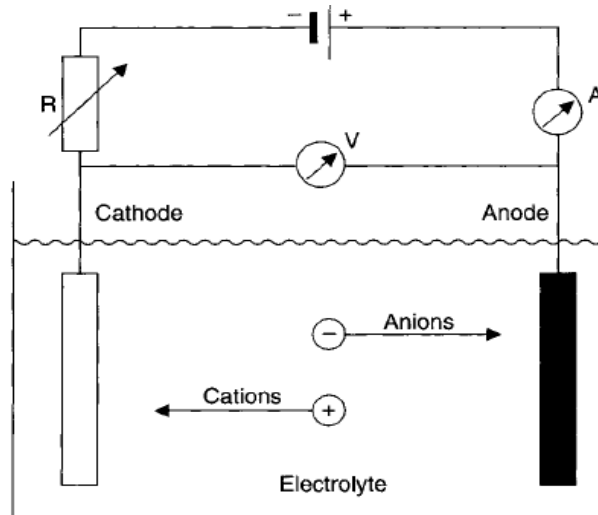
Fig. 1.1. Schematic representation of DC electroplating

The cathode, on which the metal/alloy is deposited; and anode, which itself is either a non-metallic conductor such as graphite or the coating metal itself. The primary purpose of anode is to complete the electrical circuit, and as metal cations are removed from solution as the metal, one or more balancing processes must take place at the anode to remove anions and thereby maintaining overall charge neutrality in solution. The anode may or may not fulfill the second function, which is to provide a source of fresh metal ions to replace what has been removed from solution by deposition at the cathode.

6

When an electric current passed through an electrolyte having metal ions, the electrochemical changes will take place at the electrode surface at the expense of applied current. The cations move towards the cathode where they are discharged, and deposited as metal/alloy.

$$M^{+2} + 2e^- \ \square \quad M_{(lattice)} \tag{1.1}$$

The anode dissolves to replace the metal ions removed, and thereby maintaining the metal ion concentration in the plating bath.

$$M \ \square \quad M^{+2} + 2e^- \tag{1.2}$$

The overall process is known as electrolysis. In case of insoluble anodes such as stainless steel or platinum, the overall reaction at the anode is oxidation of water.

$$2H_2O \ \square \quad 4H^+ + O_2 + 4e^- \tag{1.3}$$

Generally, one can observe the following three main steps during electroplating of metals/alloys:

(i) Ionic migration, meaning that the hydrated ion(s) in the electrolyte migrate(s) toward the cathode under the influence of applied potential as well as through diffusion and/or convection.

(ii) Electron transfer, meaning that at the cathode surface hydrated metal ion(s) enter(s) the diffusion double layer where the water molecules of the hydrated ion are aligned by the weak field present in this layer. Subsequently, the metal ion(s) enter(s) the fixed double layer, where, due to the higher field present, the hydrated shell is lost. Then on the cathode surface, the individual ion is neutralized and is adsorbed.

(iii) Incorporation, meaning that the adsorbed atom wanders to a growth point on the cathode and is incorporated in the growing lattice.

The electrodeposition technique has certain advantages over other methods of coatings and they are:

➢ Electrodeposited coatings have high hardness, good electrical and thermal conductivity, solderability and reflectivity.

➢ Electroplating being an atomistic deposition process, the crystal structures of electrodeposited coatings are fine, whereas in other processes the crystal structures are coarse.

➢ In electrodeposition the coating thickness can be easily controlled, whereas in galvanization and other processes, the coating thickness cannot be controlled easily.

➢ It is considered as the most reliable method of applying coatings of metals having very high melting points such as copper, nickel, chromium, silver, iron, gold and platinum than any other methods.

1.3.2 Faraday's laws of electrolysis

During the electrolysis, the extent of deposition or dissolution is determined by the quantity of electricity passed, the process of electrodeposition is governed by Faraday's laws of electrolysis, as stated below (Parthasaradhy 1989):

i) Faraday's first law of electrolysis

The mass of the substance altered at an electrode during the electrolysis is directly proportional to the quantity of the electricity consumed at the electrode. Quantity of the electricity is the electric charge measured in coulombs.

$$m = \frac{Q\,M}{z\,F} \qquad\qquad (1.4)$$

Where 'm' is the mass of the deposit produced at the electrode (grams) and 'Q' is the electric charge (coulombs) required for the process, M is the molar mass of the substance, $F = 96,485$ C mol^{-1} is the Faraday constant, z is the valance number of ions of the substance.

ii) Faraday's second law of electrolysis

For a given quantity of electric current through different electrolytes, the mass of the metal deposited or dissolved at an electrode is directly proportional to the electrochemical equivalent weight of metal deposited or dissolved.

$$\mathbf{m} \;=\; \frac{\mathbf{A} \times \mathbf{I} \times \mathbf{t}}{\mathbf{z} \times \mathbf{F}} \qquad\qquad (1.5)$$

Where 'A' is the atomic weight of the metal deposited or dissolved, 'I' is the actual current passed in ampere, 't' is the time in seconds, z is the valance number of ions involved in the reaction, and F is the Faraday constant $= 96,485$ C mol^{-1}.

Faraday: The passage of 96,485 coulombs or one Faraday (F) of electricity is always accompanied by an electrochemical equivalent weight of the metal being deposited on the cathode, or dissolved from the anode (Glasstone 1960).

1.4 Effect of variables on electrodeposition

Among many variables which are responsible for the overall quality of electrodeposit, the following are important.

1.4.1 Metal ion concentration

Normally during electroplating the metal salt concentration is kept high, because a high c.d. can be employed for high metal content in the solution. In general, a decrease in metal ion concentration decreases the crystal size and results in fine adherent coating films. The low free metal ion concentration in a strong solution of metal compounds can be achieved either by the addition of a compound with a common ion, or by the formation of complex compounds or ions, as in cyanide baths of copper (Brenner 1963, Parthasaradhy 1989).

However, in case of alloy deposition, the most important variable is the concentration of two or more parent metals in the bath. In general, the ratio of the metal in an electrodeposited alloy differs considerably from their ratio in the bath. Only under

some special conditions, the ratio of the metals is same in both bath and alloy. The concentration of the parent metals in the bath can be varied by three methods.

(i) Variation of metal ratio

The total metal content of the bath is kept constant while the ratio of one metal to the other is varied. This method is the most important, because the composition of alloy is more responsive to the metal ratio of the bath than to any other variable. In this method, it is preferable to keep the total number of moles of the parent metals in the bath constant, rather than the total weight of the metal.

(ii) Variation of total metal content

The ratio of the two parent metals in the bath is kept constant while the total metal concentration is varied. The composition of an electrodeposited alloy varies over only a limited range as the total metal content of the bath is varied. For this reason, this type of variation is not very frequently studied.

(iii) Variation of a concentration of a single metal

The concentration of one parent metal is kept constant in the bath while increments of the other parent metals are added. The above three procedures, which are commonly used in the investigation of alloy plating because they are simple to perform.

1.4.2 Current density

The c.d., the applied current divided by the surface area, expressed as A dm^{-2} strongly influences the plating adherence, plating quality and deposition rate. The higher the c.d., the faster the deposition rate, although there is a practical limit enforced by poor adhesion and plating quality when the deposition rate is too high. In the past three or four decades, specific interest in pulse plating and periodic reverse pulse plating (where the current is either interrupted or reversed periodically) has increased significantly (ASTM B374 1996). These techniques find distinct applications in the development of some special coatings. In general, raising the c.d. increases the proportion of the readily depositable metal in the deposit. The extent of change is likely to be greater in simple primary salt solutions than in complex salt solutions and greater when the codepositing

metals are in complex with common anion than when the anions of the complex ions are different. In the latter case, when the metals are associated with different complex ions, an appreciable change in c.d. can be permitted with little change in plating composition. It is an established fact that a periodic change in the cathode c.d. allows the growth of coating on the substrate with periodic change in the microstructure of the coatings, and consequently, its properties (Rangakrishnan et al. 2002, Kanani 2006). Hence the cyclic multilayer alloy, or composition modulated multilayer alloy coatings can be developed, with a great degree of accuracy and reproducibility using proper power sources capable of generating different power patterns (Cohen et al. 1983). i.e. modulation in composition may be effected by proper manipulation of the cathode current densities, combined with plating thicknesses.

1.4.3 Temperature

The operating temperature is the vital parameter for the consistent performance of any deposition bath. Deviations of more than 5°C from optimum temperature are sufficient to harm plate quality, deposition rates, and other properties. Baths can usually be formulated, however to operate satisfactorily at any given temperature within a relatively wide range (typically, up to 60°C). The advantages of higher temperatures include higher plating rates, improved anode corrosion, and the ability to operate more dilutes baths with no loss in performance. For protective coatings, the ability to use higher plating currents with increased deposition rates is of practical importance. While electroplating an alloy, the increase of bath temperature usually tends to increase in the proportion of nobler metal in the alloy deposit. The increase in temperature decreases the polarization of the nobler metal, relatively more than the polarization of the less noble metal.

1.4.4 Agitation

The increase of agitation on the electrodeposition process has a same effect as the temperature. As can be expected, with bath agitation the effective thickness of diffusion layer diminishes; hence the diffusion rate will increase. This thickness will vary from

species to species. A diffusion layer is not formed immediately on turning on the voltage/current. It takes on the order of several seconds, depending on agitation. Agitation brings fresh nobler metal ions to the cathode film and decreases the cathode layer thickness, which leads to increase in proportion of nobler metal in the deposit. In case of deposition of alloys, an increase in agitation usually increases the amount of nobler metal in alloy plate, thus tending to offset the effect of an increase in c.d. The effect of agitation is likely to be less pronounced when the primary metal ions are associated with complex ions rather than with simple ions, and more pronounced when the two or more metals are associated with like anions rather than with unlike anions.

1.4.5 Polarization

Electrochemically, when metal deposition is accompanied by hydrogen evolution, it may be said that one deals with alloy plating in which hydrogen is the codepositing element. This is so even when hydrogen is discharged as gas since the conditions for codeposition is met. Alloy plating of metals makes it into a process of production of hydrogen and two or more metals. The evolution of hydrogen during electrodeposition of an alloy has a significant effect on the polarization and composition of the alloy deposited. If a significant amount of hydrogen is evolved, the potential of the cathode during alloy deposition may be determined almost totally by the hydrogen evolution reaction. If, as it is usually the case, over potential for hydrogen evolution is high in the preceding case, the currents corresponding to the individual metals will be close to limiting values. Under these conditions, an increase in the current will increase the amount of hydrogen evolved, resulting in a poor efficiency for alloy deposition with a minor change in the composition of the alloy deposited.
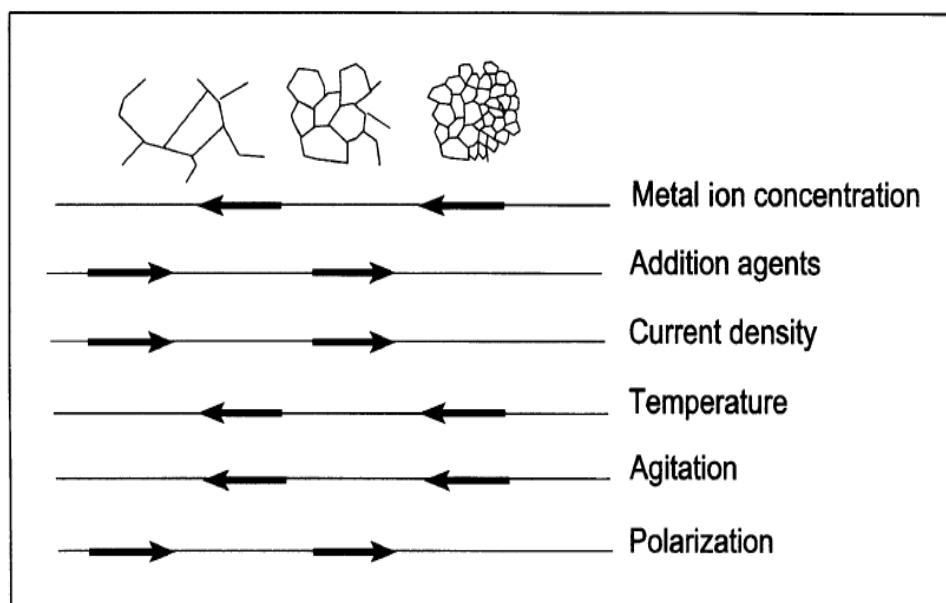
Fig. 1.2. Relation of structure of electrodeposits to operating conditions of solutions.

Though there are large numbers of other variables, which affects the structure and properties of electrodeposits, the above discussed parameters are of greater significance in the plating process, and the deposit characters. The effects of these variables on grain size can be summarized schematically as shown Fig. 1.2. The arrows in the figure indicate the tendency that an increase in the given parameter will cause in determining grain sizes in the deposit (Paunovic and Schlesinger 2006).

1.5 Cathode current density

Cathode current density is the most important factor in the electroplating process. To produce acceptable coatings, the practical electroplater must control not only the appearance but also the distribution of the metal deposited on the substrate. At constant efficiency the amount of metal deposited per unit time is directly proportional to the c.d. at each point; therefore, a nearly uniform distribution of the c.d. is required to obtain a deposit of uniform thickness. The distribution of the electric current at cathode, and hence the resulting thicknesses of electroplate on its surface, depends on the electric field

set up in the conducting plating solution. In principle, if the electric potential is known as a function of position, throughout the solution, the electroplating problem is completely solved. Thus the variation in cathode c.d. allows the growth of coatings with variation in their properties. Hence c.d. may be used as the tool for development of new materials, having new properties. To see the effect of cathode c.d. on deposition process in electroplating industry, the Hull cell, an invaluable analytical tool is being used (Naseer 2006).

Hull cell is a miniature test-plating tank with inclined electrodes shown as ab and cd in Fig. 1.3, and is used by electroplaters to check performance of plating solutions over a wide range of current densities. The two-dimensional field plot, shown in Fig. 1.3 consists of two complementary sets of lines which intersect everywhere at right angles. One set of lines, dotted in the figure, represent lines of equal potential at values intermediate between those of the two electrodes ab and cd. The current flow in the Hull cell is represented in Fig. 1.3 by solid lines which connect electrodes ab and cd. Thus the net electric field distribution along the side cd is represented by the solid lines, as shown in the Fig. 1.3.
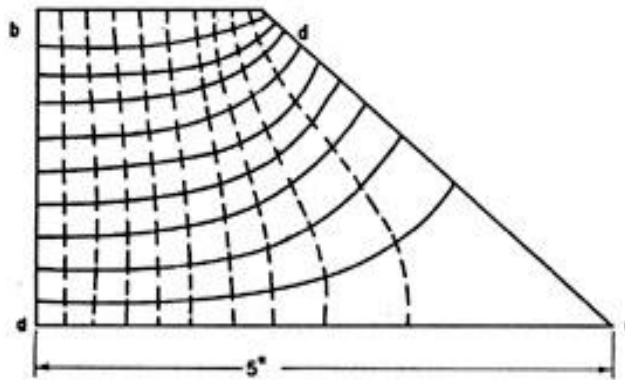
Fig. 1.3. Electric field distribution on Hull Cell panel. Electrodes *ab* and *cd* are connected by current lines (solid); equi-potential lines are dotted.

1.5.1 Hull cell - An invaluable analytical tool in electroplating

The Hull cell is a type of test cell used to qualitatively check the condition of a electroplating bath. It allows for optimization for cathode c.d. range, optimization of additive concentration, recognition of impurity effects and indication of macro-throwing power capability etc. Hull cell is named after Richard Hull, who introduced his invention to the industry in 1939. Hull cell is a miniature plating tank as shown in Fig. 1.4(a), in which the cathode is angled with respect to the anode. As a result, when a current is applied across the anode and cathode, the resulting c.d. will vary along the length of the cathode, being highest at the point it is closest to the anode. In this way, one can, within a single test run assess the effect of varying c.d. After such a run, the cathode is removed and inspected. At the highest current densities, the deposit may be burnt. At the lowest current densities, no deposition may be observed. Thus the Hull cell allows the determination of the so-called 'operating window', the c.d. range over which acceptable deposition occurs. The Hull cell is basically a trapezoidal container that holds 267 ml of solution in a depth of 48 mm of the cell. Today, Hull cell is made of an insulating material such as Perspex or PVC material, and is shown Fig.1.4 (a). To carry out the test, the electrolyte is placed in the cell and an anode of 60×75 mm size and cathode of 75×100 mm (at slanting edge) are positioned as shown in Fig. 1. 4(b). Using Hull cell, a platter could alter parameters, make additions or undertake treatments without interrupting production.

Hull cell can be used to assess any factor that produces a change in the appearance of electrodeposits over a wide range of current densities. The test is simple and quick in execution. In practice, a certain amount of skill in the interpretation of data is required. The Hull cell test is complimentary to an analytical control method and is only method to control the concentration of addition agents (like brighteners, grain refiners, levelers, stress relievers etc.). Hull cell test is a valuable guide to determine the influence of any parameter on appearance of the deposit. It is used to assess the effect of c.d. on number of solution properties like brighteners, burning ranges, leveling, ductility, covering power, throwing power and current efficiency.
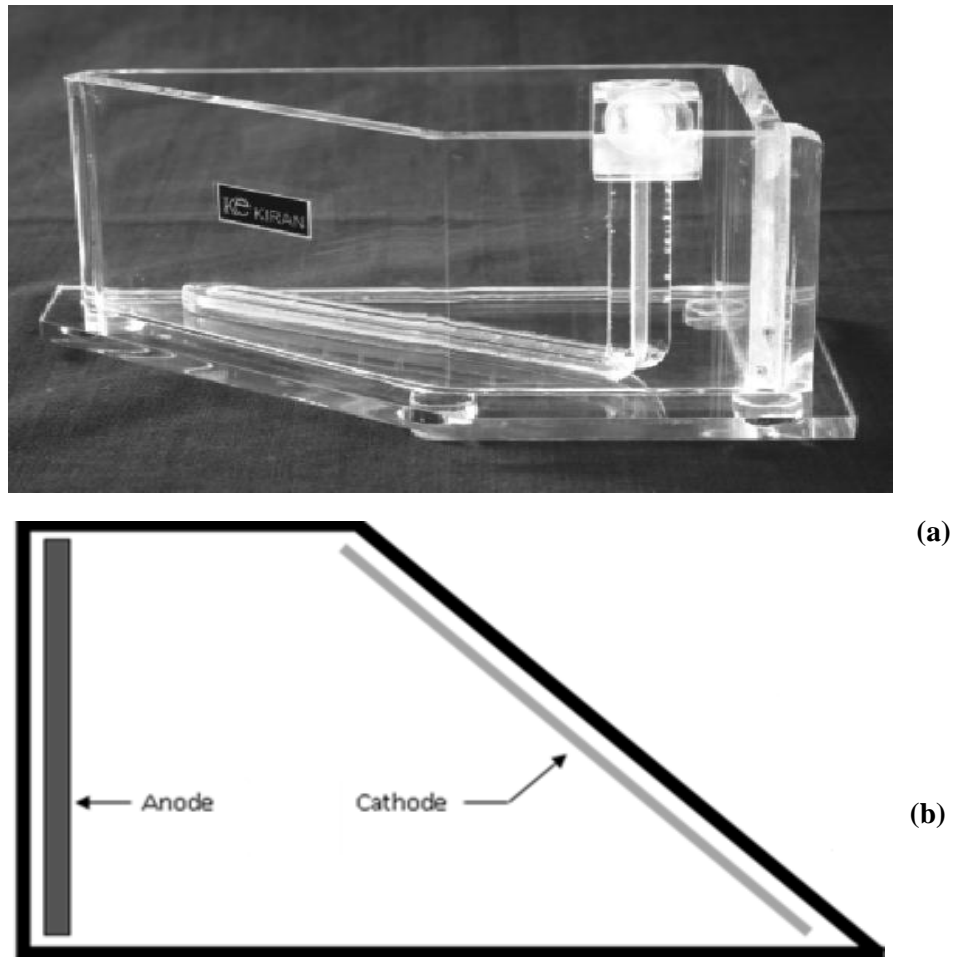
Fig. 1.4. Hull cell: (a) plan view of 267 ml Hull cell and (b) top view

By taking required electrolytic solution, the deposition can be carried out on cathode at definite cell current, such as 1 A, 2 A or 3 A etc. The corresponding current densities at definite distance from High Current Density (HCD) end can be obtained from Hull cell ruler, shown in Fig. 1.5.

HCD   **10 cm**   **LCD**

	mA cm^{-2}														
1 AMP	40	30	25	20	15	12	10	8	6	4	3	2	1	0.5	
2 AMPS	80	60	50	40	30	24	20	16	12	8	6	4	2		1
3 AMPS	120	90	75	60	45	36	30	24	18	12	9	6	3	1.5	
5 AMPS	200	150	125	100	75	60	50	40	30	20	15	10	5	2.5	

Fig. 1.5. Hull cell ruler for different cell current

C.d. at a given point along the cathode panel can also be calculated using formula,

$$I = C \left(5.10 - 5.24 \log L \right) \qquad\qquad (1.6)$$

Where 'I' is the c.d. in A dm^{-2} at any point on the cathode, 'C' is the cell current strength (I) used for the test, and 'L' is the distance in cm from HCD to the point on the cathode at which c.d. is desired to be calculated.

Thus Hull cell is an invaluable analytical tool for preventive maintenance and allowing platters to make corrections before problems to occur in production or to troubleshoot after they have occurred. Regular use of this Hull cell saves the time, money and helps to avoid disasters in plating line. Hence Hull cell is one of the most trusted testing devices in modern electroplating even today, because of its simplicity and utility. Hence, due to its invaluable use, it is said that 'a plater without a Hull cell is like an electrician without a voltmeter' (Dini 1993).

1.6 Effect of other constituents

The properties of coatings, of either metal, or alloy, can be tailored by adding other constituents into the electrolytic bath. They can be divided into groups, based on

their function as: i) primary and secondary salts ii) brightening agent iii) complexion ions iv) buffer compounds and v) salts promoting the anode solubility. For a metal or alloy deposition, any one/or many of the above additives work synergistically to impart better quality to the deposit. The function of each of these constituents in alloy bath is important to affect on one depositing metal relative to its effect on a codepositing metal.

1.6.1 Primary and secondary salts

The primary salts are largely responsible for the ion activities of depositing metal in the cathode film, since they determine the concentration and valance of the ions. Secondary salts are those of non depositing metals with or without a common anion. These salts are necessary to improve the conductivity or anode solubility or both, and influence the pH, ionic strength and ionic mobility in the cathode film.

1.6.2 Brightening agent

In metal finishing, bright or highly reflective surfaces can be of both decorative and functional importance. Reflective surfaces are characterized by a crystallite size at the surface of less than 0.3 μm^2. Thus, highly reflective deposits are found under conditions where fine-grained deposits are formed. To achieve this, it is the long-established practice to add metallic or organic compounds, known as brighteners or brightening agents. Their use is based on empiricism, there being no certain means of predicting their effects. In the same way, selecting the most appropriate such compound(s) will usually be based on trial-and-error. Generally, there are two types of brighteners. They are primary brightener, or brightener carrier and secondary brighteners. The primary brighteners generally lead to a significant grain refining action during deposition, while this greatly increases the brightness of the metal, it will not impart a mirror-finish. These primary brighteners are essential components of a complete brightening system, in that they reinforce the efficacy of secondary brighteners. The secondary brighteners are rarely used without the primary. Secondary brighteners, even at very low concentrations, impart a near-mirror finish to the deposited metal.

There are three possible mechanisms for bright deposition: (i) diffusion-controlled leveling, (ii) grain refining, and (iii) randomization of crystal growth. The theory of random electrodeposition, which asserts that there are two basic mechanisms of deposition: selective and random. Selective deposition occurs when the atoms deposit on favorable surface sites. Favorable sites for deposition are kinks, steps, and the surface ends of screw dislocations. In random deposition, there is no such regularity of growth on favorable sites. Deposition occurs randomly on all available surface sites. Random deposition can be achieved using additives that produce random distribution of isolated surface sites uncovered by the additive and available for deposition. This random distribution of uncovered (free) sites must be in a state of rapid flux from the site to site. With large surface coverage many selective, favorable sites will be blocked, and random deposition will be favored. Random coverage of a surface is considered to be essential for bright deposition. The rate of adsorption and desorption of additive must be of the same order of magnitude as that of the cathodic deposition process. If they are much smaller, additive molecules can be entrapped in the deposit, and this can lead to a selective deposition mechanism. Random deposition can also be promoted by an increase in c.d.

1.6.3 Addition agent

Most solutions used in electrodeposition of metals and alloys contain one or more inorganic or organic additives that have specific functions in the deposition process. These additives affect deposition and crystal-building processes as adsorbate at the surface of the cathode. Thus, adsorbate-surface interaction mainly decides the quality of the coatings. There is no entirely satisfactory definition for an addition agent. As a result, composition of the deposit and deposition efficiencies can be altered and the nature of the soluble anode dissolution changed by addition agents. In many cases, no clear distinction can be made between addition agent and buffer functions, since many substances act in both capacities. Their main function; when properly administered is to develop sound metallic plates of desired physical properties. Without the addition agent, the deposit

would be powdery, brittle or irregular. The addition agent are said to alter the limiting c.d. of one or both metals to change the polarization or to increase the current efficiency at the anode or cathode or both (Brenner 1963).

1.6.4 Complexing ions

A large proportion of the electrodeposited metals are obtained from solution in which the metal is present in the form of a complex, instead of in the form of simple ions. For several reasons, the complex ions in bath have better throwing power. They yield fine grained, smoother and brighter deposits, and they permit an active metal to be coated by a nobler metal, without the latter depositing by immersion. The great advantage of baths of complex ions for alloy plating is that in such baths it is often possible to bring the electrode potentials of metal close together. In solutions of some complexing ions, whether the solution is acid or alkaline, the electrode potentials of all metals are shifted to more negative (less noble) potentials, and this often brings them closer together.

Examples of some complexing agents are; salts of organic hydroxyl acids have great power for complexing and keeping metals in alkaline solution. Citrates and tartrates have been most used, but many others such as hydroxyacetate, malonate, gluconate are equally effective. Several types of nitrogen containing compounds readily form soluble complexes with metals, but they have not been successful where some of the common complexing agents have failed. Among the amines, which have been used as complexing agents, is ethylene diamine, ethylene triamine, triethanolamine. The amino acids are other forms of complexing agent, the simplest one, glycine readily forms complex metallic ions (Brenner 1963, Kanani 2006).

1.7 Characteristics of electrolytic bath

Electrodeposition of metal coatings in industrial metal finishing is usually based on the aqueous electrolytes, known as electrolytic baths. Aqueous electrolytes used in metal finishing for electrodeposition of metal coatings are principally the solutions of metal salts in an acid or alkali in solution, dissociates to form electrically charged anions

and cations. In addition, there will be additives, complexing agents to promote the electrodeposition process or optimize the deposit properties. Many electrolytes used in metal finishing are based on complexes. The characteristics of these baths such as covering power, throwing power and efficiency are very important to obtain the bright coatings showing industrial applications.

1.7.1 Efficiency of plating

The cathode current efficiency (CCE in %) of electrodeposition is the percentage of total current usefully employed for cathodic deposition of the metal. This can be calculated from the relationship,

$$\text{CCE (\%)} = \frac{\text{Measured mass gain}}{\text{Theoritical mass gain}} \times 100 \tag{1.7}$$

Theoretical mass gain can be calculated from Faradays law by measuring the quantity of the electricity that flows through the solution for known time.

1.8 Mechanism of electrodeposition

The electrodeposition of metallic layers from aqueous solution is based on the discharge of metal ions present in the electrolyte at a cathode surface. The metal ions accept an electron from the electrically conducting material at the solid-electrolyte interface and then deposit as metal atoms onto the surface. The electrons necessary for this to occur are either supplied from an externally applied potential source or are surrendered by a reducing agent present in solution, in case of electroless reduction. The metal ions themselves derive either from metal salts added to the solution, or by the anodic dissolution of the so-called sacrificial anodes, made of the same metal that is to be deposited at the cathode. The metal deposition reaction takes place in two consecutive and coupled stages. The first to this is the formation of thermodynamically stable crystal nuclei at certain points on the cathode followed by their growth. Thus, the property of electrodeposits depends on nucleation and growth processes which constitute

21

electrocrystallization (Paunovic and Schlesinger 2006). The essence of electrode kinetics is charge transfer across the interface. A profound understanding of the structure of the electrical double layer, as discussed by Helmholtz, Gouy-Chapman and Stern is needed for the discussion of the mechanism of charge transfer (Dini 1993, Budevski et al. 1996). There are other important factors, such as catalysis and adsorption, mass-transport limitations and so on, all of which may influence the rate and mechanism of charge transfer, to some extent, but it is the very act of charge transfer that matters. It is same as the conversion of chemical energy to electrical energy, as in a fuel cell or a battery during discharge (Eliaz et al. 2008).

In fact, the process of electrodeposition is more complex, involving a number of intermediate stages. The most important of these are:

> Transport of the hydrated metal ion or complex from bulk solution to the cathode.
> Stripping the hydration sheath from the metal ion at the metal-solution interface.
> Charge transfer with the formation of an adsorbed atoms (ad-atom) at the cathode surface.
> Formation of crystal nuclei by diffusion of the ad-atoms at the cathode surface.
> Fusion of thermodynamically stable crystal nuclei to form a metallic layer.

These individual steps are shown together in Fig. 1.6, with the understanding that this is a simplified depiction of the actual process.

Transport of metal ions from the bulk solution to the cathode surface is primarily due to convection and diffusion. The discharge of ad-ions to form ad-atoms takes place within the electrolyte double layer, which forms spontaneously at the metal-solution interface. Although the metal ions loose most of their charge in this process, residual charge remains, and thus a part of their hydration sheath. In this state, and after passing through the electrolytic double-layer, they are adsorbed on the cathode surface where they form ad-atoms. In order that a coherent metal film is formed, two further coupled stages must occur, known as nucleation and (crystal) growth, or a process called

electrocrystallization. Nucleation results from diffusion controlled migration of the ad-atoms on the surface. The growth process begins once the nuclei have reached a critical size.
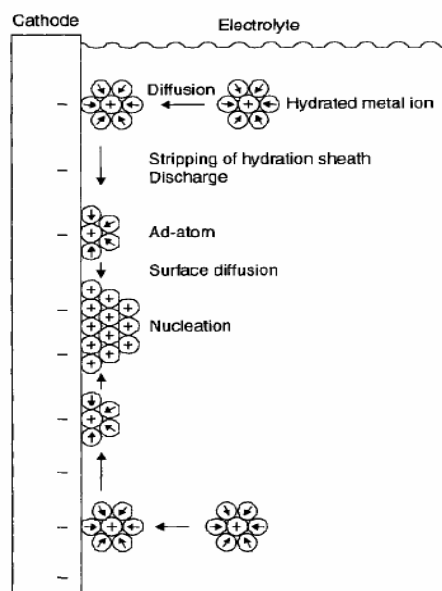
Fig. 1.6. Migration of hydrated metal ions to a cathode, surrender of the hydration sheath, formation of M-atoms, formation of crystal nuclei at the cathode surface

1.9 Advantages of electroplating

The technique of electrodeposition offers several important advantages over other coating methods. They are:

- This technique is fairly simple and relatively cheap.
- The laws governing, scaling up and scaling down of electrochemical processes are well understood.
- Geometrically complex or non line-of-sight surfaces can be coated.
- Proper design of the cell and the counter electrode can ensure the metal deposition.
- Production of coatings with close control over the property by proper manipulation of operating conditions is possible.

- Relatively low processing temperature allowing the formation of highly crystalline deposits with possibly lower residual stresses.
- Synthesis of nano/micro structured multilayer coatings having novel properties, using different current/voltage waves.
- Dense materials with high purity, low defect density and narrow distribution of grain size can be produced.
- Electrodeposited materials show distinct property of extreme hardness and excellent wear resistance.

Representative applications of electrodeposition include among others, gold-plated brass jewellery; copper plating for fabrication of interconnects in electronic packaging; hard chromium plating in aircraft applications; zinc-nickel plating on steel components for protection against corrosion; silver-plated mirrors; tin-lead coatings for soldering on printed-circuit boards; plating of nickel, iron and copper in fabrication of micro-electro-mechanical systems; mutual alloys of Fe-group metals for computer applications etc. (Landolt 2002, Kanani 2006).

1.10 Electrodeposition of alloys

The properties of alloy deposits are superior to those of single-metal electroplates, and are widely described in the literature (Brenner 1963). In other words, it is recognized that, alloy deposition, provides properties not obtained by employing electrodeposition of only single metals. It is further asserted that relative to the single-component metals involved, alloy deposits can have different properties in certain composition ranges. They can be denser, harder, more corrosion resistant, more protective of the underlying base metal, tougher and stronger, more wear resistant, superior with respect to magnetic properties, more suitable for subsequent electroplate overlays and conversion chemical treatment, and superior in antifriction applications. Electrodeposited alloys may or may not be the same in phase structure and properties as those formed metallurgically. Electrodeposited alloys find a wide range of applications in the electronics, metals and surface finishing industries, automobile industries. A large number of binary and ternary

alloys have been plated from aqueous solutions, for micro fabrication or surface coating (Kanani 2006). The compositions of electrodeposited alloys are governed by the kinetics of the partial electrode reactions, and it can be modeled in terms of mixed potential theory, commonly used in corrosion science (Landolt 2002). Detailed description on the principles and types of alloy plating is given by Brenner in his treatise (Brenner 1963).

1.10.1 Principles of alloy plating

The most obvious requirement of alloy codeposition is that the two parent metals have deposition potentials that are close together. However, since there is no generalization covering the proximity of the potentials, this condition is not considered as the principle. However other important governing principles of alloy plating are:

1. *If an alloy plating bath, which is in continuous operation, is replenished with two metals in the constant ratio, M/L (for example, by adding metallic salts or using soluble anodes), the ratio of the metals in the deposit will approach and ultimately take on the value M/L.*

2.   *An increase in the Metal- percentage (ratio) of the parent metal in an alloy-plating bath result in an increase in its percentage (ratio) in the deposit.*

3.   *In alloy deposition, the ratio of the concentration of the more readily depositable metal to   the other is smaller at the cathode - solution interface than in the body of the bath.*

4. *In the deposition of alloys from the normal alloy plating systems, the most fundamental mechanism is the tendency of the concentration of the metal ions at the cathode - solution interface to approach mutual equilibrium with respect to the two parent metals.*

Both principles (3) and (4) leads to the relation, $C_M/C_L < C^0_M/C^0_L$, where C_M and C_L are, respectively the concentration of the more readily and less readily depositable metal at the cathode - solution interface, and C^0_M and C^0_L are the concentration of the metals in the body of the bath.

25

5. *A variation in alloy plating conditions that brings closer together the potentials for the deposition of the parent metals separately. i.e., decreases the interval of the potential between them, increases the percentage of the less noble metal in the electrodeposited alloy and vice versa.*

Corollary: The shift in the current density- potential curve of alloy deposition that results from a variation in plating condition is in the same direction (+ or -) as the shift in the potentials of the parent metals.

6. *In depositing alloys in which the content of the less noble metal increases with the c.d., the operating conditions for obtaining the more constant composition of the deposit are:(a) Constant potential, if the uncontrollable variables affect the potentials of the nobler metals. (b) Constant c.d., if the uncontrollable variables affect the potentials of the less noble metal. Conditions (a) and (b) are interchanged if the content of the less noble metal decreases with c.d..*

1.10.2 Types of alloy deposition

Alloy plating can be classified into the following five types

i) Regular codeposition ii) Irregular codeposition iii) Equilibrium codeposition iv) Anomalous codeposition and v) Induced codeposition.

i) Regular codeposition

This is characterized by the deposition being under diffusion control. The percentage of nobler metal in the deposit is increased by those agencies that increase the nobler metal content of the cathode diffusion layer like, increase in the total salt content of the bath, decrease of c.d., elevation of temperature, and increased agitation. Regular codeposition is most likely to occur in baths containing simple metal ions, but may occur in baths containing complex ions. Sn-Ni and Ni-Co are the examples of this type of codeposition.

ii) Irregular codeposition

In this type, the effect of plating variables on the composition of the deposit is much smaller than with the regular codeposition. It is most likely to occur with the solution of complex ions. Brass plating is an example of this codeposition. In this brass plating, the cyanide as the complexant considerably brings the equilibrium potentials of nobler metal copper to the value of zinc equilibrium potential and enables the codeposition easily.

iii) Equilibrium codeposition

This is characterized by the deposition from a solution, which is in chemical equilibrium with both of parent metals. Cu-Bi and Pb-Sn alloys fall in this category. The ratio of metals in the deposit is the same as that in the bath.

iv) Anomalous codeposition

In electrodeposition of Zn-Fe group metal alloys, the wt. % of Zn in the deposit is much higher than in the electrolytic bath. However, one would expect to obtain an electrodeposits of nearly pure Ni due to its strong thermodynamic nobility ($E_{Zn}^0 = -0.76V$ and $E_{Ni}^0 = -0.25V$). Actually, it is not the case, instead, under most practical conditions; the ratio of the less noble metal (Zn) to the nobler metal (Ni) in the deposit is larger than in the bath. This phenomenon is known as "anomalous codeposition", described by Brenner in his comprehensive treatise (1963). Anomalous codeposition is rather rare, and is frequently associated with the electrodeposition of Zn-M (where M stands for Ni, Co and Fe) alloys and mutual alloys of iron group metals, namely Fe-Ni, Fe-Co and Co-Ni. The phenomenon deserves a considerable amount of study, since its explanation would greatly advance our knowledge of electrode polarization in general and alloy deposition in particular. The behavior of metals in anomalous codeposition is not consistent and clear. Under certain conditions of c.d. and temperature, the metals may codeposit in a normal fashion and under other conditions in anomalous manner. Among many models proposed to explain the anomalous codeposition the one, namely, hydroxide suppression

mechanism, proposed by Dahms and Croll (1965) is the most satisfactory (Paunovic and Schlesinger 2006). This was later supported by a number of workers, who measured a rise in pH near the cathode surface during the electrodeposition. As per this model, during deposition of Fe-Ni alloy it was assumed that consequent to hydrogen evolution, there will be raise in pH in the vicinity of the cathode leading to the formation of $Fe(OH)_2$. The $Fe(OH)_2$ layer thus formed suppress the diffusion of Ni^{+2} ions towards cathode, and thereby decrease the Ni content in the electrodeposited alloy.

v) Induced codeposition

It occurs whenever a metal like molybdenum, tungsten, vanadium, and titanium, which cannot be deposited alone from simple salt solutions. However, these metals readily codeposit with the iron group metals. The deposition of Ni-Mo, Ni-Ti and W-Co alloys are typical examples of this type of codeposition. Metals which stimulate the deposition are called inducing metals, and the metals which do not deposit by themselves are called reluctant metals. The effects of the plating variables on the composition of the alloys of induced deposition are more vagaries and unpredictable than the effects on the composition of alloys of any of the other types of codeposition.

1.11 Composition modulated alloy coating

In recent years, composition modulated alloy (CMA), or more correctly composition modulated multilayer alloy (CMMA) coatings are of great scientific interest due to their wide spread applications in materials research (Rangakrishnan et al. 2002). These materials basically consist of very thin layers of different metals/alloys arranged in an alternate fashion, in nanometeric scale. These coatings are also called as cyclic multilayer alloy coatings. Here the phrase 'cyclic' is used to mean the successive deposition of layers of alloys having two or more composition. The properties of these coatings are found to be improved with increase in number of layers. Though number of such layers is unlimited in theory, practically it is only up to a certain optimal numbers

(Kanani 2006). Schematic representation of CMA coating (having alternate layers of two metals) is shown in Fig.1.7.

.
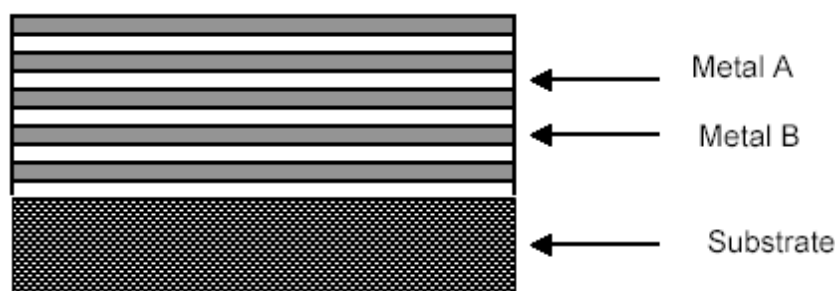
Fig. 1.7. Schematic representation of cyclic multilayer coating

The electrolytic deposition being an atomistic deposition process, it is possible to bring modulation in properties of the coating just by brining modulation in deposition conditions. As a result of the layering near atomic dimension, the nano-structured multilayered deposits can possess remarkable and sometimes unique properties not attainable in normal metallurgical alloys. These properties include X-ray optical properties, magneto-optical properties, improved hardness, wear and corrosion resistance (Haseeb et al. 1992, Simmovich et al. 1994). The CMA coatings show wide applications in various industries, including those of the aircraft, aerospace, automotive, household appliances and electronics.

The attractiveness of electroplating for the synthesis of advanced materials is linked to the large selection of plating conditions, which allows the tailoring of the characteristics of electrodeposited materials. A periodic variation of the plating conditions allows the growth of coatings on the substrate having a periodic variation in their structural properties. The experimental procedure adopted for production of multilayer alloy coatings, pertaining to this thesis is detailed in chapter 3.

1.11.1 Methods of production of CMA's

There are two approaches to develop CMMA coatings, namely physical method and electrolytic method. Physical Vapor Deposition (PVD), Chemical Vapor Deposition, sputtering and molecular beam epitoxy techniques are few among many physical methods. Several coating systems have been prepared by PVD method, such as Si/Nb and Co/X where X is either Au or Pd or Cu. The above methods have several advantages for specific applications, but due to some limitations of above methods such as high capital cost, high energy cost, etc., an alternative method is required. Blum first introduced the electrodeposition of multilayered alloy on Cu-Ni in 1920s. Later on Brenner deposited Cu/Bi by varying c.d. Electrodeposition offers certain advantages over the other conventional methods. It is a cheap and well-established industrial process and is a precisely, controlled room temperature operation. Thus, the risk of inter-diffusion is low and the deposition rate is fast with low energy requirements. Binary, ternary and quaternary alloys over a wide range of composition, and structures are easily obtainable by this technique. Electrodeposition has wide applications in various industries, including those of the aircraft, aerospace, automotive, household appliances and electronics. CMA coatings can be developed by electrolytic methods by the following routes: i) Single Bath Technique (SBT) ii) Dual Bath Technique (DBT)

i) Single bath technique

In SBT, the metal ions required to form two or more layers are dissolved in a single electrolyte and cathode potential is made to change alternatively. To avoid their simultaneous deposition, a large potential difference must exist between the deposition potential of metals. If such potential difference is not there, they are made to differ by many hundreds of milli-volts by adding appropriate complexing agents. The most satisfactory approach is to create a situation where modulation of current will result in the deposition of different composition at higher or lower currents.

ii) Dual bath technique

The DBT involves the deposition alternate layers of two components from separate baths. Very little work has been done on dual bath electrodeposition, due to inherent difficulties associated in its operation. Production of multilayer using the SBT offers the following advantages over DBT:

- No need to transfer work from one bath to another.
- No intermediate processing between baths required.
- Current density modulation does not require elaborate equipment.
- Process is less time-consuming.

Against this, few drawbacks of SBT should be noted, and they are:

- A specially formulated electrolyte for specific composition.
- Range of possible deposits is limited by availability of metal salts and metal complexes.
- It is not always possible to avoid some alloying at the interface between two layers.
- Metal ions in the electrolyte should have reduction potentials that are sufficiently far apart so that nearly pure layers can be selectively deposited. Thus, the selection for CMA is limited.

1.11.2 Applications of CMA coatings

As a result of the layering in micrometric/nanometric level, the CMMA coatings can possess unusual properties different from bulk properties. Since Zn-Fe group metals alloys, and mutual alloys of Fe-group metals exhibit n-number of properties, their CMA electrodeposits finds wide applications in various industries, including those of the aircraft, aerospace, automotive, household appliances, electronics etc. Further, in extremely high temperature and/or corrosive environments, and in the environments where the use temperatures are in access of 1000 degrees F (Jet engines, power generation applications, chemical plants, and oil rigs and in construction industry), these CMMA coatings find their applications. The attractiveness of electroplating for the

synthesis of advanced materials is linked to the large selection of plating conditions, which allows the tailoring of the characteristics of electrodeposited materials.

1.12 Corrosion and its control

Corrosion is a vexing problem in every use of every metal/alloy due to its interaction with oxygen, water, salt and gases present in the environment. Due to corrosion, about one fifth of steel production is degraded, gets lost or disappears. Under favorable corrosion conditions, all metals corrode and the most serious offender is iron and its alloys. Chemicals, soils, atmosphere (rural, industrial, marine or combination of these), foodstuffs, organic materials, acids, oxidizing agents, water, dissimilar metal contacts and high temperature are the most common causes of corrosion.

1.12.1 Corrosion protection

Protection of metals against corrosion can be distinguished as electrochemical and non-electrochemical. The non-electrochemical ways include dense protective films that isolate the metal against effects of the medium and may be paint, polymer, bitumen, enamel, etc. Electrochemical methods of protection include different percepts like: (i) Electroplating of the surface with a thin protective layer of a more corrosion resistant metal (ii) Electrochemical oxidation of the surface or application of other types of surface layer (iii) Control of polarization characteristics of the corroding metal, and (iv) Control of potential of the corroding metal. The polarization characteristics of a corroding metal can be controlled by the addition of various additives to the solution called corrosion inhibitors which adsorb on the metal and lower the rate of the cathodic and/or anodic reaction. Various organic compounds with -OH, -SH, $-NH_2$, -COOH and so on, as the functional groups are used as inhibitors.

1.12.2 Corrosion prevention by metallic coatings

i) Single metal coatings

To protect easily corrodable metal object several metallic coatings have been used, such as Cu, Ni, Zn, Sn, Cd, etc., and its alloys (Fontana 1987). Copper and nickel are examples of cathodic coatings, which are chemically less active than steel. In salt solutions, metals protect steel by shielding it from corrosive environments and are effective as long as they completely envelop the steel surface. Being less reactive than steel a given thickness of coating lost much longer than an equivalent thickness of steel. However, if discontinuities appear on coatings, a galvanic action will set up between the coating as a cathode and steel as an anode in the presence of moisture. Zn and Cd are the examples of anodic coatings. Anodic coatings protect steel from corrosion initially just as cathodic coatings by shielding it from corrosive environments, but being chemically active they are attacked more rapidly than cathodic coatings and still protect the steel by galvanic action where it acts as an anode and the underlying steel as the cathode. Cadmium, like zinc, also provides sacrificial protection to iron, steel, brass and aluminium, especially in marine and alkaline environments.

In addition to their good corrosion protection, it provide a low coefficient of friction and therefore good lubricity, predictable torque characteristics, good electrical conductivity, protection from galvanic corrosion (in particular when in contact with aluminium), easy solderability, low volume corrosion products and reduced risks of operating mechanisms being jammed by corrosion debris for many components in a wide range of engineering applications throughout industry. Hence cadmium coatings are particularly useful in the electrical, electronic, aerospace, mining, offshore, and automotive and defense industries where they are applied to bolts and other fasteners, chassis, connectors and other components.

Though cadmium and zinc are two metals used much interchangeably on non-critical hardware because they provide generally similar corrosion protection through the same principle of anodic protection. When it became accepted that cadmium is a chronic cumulative poison similar to lead and mercury in its effects, cadmium gradually became

restricted to use only on those applications where its unique combination of properties could not be met by zinc plating or zinc alloy plating. As the pressure to eliminate cadmium grew, cadmium plating continues to be used less and less. In fact it is prohibited from many applications in many countries because of its health effects.

ii) Alloy coatings

Electrodeposited Zn-based alloys of Fe group metals have achieved an important position in the protection of ferrous substrate throughout the world. Zinc alloys can be easily designed electrochemically to produce different corrosion potential to maintain the sacrificial protection of zinc at a slower dissolution rate. Some of these alloys are excellent replacement to cadmium in many applications (Pushpavanam and Michaee 2004). Even though alloy coatings are produced by thermal or electrodeposition technique in a wide range of composition, only certain composition yield better corrosion protection in a particular environment than pure electrodeposits, i.e., the composition of the alloy may be tailored to meet a particular environment. Sn-Zn alloy of 80% Sn has the superior protective power than the parent metals and the presence of tin decreases the rate of anodic attack on zinc. This alloy combines the protective value of tin with sacrificial nature of zinc and does not form typical white corrosion product seen with the zinc electroplate (Short and Dennis 1997). The best protection is offered by 70% tin alloy.

The electrodeposited Zn-based alloys of Fe group metals, or alternatively Zn-M alloys (where M =Ni, Co and Fe) are of much interest for the protection of steel substrates against corrosion (Fratesi and Roventi 1996, Sohi and Jalali 2003, Soares et al. 2006). Among the Zn-based alloys of Fe group metals, Zn-Ni alloy has been studied extensively and put into practical uses in the mass production of steel sheets for automobile bodies, and for small components such as nuts and bolts (Short et al. 1984, Roventi et al. 2000, Ramazan and Gulfeza 2007). Although Zn-M alloy coatings show better corrosion resistance than pure zinc coatings, further research for getting better protective properties is of distinct commercial interest.

1.12.3 Evaluation of metallic coatings

Though the coatings are applied for other purposes like appearances, wear resistance, reflectance, etc., major requirement of electroplated coating is good corrosion protection. Generally, the composition and structure of the deposit are detrimental to its corrosion behavior. Hence corrosion tests are highly desirable for quality control in the plating process and its improvisation apart from understanding the mechanism of coating failures. Corrosion tests can be mainly divided into two types (i) field and service tests (ii) laboratory tests.

i) Field and service tests

Service tests, including atmospheric exposure tests are inherently the most reliable for determining the performance of the coatings in service. Such tests find extensive use in the general field of corrosion. For electroplating industries atmospheric exposure tests are particularly useful in evaluating coating systems and improving the plating processes for outdoor service. In exposure tests, the specimens are kept in various locations having various atmospheres like marine, industrial, rural, etc. and coatings are evaluated at frequent intervals. This test is time consuming, and one has to wait for years together to find out the failure.

ii) Laboratory tests

The laboratory tests are very quick and enable to predict the life of coatings exposed to out-door atmosphere. Laboratory tests include accelerated tests and electrochemical tests. In the first case, the salt spray test has received extensive use for electroplated coatings; in principle, it consists of exposing the test specimen to a controlled fog of neutral salt water or salt solution containing sodium chloride. Apart from this, sulfur dioxide test can also be used for evaluating the coating, which involves exposure of test specimens to a humid atmosphere containing sulfur dioxide. The corrosion of metals in aqueous electrolytes occurs by an electrochemical mechanism.

This implies that there are distinct cathodic and anodic reactions occurring at the metal surface which comprises the corrosion process. Electrochemical methods of corrosion measurements are carried out using instruments.

1.13 Electrochemical theory of corrosion

In aqueous environments, the majority of metallic corrosion processes are electrochemical. The reaction at the less stable anodic sites (A) on metal M (e.g., where there are dislocations, imperfections) can be explained by a simplified equation:

$$M_{(s)} \; \square \quad M^{+n}_{(aq)} + n\,e^{-}_{(s)} \qquad (1.8)$$

The corresponding cathodic reaction occurs at the cathodic sites (C) at the metal/solution interface:

$$R_{(aq)} + n\,e^{-}_{(s)} \rightarrow R^{+n}_{(aq)} \qquad (1.9)$$

The species R is an oxidizing agent in solution that can receive electrons from the metal. In the corrosion process, all the electrons produced by the anodic reaction move through the remaining metal to the cathodic site and are accepted by the oxidizing agent. The overall reaction of the corrosion process is represented by Equation 1.10, and is shown schematically in Fig. 1.8.

$$M_{(s)} + R_{(aq)} \rightarrow M^{+n}_{(aq)} + R^{+n}_{(aq)} \qquad (1.10)$$
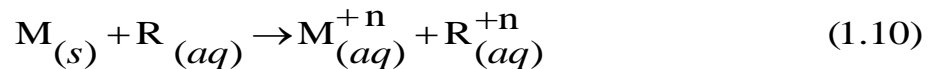
On the metal surface, many short-circuited galvanic cells may set up, and the metal will continue to dissolve in the presence of excess oxidant, and this process is spontaneous (negative ΔG) as long as the equilibrium (reversible) potential for $M_{(s)} + R_{(aq)}$ is more negative than that of $M^{+n}_{(aq)} + R^{+n}_{(aq)}$. Several cathodic reactions can occur in aqueous solution corresponding to the metallic dissolution reaction.
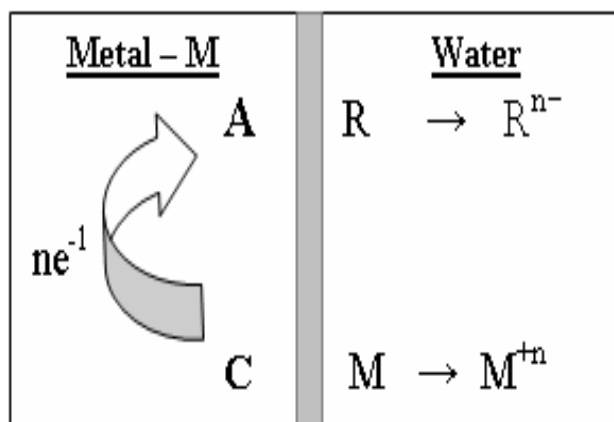
Fig .1.8. Schematic representation of corrosion process involving the metal dissolution in water containing an oxidizing agent R

In acidic solutions containing oxygen the main cathodic reaction is:

$$O_{2(aq)} + 4H^+_{(aq)} + 4e^-_{(s)} \rightarrow 2H_2O_{(l)} \qquad (1.11) \qquad (E^0 = +1.229\,V)$$

In basic environments where there is sufficient oxygen, the following cathodic reaction predominates:

$$O_{2(aq)} + 4H_2O_{(aq)} + 4e^-_{(s)} \rightarrow 2H_2O_{(l)} \qquad (1.12) \qquad (E^0 = +0.401V)$$
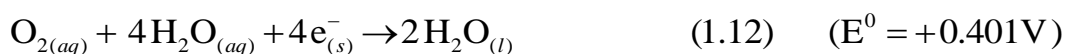
1.14 Corrosion kinetics

The rate of reduction depends essentially on the rate at which the oxidant, e.g., H^+ is transported in solution up to the cathodic site and also on the rate of electronation. The corrosion behavior of iron in dilute mineral acid solution (HCl) can be taken to illustrate the importance of the kinetic factors in determining the rate of corrosion. The electrochemical characteristics of the system can be represented by the Evan's diagram schematically shown in Fig.1.9 (Jones 1996). If an iron piece is immersed in HCl solution containing some ferrous ions, the electrode cannot remain at either of these two reversible potentials but must lie at some other potential. Iron is metallic and a good conductor of

electricity and therefore, the entire surface must be at a constant potential. The total rates of oxidation and reduction are equal at the intersection of polarization curves for the two processes represented by E_{corr}. The rate of hydrogen evolution to the rate of iron dissolution will be equal and this is expressed in terms of corrosion current density, $i_{corr.}$ For most of the metals, the corrosion c.d. of 1 $\mu A\ cm^{-2}$ will be equal to a CR of 1 millimeter per year (mm y^{-1}).
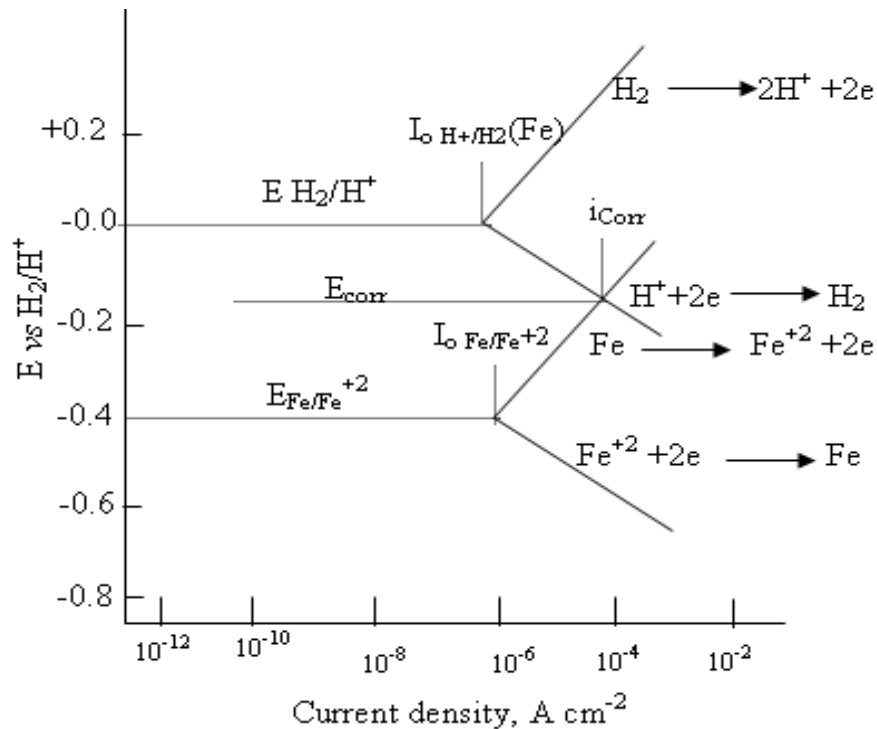
Fig.1.9. Electrode kinetic behavior of pure iron in acid solution (schematic)

There are two important electrochemical approaches for measurement of corrosion kinetics, or corrosion rate (CR). They are:

- Potentiodynamic polarization or Tafel's extrapolation method (DC method).
- Electrochemical impedance spectroscopy (EIS) or Alternate Current (AC) method.

1.15 Potentiodynamic polarization method

The potentiodynamic polarization or Tafel extrapolation method for determining the (CR) was used by Wagner and Traud to verify the mixed-potential theory (Fontana 1987, Jones 1996). The metal sample is termed the working electrode, and cathodic current is supplied to it by an auxiliary electrode composed of some inert material such as platinum. Current is measured by the ammeter, and the potential of the working electrode is measured with respect to a reference electrode by a potentiometer-electrometer circuit. The electrode potential versus the log of c.d. is determined using electrochemical procedures. In a representative diagram shown in Fig. 1.10, the solid lines corresponds to polarization curves, as the electrode potential is made more positive or negative about the open circuit potential (OCP).
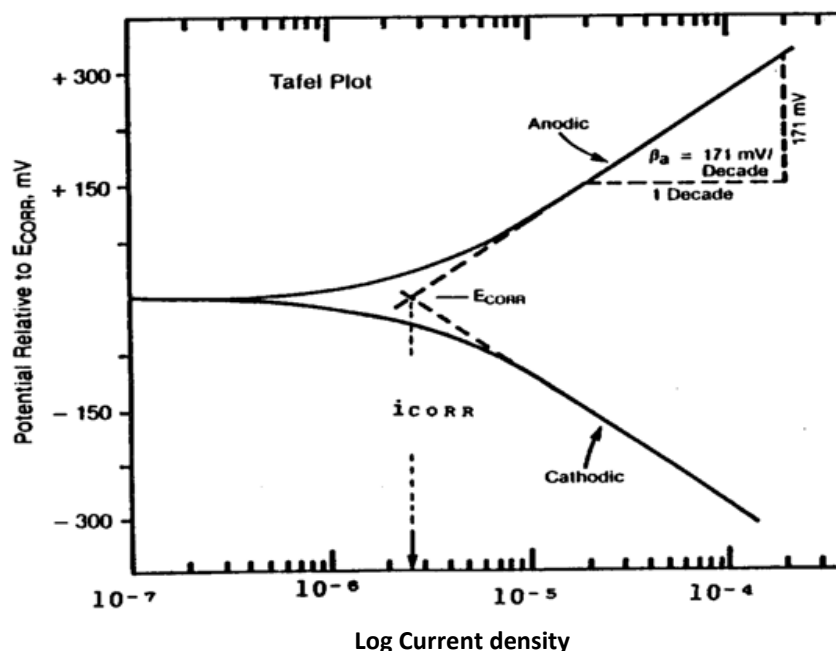
Fig. 1.10. Typical potentiodynamic polarization behavior (Tafel plot)

At potentials approximately 200 mV more positive than the OCP, the electrode potential versus log c.d. is linear. The slope of the oxidation reaction that represents metal becoming soluble metal ion is linear. The slope is called anodic Tafel slope, represented

by β_a. The curve shows that for an active metal, as the electrode potential is made more positive, or as the solution becomes more oxidizing, the metal dissolution increases. The cathodic branch of the polarization curve is the solid line at more negative potential than the OCP; a cathodic current to the metal specimen is measured. The slope of the linear portion of the polarization curve is the cathodic Tafel slope, represented by β_c. As the potential is made more negative, the rate of the reduction reaction increases. The relationship for anodic and cathodic processes under activation polarization is

$$\eta_a = \alpha_a + \beta_a \log i \tag{1.13}$$

$$\eta_c = \alpha_c + \beta_c \log i \tag{1.14}$$

Where,

η_a = anodic polarization or anodic over potential

η_c = cathodic polarization or cathodic over potential

α_a and α_c, = anodic and cathodic Tafel constant

β_a and β_c = anodic and cathodic Tafel slope

$\log i$ = logarithm of the current

The linear portion of the cathodic branch and anodic branch of the polarization curve can be extrapolated back to the intersection at OCP, and the approach is called Tafel's extrapolation method. The value of the current at this intersection yields the i_{corr}, which is equal to the rate of the anodic or cathodic reaction under freely corroding conditions. Thus extrapolation method can be used to determine the CR of metals, when either the cathodic or anodic branch exhibits a well-defined linear region.

1.16 Electrochemical impedance spectroscopy

EIS is a very versatile electrochemical tool to characterize intrinsic electrical properties of any material and its interface. The basis of EIS is the analysis of the impedance (resistance to alternating current) of the observed system in subject to the applied frequency and exciting signal. This analysis provides quantitative information about the conductance, the dielectric coefficient, the static properties of the interfaces of a

system, and its dynamic change due to adsorption or charge-transfer-phenomena. EIS uses alternate current (AC) of very low amplitude (10mV). This facilitates a non-invasive observation of any sample without any or less influence on the electrochemical state.

The well known EIS technique differs from DC method by using AC. In DC method Ohm's law is limited to only one circuit element, i.e., the ideal resistor. An ideal resistor has several simplifying properties:

❖ It follows Ohm's law at all current and voltage levels

❖ Its resistance value is independent of frequency

❖ Current and voltage signals through a resistor are in phase with each other.

Ohm's law defines resistance R in terms of the ratio between voltage E and current I as*:*

$$R = \frac{E}{I}$$ (1.15)

But the real electrochemical systems, however, contains circuit elements that exhibit much more complex behavior, and hence in place of resistance one can use *impedance*, which is more general circuit parameter. Impedance is also a measure of the ability of a circuit to resist the flow of electrical current. Unlike resistance, it is not limited by the simplifying properties listed above. In EIS, the impedance behavior is being studied by the application of an AC signal (sinusoidal wave). The form of the current–voltage relationship of the impedance in an electrochemical system can also be expressed as (Yuan et al. 2010),

$$Z(\omega) = E(t) \ / \ I(t)$$ (1.16)

Where, $Z(\omega)$ is the impedance in ohms (Ω) as function of frequency (ω), and E (t) and I (t) are the time dependent voltage and current. Impedance (symbol Z) is a measure of the overall opposition of a circuit to current, in other words: how much the circuit impedes the flow of current. Hence the EIS takes into account the effects of capacitance and inductance apart from the resistance. Impedance is measured in ohms with symbol Ω.

Impedance is more complex than resistance because the effects of capacitance and inductance vary with frequency of the current passing through the circuit. This means the impedance varies with frequency. The effect of resistance is constant regardless of frequency. Four electrical quantities which determine the impedance (Z) of a circuit are: resistance (R), capacitance (C), inductance (L) and frequency (f). Hence, the term 'impedance' is often used (quite correctly) for simple circuits which has capacitance or inductance.

1.16.1 Reactance (X)

Reactance is another word for resistance, and is a measure of the opposition of capacitance and inductance to current. Reactance varies with the frequency of the electrical signal used. Reactance is measured in ohms. There exists two contribution to the total reactance, X. They are capacitance reactance X_C and inductance reactance X_L.

i) Capacitive reactance (Xc)

$$X_C = 1/2\pi f C \tag{1.17}$$

Where   Xc = reactance in ohms (Ω)

       f = frequency in hertz (Hz)

       C = capacitance in farads (F)

The value of Xc is found to be large at low frequencies and vice versa. At a low frequency limit, the AC becomes equivalent to DC making Xc to become infinite (total opposition). Hence, by rule the capacitors pass AC but block DC.

ii) Inductive reactance (X_L)

$$X_L = 2\pi f L \tag{1.18}$$

Where X_L = reactance in ohms (Ω)

       f = frequency in hertz (Hz)

       C = capacitance in farads (F)

The value of X_L is found to be large at high frequencies and vice versa. At high frequency limit, X_L tends to become very large. The large value of X_L at high frequency implies that, inductor impedes the current flow. Hence, by rule the inductors pass DC but block high frequency AC. Thus the contribution to total impedance, Z from different components, R, C and L in an AC circuit may be summarized as below. (Russell and Mann 1990).

Hence, the total reactance, X is the difference of two, and may be written as,

$$X = X_L - Xc \qquad\qquad (1.19)$$

The contribution to the total impedance Z from a resistor, capacitor and an inductor is given by the relation shown in the Table 1.1.

Table 1.1. Contribution to total impedance (Z) from resistor (R), capacitor (C) and Inductor (L)

Resistor	Capacitor	Inductor
Resistance, R	Capacitive reactance, X_C	Inductive reactance, X_L
$V_R/I = R$	$V_C/I = X_C = I/\omega_c$	$V_L / I = X_L = \omega_L$
V and I in phase	V lags I by $\pi/2$	V leads I by $\pi/2$

The above information is shown graphically in Fig. 1.11. It is easy to remember the frequency dependency of impedance by considering zero frequency AC as DC. An inductance is like a closed circuit (like piece of wire) and its impedance at low frequency AC is zero. At low frequency AC, a capacitor is an open circuit, and hence its impedance reaches infinity.
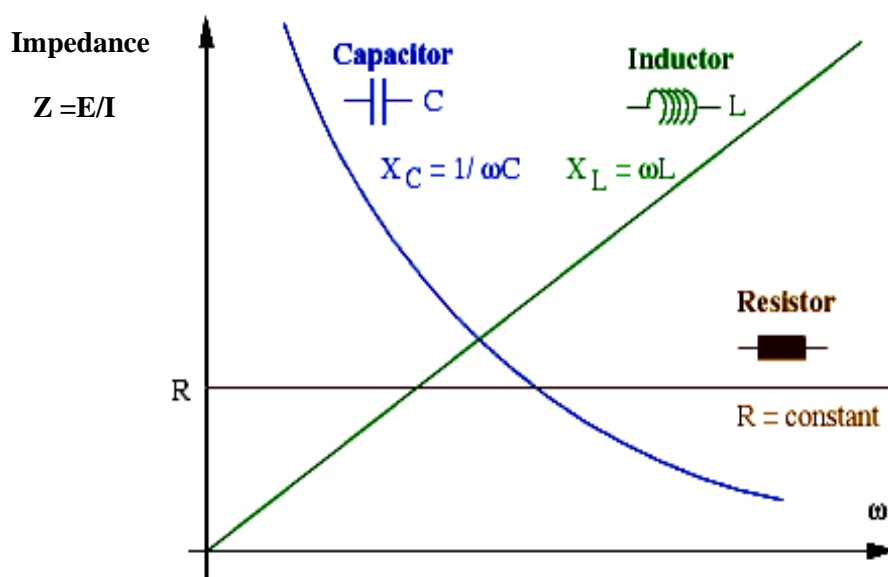
Fig. 1.11. Variation of R, X_C and X_L with frequency

Generally, the impedance spectrum of an electrochemical system can be presented in Nyquist and Bode plots, which are represents the impedance as a function of frequency. A Nyquist plot is displayed for the experimental data set Z ($Z_{re,i}$, $Z_{im,i}$, ω_i), (where i = 1, 2, …, n) of n points measured at different frequencies, with each point representing the real and imaginary parts of the impedance ($Z_{re,i}$, $Z_{im,i}$) at a particular frequency ω_i. Bode's magnitude and phase angle plots are alternative representation of the impedances, obtained by drawing phase angle, θ vs. logω and |Z |vs. logω respectively. Both plots usually start at a high frequency and end at a low frequency, which enables the evaluation of solution resistance more quickly.

The capacitance and inductance cause a phase shift between the current and voltage, which implies that the resistance and reactance cannot be simply added on to give impedance. Instead they must be added as vectors with reactance at right angles to resistance as shown in the Fig. 1.12.

44
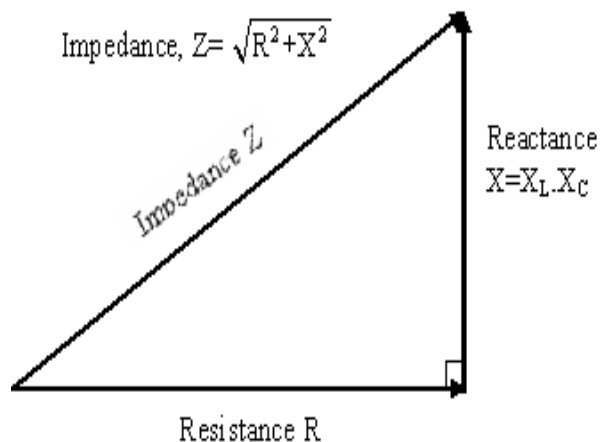
Fig. 1.12. Impedance, Z as a resultant of vector addition of reactance, X and resistance, R

Accordingly, Nyquist plot represents such data points corresponding to total impedance Z, having both real and imaginary, i.e. $Z^{'}$ and $Z^{''}$ components at various frequencies.

1.16.2 Advantages of EIS over DC technique

➢ AC impedance techniques use very small excitation amplitudes, usually in the range of 5-10 mV peak-to-peaks. Excitation amplitudes of this order perturb the electrochemical test system to a minimum extent, thus reducing errors caused by the measurement technique itself.

➢ The EIS data reflect the following parameters such as (i) charge transfer resistance of the corrosion (dissolution) reaction of metallic specimens, (ii) double layer capacitance of the metal / electrolyte interface, (iii) diffusion impedance of the dissolved metallic ions, (iv) potential-dependent adsorption/desorption phenomena at the interface, (v) impedance of passive film at the interface.

> ➢ Thus AC impedance measurements provide data on both electrode capacitance and charge transfer kinetics, the technique can provide valuable mechanistic information.

> ➢ The AC impedance technique does not involve potential scan and hence can be applied to low conductivity solutions where DC techniques are subject to serious potential control errors.

1.17 Magnetic properties

The magnetic properties exhibited by various materials can be classified into 5 types and they are as follows: (i) Para magnetism, (ii) Diamagnetism, (iii) Ferromagnetism, (iv) Ferromagnetism, and (v) Antiferromagnetism. The most important class of magnetic materials is ferromagnets, i.e. compounds of Fe, Co, Ni and Mn. The magnetic moment of an atom is by interatomic exchange, governed by Hund's rule which favors parallel spin alignment on atomic scale. In addition ferromagnetism requires inter atomic exchange, to ensure parallel alignment of the moment of neighboring atom Hysteresis loops are commonly used for studying the ferromagnetic behavior of materials. When an external magnetic field is applied the atomic dipoles align themselves to the external field. Even when the external field is removed, part of the alignment will be retained and the material is then said to be magnetized. The relationship between magnetic field (H) and magnetic flux density (B) is not linear in ferromagnets and ferrimagnets. The dependency of magnetic field density with applied magnetic field strength shown schematically in Fig. 1.13, and the different stages involved are explained as below:

i) *Magnetic saturation*

It may be observed that with increase in field strength, the flux density will also increase following a curve but only till a certain point (a), as shown in the Fig. 1.13. Further increase in field strength above this point, will result in no change in flux density. This condition is called as magnetic saturation (Ms).
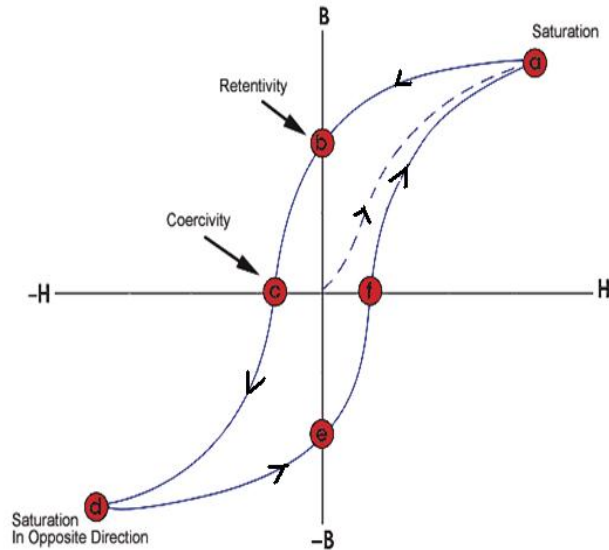
Fig.1.13.   Hysteresis loop showing the dependency of H with B

(ii) Remanant magnetization

If the field strength is reduced further, the magnetic moments relax and take up their normal positions. However the demagnetization does not follow the magnetization route in reverse. Consequently, at zero magnetic field strength, the material still retains a certain amount of magnetization which is called a remanence, point (b) in Fig. 1.13.

(iii) Coercive force

In order to reduce the magnetization to zero, a magnetic field strength has to be applied in the reverse order till point (c) in Fig 1.13. This reverse field needed to reduce the magnetization to zero, is called as coercivity. The same procedure follows in the opposite side, if the direction of magnetic field is reversed.

1.18 Scanning Electron Microscopy

Scanning electron microscopy (SEM) is the most widely used of all electron beam instrument. It owes its popularity to the versatility of its various modes of imaging, the excellent spatial resolution of its images, the ease with which the micrographs that are generated can be interpreted, the modest demands that are made on specimen preparation, and its 'user-friendliness' (Amelinckx 1996). At one end of its operating range, the SEM provides images, which can readily be compared to those of conventional optical microscopes, while at the other end its capabilities are complementary to instruments such as scanning tunneling (STM) or atomic force (AFM) microscopes. The SEM is a mapping, rather than an imaging device, and so is a member of the same class of instruments as the facsimile machine, the scanning probe microscope, and the con-focal optical microscope. The sample is probed by a beam of electrons scanned across the surface. Radiations from the specimen, stimulated by the incident beam are detected, amplified, and used to modulate the brightness of a second beam of electrons scanned, synchronously with the first beam, across a cathode ray tube display.

The magnification of the specimen in SEM is geometric in origin and may be changed by varying the area scanned on the sample. The arrangement makes it possible for a wide range of magnifications to be obtained, and allows rapid changes of magnification since no alterations to the electron-optical system are required. Multiple detectors can be used to collect several signals simultaneously, which can then be displayed individually, or combined, in perfect register with each other. It is this capability in particular which makes the SEM so useful a tool since multiple views of a sample, in different imaging modes, can be collected and compared in a single pass of the beam.

1.19 Energy Dispersive X-ray spectroscopy

Energy dispersive X-ray spectroscopy (EDX) is an analytical technique used for the elemental analysis or chemical composition of sample, interfaced with SEM machine.

The technique relies on the investigation of a sample through interactions between electromagnetic radiation and matter, analyzing X-rays emitted by the matter in response to being hit with charged particles. Its characterization capabilities are due in large part to the fundamental principle that each element has a unique atomic structure allowing X-rays that are characteristic of an elements atomic structure to be identified uniquely from one another. To stimulate the emission of characteristic X-rays from a specimen, a high-energy beam of charged particles, such as beam of X-rays, is focused on the sample being studied. At rest, an atom within the sample contains ground state (or unexcited) electrons in discrete energy levels or electron shells bound to the nucleus. The incident beam may excite an electron in an inner shell, ejecting it from the shell while creating an electron hole where the electron was. An electron from an outer, higher-energy shell then fills the hole, and the difference in energy between the higher-energy shell and the lower energy shell may be released in the form of X-ray. The number and energy of the X-rays emitted from a specimen can be measured by an energy dispersive spectrometer. As the energy of the X-rays is characteristic of the difference in energy between the two shells, and of the atomic structure of the element from which they were emitted, this allows the elemental composition of the specimen to be measured (Ray 2005). The likelihood of an X-ray escaping the specimen, and thus being available to detect and measure, depends on the energy of the X-ray and the amount and density of material it has to pass through, which may reduce the accuracy of detection.

LITERATURE REVIEW,

SCOPE AND OBJECTIVES

2.1 Introduction

Electroplating is one of the oldest approaches of surface finishing technology for protection of many metals and alloys against corrosion. By the mid-nineteenth century, development of the dynamo led to electrochemical deposition of many metals on an industrial scale. Nowadays electroplating is one of the most promising methods in surface engineering due to genuine reason of its simplicity and less cost. Today there are hardly any industries without using one way or other the advent of electroplating to get market values to their products. Generally, coatings are applied to metal substrates for several purposes.

The electrodeposition of mutual alloys of Fe-group metals has been investigated extensively from the decades because of their particular magnetic and mechanical properties. Several serious research works have been reported in the past decades, to optimize many new mutual alloy baths, with special emphasis on production and properties of electrodeposits. Many attempts have been made to develop the mutual alloys of Fe-group metals using different conditions of additives, including different power patterns; namely, direct current (DC), pulsed current (PC) and modulated dual pulse current/voltage for enhanced magnetic properties and corrosion resistance. This chapter is devoted for literature review on electrodeposition of mutual alloys of Fe-group metals and their characterization, developed using different current pulses, and followed by scope and objectives of the thesis.

2.2 Literature review

Electrodeposition is a unique technique in which a variety of materials can be synthesized including metals, ceramics and polymers. Electrochemical strategies offer

unique possibilities for development of nano-structured new materials showing novel properties. Hence, today electroplating technology is responding in both revolutionary and evolutionary ways, and consequently it has evolved into an important part of nanotechnology. Using this technique of nanoplating, it is possible to obtain pore-free nanocrystalline metal/alloy systems, having distinct properties. The subject of alloy electroplating is being dealt with an ever-increasing number of scientific publications. Typical purposes include improved corrosion resistance, magnetic properties, wear resistance, and many mechanical properties along with bright appearance. The type of electrodeposited films based on metal/alloy system has a significant role to achieve desired properties to meet the desired industrial applications.

The three important Fe-group metals, namely Ni, Fe, and Co codeposit to form the three possible binary alloys and ternary alloys. They are called mutual alloys of Fe-group metals, and are probably the most easily deposited of all alloys for three reasons: i) the standard potentials of the three metals are close together (Fe, -0.440 V, Co, -0.277 V and Ni, -0.250 V) and hence the resulting alloy naturally offer better corrosion protection. ii) It has been reported by many workers that the noble metal content in the Fe-group metal alloys is the crucial component of their electrical and magnetic properties including their corrosion resistance. In other words, the alloy becomes electrochemically nobler iii) The metals are deposited at high polarization effect.

2.2.1 Electrodeposition of monolayer alloys of Fe-group metals using direct current

In electrodeposition of alloy, the c.d. plays an important role on the deposit characters such as composition, structure, and properties. Therefore it is possible to control the composition by changing the cathode current density (c.d.). Originally the electroplating technology was confined to develop only monolayer coatings of metal/alloy using constant current, or D.C, where modulation in composition is expected at different applied current densities. Though there are innumerable reports pertaining to electrodeposition and characterization of monolayer coatings of Fe-group alloys (such as

Fe-Ni, Fe-Co and Co-Ni) developed from different baths, the following are few to be worth mentioned. Detailed literatures pertaining to individual alloys are discussed in brief in respective chapters.

i) Electrodeposition of Fe-Ni alloy

The great research interest in development and characterization of Fe-Ni thin films originates from their operational capacity, economic possibilities, magnetic and other properties. These alloys were found to exhibit good corrosion resistance properties with good leveling, ductility and brightness. Further, due to their magnetic properties these alloys find applications in the area of memory devices for computers, perpendicular magnetic recording media, and as stampers for disk pressing (Andricacos and Romankiw 1994). Electrodeposition of Fe-Ni alloys follows anomalous type of co-deposition with preferential deposition of less noble metal, i.e. Fe compare to noble Ni (Afshar et al. 2002). Dahms and Croll (1965) have investigated the role of pH at the cathode surface and its effect on the codeposition. They found an increase of pH at the cathode interface, and subsequent hydrolysis is responsible for anomalous codeposition of iron group metals, similar to the electroplating of Zn-Fe group metal alloys. A kinetic model was proposed to provide a simple explanation of the anomalous behavior of Fe-Ni codeposition in the absence of hydrogen (Matlosz 1993). Characteristic anomalous codeposition was observed in both DC and PC. (Grimmett et al. 1993). The latest and the most accepted model for the mechanism of Fe-Ni was confirmed with EIS study. It was proposed that Ni^+_{ads} and Fe^+_{ads} species compete for adsorption, and $Fe(OH)_2$ formed inhibits the diffusion of more noble Ni^+ ions towards cathode, and suppresses its reduction on cathode.

Recently, much attention has been paid to the study of nanocrystalline Fe-Ni alloys due to their interesting mechanical and magnetic properties. Both face centered cubic (fcc) and body centered cubic (bcc) nickel-iron solid solutions have been produced using electrodeposition techniques. The Fe-Ni alloys obtained through electrodeposition method are found to be different from those obtained by other methods (Trudeau 1999).

During electrodeposition of bcc iron-nickel alloys, the serious drawback of the nanocrystalline electrodeposits is generation of internal stresses (Czerwinski 1996). The level of internal stresses generated in electrodeposits is high enough to exceed the fracture strength of the alloys, resulting in cracking (Czerwinski 1998). The internal stress level can be reduced by adding inhibitors (Oniciu and Muresan 1991). For conventional bcc iron-nickel alloys, at room temperature, a maximum strength occurs at approximately 15- 20% nickel (Petrovic 2001). However, the few reported results for the conventional polycrystalline fcc nickel-iron alloys suggest that the strength of these alloys is independent of composition (Aggen 1990). In order to obtain a high wear resistance, very often exceeding the values typical for tempered steel, Fe-Ni alloys have to be deposited under a condition of high polarization. As a result, electrodeposits are under high internal stress, which frequently causes microcracks (Czerwinski et al. 1998). Tensile stress, typical for Fe-Ni alloys, and microcracks limit the exploitation of the coatings: they may cause localized corrosion and a decrease in fatigue life of the coated part, in some cases up to 40% (Safranek 1973). Considerable improvement in the corrosion resistance of bulk Fe-Ni alloys with increased Ni content has been observed. Uhlig (1974) explained this behavior by electron configuration theory of passivity. Corrosion studies of bulk Fe-Ni alloys in various electrolytes indicated that corrosion rate is not only dependent on the film composition but also on the electrolyte. The anodic dissolution rate of Fe-Ni coatings were found to vary with crystal orientation was reported by Marcus et al. (1986).

A number of experimental studies have shown that by decreasing the average crystal size of a material below 20 nm, it is possible to improve its functional properties at the cost of its magnetic properties. Against to this, some surprising results were obtained when nanostructured magnetic Fe-Ni alloys are synthesized by electrodeposition. It was observed that grain size as well as the composition of the deposits is strongly dependent on the electrolyte composition and deposition parameters. An increase in Ni to Fe ratio in the bath has been reported to decrease the iron content of

the alloy and increase its grain size (Cheung et al. 1995). In some cases, additives were used for decreasing grain size of alloys (Fricoteaux and Rousse 2008). Direct and pulse current were used to produce bulk Fe-Ni alloys in nano-size scale. The mechanism of nanocrystalline Fe-Ni electrodeposition were also studied using electrochemical impedance technique (Sanaty-Zadeh et al. 2009).

ii) Electrodeposition of Co-Ni alloy

Nickel-based alloys are used widely in aerospace, energy generation and corrosion protection, especially in corrosive environments at high temperatures. On co-depositing cobalt with nickel hardens the nickel in a sulphur free form by forming a solid solution, and they are ductile than those hardened by sulphur containing additives (Srivastava et al. 2006). Cobalt and nickel forms a solid solution over the whole concentration range (Barker 1992). This ability enables the potential uses of their magnetic properties in wide range of conditions. This makes Co-Ni alloy of special interest to the microelectronics industry (Golodnitsky et al. 2002). Further, Co-Ni films are expected to show greater resistance to corrosion than Ni-Fe films (Gomez et al. 2005). Co-Ni alloys have been studied extensively for magnetic applications especially in micro-system technology for the manufacture of sensors, actuators, micro relays and inductors (Wang et al. 2005). These alloys have been deposited from a variety of simple and complex baths, and they exhibit co-deposition of anomalous type (Correia and Machado 2000). The anomalous codeposition could be related to the intrinsically fast kinetics of cobalt deposition. Along with kinetic study it also had been found that no anomalous codeposition of nickel-cobalt occurred in the complex ion bath (Ch and Piron 1996). It was found that the extent of anomaly of mutual alloy deposition decreases in case of pulse reverse plating at low current densities (Tury et al. 2006). Pulse parameter effects on the composition morphology and structure of Ni-Co alloys electrodeposition from chloride bath. (Lallemand et al. 2005).

Investigations on Ni–Co alloys with different composition and microstructure showed that physical and electrochemical properties strongly depend on the Co-content

of the alloy. The amount of cobalt in Ni–Co deposit can be controlled by experimental parameters, such as electrolyte composition, pH, c.d., temperature and stirring speed (Golodnitsky et al. 2002). The effect of these parameters on the mechanical properties such as hardness, strength, residual stress and magnetic properties has been dealt in detail in literature (Brenner 1963). Few studies have been reported on the tribological behavior of these coatings. Co-rich alloys exhibit lower friction coefficient and higher wear resistance compared to Ni-rich alloys. They have attributed this behavior to the hcp crystal structure in Co-rich alloys (Wang et al. 2005). Co-Ni coatings on stainless steel exhibit good corrosion resistance in saturated sodium chloride solution.

iii) Electrodeposition of Co-Fe alloy

Fe-Co alloys have been extensively studied in the past due to their wide range of applications in magnetic devices due to their high saturation magnetizations and low coercivities (Zhou et al. 2008). Nano-crystalline soft ferromagnetic of Fe-Co have highly desirable materials for high temperature applications like magnetic bearings for high-speed motor, flywheels, gas turbine engines, etc.(Turgut et al. 2000). The property of Fe-Co strongly depends on the structure, composition and morphology of the deposit (Kakuno et al. 1997).

Electrodeposition is an inexpensive method for generating Fe-Co films with a high technological potential. The effect of applied magnetic field on the morphology and texture of Fe-Co alloy coatings have been studied (Shao et al. 2003). The composition of electroplated Fe-Co film was found to be influenced by the addition of sodium saccharin, which has a favorable effect on deposit quality and bath stability. The codeposition of cobalt and iron leads to a reduction of the reaction rate of more noble component, and an increase in reaction rate of the less noble component was observed when the organic additives are adsorbed on the electrode surface (Lallemand et al. 2004). The electrodeposited Fe-Co from chloride and sulfate baths has suggested that, the current efficiencies from chloride bath were significantly higher than that from sulfate one. High current efficiencies, around 52%, was independent of Fe^{2+} concentration in chloride

baths, but decreased to level of 18% in sulfate baths (Kim et al. 2003). These results were justified by the catalytic effect of chlorine, through formation of ion bridge between the electrode and the metal ion being discharged. Further, the deposition of Co-Fe alloy was found to be influenced by plating parameters such as electrolyte composition, c.d., bulk pH value etc. on deposit characters such as morphology, structure, magnetic properties etc. Similarly, several studies have been reported on electroplating mechanism and textural characteristics of mutual alloys of Fe-group metals as reported by Matlosz (1993), and in references cited therein.

2.2.2 Electrodeposition of monolayer alloys Fe-group metals using pulsed current

Deposition of mutual alloys of Fe-group metals (Ni, Co and Fe) is of interest due to the anomalous type of co-deposition. Majority of electrodeposition of mutual alloys of Fe-group metals have focused deposition suing direct current. However, there are few reports with regard to the deposition of mutual alloy of Fe-group metals through pulse plating, pulse reverse plating. It was observed that under certain coating conditions, the characteristic anomalous codeposition was changed to normal type, with change in hardness, porosity, surface topology, internal stress of the deposits (Grimmett et al. 1988). The pulse plating in the un-agitated bath of Fe-Ni is similar to the one with direct current wave form at low c.d. (Grimmett et al. 1990). It was also found that the anomaly of mutual alloys decreases in case of pulse reverse plating at low current densities (Tury et al. 2006). Pulse parameters were found to effect the composition, morphology and structure of Ni-Co alloys (Lallemand et al. 2005). Organic additives were found to affect the electrodeposition of Co-Fe alloy when coating was carried out using direct current and pulse current. Co-Fe alloy coatings obtained by pulse current was found to exhibit unique surface morphology, with decreased grain size and increased hardness (Sanaty et al. 2009). It has been observed that the cyclic voltametry and pulse reverse plating techniques were the novel methods for the preparation of Fe-Co and Fe-Co-Ni nanowires, as reported by Bai et al. (2003). The addition of nickel into the Fe-Co alloy was observed to extend the diameter of metal nanowires

2.2.3 Composition modulated multilayer alloys of Fe-group metals

In recent years, advances in electrodeposition technologies have led to the development of nano-structured multilayer alloy coatings showing unique properties. They are called composition modulated multilayer alloy (CMMA), or simply, cyclic multilayer alloy (CMA) coatings. As implied by the name, cyclic multiple-layer alloy electrodeposition involves the formation of an inhomogeneous alloy consisting of lamellae of different composition, as shown schematically in Fig. 2.1 for a binary alloy composed of species A and B (ASM Handbook 1994). Each lamella of species A (or species B) in the film has a nearly uniform thickness λ_A (or λ_B). The modulation wavelength ($\lambda = \lambda_A + \lambda_B$) characterizes the imposed compositional microstructure and typically takes a value anywhere from angstroms to microns in thickness. Multiple-layer thin films with spatially periodic compositional microstructures of the type shown in Fig. 2.1 are sometimes referred to in the literature as CMA's or as super-lattice alloys.
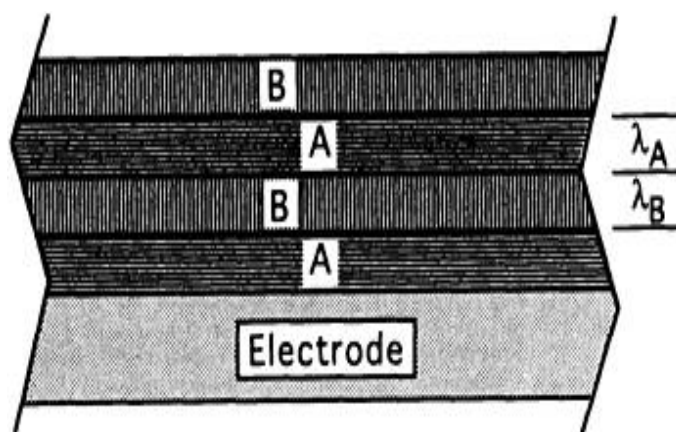
Fig. 2.1. Schematic representation of a multilayer alloy consisting of alternate layers of component A and component B

The thicknesses of the A and B are given by λ_A and λ_B, respectively. The modulation wavelength that characterizes the multiple-layer structure is $\lambda = \lambda_A + \lambda_B$. Multiple-layer alloys often exhibit a spatially periodic compositional wave throughout the film, rather than the discrete interface depicted between each lamella. Off late, to achieve

the enhanced corrosion performance the CMMA coatings have been developed. These CMMA coatings consist of a large number of thin layers of alloys, having different composition; and each layer has its own distinct role in achieving preferred performances (Ivanov et al. 2002, Jensen et al. 1998). The ability to do so by electrodeposition depends upon the solution chemistry and the operating parameters. CMMA coating technique is relatively new, and is now gradually gaining interest amongst researchers, because coatings exhibit better properties such as improved mechanical strength, micro-hardness, giant magnetoresistance (GMR) and corrosion resistance (Bull and Jones 1996, Gabe and Green 1998, Kalantary et al. 1998, Nabiyouni et al. 2002).

A wide variety of binary and ternary alloy systems have been electroplated as multiple-layer films. In many cases these alloys can be electroplated from a single electrolyte bath using either current or potential pulsing schemes. A common strategies used in many SBT is to use the hydrodynamic modulation that is synchronized in some manner with the pulsed plating. Multi-layer alloys are often found to exhibit unusual (and sometimes highly desirable) mechanical, magnetic, electrical, and chemical properties, especially when the modulation wavelength λ is of the order of nanometers. In short, multilayer alloy plating combines the best attributes of electroplating like, high output, low cost, and simple equipment with an extra degree of freedom to engineer the surface film properties. The potential impact of multilayer plating on the performance and economics of engineered surface layers appears to be large, although most commercial applications of the technology are still being developed. The CMA coating of multilayer metallic alloys with nanometer-scale modulation has prominent role in surface engineering.

While producing CMMA coating of wide compositional range, Huang et al. (2002) studied the deposition of NiFeCo/Cu from quaternary Fe, Co, Ni and Cu system. The coatings showed good GMR property, and showed dependency with number and thickness of the individual layers. Many researchers have reported the electrodeposition of multilayer Ni-Co-Cu/Cu coatings with evidence of increased GMR properties

(Nabiyouni et al. 2002). The compositions of Fe and Ni in layers were modulated by varying the deposition potential while improving the magnetic properties of even composition modulated nanowires (Liew et al. 2011). Further, Fe-Ni segments or multilayers were fabricated along the cylindrical axis of the nanowires from acidic chloride baths using anodized alumina as scaffolds (Rheem et al. 2007).

Recently, electrodepositon of monolayer Zn-Co have been made on mild steel, and their corrosion behaviors have been studied in 5% NaCl solution. In an effort to improve the corrosion performance of monolayer Zn-Co alloys by multilayer technique, CMA(Zn-Co) coatings have been fabricated using single bath technique, using different current pulses, namely square, triangular and trapezoidal (Yogesha et al. 2012). The coating configuration, in terms of switching cathode current densities, number of layers and thickness of individual layers have been optimized for peak performance of the coatings against corrosion. The experimental results revealed that CMA (Zn-Co) coatings developed using square and triangular current pulses exhibit much better corrosion resistance compared to monolayer alloys, developed from same bath for same time. A significant improvement in the corrosion resistance of multilayer Zn-Co alloy coating was found compared to corresponding monolayer Zn-Co alloy. The improvement in the corrosion performance of CMA Zn-Co coatings were explained in advanced properties of the coatings imparted by exceptional thinning of layers.

Though there are many reports on electrodeposition and characterization of Zn-Fe group metal alloys, no much work is seen to be reported with regard to electrodeposition and characterization of mutual alloys of Fe-group elements (such as Fe-Ni, Co-Ni, Fe-Co etc). Hence it is planned to develop mutual alloys of Fe group metal alloys and to examine their corrosion, electronic, magnetic behaviors. It is well known that property of the materials (developed by electrolytic method) can be improved greatly by bringing a modulation in the deposition conditions, such as current density, pH and temperature. Further, it possible to bring a significant improvement in the material property by

developing it in multilayered fashion, called composition modulated multilayer (CMM) materials. Thus, it is intended to develop new materials by proper optimization of bath composition and operating parameters and to characterize them for improved electrical and magnetic properties, including their corrosion behavior.

2.4 Conclusions from literature review

The literature survey on electrodeposition and characterization of both monolayer and multilayer coatings of mutual alloys of Fe-group metals, namely Fe-Ni, Co-Ni and Fe-Co was found to establish the following facts:

1. Electroplating technology can be effectively used for production of mutual alloys of Fe-group metals for better electrical, magnetic and corrosion properties at less cost and more accuracy.

2. The codeposition of mutual alloys of Fe-group metals exhibits peculiar anomalous co-deposition with preferential deposition of less noble metal than the nobler one. This is due to the suppressed deposition of nobler metal by hydroxide of less noble metal.

3. An increase of c.d., or the cathodic polarization causes an increase in relative amount of more noble metal in the deposit, which is the key factor required for structural modulation of the electroplates.

4. A successive change in c.d. allows the growth of coatings on the substrate, having successive change in its composition during deposition. i.e. a change of c.d. brings a change in phase structure of the coatings.

5. Multilayer coatings of mutual alloys of Fe-group metals, having patterned structures offer a promising route for development of new materials showing enhanced magnetic and corrosion properties. Hence, electrodepositon of mutual alloys of Fe-group metals are proved to be a subject of intense research both in scientific and industrial communities.

6. Impressive progress and deeper understanding of the principles of electrodeposition and availability of sophisticated power sources have led to development of variety of CMMA materials for specific engineering applications.

7. Multilayer technique provides much greater control over the working characteristics of the deposition process than hitherto. Layer thickness, performance of electroplated finishes is among the attributes that have been brought under strict control.

2.5 Scope and objectives

During electrodeposition of mutual alloys of Fe-group metals, the c.d. plays a prominent role on composition, structure and properties of the deposit. In other words, the cathode c.d. decides the deposit characters such as brightness, magnetic property, hardness, corrosion resistance etc. Generally, an increase of c.d. causes an increase of more noble metal content in the plated alloy. In such cases, it is possible to control the composition of the alloy by changing in the cathode c.d. The structure modulated alloy made in this way, offer a promising route for synthesis of new types of materials. Nanostructure coatings demonstrate surface and coating properties more superior than monolayer or non-nanostructured coatings. Hence, in these days the nano-structured multilayer materials, developed by electrolytic methods have received much attention due to their unique physical, chemical and mechanical properties, and is the subject of intensive research both in the scientific and industrial communities. Electrochemistry has a special role in producing such materials electrolytically at less cost, with high degree of accuracy and reproducibility. It is possible to develop a structure modulated coating by alternatively changing the cathode c.d. during deposition. Periodically modulated (in composition) alloys made in this way offer new properties to the coatings.

Though substantial amount of work has already been documented pertaining to the electrodeposition of mutual alloys of Fe-group metals (both monolayer and multilayer), focusing their electrical and magnetic properties, no much emphasis was given to their corrosion properties. To best of author's knowledge no work has been reported with

regard to development of corrosion resistant CMMA coatings of mutual alloys of Fe-group metals using pulsed current. Further, the effect of coating configuration on deposit characters has not been recorded, with associated structure-property relationship. Hence, in the light of experimental investigation carried out by multilayer coatings of Zn-Co alloy (Yogesha et al 2012) using square, triangular and saw-tooth current pulses, it has been decided to undertake a systematic study on optimization of new baths of mutual alloys of Fe-group metals, using common additives, namely boric acid, ascorbic acid and sulphanilic acid. The deposition conditions are optimized for development of both monolayer and multilayer coatings of alloys of Fe-group metals, and results are discussed. Further, the effects of dual and triple current pulses on corrosion protection performance of the CMMA coatings are studied.

In this direction, three new electrolytic baths, namely Fe-Ni, Fe-Co and Co-Ni have been optimized, using copper as substrate. The bath constituents and operating parameters are optimized for bright monolayer alloys of Fe group metals, using standard Hull cell method. The multilayered coatings of mutual alloys of Fe-group metals are developed galvanostatically using dual and triple current pulses. The coatings are developed under different conditions of cyclic cathode current densities (CCCD's) and number of layers. The corrosion performance of the multilayer coatings, having different coating matrices have been studied, and are compared with that of respective monolayer coating, deposited from same bath for same time. The coating configurations (in terms of CCCD's and number of layers) have been optimized for peak performance of the coatings against corrosion. The effect of different current pulses on deposit characters, consequently on corrosion performances were studied. The reasons responsible for improved corrosion resistance of CMMA coatings were explained and discussed. How the nanostructured layers of alloys having exceptional thinness (typically 1 to 100 nm) are responsible for better corrosion stability of the coatings have been analyzed using Scanning Electron Microscopy (SEM), dielectric spectroscopy and other Instrumental methods. The corrosion resistance of coatings developed using dual and triple current

pulses have been compared in relation to corresponding monolayer alloy from same bath, and results are discussed. The effect of different sets CCCD's and degree of layering have been tested and results are discussed.

The experimental results embodied in the thesis are driven by the following objectives:

1. To optimize stable baths of mutual alloys of Fe-group metals, such as Fe-Ni, Co-Ni and Fe-Co for deposition of bright coatings on copper, and to study their corrosion and magnetic behaviors.

2. To investigate the effect of c.d. on deposit characters, such as chemical composition, thickness, hardness, phase structure and surface morphology of Fe-Ni, Co-Ni and Fe-Co coatings.

3. To increase (by many fold) the corrosion resistance of monolayer coatings of Fe-Ni, Co-Ni and Fe-Co alloy through multilayer method, called CMMA coating method using dual and triple current pulses.

4. To optimize the coating configuration (in terms of CCCD's and number of layers) of multilayer coatings of Fe-Ni, Co-Ni and Fe-Co for peak performance against corrosion.

5. To examine the effect of layering on magnetic and corrosion behavior of the coatings.

6. To examine the effect of power patterns, namely dual and triple current pulses and number of layers on corrosion resistance of CMMA coatings.

7. To understand the reasons responsible for increased corrosion rate of multilayer Fe-Ni, Co-Ni and Fe-Co coatings at higher degree of layering, i.e.at higher amplitude of modulation.

8. To examine the effect current pulse, i.e. dual and triple pulse on composition modulation, and in turn on corrosion protection ability of the coatings.

9. To analyze the relation between the corrosion resistance and surface morphology of CMMA coatings in comparison with that of monolayer (non-nanostructure) coatings.

10. To understand the reason responsible for substantial increase in corrosion protection of multilayer coatings compared to monolayer by instrumental methods such as polarization, EIS, XRD, EDX and SEM.

CHAPTER- 3

EXPERIMENTAL SET UP

AND RESEARCH METHODOLOGY

3.1 Introduction

The ultimate goal of conducting research in the electroplating technology field is to investigate how to produce plated films with desirable mechanical, physical, and chemical properties that meet particular application requirements. Unfortunately electroplating of metals/alloys is a complex process associated with several sensitive factors, such as cathode surface, anode surface, concentration of bath components, nature of the medium, pH, current density (c.d.), temperature of the bath solution, anode-cathode distance, anode purity etc.

Mainly three steps are generally adopted in the plating process. They are: i) Pre-plating process ii) Plating process iii) Post-plating process. Pre plating process involves the polishing and cleaning the cathode surface and activation of anode material. It also involves the bath preparation, purification etc. In the plating process the actual electrolysis is carried out and optimization of parameters such as additive concentration, conducting salt, complexing agent, pH, temperature of the bath and optimization of c.d. for good and uniform coating. Finally, during post-treatment process, the deposit quality is required to be modified for industrial requirements by adopting standard procedures, and then characterization is performed.

There is no single experimental procedure which can cover all the aspects of electroplating of metals/alloys. Though absolute reproducibility is rather impossible to achieve in electroplating due to high sensitivity governed by several factors, the reproducibility within a reasonable limit of error is of considerable importance. A careful control of plating condition is of very importance because the properties of deposits are greatly affected by the plating conditions. Hence general procedure followed in the thesis,

for production and characterization of mutual alloys of Fe group metal coatings are given in the following sections. The experimental procedures adopted for optimization of electrolytic baths have been explained. Various methods followed in process and product characterization were discussed. Methods and materials used in the present study are given as common experimental procedures as below.

3.2 Experimental materials and methods

3.2.1 Chemicals and materials

All chemicals used are of laboratory grade (LR) or analytical grade. The chemicals used and their manufacturers are given in Table 3.1.

Table 3.1. The list of chemicals used and their manufacturers

Chemicals	Chemical Formula	Name of Supliers
Nickel sulphate	$NiSO_4.6H_2O$	Merck, India
Cobalt sulphate	$CoSO_4.7H_2O$	Merck, India
Ferrous sulphate	$FeSO_4.7H_2O$	Merck, India
Sulphanilic acid (SA)	$C_6H_7NO_3S$	Merck, India
Ascorbic acid (AA)	$C_6H_8O_6$	Merck, India
Boric acid (BA)	H_3BO_3	Merck, India
Hydrochloric acid	HCl	Rankem, India
Sodium hydroxide	NaOH	Nice, India
Sulphuric acid	H_2SO_4	Rankem, India

The all depositions of monolayer and multilayer coatings of Fe-Ni, Co-Ni and Fe-Co alloys have been accomplished under identical conditions of pre-cleaning, and common procedures were used for determining wt. % of noble metal (M) content in baths and coatings.

3.2.2 Surface cleaning

Success of electroplating or surface modification depends on removing contaminants and films from the substrate. Hence following procedure was followed to ensure good adhesion of the coatings. Copper panels of various sizes (10.0×5.0 cm^2, 5.0×5.0 cm^2 and 2.5×3.0 cm^2) were pretreated by mechanical polishing. Then they were ground to polish using emery coated mops of gradually decreasing grit sizes. The mirror polished specimens were then degreased with trichloroethylene (TCE) as solvent. Lastly, they were electrocleaned cathodically for 2 minutes and then anodically for 30 seconds, using bath given in Table 3.2. Later the specimens were washed in running water, rinsed in distilled water followed by a dip for 10 second in 5% H$_2$SO$_4$. Finally, washed and rinsed with distilled water, and then immediately taken for deposition. The composition of electrocleaning bath is given below:

Table 3.2. The composition of electro-cleaning bath

Sodium hydroxide	35 g L^{-1}
Sodium carbonates	25 g L^{-1}
Sodium lauryl sulfate	1.0 g L^{-1}
Temperature	303 to 353 K
Current density(c.d.)	6.0 A dm^{-2}
Duration	2 min cathodically followed by 30 seconds to 1 min anodically

3.2.3 Purification of electrolytes

A good electrodeposition to expect, proper preparation and preconditioning of the electrolyte is must. To achieve good coatings of required physical and chemical properties, the electrolytes used in the present study are prepared as follows. Nickel sulphate hexahydrate/cobalt sulphate heptahydrate/ferrous sulphate heptahydrate were dissolved in distilled water, depending on the requirement. Known amount of boric acid,

ascorbic acid and sulphanilic was mixed with electrolyte (Ni, Co and Fe salt solution). Then all solutions were mixed together, and stirred well. The solutions were then filtered Whatmann-40 filter paper. The pH of the plating solution was adjusted to the required value, using dilute NaOH or H_2SO_4, using digital pH Meter (Systronics, μ pH system-362).

3.2.4 Optimization of bath's composition

The chemical constituents and operating parameters of each bath have been optimized by standard Hull cell method, described elsewhere by passing 1.0 A cell current for 5 min, under still condition. The basic principle and importance of Hull cell in optimization of electroplating bath in Lab scale is discussed in Section 1.5. The Hull cell of 267 ml capacity, made of perplex material was used for fixing the bath chemistry, c.d. range, additive concentration, recognition of impurity effects and indication of brightness region in various baths.

3.2.5 Electrodeposition of monolayer and multilayer coatings

Electrodeposition of monolayer and multilayer coatings of binary alloys of Fe-group metals namely, Fe-Ni, Co-Ni and Fe-Co were carried out using DC power analyzer (N6705A, Agilent Technologies, USA), under identical condition of agitation. All depositions were carried out for same duration (10 minutes), for comparison purpose on active surface area of 7.5 cm^2. All monolayer (bulk) coatings were developed using direct current (D.C.), or constant current pulse. With theme that the periodic change in the cathode c.d. allows the growth of coating having periodic change in the composition, the CMMA coatings of different gradations in compositions were developed. The objective of improving the corrosion resistance of monolayer coatings by multilayer coating is guided by the following principles*:*

1. *Successive change in c.d. allows the growth of layers having successive change in its chemical composition.*

2. *The layering of alloys having different noble metal content leads to the formation of distinct interface*

3. *Better corrosion protection can be achieved by exceptional thinning of layers, which in turn leads to increased specific surface area of coatings.*

Having guided by the above principles of composition modulated multilayer alloy (CMMA) coatings of Fe-group metals were deposited using square waves having dual and triple pulses, by making the c.d. to cycle between two and three values. The schematic of current pulses used for monolayer (Direct Current) and multilayer (dual and triple current pulse) are shown in Fig. 3.1.
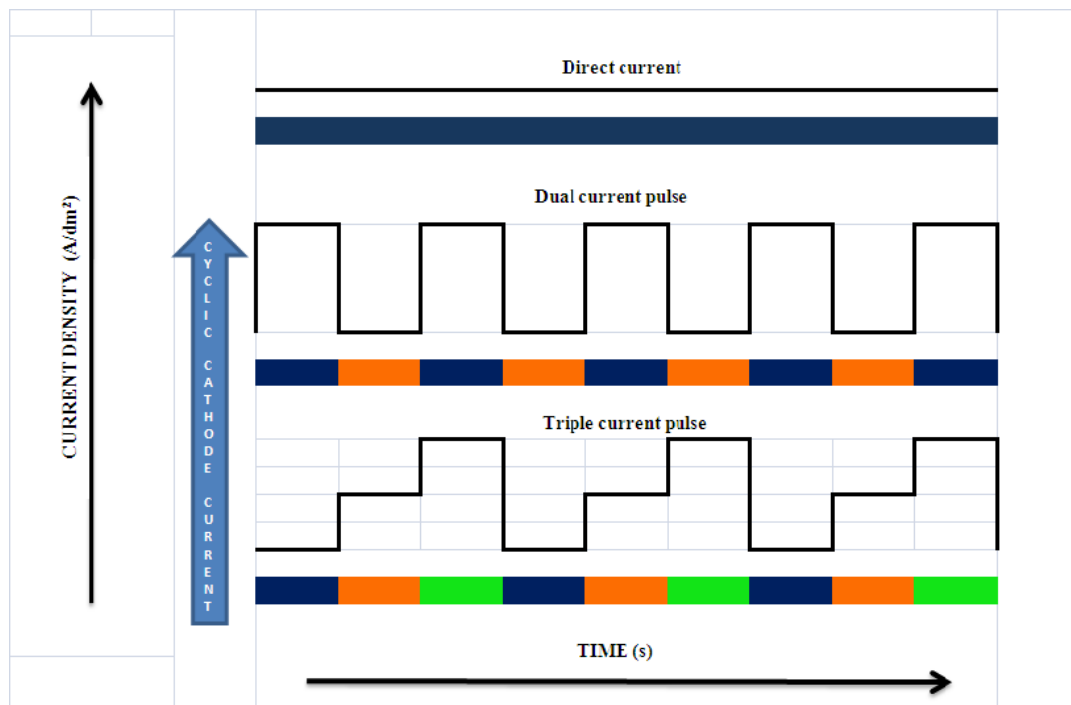
Fig. 3.1. Schematic representation of different power patterns used for deposition of monolayer and multilayer coatings of Fe-group alloys, using DC power Analyzer (N6705A, Agilent Technologies, USA) Direct (constant) current for monolayer; and dual and triple current pulses for sharp change in composition in multilayer coating

3.2.6 Optimization of baths to develop multilayer coatings of iron-group mutual alloys

Three binary alloy baths, namely Fe-Ni, Co-Ni and Fe-Co alloys have been developed through standard Hull cell method, using boric acid (BA), ascorbic acid (AA) and sulphanilic acid (SA) as common additives. The bath composition and operating variables, such as pH, temperature and c.d. have been optimized based on visual observation of the coatings, and their corrosion performances were evaluated, and results are discussed in following chapters. In an effort to increase the corrosion stability of the Fe-Ni, Co-Ni and Fe-Co alloy coatings, each Fe-Ni, Co-Ni and Fe-Co alloy coatings have been tried through multilayer approach, using dual and triple current pulses. Since the corrosion protection of multilayer Fe-Ni, Co-Ni and Fe-Co coatings is due to sacrificial and barrier protection of alternate layers, finding their right combination for full (optimal) protection by fixing right cathode current densities is the most important part of CMMA coating. Hence, the coating configurations were optimized in terms of cathode current densities and number of layers. The results are discussed with possible reasons for improved corrosion protection of multilayer coatings in Chapters 5, 7, and 9.

3.2.7 Notations used for representing coatings

It should be noted that, in the present study the cathode c.d., during deposition is made to cycle, or change between two pre-set values. i.e. alloy of one composition deposits at low c.d., and alloy of other composition deposits at high c.d. Here the cathodic current is made to cycle between two values, sharply at different time intervals, as shown in Fig 3.1. Hence, unlike regular pulse plating, in the present study, at no time the c.d. comes to zero. i.e. there is no off-time. Hence pulse plating parameters like, pulse duty-cycle, pulse frequency are not relevant with regard to electrodeposition. It is only to understand that the D.C. of different current strength has been sent in pulsed manner, which enabled the development of coatings having different composition. Accordingly, the current is cycling between low and high current densities, called cyclic cathode current densities (CCCD's).

By convention in this thesis, all monolayer alloy coatings are represented by monolayer $(M-M')_1$, where M and M′ represents the constituting metals of the alloy; and 1 represents the optimal c.d. at which monolayer M-M′ alloy coatings being developed using DC. The multilayer coatings developed, at two cycling cathode current densities are represented as: CMMA $(M-M')_{1/2/n}$, where 1 and 2 represents the lower and higher cathode current densities, between which the current is made to cycle; and 'n' represents the number of cycles the deposition is allowed to occur in total plating time (10 minutes). Further, CMMA coatings developed using dual and triple current pulses are conveniently represented, respectively as $(M-M')_{1/2/n/dual}$ and $(M-M')_{1/2/n/\ triple}$.

3.3 Instruments used

Electrochemical characterization of electrodeposits by various techniques, such as potentiodynamic polarization, cyclic voltammetric and EIS studies were carried out using Potentiostat/Galvanostat (*VersaSTAT-3,* Princeton Applied Research, USA). An X-ray diffraction (XRD) investigation of electroplates obtained at different current densities were carried out using an X-ray diffractometer D8 (Bruker AXS). Cu Kα (λ=0.15405 nm) radiation, in continuous scan mode with a scan rate of $1°min^{-1}$ was used. Surface morphology and composition of the coatings were examined by Scanning Electron Microscopy (SEM), interfaced with Energy Dispersive X-ray (EDX) Analyzer facility (JSM-6380 LA from JEOL, Japan). Magnetic properties of the films were measured by a vibrating sample magnetometer (VSM) (ADE-DMS, EV-7).
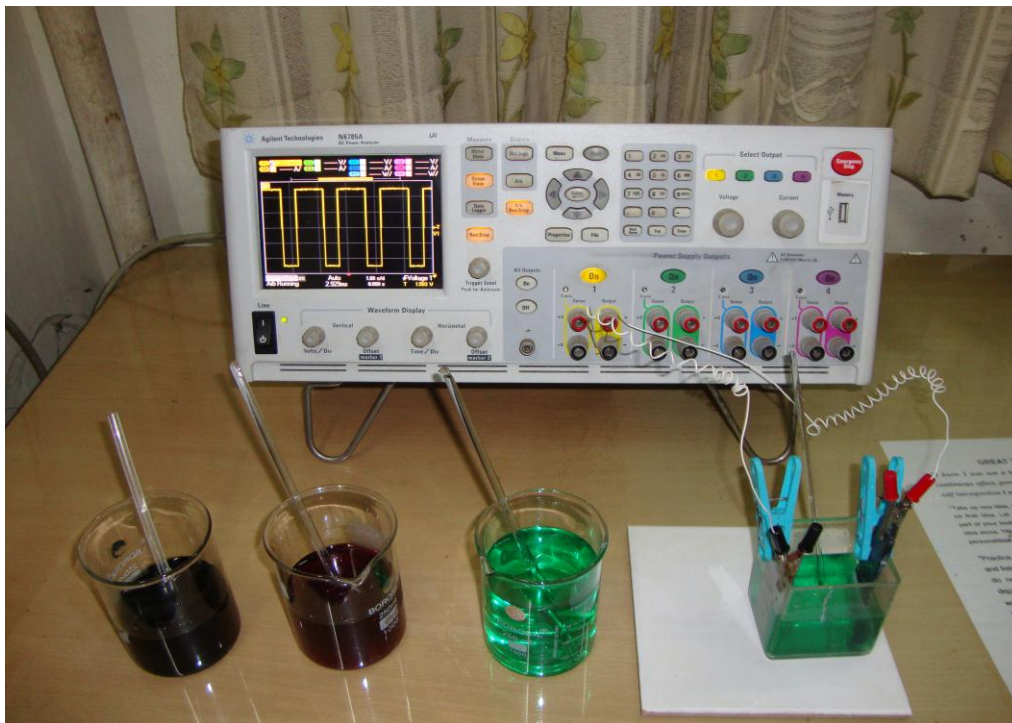
Fig. 3.2. Experimental setup used for deposition of multilayer alloys of Fe-group metals using DC power analyzer (N6705A, Agilent Technologies, USA) (Square current having dual pulse may be seen on the screen)

Micro hardness of the deposits was measured using digital Micro Hardness Tester (CLEMEX). Thicknesses of the deposit were measured by Faraday's law. Adhesions and brightness of the coatings were tested using, respectively Adhesion Tester (CC2000, DIN ISO 2401). The experimental setup used for deposition of monolayer and multilayer alloys of iron group metals is shown in Fig. 3.2.

3.4 Process and product analysis

i) Cathode current efficiency

The cathode current efficiency (CCE) of the plating bath was calculated from the weight of the deposit plated at known current and time and electrochemical equivalents of the alloy, using equation 3.1.

$$\text{CCE} = \frac{\text{measured mass gain}}{\text{theoretical mass gain}} \times 100 = \frac{w}{\dfrac{E_w \times I \times t}{F}} \times 100 = \frac{wF}{It} \sum \frac{c_i n_i}{M_i} \times 100 \qquad (3.1)$$

where w is the measured mass of the deposit (g), t is the deposition time (s), I is the total current passed (A), E_w is the equivalent weight of the alloy (g equiv^{-1}), c_i is the weight fraction of the element in the alloy deposit, n_i is the number of electrons transferred per atom of each metal, M_i is the atomic mass of that element and F is the Faraday's constant (96,485 C equiv^{-1}). Density of the alloy can be calculated, similar to the calculation of equivalent weight of the alloy, using the density and percentage of the individual metal (Brenner 1963). Generally in plating, increase of c.d. decreased the CCE and increase of metal content in the electrolyte. Bath temperature and agitation generally increased the cathode efficiency.

ii) Partial current density

The partial deposition current densities were calculated from the mass gained and the chemical composition of the deposit, using the equation:

$$i_p = \frac{w}{A\,t} \times \frac{c_i\,n_i\,F}{M_i} \qquad (3.2)$$

where i_p is the partial current density of element i (A cm^{-2}) and A is the surface area of the cathode (cm^2), w is the measured mass of the deposit (g), t is the deposition time (s), c_i is the weight fraction of the element in the alloy deposit, n_i is the number of electrons transferred per atom of each metal, M_i is the atomic mass of that element and F is the Faraday's constant (96,485 C equiv^{-1}).

iii) Cyclic voltammetry study

Cyclic voltammetry (CV) study was performed in a conventional three-electrode cell to better understand the process of electrodeposition to identify the effect of additives, namely BA, AA and SA. Saturated calomel electrode (SCE) electrode was used as the reference electrode, and platinum as counter. The optimal bath compositions were used for this study. All chemicals used were either LR grade or Analytical grade. Double distilled water was used for preparation of electrolyte solutions. Before carrying out the experiments, the pH of the solution was adjusted to the optimal value and the bath temperature was stabilized to 303K. Before each experiment, the electrode was activated by immersion in dilute HNO_3. The CV experiments were conducted in a quiescent solution, without purging. Initially, three scan rates were evaluated: 10, 20, 50 and 100 mV s^{-1}. However, the peaks in the CV spectra became more distinct at 50 mV s^{-1}, thus this scan rate was further used.

iv) Thickness

The thicknesses of each coating were calculated from Faradays law using equation:

$$t \ = \ \frac{E \times i \times CCE \times \Delta T}{d \times F} \tag{3.3}$$

Where 't' is the thickness of the deposit, E is an electrodeposit coating equivalent, *i* is a film deposition c.d., CCE is a current efficiency, ΔT is a time interval, and 'd' is the density of the deposit and F is Faradays constant. The validity of measured thickness was verified using digital Thickness Tester also.

v) Corrosion cell

All corrosion studies reported in this thesis were carried out in 1.0 HCl solution, as representative aggressive corrosion medium) maintained at 303 K prepared in distilled water contained in a three electrode configuration cell (250 ml) having working electrode, counter electrode and reference electrode. The cell is designed in such a way that anode and cathode can be fixed parallel to each other at 4 cm distance. SCE electrode

was used as the reference electrode. The Luggins tube was used measure the potential at the surface of specimen through the agar-agar-KCl salt bridge. In all electrochemical studies the electroplated copper panels was used as the working electrode. Potentiodynamic polarization studies were performed at a scan rate of 1.0 mV s^{-1} in a potential ramp of $\pm$ 0.25V around open circuit potential (OCP). The experimental setup used for corrosion study is shown in Fig. 3.3. The corrosion data, like corrosion current density (i_{corr}), corrosion potential (E_{corr}) and corrosion rate (CR) in millimeter per year (mm y^{-1}) were determined by Tafel's extrapolation method. The CR of coatings, expressed in mm y^{-1} was calculated using equation 3.4, given below
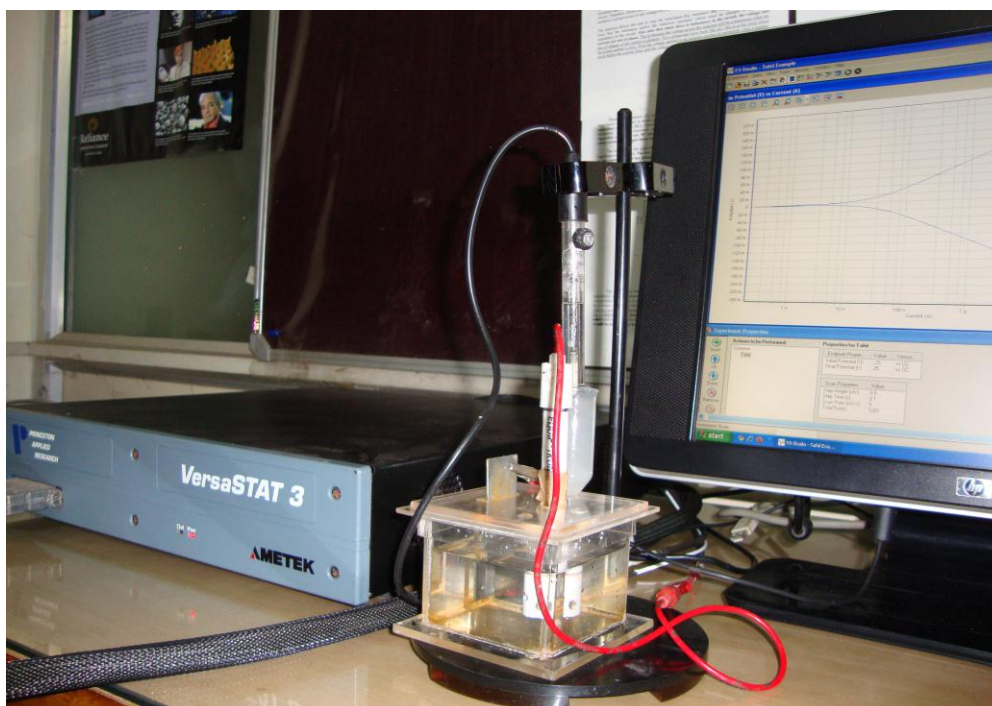
Fig. 3.3. Experimental setup used for the corrosion study of electroplated mutual alloys of iron group metal

$$CR = 0.129 \times i_{\text{corr}} \frac{\text{E}}{\text{D}} \qquad (3.4)$$

Where, E is gram equivalent weight and D is density in g cm^{-3}.

The electrochemical impedance spectroscopy (EIS) studies have been made in the frequency range from 100 kHz to 10 mHz, using ±10 mV perturbing voltage. Possible corrosion mechanism in multilayer coating has been identified by acid drop test, followed by SEM analysis. The corrosion protection efficacies of multilayer alloys have been analyzed in terms of their double layer capacitance and dielectric properties.

ELECTRODEPOSITION OF MONOLAYER Fe-Ni ALLOY COATINGS AND THEIR CHARACTERIZATION

4.1 INTRODUCTION

Development of new materials and understanding their surface and functional properties are at the root of progress of material science. This is particularly true for development of new magnetic materials for variety of their applications. In this regard, the deposition of binary alloys of Fe-group metals, namely Fe-Ni, Fe-Co and Ni-Co by electrochemical reduction in aqueous solutions has long been a subject of scientific and technological interest with the earliest studies dating back to the beginning of last century (Matlosz 1993). The solid state properties of these alloys which received considerable attention are their magnetic properties and excellent corrosion resistance. They are used primarily as soft magnetic materials in the area of high-speed random-access memories (RAM) of computers (Štefec 1973). The relationships among the plating variables of Fe-Ni alloys are found to be further complicated by nature of co-deposition which is observed in all mutual alloys of Fe-group metals.

The co-deposition of mutual alloys of Fe-group metals exhibits peculiar phenomenon of 'anomalous co-deposition'. This term introduced by Brenner is being used to describe the preferential deposition of the less noble metal, Fe to the more noble metal, Ni (Brenner 1967). In other words, the reduction of Ni is inhibited while the deposition of iron is enhanced when compared to their individual deposition rates. Hence, electrodeposition of Fe-Ni alloys has attracted considerable attention due to their special characteristic nature and wide range of unique properties. The phase structures of these alloys have been analyzed by electrochemical techniques, such as galvanostatic and

potentiostatic methods, and more often by anodic linear sweep voltammetry (Despic et al. 1995). The literature pertaining to electrodeposition of mutual alloys of Fe group metals is rather exhaustive, and many serious research works have been reported (Despic et al. 1995, Ricq et al. 2001, Bento and Mascaro 2002, Jartych 2002, Myung and Nobe 2001). It has been identified that Fe- group metal alloy solid solutions produced by electrodeposition technique exhibits both face centered cubic (fcc) and body centered cubic (bcc) structures. These alloys were found to exhibit many useful properties such as high internal strength, hardness, high corrosion resistance and unusual magnetic properties. Many magnetic alloys with different compositions were widely employed for various purposes. Ferromagnetic alloys, like Fe-Co and Fe-Ni are few among many. They received considerable attention for their applications in modern industries, such as in rockets, computers, space technology, etc. However, data on magnetic properties and corrosion resistance of electroplated Fe-Ni alloys are difficult to correlate due to complexicity involved in plating conditions and associated peculiar anomalous codeposition. Hence, it is difficult to distinguish between the factors that significantly affect them (Leith et al 1999, Bockris JO´M et al. 2000). Thus it is hard to develop Fe-Ni coatings of desired properties from aqueous electrolyte. In other words, the magnetic properties and corrosion behaviors of Fe-Ni alloy deposited from each bath is unique, in terms of the bath composition and operating parameters.

This chapter presents the results of investigation on optimization of deposition conditions for monolayer Fe-Ni coatings on copper using D.C. (without modulation in current pulse). The effect of current density (c.d.) on surface structures, magnetic properties and corrosion behaviors of the coatings has been studied and results are discussed.

4.2 OPTIMIZATION OF Fe-Ni ALLOY BATH

The optimal composition and operating parameters of the bath was arrived by standard Hull cell method, and is given in Table 4.1. Variety of Fe-Ni coatings having different composition formed on Hull cell panel indicated that c.d. plays an important

role on plating process. While overcoming the practical difficulties in developing a stable electrolytic bath for deposition of binary magnetic Fe-Ni alloy, boric acid (BA) and ascorbic acid (AA) were used, as stabilizers. A drastic increase in pH of the electrolytic bath was found after plating. Hence, BA was used as buffer; preventing the increase of pH after each deposition. A chemically stable bath was achieved by adding AA, as antioxidant to prevent oxidation of Fe^{2+} into Fe^{3+} ions. Sulphanilic acid (SA) was used as brightener, to impart mirror finish to the coating. The bath constituents and operating parameter under optimal conditions are given in Table 4.1. The deposit over the wide c.d. range of the Hull cell panel was found to be bright, i.e. in the range of 1.0-8.0 A dm^{-2}. The Fe-Ni alloys having varied compositions were developed at different c.d.'s, keeping anode and cathode parallel to each other. The effect of c.d. on wt. % of Ni, hardness, and crystallite grain size of the coatings are discussed in the following sections.

Table 4.1. The composition and operating parameters of optimal bath for deposition of bright Fe-Ni alloy on copper

Bath ingredients	Concentration (g L$^{-1)}$	Purpose	Operating parameters
$FeSO_4.7H_2O$	16	Metal salt	c.d. : 1.0-8.0 A dm^{-2}
$NiSO_4. 6H_2O$	100	Metal salt	pH: 3.5
H_3BO_3	30	Buffer	Temperature: 303K
L-Ascorbic acid	8.0	Antioxidant	Anode: Pure nickel
Sulphanilic acid	1.0	Brightener	

All depositions were accomplished galvanostatically on copper at different c.d.'s from optimal using DC power source (N 6705A, Agilent Technologies, USA). The pH of bath solution before and after every deposition was measured, and the change of pH was noted. Solution pH was adjusted to 3.5, using either H_2SO_4 or NaOH. The polished copper panel after deposition was rinsed with distilled water, and then air dried. The

thickness of each coating was calculated from the weight of deposit using Faraday's law. The hardness of the deposit was measured by Vickers method using Micro-Hardness Meter.

Magnetic properties of the Fe-Ni films were measured by a vibrating sample magnetometer (VSM) (ADE-DMS, EV-7). The VSM was calibrated using the standard calibration sample of nickel with 99.99% purity. The calibration was done at an applied magnetic field of 15,000 Oe, and a temperature of 293K. Hysteresis loops were generated using a sweep time of 20 minutes and a maximum field of 15000 Oe. The dimensions of the Fe-Ni coating samples used in the VSM measurements are 5 mm × 5 mm. The corrosion behaviors of coatings were evaluated in 1M HCl using Potentiostat/Galvanostat (VersaSTAT3, Princeton Applied Research) by electrochemical impedance followed by potentiodynamic polarization method. A three-electrode set-up was used for corrosion study, described elsewhere (Jones 1996). A saturated calomel electrode (SCE) was used as the reference electrode. The potentiodynamic polarization curve of E vs. Log I was obtained at 1 mVs^{-1} scan rate. The corrosion c.d. (i_{cor}) was measured by Tafel extrapolation method. The corrosion c.d. (i_{cor}) was obtained from Tafel constants (b_c, the cathodic constant and b_a, the anodic constant) were obtained by Tafel's extrapolation method. Before the measurements, the sample was put into the electrochemical cell and was allowed to reach stationary potential, which usually took approximately 60 seconds. EIS signals were recorded using AC signal of 10 mV amplitude, at a frequency range from 10 mHz - 100 kHz. Surface morphology and composition of Fe-Ni alloy coatings were examined by Scanning Electron Microscopy (SEM), interfaced with Energy Dispersive X-ray (EDX) Analyzer facility (JSM-6380 LA from JEOL, Japan). The phase structures of the coatings were identified by XRD (JEOL JDX-8P), using Cu Kα (λ=1.5406 Å) radiation in continuous scan mode at scan rate of 2°min^{-1}. The grain size was evaluated using Scherrer formula, D=Kλ/βcosθ, where *D* is crystalline size, *K* is constant, λ is incident wavelength, β is full width at half maximum intensity and θ is Braggs angle.

4.3 RESULTS AND DISCUSSION

4.3.1 Cyclic voltammetry study

The cyclic voltammetry (CV) is an extremely useful technique as it can provide useful information about redox reactions in a form which is easily obtained and interpreted. Hence CV technique was used to identify the role of additives in codeposition of Fe-Ni alloy and to analyze the reduction and oxidation peaks. Cyclic voltammogram was obtained using platinum (Pt) as working electrode, pH = 3.5 at scan rate υ = 10 mVs^{-1}in presence and absence of additives, as shown in the Fig. 4.1. Preliminary electrochemical study was carried out using optimal bath having only the additives (without metal ions). The shape of the voltammogram revealed that additives are electrochemically inactive. The CV corresponding to only metal ions demonstrated that the deposition of Fe and Ni proceeds along with the hydrogen evolution reaction. The oxidation peak is found to be shaped by the current contributions of oxidation of both Fe and Ni.
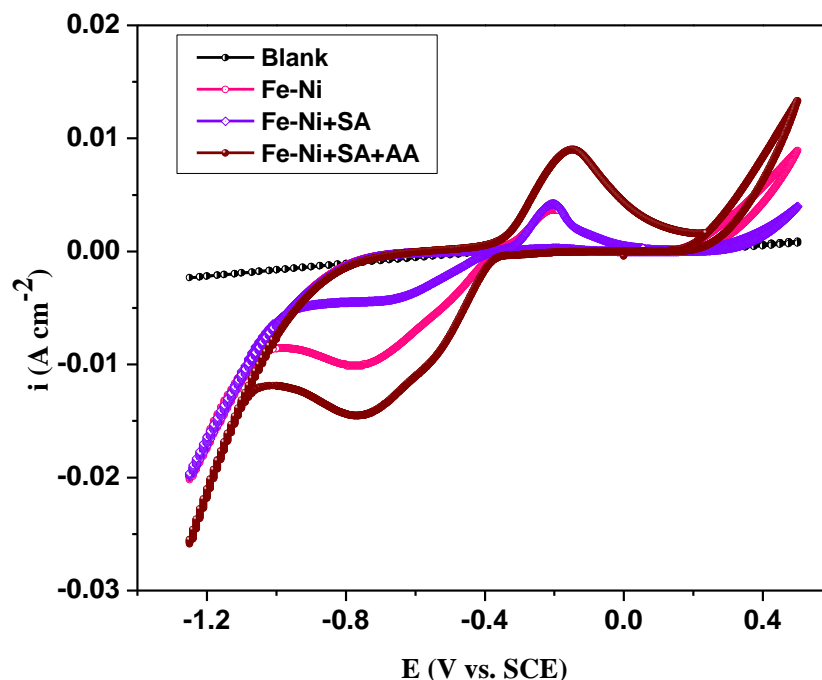
Fig. 4.1. Cyclic voltammograms for Fe-Ni bath demonstrating the effect of AA and SA

Drastic change in cathodic current due addition of SA may be rationalized by the combined effect of i) increased mass-transfer process and ii) decreased hydrogen evolution. These factors amounted to the under potential deposition (UPD) of Fe-Ni alloy having more wt. % Ni with better appearance.

Further, the addition of AA was found to increase the cathodic current due to increase in mass transfer of deposition process. Similarly, peak anodic current was found to increase drastically, indicating the dissolution of alloy with different composition. Thus, the constancy of peak cathodic potential on addition of SA and AA indicated that the composition of Fe-Ni alloy is dictated by the mass transfer process, not by kinetics of deposition, supported by the shape of voltammograms. Consequently, deposition of bright and uniform Fe-Ni alloy became possible due to favored the mass transfer process by reducing the hydrogen evolution at cathode. Therefore, the improved appearance of the coating is due to increase in wt. % of Ni, or due to decrease in hydrogen evolution, explained by hydroxide suppression mechanism.

4.3.2 Effect of c.d.

i) Wt. % of Ni in the deposit

The composition of electroplated Fe-Ni alloys may be described by the percentage of one alloy component, e.g., nickel, plotted against the relative percentage of the respective metal ions, i.e., Ni^{2+} in the plating bath (Štefec 1973). It should be noted that in the present Fe-Ni alloy bath given in Table 4.1, the wt. % of Ni and Fe in the bath are found to be respectively, 88 % and 12 %. Neglecting the deviation at very low c.d., an increase of Ni wt. % in the deposit with increasing applied c.d. was observed. This is supported by deposition principle of mutual alloys of Fe-group metals that an increase in the c.d. or temperature results in an increase of more noble metal in the deposit. The variation in the wt. % of Ni in the deposit with c.d., shown in Fig. 4.2, revealed that under no conditions of c.d., wt. % of Ni in the deposit has reached the bath composition. i.e., the wt. % of Ni in the deposit was found to be always less than that in the bath. Hence it

may be inferred that the proposed bath follows anomalous type of deposition at all conditions of c.d. employed in this study.
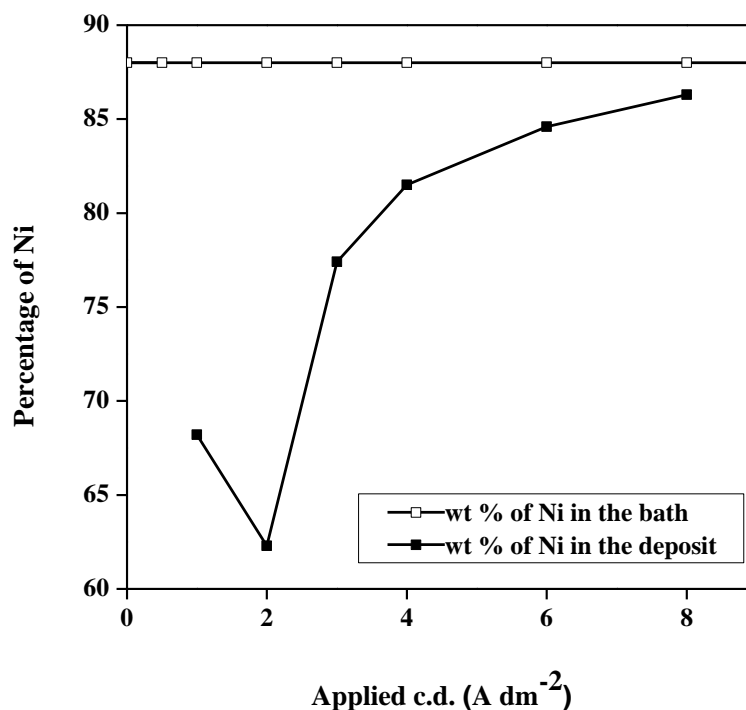
Fig. 4.2. Variation in wt. % of Ni in the deposit with applied c.d., deposited from optimal Fe-Ni bath at 303 K and pH= 3.0

Further, it was observed that at c.d. greater than 2.0 A dm^{-2}, the wt. % of Ni in the deposit was found to increase with c.d. At 4.0 A dm^{-2}, the bath produced a sound and bright deposit having ~ 81.5 wt. % of Ni. This increase in Ni content with c.d. (Fig. 4.2) indicates that the deposition process is tending towards normal type. But at low c.d. (< 2.0 A dm^{-2}) the bath exhibited the opposite trend, i.e., it decreased with increase in c.d., as shown in Fig. 4.2. This is due to the tendency of bath to co-deposit in anomalous type than normal type, as envisaged by Brenner (Brenner 1967). This observation at low c.d. and elevated temperature are characteristic of all mutual alloys of Fe-group metals due to drastic change in mass transport process during deposition.

ii) *Partial c.d. and cathode current efficiency*

The partial current density for single metal deposition, namely, Fe and Ni from sulfate bath at various applied c.d.'s are shown in Fig.4.3. The partial current density of hydrogen is determined as the difference of the metal current from the total applied current (Hegde et al. 2010). In the range of c.d.'s employed, the hydrogen side reaction dominates the deposition.
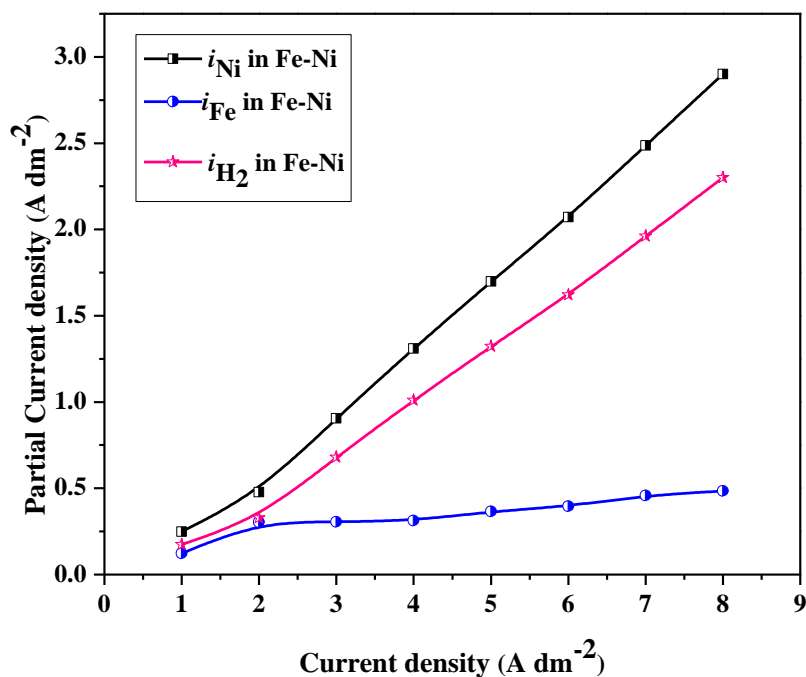
Fig. 4.3. The variation of partial current densities of Fe, Ni and H_2 with applied c.d.

Large overpotentials are required for significant Fe or Ni deposition, and hence the Fe and Ni partial current densities increase with applied c.d.'s. These results are compliance with increased of cathode current efficiency (CCE) shown in Table 4.2. The increase of partial current density of Fe and Ni with applied c.d. has resulted in increase in CCE of the bath. The effect of c.d. on the appearance and corrosion resistance of the Fe-Ni alloy was studied. The CCE was calculated from the mass gained, the charge passed and the chemical composition of the deposit.

Table 4.2. Effect of c.d. on deposit characters of monolithic Fe-Ni alloy deposited at 303K

c.d. ($A\ dm^{-2}$)	CCE (%)	Deposit Thickness (μm)
1.0	78	1.56
2.0	79	3.31
3.0	81	4.94
4.0	82	6.76
6.0	83	10.25
8.0	85	14.05

iii)Thickness of deposit

The applied c.d. was found to show direct dependency on thickness of deposit as evidenced by the data given in Table 4.2. The observed dependency of thickness with c.d. may be due to the adsorbed metal hydroxide (alkalization), caused by the steady increase in pH due to hydrogen evolution.

iv)Adhesion

The adherence of Fe-Ni alloy coatings at different c.d. was tested. It was found that all coatings except at high c.d., the coatings are bright, hard and adherent on Adhesion Testing. They were found to be completely smooth cut edges and none of the squares of the deposit is detached from the substrate indicating that coating at the optimal condition has excellent adhesion.

v) Effect of pH

The pH of the bath was varied from 2.0 to 5.0. However, the appearance and stability of the bath was found to be unchanged with pH up to 3.5. However above pH = 4.0 the bath was found to be unstable due to precipitation.

4.3.3 Surface morphology

The effect of c.d. on the surface morphology of coatings was studied by Scanning Electron Microscopy (SEM). The microstructure of the coatings deposited at different c.d.'s is shown in Fig. 4.4. It should be noted that the surface morphology of electroplated Fe-Ni coating is greatly influenced by c.d. employed. Sanaty et al. observed that increasing the iron content in the deposit decreases the grain size (2009).
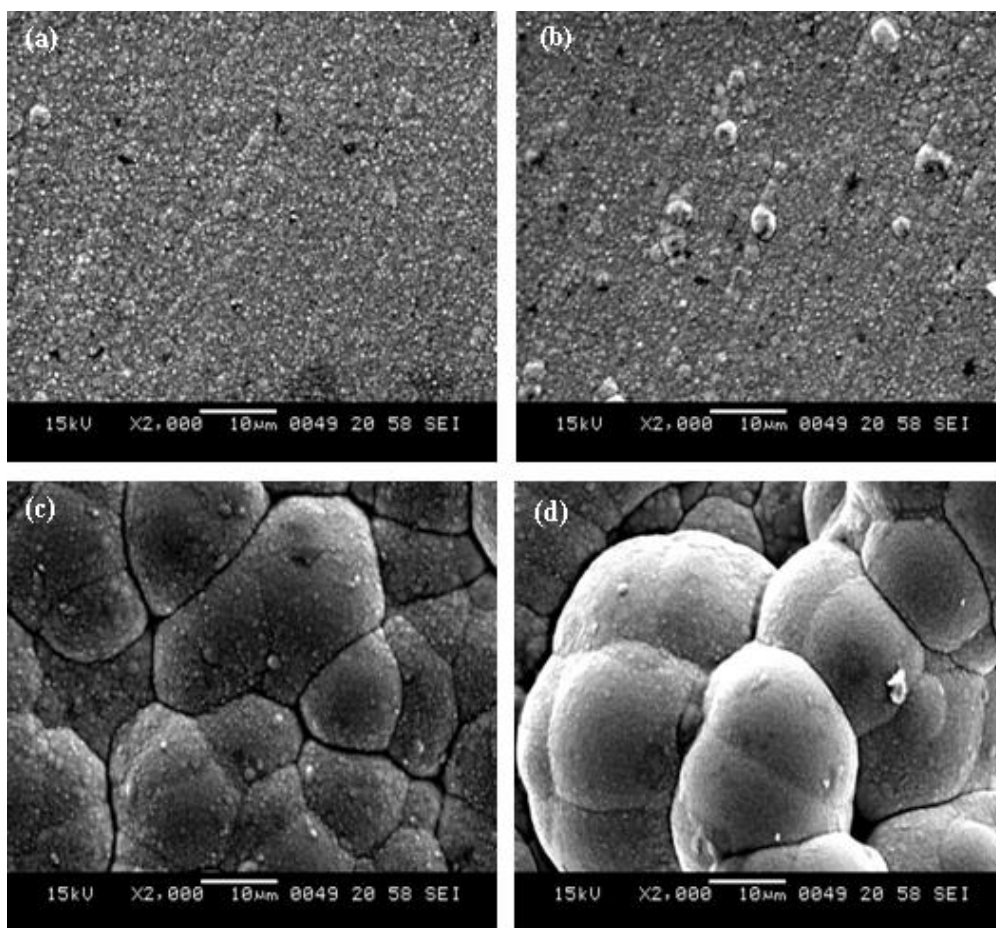
Fig. 4.4. SEM micrographs Fe-Ni coatings deposited from optimized bath at (a) 2.0 A dm^{-2} (b) 4.0 A dm^{-2} (c) 6.0 A dm^{-2} (d) 8.0 A dm^{-2}

Generally, crystallization occurs either by the buildup of old crystals, or by the formation and growth of new ones. These two processes are in competition with each other, and are influenced by different factors. Low surface diffusion rates, high population of adatoms and high over-potentials are factors responsible for creation of

new nuclei (Ebrahim and Li 2003). Hence, at low c.d. the deposit was found to be very smooth and uniform as shown in Fig. 4.4(a). It was observed from Fig. 4.4, as the c.d. increased the grain size also increased. At very high c.d. (8.0 A dm^{-2}) the deposit was found to be very porous, with globular structure. It may be due to high wt. % of nobler Ni in the deposit, caused by reduced inhibitory action of hydroxyl ions.

4.3.4 Phase structure

The crystal orientation of electrodeposited Fe-Ni alloys with different compositions can be characterized by means of XRD analysis. The identification of phase structure of the deposits was made from the peak profiles of the X-ray reflection plotted as a function of 2θ, as shown in Fig. 4.5. XRD signals of Fe-Ni coating at 2.0 A dm^{-2} showed single phase bcc related to Fe crystal structure. As cathode c.d. increased, the wt. % of Ni in the deposit increased. Accordingly an increase in fcc phase structures corresponding to increased Ni content was observed.
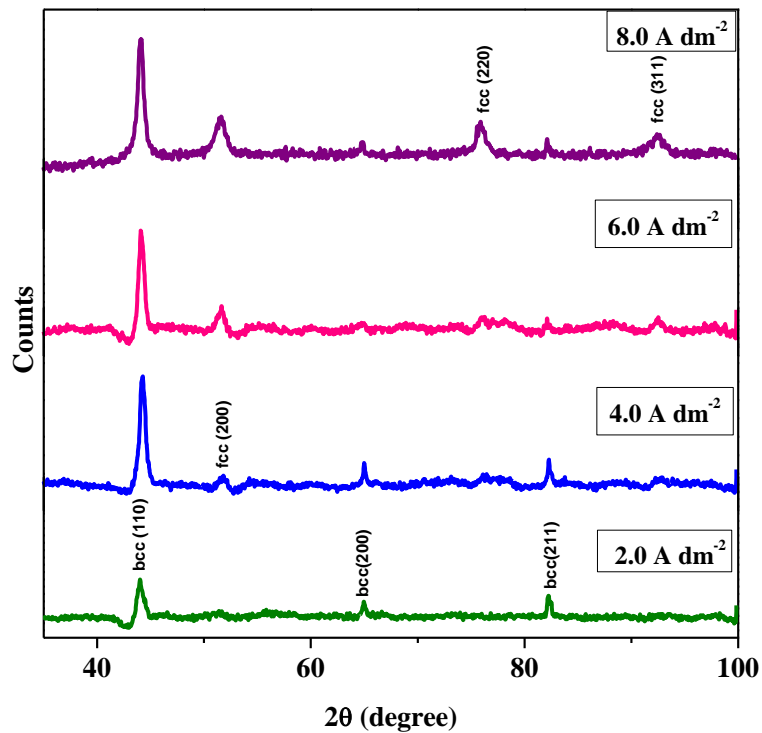
Fig. 4.5. X-ray diffraction patterns of Fe-Ni alloy deposited at different c.d.'s, from the optimized bath at 303K

At 4.0 A dm^{-2}, the alloy consisting of both bcc and fcc crystal structures was formed as confirmed by related pattern. Since the Ni peak pattern coincides with the peak pattern of FeNi$_3$, the existence of inter-metallic FeNi$_3$ structure is quite evidenced. This is further supported by study on nanocrystalline Ni-Fe alloy (Li and Ebrahimi 2003). Accordingly there exists a larger probability of formation of an ordered FeNi$_3$ intermetallic structure due to faster grain boundary diffusion. To know the preferred orientation of the deposit in detail, the texture coefficient (T$_C$) value was employed. Based on the relative intensities of the bcc and fcc peaks, it is possible to find the T$_C$ value of Fe-Ni electrodeposit using XRD data. The method developed by Be'rube' and L'Esperance has been used for calculating the value of T$_C$, and is given by following equation.

$$T_C(hkl) = \frac{I(hkl)}{I_0(hkl)} \times \frac{\sum I_0(hkl)}{\sum I(hkl)} \tag{4.1}$$

where *I(hkl)* is the peak intensity of Fe-Ni electrodeposits and *ΣI(hkl)* is the sum of intensity of all the diffraction peaks. The index 0 refers to the intensities of the peaks of standard Fe-Ni sample. If the T$_C$ is greater than 1.0, it indicates the existence of preferred orientation. It may be noted that volume fraction of bcc is found to be higher than that of fcc at low c.d. As the c.d. increased fcc phase predominated over the bcc phase.

Fig. 4.6 (a) and 4.6 (b) shows the relationship between the applied c.d. and the T$_C$ of bcc and fcc phases respectively. In the bcc phase, the T$_C$ values for the (200) and (211) orientations are greater than unity. It indicates that the preferred orientation of the deposit at low c.d. is of dual fibre texture, i.e., (200) and (211). However at 4.0 A dm^{-2}, (211) fibre texture decreased and disappeared altogether at high c.d. side. On the other hand, in the fcc phase, (111) fibre texture predominates. On further increasing the c.d., the preferred orientation of the fcc phase changed sharply from (111) to the (220). Thus from the XRD patterns and the T$_C$ values, it may be concluded that at low c.d., the volume fraction of bcc is greater than that of fcc with predominance of (200) and (211)

91

fibre texture. Hence as c.d. increased, the volume fraction of fcc increased. Therefore fcc (220) fibre texture developed strongly as shown in Fig. 4.6 (b).
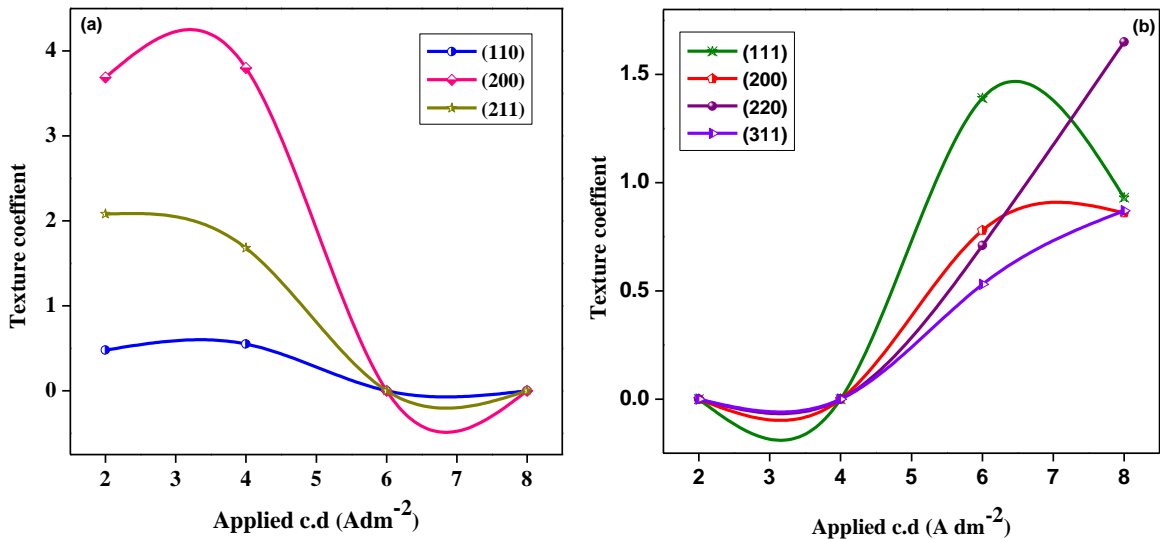
Fig. 4.6. Variation of texture coefficient, T_C of electrodeposited Ni-Fe alloy with applied c.d. of (a) bcc phase, and (b) fcc phase

4.3.5 Micro hardness

The micro-hardness of Fe-Ni alloy deposited from the proposed bath was found to increase with the c.d. employed for its deposition. As seen in Fig. 4.7, there was an increase in hardness with c.d., i.e. with decrease in Fe content.

This is in contradiction of the results reported in the literature (Li and Ebrahimi 2003), wherein an increase in hardness was observed with increase in Fe content. McCrea et al observed a moderate decrease in hardness with increasing Fe content in the fcc range; and a significant increase with Fe content in the bcc range (2003). However, Cheung et al. showed that the hardness of Fe-Ni alloy increased with Fe content up to 16.5 %, and then decreased (Cheung et al. 1995). Therefore at higher c.d., the coating

with intermetallic $FeNi_3$ phase structure has formed, evidenced by XRD analysis and is responsible for overall hardness of the electrodeposits.
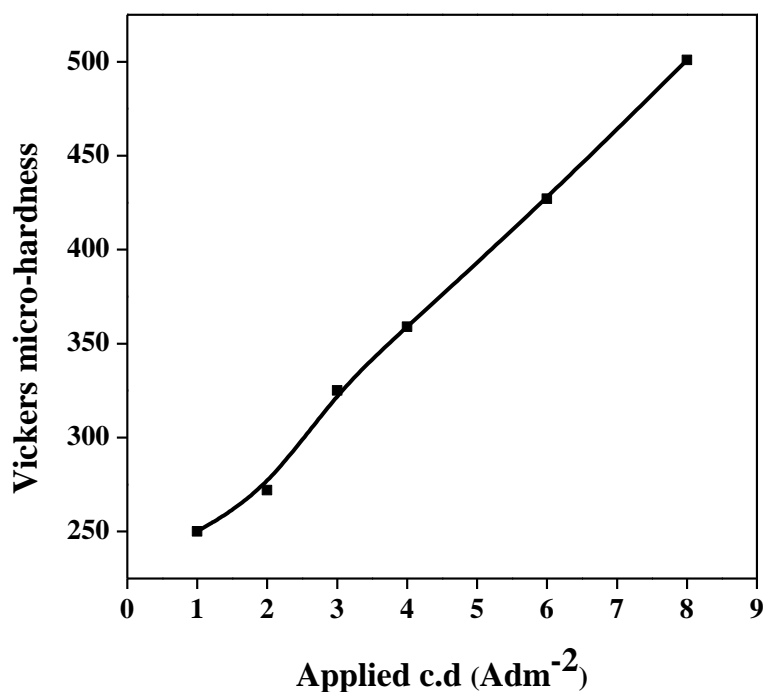
Fig.4.7. Variation of micro-hardness of Fe-Ni coatings deposited at different applied c.d., as function of Fe content in the alloy

4.3.6 Magnetic property

It is well known that the magnetic properties of electroplated materials depend on the chemical composition and grain size (Suryanarayana 1995). The magnetic properties of Fe-Ni coated films were measured at room temperature using VSM. The hysteresis curve of Fe-Ni films are shown in Fig. 4.8. It was found that the Fe-Ni alloys exhibit ferromagnetic property, but no super-paramagnetic phenomenon was observed. The saturation magnetization, M_s and coercivity, H_c of Ni-Fe deposits at different c.d.'s are given in Table 4.3.

Table 4.3. Variation of saturation magnetization, M_s and coercivity, H_c of electrodeposited Fe-Ni alloy with applied c.d.

Applied c.d. $(A\ dm^{-2})$	M_s $(emu\ g^{-1})$	H_c (Oe)
2.0	3.51	17.60
4.0	6.16	15.95
6.0	8.13	15.00
8.0	9.50	14.00

The observed decrease of M_s, and an increase of H_c with deposition c.d. may be explained as follows: Bulk Fe and bulk Ni are known to be ferromagnetic with M_s value equal to 220 emu g^{-1} and 55 emu g^{-1} respectively. The decrease of M_s with increase in c.d. is due to decrease of grain size from bulk to nano. It is known that M_s is dependent on the number of magnetic molecules in a single magnetic domain, and hence it is proportional to the size of the material (Wu and Chen 2003).

Generally, the M_s value increases with Fe content in the deposit (Myung and Nobe 2001). The most striking feature here is that with the increase in Fe content, the M_s value is found to decrease. Moreover, the presence of $FeNi_3$ super lattice phase contributed to the magnetization (Štefec1973). Further, the coercivity value is found to decrease constantly with c.d. as reported in Table 4.3. Generally, smaller grain size contributes to an increased value of coercivity (Liu et al. 2006). In the present study, the coercivity can also be linked to the phase structure of the alloys. As seen in XRD study, phase transformation from bcc to fcc occurred with an increase in applied c.d. Ibro and co-workers have found that materials with single bcc phase show high coercivity (Tabakovic et al. 2000). Hence at 2.0 A dm^{-2}, bcc phase was dominated leading to a high coercivity. As the c.d. increased to 4.0 A dm^{-2}, along with bcc phase the alloy exhibited a slight fcc phase. In other words, there was a formation of mixed phase which leads to reduction in coercivity.
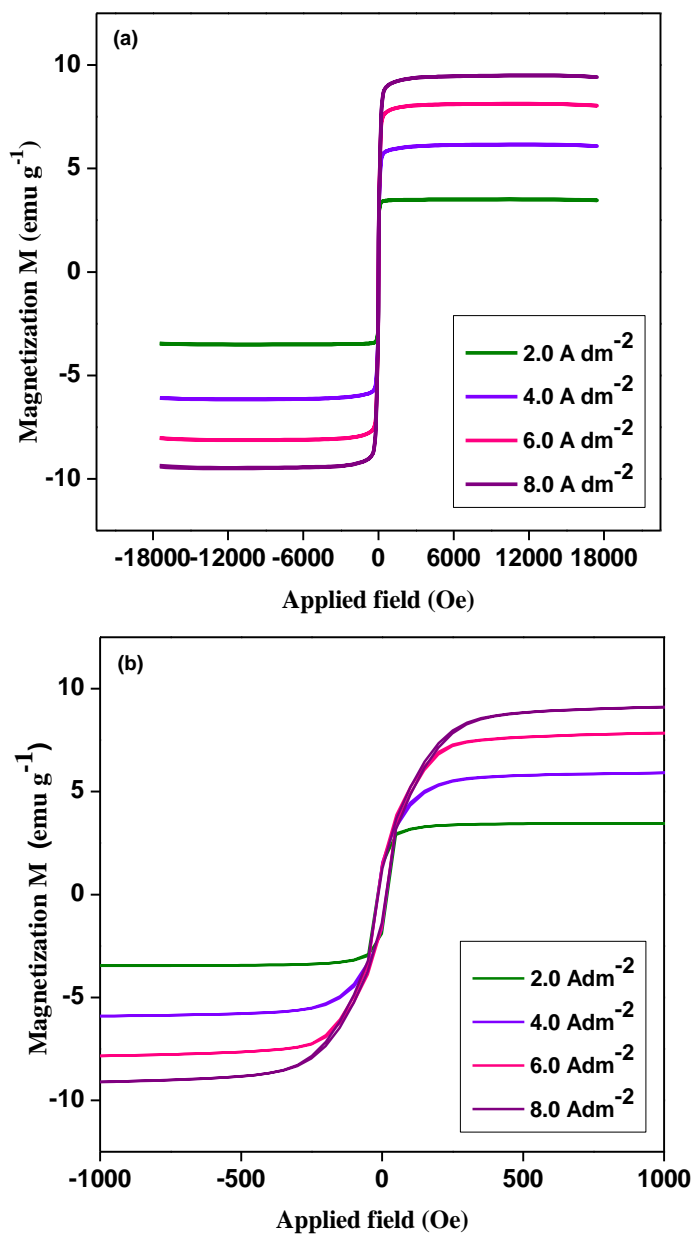
Fig. 4.8. (a) Magnetization curve of Ni-Fe coatings deposited at different applied c.d.'s and (b) enlarged view at close proximity of applied magnetic field
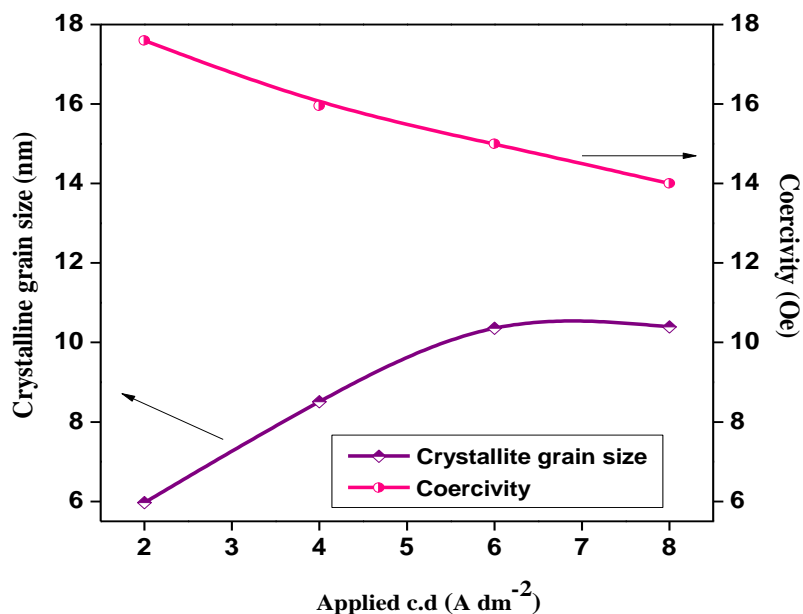
Fig. 4.9. Variation of crystalline grain size and coercivity of electrodeposited Fe-Ni alloy over range of applied c.d.

At higher c.d. there exists a complete transition of bcc to fcc phase, consequently the coercivity decreased. The variation of crystallite grain size and coercivity of the electrodeposited of Fe-Ni alloy coatings with applied c.d.'s are shown in Fig. 4.9.

It may be observed that crystallite grain size and coercivity show almost inverse dependence with each other over the range of applied c.d. studied, in compliance with discussion made earlier.

4.3.7 Potentiodynamic polarization study

The corrosion behaviors of electrodeposited Fe-Ni coatings have been evaluated by potentiodynamic polarization method. The corrosion rates (CR) were calculated by Tafel's extrapolation method. Tafel behavior of the coatings at different c.d., like 2.0, 3.0, 4.0, 6.0 and 8.0 A dm^{-2} is shown in Fig.4.10, and corresponding corrosion data are reported in Table 4.4.
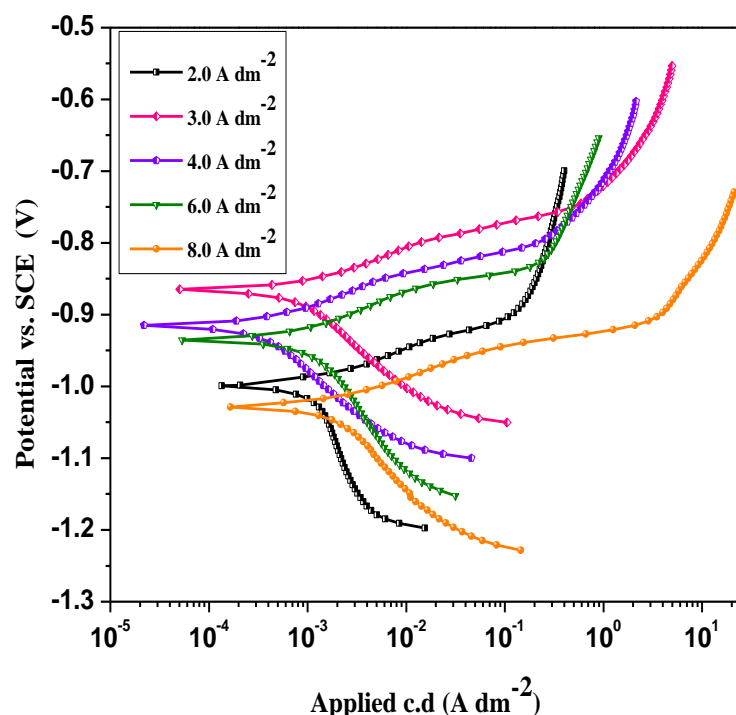
Fig. 4.10. Potentiodynamic polarization behavior of Fe-Ni coatings at different c.d.s, deposited from optimal bath at 303K

It should be noted that Fe-Ni alloys deposited at different c.d.'s are characterized by high E_{corr}, and the passivity regime begins at less negative potentials. Further, the CR decreased with an increase of c.d., as a function of changed phase structure of the deposits. It is observed that Fe-Ni coating, at 4.0 A dm^{-2} exhibits least CR (7.40 mm y^{-1}) due to characteristic phase structure of the deposit.

The XRD signal corresponding to the coating deposited at 4.0 A dm^{-2} in Fig 4.5 shows an intermediate transitional phase from bcc to fcc. During this transition, the Fe content tends to decrease and Ni content tends to increase. Ni being nobler compared to Fe, a decrease of corrosion rate was observed. But, further increase of c.d. resulted in decrease of CR as shown in Table 4.4. This is attributed to high porosity of the coatings

due to FeNi$_3$ phase, consequent to increased Ni content. This is in compliance with the surface morphology of Fe-Ni coatings as shown in Fig. 4.4.

Table 4.4. Corrosion parameters of Fe-Ni alloy coating deposited from the optimized bath at different c.d.s

c.d. (A dm^{-2})	-E_{corr} (V vs. SCE)	i_{corr} (μA cm^{-2})	CR (mm y^{-1})
1.0	1.055	1644.5	18.49
2.0	0.995	1046.9	11.77
3.0	0.865	860.7	9.68
4.0	0.913	650.3	7.40
5.0	0.833	942.6	10.73
6.0	0.934	1080.1	12.13
7.0	1.077	1339.2	15.06
8.0	1.027	1458.4	16.40

4.3.8 Electrochemical impedance spectroscopy

Electrochemical impedance spectroscopy (EIS) is a useful experimental tool to characterize frequency response of a device. The measurement proceeds by applying a low amplitude alternating voltage ΔV to a steady-state potential Vs, with $\Delta V (\omega) = \Delta V_{max}e^{j\omega t}$, where j= -1, ω is the pulsation (angular frequency) and ΔV_{max} the signal amplitude. This input signal leads to a sinusoidal output current ΔI, with $\Delta I(\omega) = \Delta I_{max}e^{j(\omega t+\phi)}$ where ϕ is the phase angle of the current versus the voltage and ΔI_{max} the signal amplitude. The electrochemical impedance $Z(\omega)$ is defined as $Z (\omega) = \Delta V/\Delta I = |Z(\omega)| e^{-j\phi}=Z'+ jZ''$, where Z' and Z'' are respectively the real part and the imaginary part of the impedance, defined as $Z'^2+ Z''^2=|Z(\omega)|^2$. Experimental data extracted from this

measurement are usually plotted in a Nyquist diagram which represents the imaginary part of the impedance versus the real part over a particular frequency range.
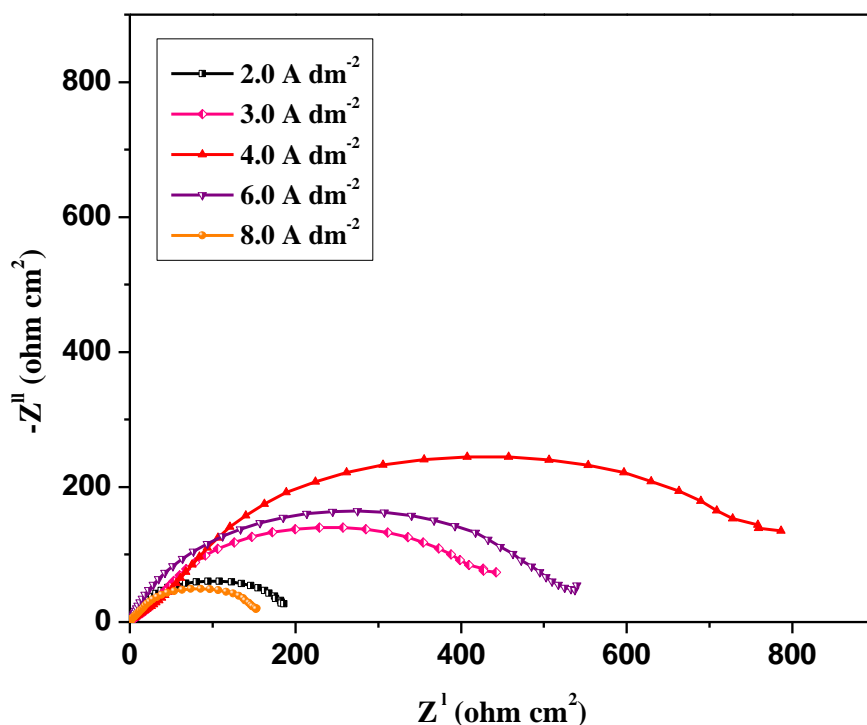
Fig. 4.11. Nyquist plots of Fe-Ni alloy coatings (monolayer) obtained at different current densities, from optimal bat at 303K

The corrosion behaviors of the coatings were studied in 1 M HC by EIS method. Measurements were carried out at frequency range from 100 kHz to 0.01 Hz at open circuit potential. The Nyquist representations of the impedance of the coatings developed under different cathode c.d.'s are shown in Fig. 4.11.

The observed single semi circle in impedance response indicates that single charge transfer process is involved during dissolution of coatings. Deviation of perfect circular shape is often referred to the frequency dispersion of interfacial impedance. This

anomalous behavior is generally attributed to the inhomogeneity of the metal surface arising from surface roughness or interfacial phenomena. Generally, at higher frequencies the interception of real axis is ascribed to the solution resistance (R_s) and at the lower frequencies, the interception with real axis is ascribed to the charge transfer resistance (R_{ct}).
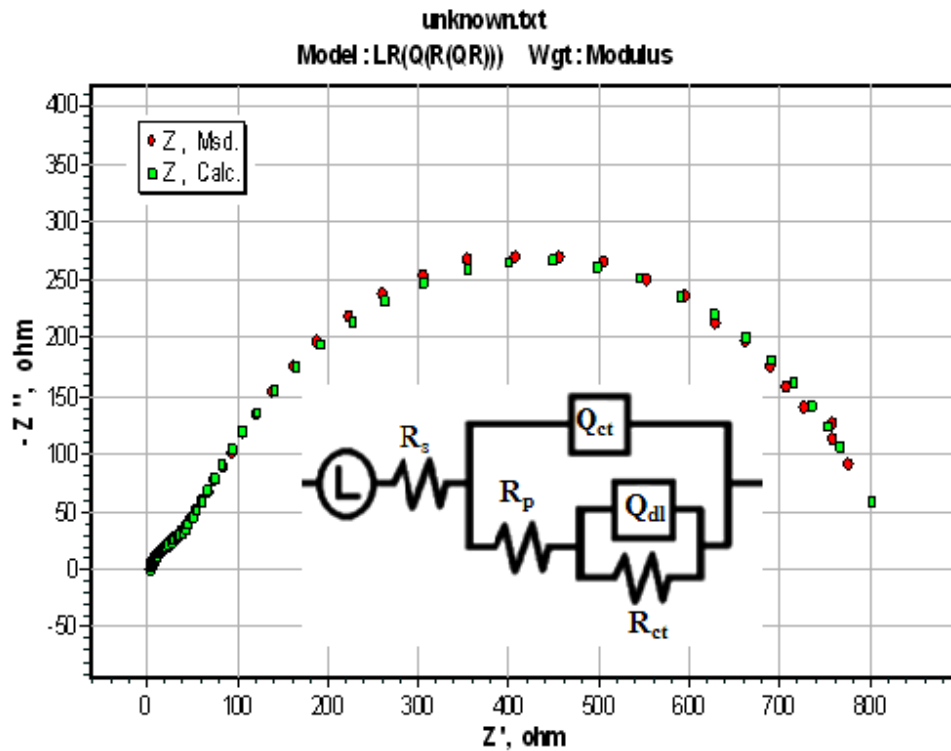
Fig. 4.12. Equivalent circuit {LR(Q(R)(QR))} with best fitment for monolithic Fe-Ni alloy, at optimized c.d. = 4.0 A dm^{-2} (using ZsimpWin software)

Hence, in Fig. 4.11 it may noted that R_{ct} value increased as the deposition c.d. increases from 2.0 A dm^{-2} to 4.0 A dm^{-2} then decreased. This shows that the Fe-Ni alloy deposited at 4 A dm^{-2} is found to have high corrosion resistance compared to all coatings at other c.d.'s. The best corrosion protection of the coating corresponding to optimal c.d. is due to increased capacitive reactance, X_c (or less electrical conductivity) caused by less capacitance of electrical double layer, Q_{dl}.

An equivalent circuit corresponding to monolayer Fe-Ni alloy, shown in Fig. 4.12 was used for simulation of the impedance data. The circuit consists of double layer capacitance (Q_{dl}), which is parallel to charge transfer resistance (R_{ct}); both of which are in parallel with coating capacitance (Q_{ct}) and charge transfer resistance for the porosity of the coating (R_p). As same experimental set up was used for impedance study, the value of R_s was considered to be constant. When the coated sample is immersed in the electrolyte, the corrosion is expected to initiate rapidly at the pores present in the coating because of low coating thickness. This leads to the formation of localized galvanic cells, which dominate the galvanic corrosion process. In such cases, electrochemical interface can be divided into two interfaces: electrolyte/coating and electrolyte/substrate.

The impedance profile shown in Fig. 4.12 can be described by transfer functions, corresponding to the proposed equivalent circuit (shown in inset). The optimum numerical values of the equivalent circuit parameters are listed in Table 4.5. The constant phase element (CPE) must be introduced in the equivalent circuit to account for frequency dispersion originating from heterogeneity or roughness of the electrode surface. The double layer capacitance, C_{dl} then should be substituted by the CPE whose impedance, Z_{CPE} may be described (Macdonald 1987) as:

$$Z_{CPE} = 1/[\, Y_0 \,(jw)^n\,] \tag{4.1}$$

Where Y_0 is the magnitude of the CPE, n is the exponent (phase shift), ω is the angular frequency and j is the imaginary unit, 'n' is a constant, called exponent ($-1 < n < 1$). When n =1, a purely capacitive behavior is observed, whereas when n=0 the CPE is considered to be a resistor (a real frequency-independent parameter).

Table 4.5. Impedance data of Fe-Ni alloy coatings deposited at different c.d.'s from optimized bath at 303K

c.d. (A dm^{-2})	$L \times 10^{-6}$ (H cm^2)	Q_{coat} (μF cm^{-2})	n_c	R_{pore} (Ω cm^2)	Q_{dl} (μF cm^{-2})	n_{dl}	R_{ct} (Ω cm^2)
1.0	0.713	51.22	0.80	11.77	91.80	0.73	232.9
2.0	1.108	34.71	0.74	29.98	85.68	0.84	446.4
3.0	2.346	29.97	0.72	33.11	51.62	0.73	450.8
4.0	8.628	12.24	0.72	58.88	41.20	0.73	801.3
5.0	4.171	19.55	0.62	50.68	50.72	0.80	641.1
6.0	1.336	59.81	0.83	28.83	62.92	0.80	385.9
7.0	0.757	62.43	0.67	15.16	73.65	0.81	326.8
8.0	0.728	94.23	0.82	5.14	145.30	0.80	136.0

From EIS data given in Table 4.5 it is seen that the charge transfer resistance, R_{ct} for Fe-Ni coating deposited at 4.0 A dm^{-2} is found to be least. Further, for coatings developed at different c.d.'s, the value of n is tending towards 1. This indicates that the corrosion protection of the alloy system is capacitor controlled.

4.4 CONCLUSIONS

A new acid sulphate bath has been proposed for deposition of Fe-Ni alloy on copper and following observations were made as conclusions:

1. The bath exhibits anomalous type of codeposition at all c.d.'s studied. The property of coatings, consequent to its composition is dictated by the deposition c.d.

2. XRD study revealed that volume fraction of bcc structure is higher than that of fcc at low c.d.; and fcc phase becomes predominant over the bcc phase as c.d. has increased.

3. Saturation magnetization (M_s) and coercivity (H_c) of the coatings respectively increased and decreased with c.d. These properties are associated with the crystallite grain size and phase structure of the coatings.

4. Corrosion study demonstrated that at 4.0 A dm^{-2}, the bath produces the least corrosive Fe-Ni coating (CR = 7.40 mm y^{-1}) with about 81.5 % of Ni content, compared to the one at other c.d.'s. Further, the XRD study revealed that at this c.d., phase structure of the alloy has changed from bcc to fcc pattern**.**

5. The impedance data from the EIS measurements showed that the values of charge transfer resistance, R_{ct} and the pore resistance R_{pore} increased with c.d. only up to 4.0 A dm^{-2} and then decreased. The peak performance of Fe-Ni alloy coating at optimal c.d. is due to the combined effect of double layer capacitance and coating capacitance.

ELECTRODEPOSITION AND CHARACTERIZATION OF MULTILAYER Fe-Ni ALLOY COATINGS

One emerging area of materials research is development of new metals and alloys having a spatially periodic composition in one dimension with ultrafine nanostructures. Such class of materials is popularly known as composition modulated multilayer alloys (CMMA). As a result of layering at a near atomic dimension, i.e. by nano/micrometric layering these CMMA materials can possess remarkable and some time unique properties not attainable in normal metallurgical alloys. These properties include X-ray optical properties, magneto-optical properties, improved hardness, wear and corrosion resistance (Bull and Jones 1996, Gabe and Green 1998, Nabiyouni et al. 2002, Kalantary et al. 1998). Thus CMMA coatings show wide applications in various industries including those of the aircraft, aerospace, automotive, household appliances and electronics. CMMA coatings are those in which alloy composition can be varied either as a step function to produce multilayers or gradually changed to give compositionally graded coatings (Jensen et al. 1998). The ability to do so by electrodeposition depends upon the solution chemistry and the operating parameters, and has been summarized as theoretical concepts by Despic and Jovic (1987). Practical realization of a useful coating however depends additionally on metallurgical considerations in which an acceptable coating should have desirable or advanced properties, in terms of their mechanical, chemical or physical properties. The metallurgical factors depend upon being able to define the layer thickness and composition and to obtain a coating that is functional through appearance, smoothness and macro-leveling nature.

Though there are different approaches to develop multilayer coatings, the most convenient one is by electrolytic method due to its simplicity and less expense. In

electrolytic method there are two approaches, known as the dual bath technique (DBT) and single bath technique (SBT) (Chawa et al. 1998). DBT involves the deposition of constituents from two separate plating baths. In SBT, the metal ions required to form both deposit layers are contained in the single electrolyte and the alloy deposition is achieved by changing alternatively the plating current/potential, possibly in combination with a modulation in mass transport towards the cathode. Both techniques are known to have their own advantages and disadvantages. However, the drawbacks of the DBT have been deemed to outweigh the benefits, so that the SBT approach is used instead.

Though gradations in composition are possible through modulation in cathode c.d., agitation, temperature etc., the gradation in composition can be better controlled by modulation in cathodic c.d. with great degree of accuracy and reproducibility, using microprocessor controlled power sources (Ivanov et al. 2002, Brenner 1963, Kanani 2006, Cohen et al. 1983, Ganeshan et al. 2007). This technique, in principle is straight forward to design and fabricate new materials. Cyclic multilayered alloy coating with periodic change in composition can be obtained from an electrolytic bath using variety of current pulses. The square current pulses may be 'dual' (for sharp change in composition in two layers) and 'triple' (for sharp change in composition in three layers) type for imparting modulation in composition. Thus the properties of coatings can be tailored by proper manipulation of coating configurations meet various desired engineering applications.

The present chapter looks at development of multilayer coatings of Fe-Ni alloy on copper using dual and triple current pulses. The optimized conditions for development of most corrosion resistant coatings are reported. The experimental study is driven by the objective to improve the corrosion performance of monolayer Fe-Ni alloy by multilayer coating technique, and to understand how a periodic change in the current pulses can bring change in the deposit characters. CMMA coatings were developed using same optimized bath detailed in Chapter 4. This chapter unfolds into three sections. The Sections 5.1 and 5.2 are devoted for optimization of deposition conditions for

development of CMMA Fe-Ni coatings using dual and triple current pulses, respectively. The corrosion performance of multilayer Fe-Ni coatings developed using dual and triple current pulses in relation to that of monolayer coatings are discussed in Section 5.3

SECTION 5.1 Development and characterization of multilayer Fe-Ni coatings using dual current pulse

5.1.1 Electrofabrication of Fe-Ni alloy coatings

The optimization of a stable Fe-Ni bath for deposition of bright monolayer Fe-Ni alloy using direct current (DC) has been discussed in Chapter 4. The effect of c.d. on wt. % of Ni, thickness, hardness, corrosion resistance and change in phase structures were discussed. The experimental investigation has established the fact that Fe-Ni coating deposited at 4.0 A dm^{-2} found to be bright with least corrosion rate (7.40 mm y^{-1}), and has been taken as its optimal c.d. The effect of dual current pulses on deposit characters of multilayer Fe-Ni coatings has been studied. The cyclic cathode current densities (CCCD's) and number of layers have been optimized for best performance of the coatings against corrosion. The power patterns used for development of CMMA coatings (both dual and triple current pulses) in comparison with that used for monolayer coating is shown schematically in Fig. 3.1. To assess the coating characteristics all coatings (both monolayer and multilayer) were carried out 10 minutes (~15µm thickness) using same electrolytic bath.

5.1.2 Optimization of cyclic cathode current densities

Electroplating is being an atomistic deposition process; it can be used to synthesize nano-structured material with extreme control over deposition conditions. Any modulation in mass transfer process at the cathode during plating brings modulation in the property of the coatings. It is well known that in the case of mutual alloys of iron group metals, even a small change in the composition, latter may result in significant change in properties due to change in the phase structure. With this incentive, it has been attempted to bring modulation in composition, in turn in phase structure of alternate layers using square type current having two pulses (Ganesan et al. 2007). The precise control of the CCCD's allowed the production of alternate layers with different composition of alloys with no interlayer diffusion.

108

CCCD's should be properly selected before to go for higher degree of layering. This procedure was adopted to ensure the right combination of layers with distinct interfaces. Hence to begin with, multilayer coatings having only 10 layers were developed at different sets of CCCD's, and their corrosion behaviors were studied. Different sets of CCCD's were tried to have right combination of successive layers to give extended protection to base metal (copper) against corrosion. Among the various sets tried, the less corrosion rate (CR) was measured in the coatings produced at difference of 2.0 A dm^{-2} and 4.0 A dm^{-2} between CCCD's as shown in Table 5.1. Many combinations of CCCD's have been selected for studying the effect of layering, as described in the following section and in Table 5.2.

Table 5.1. Corrosion rate (CR) of multilayer (Fe-Ni) coatings at different sets of CCCD's (with 10 layers), developed from the optimized bath at 303K

CCCD's (A dm^{-2})	$-E_{corr}$ vs SCE (V)	i_{corr} (μA cm^{-2})	CR (mm y^{-1})
CMMA Fe-Ni coatings developed at difference of 2.0 A dm^{-2} between CCCD's			
(Fe-Ni)$_{2.0/4.0}$	0.887	229.4	2.57
(Fe-Ni)$_{4.0/6.0}$	0.677	230.9	2.59
(Fe-Ni)$_{6.0/8.0}$	0.687	313.7	3.49
(Fe-Ni)$_{3.0/5.0}$	0.597	370.1	4.11
CMMA Fe-Ni coatings developed at difference of 4.0 A dm^{-2} between CCCD's			
(Fe-Ni)$_{2.0/6.0}$	0.993	306.4	3.44
(Fe-Ni)$_{4.0/8.0}$	0.582	381.0	4.23
(Fe-Ni)$_{3.0/7.0}$	0.647	596.0	6.63

5.1.3 Optimization of number of layers

The properties of multilayer coatings including their corrosion performance can be improved by proper layering. i.e. by controlling the nucleation process during successive layering. These properties may often to be improved by increasing the total number of layers, usually up to an optimal number as long as the adhesions between layers are assured (Kanani 2006). Therefore at optimal CCCD's, i.e. 2.0-4.0 A dm^{-2} and 2.0-6.0 A dm^{-2} CMMA coatings with 10, 20, 60, 120, 300, 400 and 600 layers were developed and their CR's were measured by potentiodynamic polarization method. The CR's of the coatings were found to decrease with number of layers in each set of CCCD's as reported in Table 5.2.

However, at 2.0/4.0 A dm^{-2}, the CMMA coating with 300 layers showed minimum CR (0.32 mm y^{-1}) in relation to monolayer Fe-Ni alloy coating (7.40 mm y^{-1}) developed using D.C. as shown in Table 5.2. Hence, it may be noted that multilayer Fe-Ni coating presents much better corrosion resistance compared to corresponding monolayer Fe-Ni alloy, deposited from same bath. Though there is substantial decrease of CR with layering at 2.0-6.0 A dm^{-2} also (shown in Table 5.2), the result pertaining to 2.0/4.0 A dm^{-2} was more encouraging due to least CR and better homogeneity of the deposit. However, an attempt of increasing the corrosion resistance further by increasing number of layers in each set of CCCD's has resulted in increase of CR, as shown in Table 5.2.

The increase of CR at higher degree of layering, i.e. with 600 layers is due to shorter relaxation time for redistribution of metal ions at the diffusion layer, during plating (Kanani 2006). The phenomenon may be explained as follows: metal ions (Fe^{2+} and Ni^{2+}) from the bulk of the electrolyte diffuse towards the cathode and to get discharge as metal atom. This process of diffusion is controlled mainly by applied cathode c.d. As the number of layers increased, the time for the deposition of each layer is small (as the total time for deposition remained same, 10 min). At higher degree of layering, there is no sufficient time for metal ions to relax against diffusion under given c.d., and to deposit on cathode by brining change in composition. As a result, at higher degree of layering modulation in composition is not likely to take place. In other words,

110

on exceptional thinning of layers, the coating is tending to become monolayer showing less corrosion resistance. Hence extended protection of the multilayer Fe-Ni coating is due to combined effect of composition of individual layers (modulation) and increase in the number of interfaces. Based on corrosion protection efficacy, CMMA Fe-Ni alloy having $(Fe-Ni)_{2.0/4.0/300}$ configuration has been proposed as the optimal for multilayer coating, with individual layer thickness ~ 50 nm. Finally, it may be concluded that the extended corrosion protection of multilayered coating is due to electrofabrication of layers of alloys in nano/micrometric scale.

Table 5.2. Decrease of corrosion rate (CR) of multilayer Fe-Ni coatings with increase in number of layers, deposited from optimal bath at 303K

CCCD's $(A\ dm^{-2})$	Number of layers	Time for each layer (s)	Average thickness of layer (nm)	$-E_{corr}$ vs SCE (V)	i_{corr} $(\mu A\ cm^{-2})$	CR $(mm\ y^{-1})$
	10	60	1400	0.887	229.4	2.57
	20	30	700	0.904	131.4	1.47
	60	10	233	0.894	97.17	1.09
	120	5	116	0.914	75.60	0.84
$(Fe-Ni)_{2.0/4.0}$	300	2	46	0.924	28.77	0.32
	400	1.5	35	0.913	46.39	0.52
	600	1	23	0.914	54.13	0.60
	10	60	1400	0.993	306.4	3.44
	20	30	700	1.003	223.4	2.51
	60	10	233	1.013	163.0	1.83
	120	5	116	1.032	95.39	1.07
$(Fe-Ni)_{2.0/6.0}$	300	2	46	1.032	69.62	0.78
	400	1.5	35	1.043	73.03	0.82
	600	1	23	1.024	77.73	0.87
$(Fe-Ni)_{4.0}$	monolayer	600	14000	0.913	650.3	7.40

5.1.4 Corrosion study

i) Potentiodynamic polarization study

The polarization behavior of multilayer $(Fe\text{-}Ni)_{2.0/4.0}$ coatings having different number of layers is shown in Fig. 5.1. It was observed that the corrosion resistance of the coatings increased with layering only up to 300 layers, as evidenced by their corrosion current (i_{corr}) values reported in Table 5.2. The progressive decrease of i_{corr} with layering, as seen in Fig. 5.1 indicates that improved corrosion resistance is due to layering of alloys having different composition. Polarization curve corresponding to $(Fe\text{-}Ni)_{2.0/4.0/300}$ configuration, shown in Fig. 5.1 suggested that this coating is the most corrosion resistant than others.

Further, the shape of cathodic polarization curve corresponding to different number of layers (Fig. 5.1) indicate that progressive decrease of corrosion rate, of course up to 300 layers is due to progressive decrease of exchange current density (i_0) for hydrogen evolution reaction.
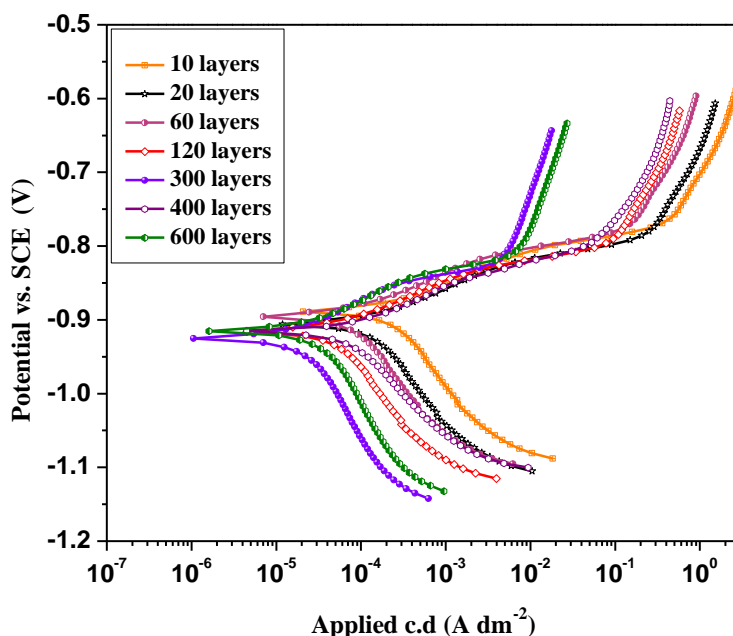
Fig. 5.1. Potentiodynamic polarization curves of multilayer $(Fe\text{-}Ni)_{2.0/4.0}$ coatings having different number of layers, developed using dual current pulses from optimal bath at 303K

The value of i_0 was obtained by extrapolating cathodic curve to intersect the open circuit potential of the coating. Hence, the i_0 for evolution of hydrogen (equivalent to the reversible rate at equilibrium for reaction, $2H^+ + 2e \leftrightarrow H_2$) is found to be decreased as the number of layers increased. A drastic change in i_0 was thus observed when layers are increased from 10 to 300, as seen in Fig. 5.1. Hence, increased corrosion protection of CMMA $(Fe-Ni)_{2/4/6/300}$ is due to reduced i_0 for evolution of hydrogen on coated surface, which decreases as number of layers increased.

As discussed earlier at high degree of layering, the deposition time for each layer is very short as mentioned in Table 5.2. Consequently, modulation in composition is not likely to take place, and hence multilayer deposit tends to become monolayer showing less corrosion resistance (property of bulk material).

ii) Electrochemical impedance spectroscopy
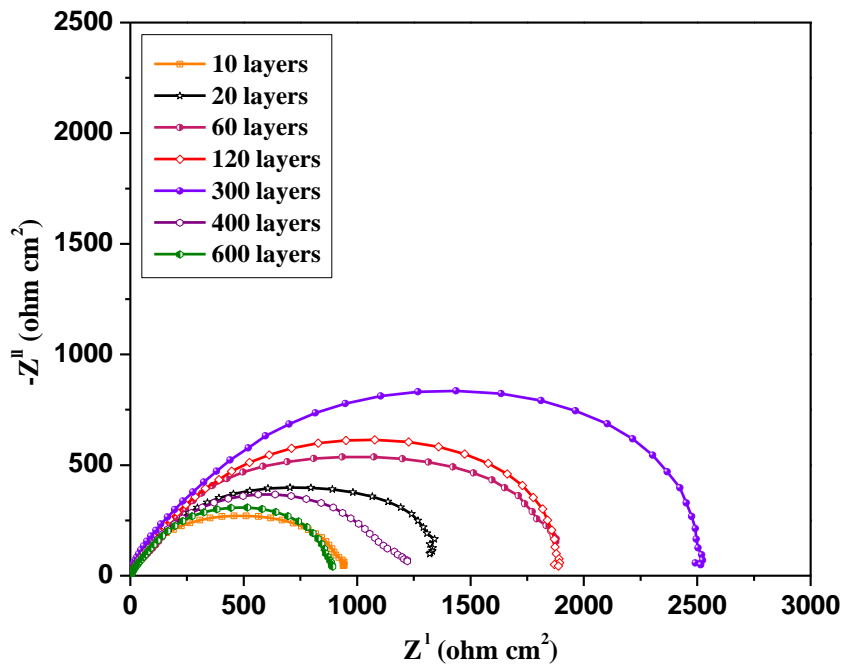
Fig. 5.2. Real versus imaginary resistance values of multilayer $(Fe-Ni)_{2.0/4.0}$ coatings having different number of layers, developed using dual current pulse from optimal bath at 303K

The EIS measurement was carried out in a 1 M HCl solution. The coated samples are masked with cellophane tapes with leaving 1 cm^2 exposed area. The impedance measurement was made at AC voltage of ± 10 mV over a frequency range of 10 kHz–10 MHz. The current responses were measured and data were analyzed by Nyquist and Bode plots. Generally, in these plots the three different parts indicated with high frequency, medium frequency and low frequency reflect the interfacial behavior of the coated film. The interface behavior of the coating at optimal configuration in solution environment was modeled with electrical equivalent circuit. The values of the circuit element such as polarization resistance (R_p), solution resistance (R_s) were determined.

Nyquist responses of (Fe-Ni)$_{2.0/4.0}$ coatings, having different number of layers is shown in Fig. 5.2. The existence of single semicircle for all coating configuration showed that single charge transfer process is involved in dissolution. Impedance responses clearly indicated that the polarization resistance, R_p increased progressively as the number of layer increased.
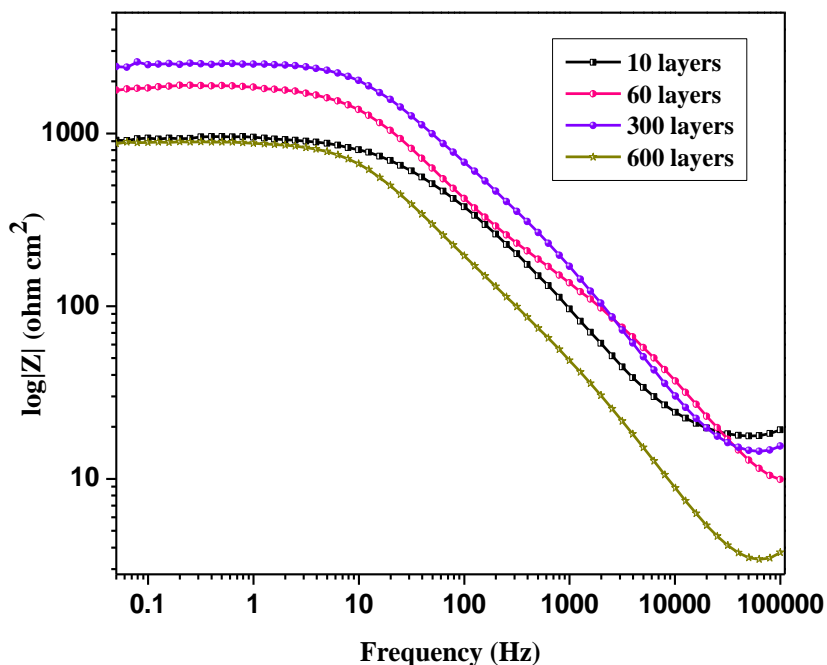
Fig. 5.3. Bode's modulus plots for multilayer (Fe-Ni)$_{2.0/4.0}$ coatings with different number of layers, developed from the optimized bath using dual current pulses

This is due to the fact that increased capacitive reactance of coating resulted in decreased electrical conductivity of coatings. Further, the depressed semicircles of impedance may be observed in Fig.5.2. This is often referred to frequency dispersion of interfacial impedance. This anomalous flattening behavior is generally attributed to the inhomogeneity of the metal surface arising from surface roughness or interfacial phenomena.

Bode's magnitude he plot of log |Z| vs log f shown in Fig. 5.3 displays that absolute impedance increase in the same order as Nyquist plot. Further, the corrosion protection efficacy increases with number of layers upto 300 layers and then decreased. The Bode's phase angle plot shown in Fig. 5.4 verifies once again the observed Nyquist behavior. The phase angle has approached -70º for (Fe-Ni)$_{2.0/4.0/300}$ signaling the increased capacitive reactance, or less double layer capacitance. The impedance data corresponding to (Fe-Ni)$_{2.0/4.0/300}$ was fitted into electrical equivalent circuit, shown in Fig. 5.5 and corresponding circuit element data are given in Table 5.3.
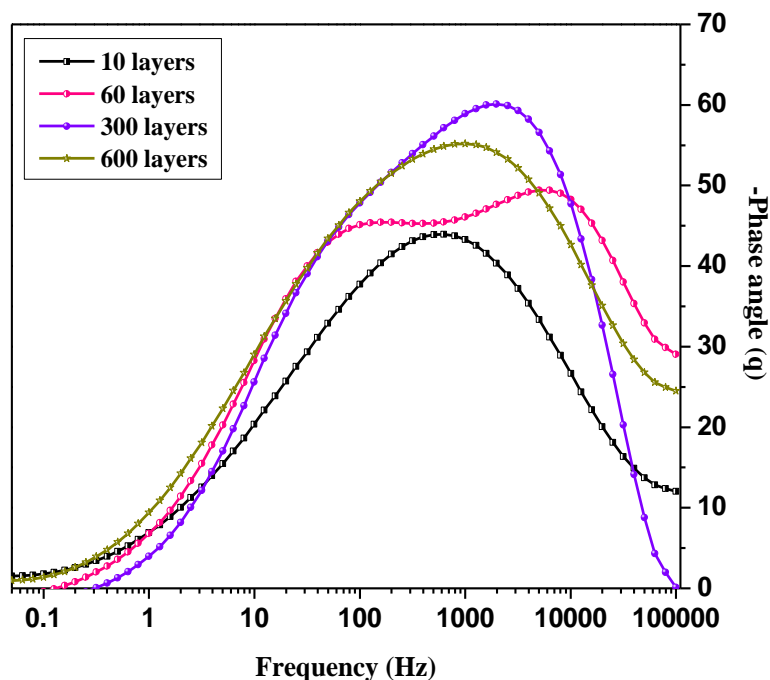
Fig. 5.4. Bode's phase angle plot for multilayer (Fe-Ni)$_{2.0/4.0}$ coatings having different number of layers, developed using dual current pulse from optimal bath at 303 K

A good agreement between experimental and fitted data was found. Two (RQ) parallel circuit combinations are used to represent the electrochemical activities of the oxide layer and the coating/solutions interface. In Fig. 5.5, R_{ct} and constant phase element (Q_1) are the charge transfer resistance and the oxide layer capacitance. R_c and Q_2 are the coating resistance and the coating capacitance, or the resistance and capacitance of the space charge layer.

Table 5.3. Impedance parameters deduced by equivalent circuit simulation for multilayer (Fe-Ni) $_{2.0/4.0/dual}$ coatings having different number of layers, deposited from optimal bath

No. of layers	L (Hcm^2) $\times 10^{-6}$	R_{ct} (Ωcm^2)	Q_1 (Ω^{-1}cm^{-2}S^{-n}) $\times 10^{-6}$	n_1	R_f (Ωcm^2)	Q_2 (Ω^{-1}cm^{-2}S^{-n}) $\times 10^{-5}$	n_2
10	0.166	793.4	0.206	0.7	141.9	1.501	0.8
20	7.001	1135	0.200	0.8	136.5	1.370	0.8
60	7.461	1673	0.145	0.8	188.9	1.029	0.8
120	1.138	1746	6.844	0.8	225.0	0.823	0.8
300	1.518	2218	5.156	0.8	306.2	0.764	0.8
400	7.465	1174	6.751	0.9	33.0	1.917	0.7
600	4.447	841.8	0.267	0.8	55.1	1.808	0.8
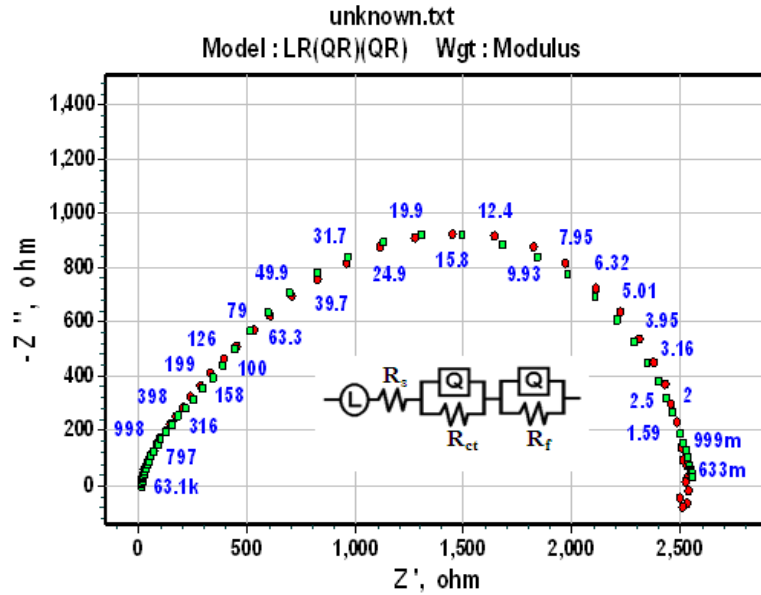
Fig. 5.5. Equivalent electrochemical circuit fitment for multilayer (Fe-Ni)$_{2.0/4.0/300/dual}$ developed using dual current pulse from optimal bath at 303K

5.1.5 Dielectric properties of multilayer coatings

EIS data points can also be used to study the dielectric properties of materials, and the technique is called dielectric spectroscopy (Gellings and Bouwmeester 1997). It is based on the interaction of an external field with the electric dipole moment of the sample, often expressed by permittivity. This technique measures the relative dielectric constant, ε_r of a system over a range of frequencies. The frequency response of the system, including the energy storage and charge dissipation properties can be identified by this method.

The capacitance is inversely proportional to the electric field between the plates, and the presence of the dielectric reduces the effective electric field. The capacitance C may be expressed as,

$$C = \frac{k\varepsilon_0 A}{d} = \frac{\varepsilon_r A}{d} \tag{5.1}$$

Where k is dielectric constant of the medium, ε_0 is permittivity of vacuum, A is surface area of parallel plates and d is the spacing distance. When coating having definite

117

dielectrics is placed between charged plates having electric field E, the polarization of the medium produces an electric field opposing the field of the charges on the plate. The relative dielectric constant is a characteristic of space between plates, and is a way to characterize the reduction of electric field due to polarization, represented as $E_{polarizatioin.}$ Then the effective electric field, $E_{effective}$ is given by relation,

$$E_{effective} = E - E_{polarization} = \frac{\sigma}{k\varepsilon_0} = \frac{\sigma}{\varepsilon_r} \tag{5.2}$$

Here σ is the surface charge density; or quantity of charge per unit area of capacitor plate (C m^{-2}). Then decrease of effective electric field between the plates will increase the capacitance of the parallel plate structure. Therefore dielectric must be a good electric insulator to minimize any DC leakage current through a capacitor (Conway 1999). Thus by understanding the dependency of surface charge density, σ with relative dielectric constant, ε_r of the interfacial medium, it is possible to have a frequency response of ε_r for different (Fe-Ni)$_{2.0/4.0}$ coatings. Thus the improved corrosion resistance of multilayer coating can be explained in terms changed dielectric property of the layered coatings. (Aarti et al. 2010, Koops 1951, Maxwell 1973, Ravinder and Latha 1999). Thus the equation for the dielectric constant, ε_r can be shown as,

$$\varepsilon_r = \frac{Z_I}{\omega C_0 \left(Z_R^2 + Z_I^2 \right)} \tag{5.3}$$

Here $C_0 = \varepsilon_0 A/t$ and ε_0 is the permittivity of free space, A is the electrolyte-electrode contact area and t is the thickness of the dielectric medium and $\omega = 2\pi f$, where f is the frequency in Hz. Where, Z_R and Z_I are the real and imaginary parts of complex impedance spectra, Total impedance Z^* is given by relation, $Z^* = Z_R + jZ_I$, where Z_R and Z_I are its real and imaginary components. Fig. 5.6 shows the dielectric constant (ε_r) of the CMMA (Fe-Ni)$_{2.0/4.0}$ coatings having different number of layers as a function of frequency f.
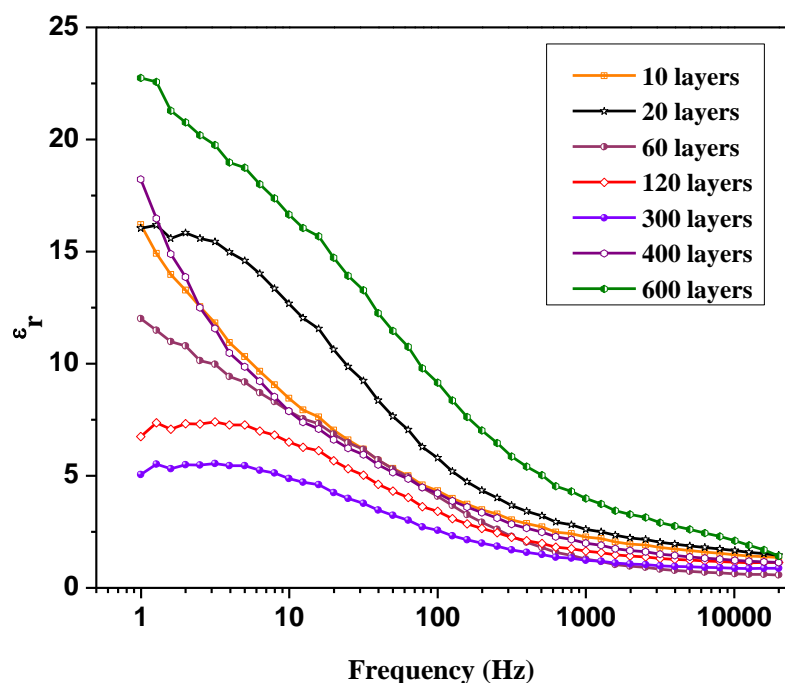
Fig. 5.6. Relative permittivity of CMMA (Fe-Ni)$_{2.0/4.0}$ coatings having varying number of layers as function of frequency, developed from optimal bath at 303 K

It may be observed that at high frequency limit, ε_r is independent of number of layers. It is due to the fact that, at high frequency there is no charging of the capacitor and the capacitor is effectively like an open circuit (vacuum). Therefore, ε_r is almost same for all coatings irrespective of the number of layers they have. At low frequency side, the frequency response of the capacitor was found to more dependent on ε_r as shown in Fig. 5.6. This is due to fact that at low frequency, AC becomes equivalent to DC, and is more sensitive to ε_r. Hence, decrease of ε_r with number of layers indicates that the polarizing ability of the Electrical Double Layer (EDL) capacitor decreases with layering (Ravinder and Latha 1999). Therefore least ε_r of CMMA (Fe-Ni)$_{2.0/4.0/300}$ coating, compared to other coatings indicates that it acts as good dielectric barrier for passage of current through the capacitor, and offers good corrosion resistance.

5.1.6 SEM Study

The formation of successive layers of alloys with distinct properties was confirmed by scanning electron microscopy (SEM). Cross-sectional view of multilayer coating having 60 layers, represented as $(Fe-Ni)_{2.0/4.0/60}$ is shown in Fig. 5.7(a). The poor contrast between layers is due to small difference in chemical composition of alloys in each layer. Inspection of the microscopic appearance of the coating after corrosion tests can also be used to understand the reason for the improved corrosion resistance of the coatings. Fig. 5.7(b) shows the multilayer $(Fe-Ni)_{2.0/4.0/10}$ configuration, after corrosion test. The image in Fig. 5.7(b) exposes the alternate layers formed during process of deposition. It is evident that the layers with lower concentration of Ni were preferentially dissolved, although eventually the copper substrate was exposed.

Improved corrosion resistance of CMMA coatings may be explained in terms of the selective dissolution of alloys in layers as envisaged by Fei and Wilcox (2005). In CMMA $(Fe-Ni)_{2.0/4.0}$ coating, the $(Fe-Ni)_{4.0}$ top layer (with high wt.% of Ni) corrode slowly, than the beneath layer $(Fe-Ni)_{2.0,}$ with low wt. % of Ni. Consequently, the resulting failures like pores and crevices occurring in the single layer will be covered by the successively deposited coating layers, and thus the corrosion agents path is longer or blocked (Dobrzanski et al. 2005). That is why, as the number of layers increased, the corrosive agent needs more time to penetrate through coating defects into the substrate material than in the case of monolayer coating. The extended protection can also be interpreted in terms of alternate layers having different composition, and hence different phase structures. According to which the corrosion protection efficacy of multilayer coatings is due to barrier effect of layers with high wt. % of Ni, and sacrificial effect of layers with less wt. % of Ni.
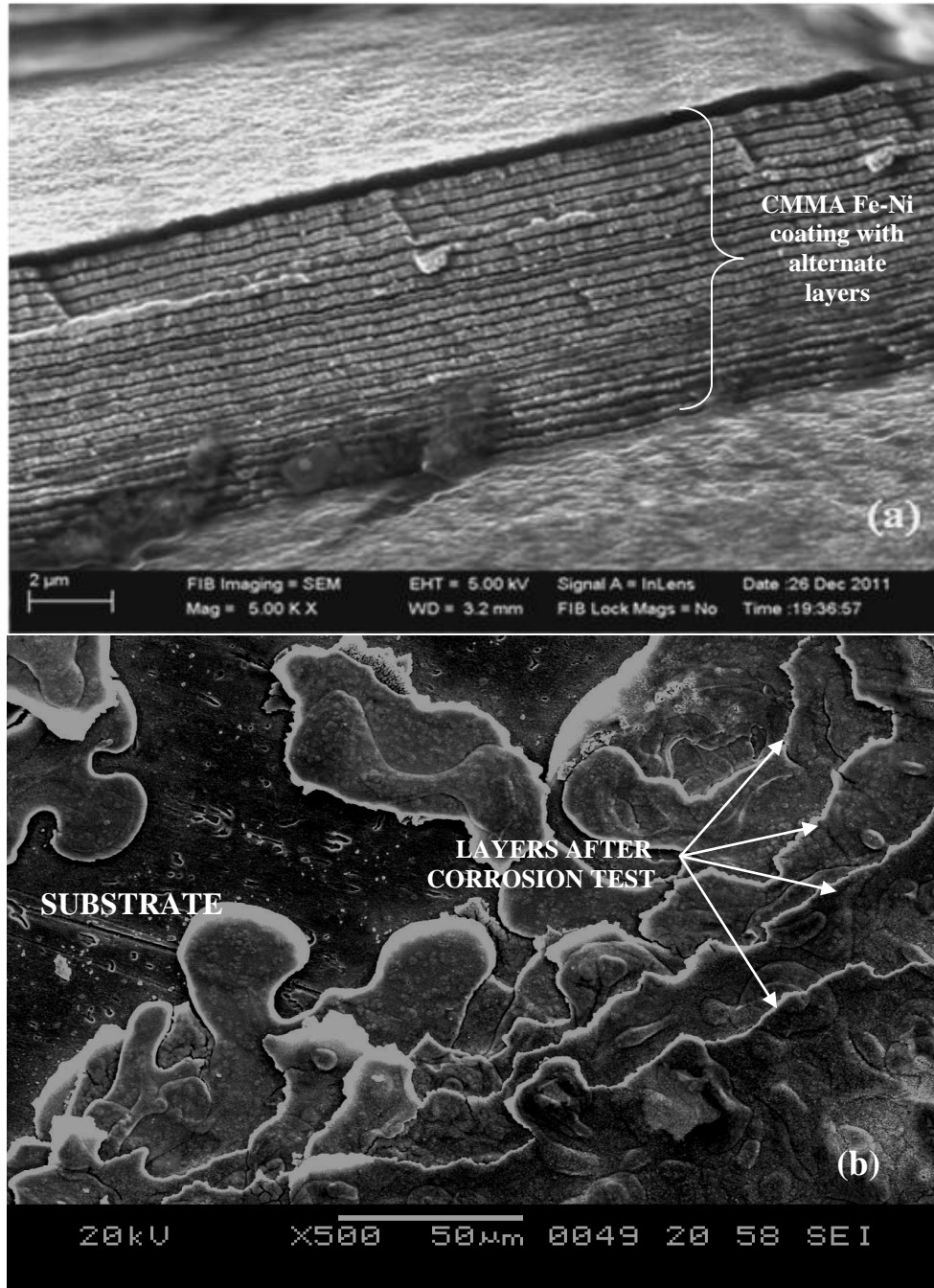
Fig. 5.7. SEM images of multilayer (Fe-Ni)$_{2.0/4.0/60}$ coatings, developed from optimized bath: (a) cross-sectional view of 60 layers, and (b) coated surface after corrosion test

121

SECTION- 5.2: Development and characterization of multilayer Fe-Ni coatings using triple current pulse

The CMMA coating technique is basically for producing laminated structure of cyclic multilayered alloys. The thickness and composition of the individual layers can be altered precisely and conveniently by cyclic modulation of cathode current/potential at the time of deposition. It is possible to modulate the structure of individual layers to obtain laminated composite coatings having desired engineering properties. Thus wear and corrosion resistances, mechanical strength, hardness as well as certain magnetic, optical, and electronic properties of the plated composites can be improved by this method. Recently variety of current pulses, like square and triangular current pulses were used to produce sharp or gradual change in compositions. The resulting deposits were found to exhibit improved properties, depending on the thickness and composition of the individual layers. The amplitude of the composition modulation diminished rapidly when layer thicknesses below certain limit, depending on the coating system. With this incentive, the multilayer Fe-Ni alloy coatings have been developed using triple current pulses, so as to cause three distinct layers with three interfaces in each cycle. Attempt has been made to optimize the coating configuration for development CMMA Fe-Ni on to copper, using triple current pulses for best performance against corrosion. The experimental results are reported in the proceeding sections.

5.2.1 Development of multilayer Fe-Ni alloy using triple current pulses

Monolayer Fe-Ni alloy with no compositional gradation was developed using direct current and results were reported in Chapter 4. Multilayer coatings having sharp change in composition in successive three layers by three fold were developed using triple current pulses. Triple current pulses have been generated by proper setting of the power source while keeping total 10 min for deposition. The pattern of the triple current pulse used for development of CMMA Fe-Ni alloy, in this section is shown schematically in Fig. 3.1. Predetermined cathode current densities were used to get laminar deposits with successively changing composition, in cyclic manner. Multilayer Fe-Ni coatings having

different configuration, i.e. with different sets of CCCD's and number of layers were developed and characterized. The coating configurations were then optimized for best performance against corrosion.

5.2.2 Optimization of cyclic cathode current densities

The corrosion resistance of multilayer coating can be improved substantially by proper manipulation of deposition variables. Among these variables, current being the most convenient to control, the coatings have been carried out using different sets cathode current densities. Modulation in composition was effected using triple current pulses, and their corrosion behaviors were studied, and corresponding data are given in Table 5.4. To start with, the 10 layered coatings were developed with different sets of CCCD's, and their effects on corrosion characters were evaluated. Among the various sets tried, the less corrosion rate was measured in the coatings produced at difference of 2.0 A dm^{-2} and 3.0 A dm^{-2} between CCCD's as shown in Table 5.4. These coatings were found to be agreeable in terms of homogeneity, brightness and uniformity. This combination of CCCD's has been selected for studying the effect of further layering.

5.2.3 Optimization of number of layers

Multilayer coatings of mutual alloys of Fe group metals have been deposited and evaluated for their improved properties such as, corrosion resistance, electrical resistivity, magnetoresistance and other advanced properties (Myung and Nobe 2001). It is known that the properties of multilayer coating can be improved by increased degree of layering. Contrary to this, the amplitude of the composition modulation is going to be diminished rapidly if layer thicknesses below certain limit (~ 1000 A°). Hence it is necessary to optimize the number and thickness of individual layers for peak performance of the coatings. Therefore, in the present study, few sets of CCCD's such as 2.0/4.0/6.0 and 2.0/5.0/8.0 A dm^{-2} etc have been selected for layering. Fe-Ni multilayer coatings with 20, 60, 120, 300, 400 and 600 layers were developed, and their corrosion rates were evaluated. The polarization behavior of the coatings having different number of layers is shown in Fig. 5.8, and corresponding corrosion data are reported in Table 5.5.

Table 5.4. Corrosion rate (CR) of multilayer Fe-Ni coatings at different sets of CCCD's (having 10 layers), developed using triple current pulses from optimal bath at 303K

CCCD's (A dm^{-2})	$-E_{corr}$ (V vs SCE)	i_{corr} (μA cm^{-2})	CR (mm y^{-1})
CMMA Fe-Ni coatings at difference of 2.0 A dm^{-2} between CCCD's			
(Fe-Ni)$_{2/4/6}$	0.894	103.46	1.16
(Fe-Ni)$_{1/3/5}$	0.946	138.68	1.55
(Fe-Ni)$_{3/5/7}$	0.875	207.56	2.33
(Fe-Ni)$_{4/6/8}$	0.862	240.06	2.70
CMMA Fe-Ni coatings at difference of 3.0 A dm^{-2} between CCCD's			
(Fe-Ni)$_{2/5/8}$	0.885	177.52	1.99
(Fe-Ni)$_{1/4/7}$	0.866	266.38	2.96

The CR's were found to decrease with number of layers in each set of CCCD's as observed in case of dual current pulses (Table 5.2). The decrease of CR's in both sets of CCCD's tried, have indicated that the observed decrease of CR is not only specific of the composition of layers but also the number of individual layers. At optimal coating configuration there will be appreciable increase in the layers, and hence specific surface area of the coatings (analogously to the surface region of nanoparticles), due to layering. Hence the monolayer coatings are going to be dominated by their interfaces. This observation is in support of the principles of nano/microstructure multilayer coatings of metals/alloys exhibiting variety of improved functional properties.

The saturation of corrosion resistance at high degree of layering in both sets of CCCD's was found. i.e. decrease of CR at higher number of layers is attributed to less relaxation time for redistribution of metal ions in the diffusion layer, as explained in Section 5.1.2. Finally, multilayer coating at 2.0/4.0/6.0 A dm^{-2} , having 300 layers

showed minimum corrosion rate (0.13 mm y^{-1}) relative to monolayer Fe-Ni alloy coating (7.40 mm y^{-1}) as shown in Table 5.5. Even though a substantial decrease of CR at 2.0/5.0/8.0 A dm^{-2} (at 300 layers) was found, the coating corresponding to 2.0/4.0/6.0 A dm^{-2} has been considered due to better appearance. Thus multilayer (Fe-Ni) $_{2.0/4.0/6.0/300}$ coating has been proposed as the optimal configuration for best performance against corrosion, from the given bath. i.e., an ideal combination of CCCD's and number of layers, at which the deposit shows peak performance against corrosion. Under this condition, the average thickness of the individual layer comes out to be about 50nm, calculated from the total thickness of the coatings and number of layers formed.

5.2.4 Corrosion study

i) Tafel's polarization study

The potentiodynamic polarization behavior of CMMA (Fe-Ni)$_{2.0/4.0/6.0}$ coatings with different number of layers (only representative plots) are shown in Fig. 5.8.
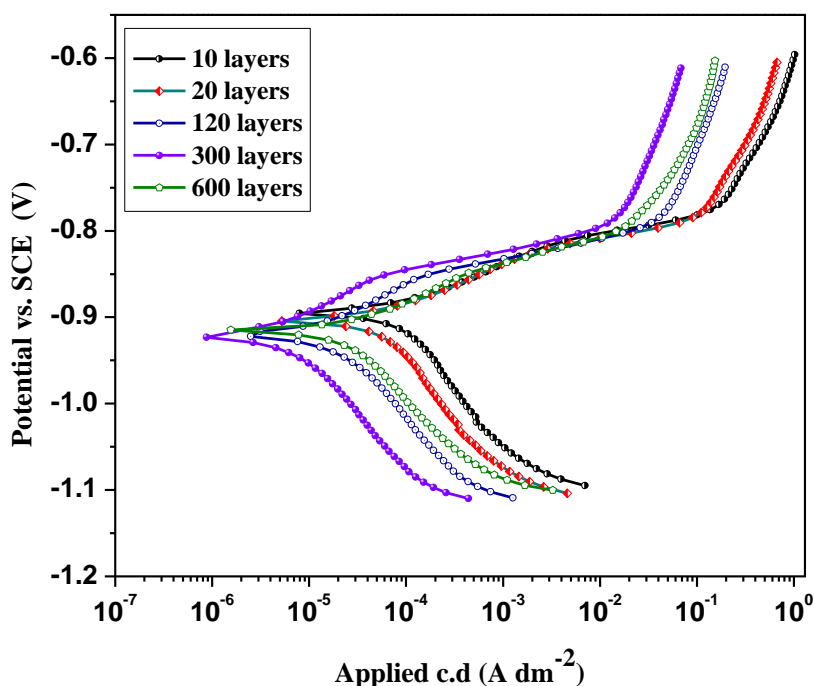
Fig. 5.8. Potentiodynamic polarization behaviors of multilayer (Fe-Ni)$_{2.0/4.0/6.0}$ coating having different number of layers developed using triple pulse, from optimal bath at 303K

It was observed that the corrosion resistance of the deposits increased substantially with number of layers as evidenced by their i_{corr} values, reported in Table 5.5. The progressive decrease of corrosion current (i_{corr}) with number of layers indicated that improved corrosion resistances are due to layering effect. A polarization curve shown in Fig. 5.8 indicates that CMMA deposit with (Fe-Ni)$_{2.0/4.0/6.0/300}$ configuration is the most corrosion resistant.

Table 5.5. Decrease of corrosion rate (CR) of multilayer coatings with increase in number of layers, developed from optimal bath at 303 K

CCCD's (A dm^{-2})	Number of layers	Time for each layer (s)	Average thickness of layer (nm)	$-E_{corr}$ vs SCE (V)	i_{corr} (µA cm^{-2})	CR (mm y^{-1})
	10	60	1400	0.894	103.4	1.16
	20	30	700	0.903	83.8	0.94
	60	10	233.3	0.912	35.7	0.40
	120	5	116.6	0.919	21.3	0.24
(Fe-Ni)$_{2.0/4.0/6.0}$	300	2	46.6	0.920	12.0	0.13
	400	1.5	35.0	0.911	14.5	0.16
	600	1	23.3	0.913	17.7	0.19
	10	60	1400	0.923	129.5	1.45
	20	30	700	0.924	97.42	1.09
	60	10	233.3	0.933	64.05	0.72
	120	5	116.6	0.949	46.78	0.52
(Fe-Ni)$_{2.0/5.0/8.0}$	300	2	46.6	0.965	30.81	0.34
	400	1.5	35.0	0.975	44.96	0.50
	600	1	23.3	0.981	65.66	0.73
(Fe-Ni)$_{4.0}$	monolayer	600	14000	0.913	650.3	7.40

Further, the shape of polarization curves indicates that corrosion process is cathodic controlled. i.e. Decrease of corrosion rate due to increased layering is attributed to the decreased i_0, i_0 for liberation of hydrogen on coated surface, as discussed in Section 5.1.4.

ii) Electrochemical impedance study

An electrochemical impedance study consists of applying the AC voltage and measure the current, associated electronics to measure the impedance of an electrochemical cell containing test sample as one of the electrodes. In alternate current (AC) impedance or EIS study, it is common to plot imaginary impedance (Z'') versus real impedance (Z') over range of frequency with provision to distinguish the polarization resistance contribution (R_p) from the solution resistance (R_s). Nyquist behavior for (Fe-Ni)$_{2.0/4.0/6.0/triple}$ coatings, having different number of layers were studied and are shown in Fig. 5.9.
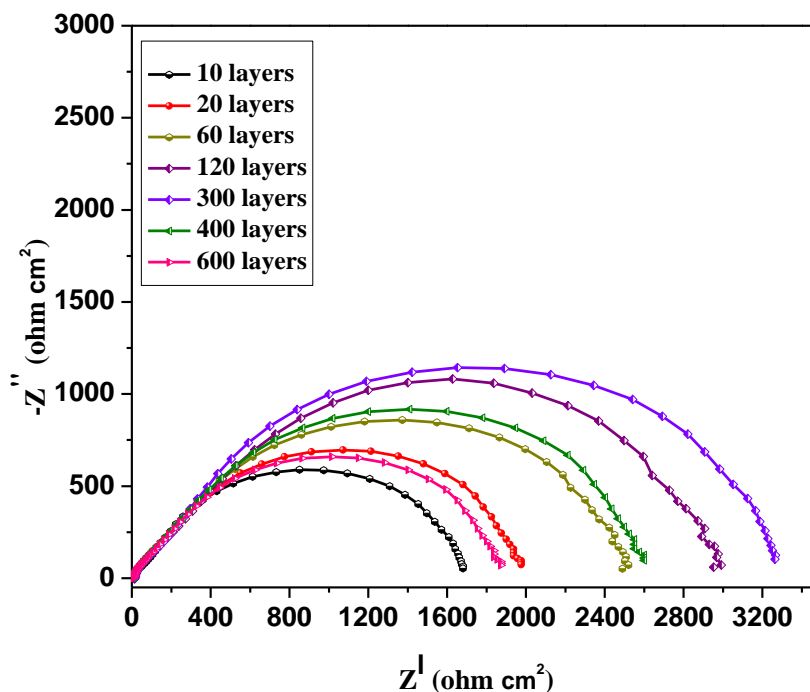
Fig. 5.9. Real versus imaginary resistance values of multilayer (Fe-Ni)$_{2.0/4.0/6.0/triple}$ coatings having different number of layers developed using triple pulse from optimal bath at 303K

Progressive increase of polarization resistance, R_p with successive layering were observed up to 300 layers, and then decreased. i.e. in coatings having 400 and 600 layers. Further, depressed semicircular Nyquist responses were ascribed to the interfacial frequency dispersion. This anomalous behavior is characteristic of coatings on metal surface, and is attributed to the in-homogeneity of the metal surface arising from surface roughness or interfacial phenomena.

Bode plot of log |Z| vs log f for multilayer coatings (only representative) is shown in Fig. 5.10. The observed plots corroborate the progressive increase of interfacial charge transfer resistance, R_p with layering (only up to 300 layers) as evidenced by Nyquist plots. Bode's phase angle plot was used to confirm the impedance data of (Fe-Ni)$_{2.0/4.0/6.0/triple}$ coatings as shown in Fig. 5.11.
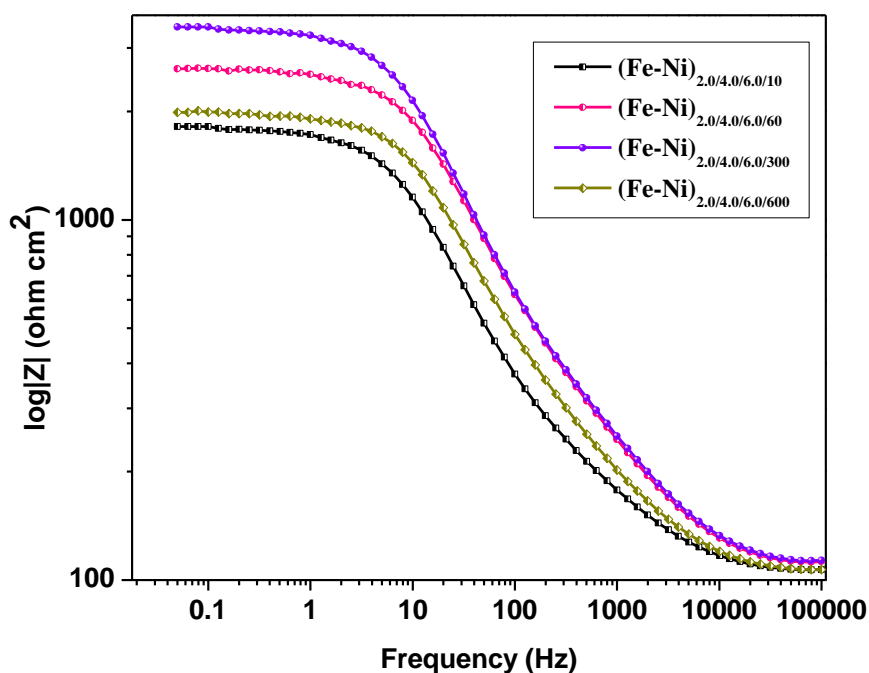
Fig. 5.10. Bode's magnitude plot for multilayer (Fe-Ni)$_{2.0/4.0/6.0}$ coatings with different number of layers developed using triple current pulses measured as function of frequency, from the optimized bath at 303 K

It is observed that the phase angle approaches -90º, indicating that the observed corrosion resistance is of capacitive impedance origin. Further, it was observed to be diminished at extreme frequency limits as shown in Fig. 5.11.

The observed impedance responses were fitted into electrical equivalent circuit having electrical components as shown in Fig. 5.12, and corresponding circuit elements are given in Table 5.6. The equivalent circuit fitment for Fe-Ni coatings, shown in inset of Fig. 5.12 presents best agreement with the experimental data and fitted data. Two (RQ) parallel circuit combinations are used to represent the electrochemical activities of the oxide layer and the coating/solutions interface. R_{ct} and constant phase element Q_1, in Fig. 5.12 are the charge transfer resistance and the oxide layer capacitance. Rc and Q_2 are the coating resistance and the coating capacitance, or the resistance and capacitance of the space charge layer.
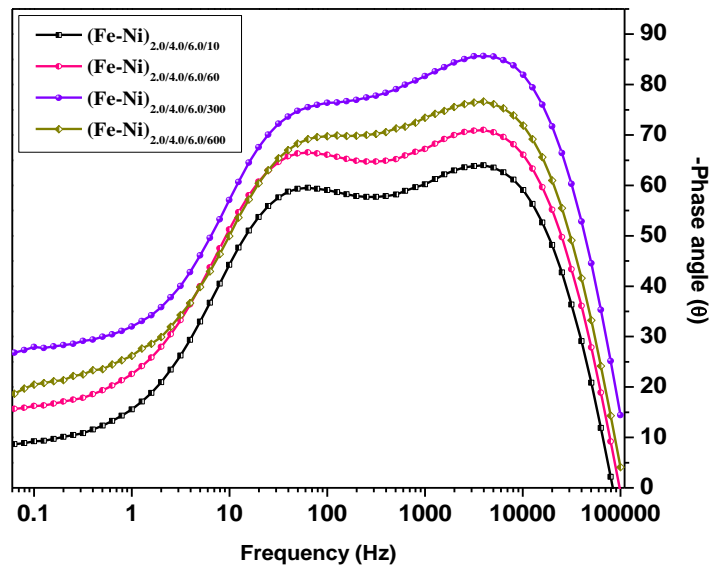
Fig. 5.11. Bode phase of multilayer $(Fe-Ni)_{2.0/4.0/6.0}$ coatings with different number of layers, developed from the optimized bath, using triple current pulses measured as function of frequency
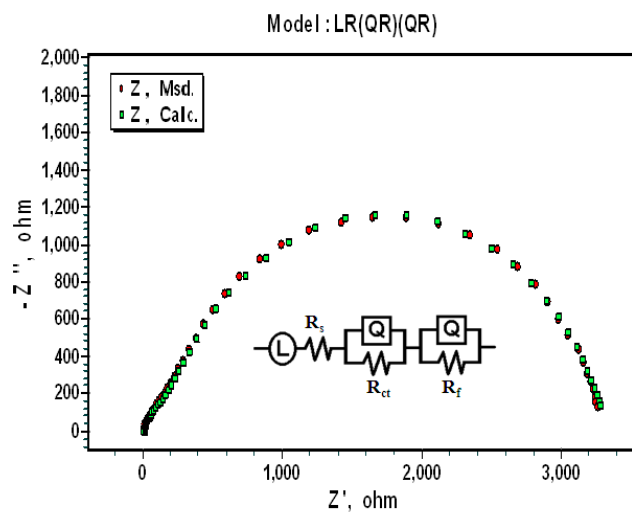
Fig. 5.12. Equivalent electrochemical circuit fitment for multilayer (Fe-Ni)$_{2.0/4.0/6.0/300}$ developed using dual current pulse, developed from the optimized bath at 303 K

Table 5.6. Impedance parameters obtained by equivalent circuit simulation of multilayer (Fe-Ni) $_{2.0/4.0/6.0}$ coatings having different number of layers, deposited from optimized bath at 303K

No. of layers	L× 10^{-6} (Hcm^2)	R$_s$ (Ωcm^2)	R$_{ct}$ (Ωcm^2)	Q$_1$ (μF cm^{-2})	n$_1$	R$_c$ (Ωcm^2)	Q$_2$ (μF cm^{-2})	n$_2$
10	6.545	5.81	1616	0.218	0.8	88.05	1.341	0.8
20	6.906	6.22	1862	0.141	0.8	130.1	0.944	0.8
60	1.188	10.41	2370	0.116	0.8	153.1	0.718	0.8
120	1.757	9.44	3154	0.161	0.8	502.0	0.691	0.8
300	1.271	11.29	3137	0.107	0.8	1709	0.013	0.8
400	9.087	8.18	2449	0.112	0.8	171.4	0.718	0.8
600	8.451	4.37	1979	0.238	0.8	63.6	0.700	0.7

5.2.5 Dielectric barrier of CMMA coatings

The relative permittivity, ε_r of the coatings were calculated from film thickness, δ and area A and coating capacitance C, using the equation:

$$\varepsilon_r = \frac{C_c \delta}{A \varepsilon_0} \tag{5.4}$$

Where, ε_0 is permittivity of the vacuum. Improved corrosion resistance of CMMA coatings can be explained in terms of the effect of time dependent electric field. i.e. frequency. Fig. 5.13 shows the variation of relative permittivity versus frequency, of the CMMA coatings having different number of layers. It was observed that the value of ε_r for all coatings is high at low frequency limit, which are diminished as the frequency is increased. At low frequency, the decrease of ε_r with increase in number of layers, indicate that the dielectric barrier of coatings has increased with layering. Thus the peak corrosion resistance of multilayer $(Fe-Ni)_{2.0/4.0/6.0/300}$ coating is attributed to decreased permittivity of the coating.
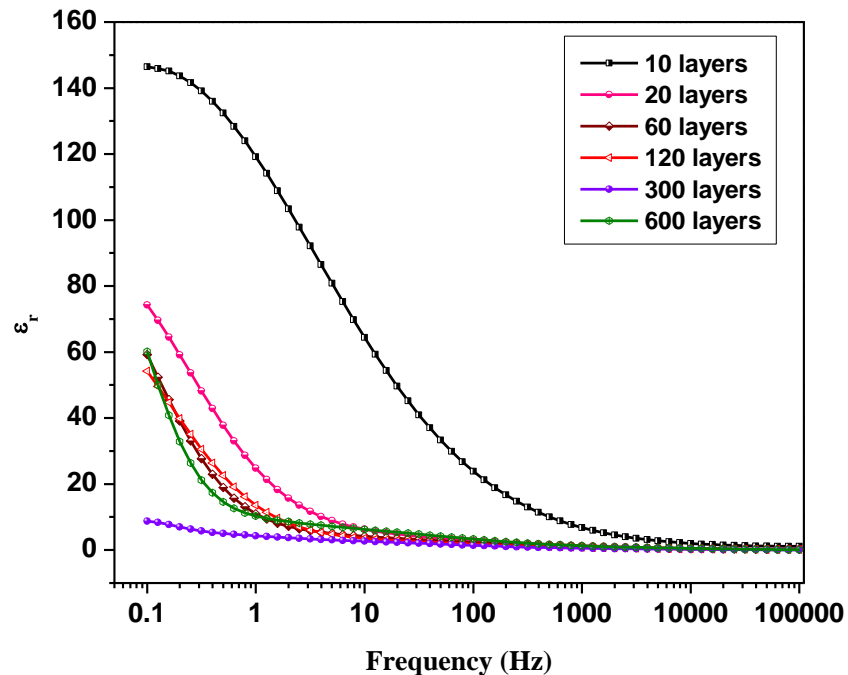
Fig. 5.13. Relative permittivity of multilayer $(Fe-Ni)_{2.0/4.0/6.0/triple}$ coatings having different number of layers developed using triple pulse measured as function of frequency

5.2.6 SEM Study

The surface morphology and formation of layers of alloys having different composition was confirmed by scanning electron microscopy (SEM) as shown in in Fig. 5.14.
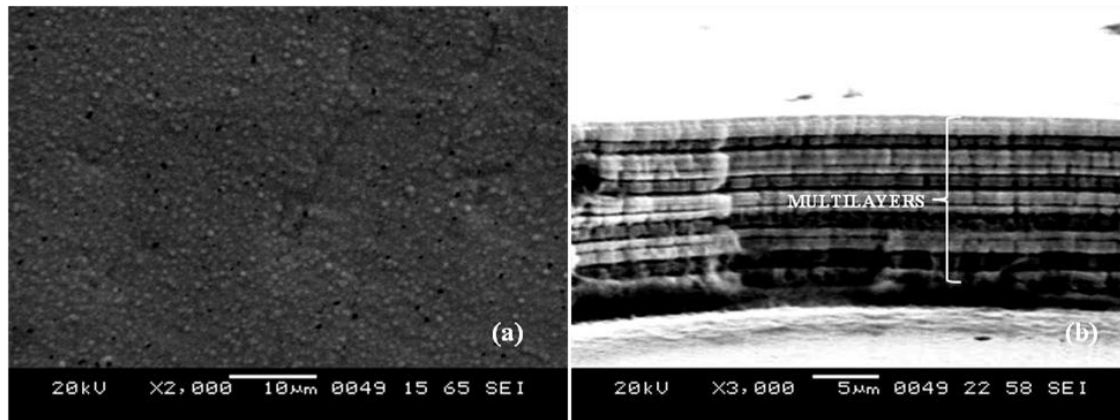
Fig. 5.14. SEM images of multilayer (Fe-Ni)$_{2.0/4.0/60}$ coatings developed from optimized bath: (a) surface morphology of the multilayer coating and (b) cross-sectional view showing 30 layers (in triplet)

Surface morphology of multilayer (Fe-Ni)$_{2.0/4.0/6.0/300}$ alloy, marked as Fig. 5.14(a), displayed a uniform fine grained structure. Cross-sectional view of CMMA (Fe-Ni)$_{2.0/4.0/60}$ shown in Fig. 5.14(b), confirms the successive deposition of alloys in layered fashion (triplet), due to passage of triple pulses. Inspection of the microscopic appearance of the surface after corrosion tests confirmed the extended protection of CMMA coatings is a layering effect, as explained in Section 5.1.6.

SECTION-5.3 Comparison of corrosion rates of multilayer Fe-Ni coatings developed using dual and triple current pulses

The effects of current pulses on corrosion resistance of multilayer Fe-Ni coatings have been studied. CMMA (Fe-Ni)$_{2.0/4.0/300/dual}$ and CMMA (Fe-Ni)$_{2.0/4.0/6.0/300/triple}$ coatings have been identified as optimal coating configuration, deposited from same bath. The corrosion performances of multilayer coatings in comparison with that of monolayer (all under optimal conditions) are summarized in Table 5.7. The corrosion data reported in Table 5.7 reveals that corrosion resistance of all multilayer coatings is more than that of monolayer coating, obtained from same optimized bath. It was found to be due to combined effect of compositional modulation and increased number of layers, having micro-sized grain structures.

Table 5.7. Comparison of corrosion rates of monolithic (Fe-Ni)$_{4.0}$ and CMMA (Fe-Ni) coatings, developed using dual and triple current pulses from same bath 303K.

Coating configuration	$-E_{corr}$ vs SCE (V)	i_{corr} (μA cm^{-2})	CR (mm y^{-1})
(Fe-Ni)$_{4.0/monolayer}$	0.913	650.38	7.40
(Fe-Ni)$_{2.0/4.0/300/dual}$	0.924	28.7	0.32
(Fe-Ni)$_{2.0/4.0/6.0/300/triple}$	0.920	12.0	0.13

5.3.1 Polarization behaviors

The comparison of potentiodynamic polarization curves of coatings obtained using D.C., dual and triple current pulses are shown in Fig. 5.15. It was observed that the corrosion rate decreased gradually as the overall numbers of layers were increased in all three types of cathodic current pulses. It may be noted that almost same corrosion rates were observed in Fe-Ni multilayer coating developed using dual and triple current pulses. Further, among the multilayer coatings, the deposit developed using triple current pulse is more corrosion resistant compared to other coatings.
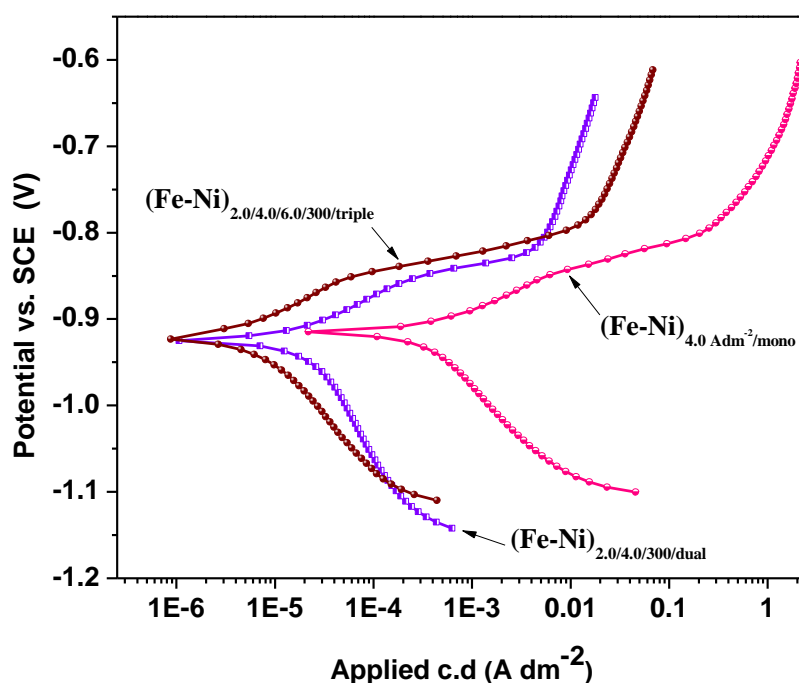
Fig. 5.15. Comparison of corrosion behaviors of monolayer (Fe-Ni)$_{4.0}$ and multilayer (Fe-Ni) coatings developed using D.C. , dual and triple pulses from optimized bath at 303K

Above observation reveals that modulation in composition of the individual layers is not only the factor responsible for improved corrosion resistance but also the number of interfaces. The modulation in composition in triple pulse is more when compared to

dual pulse. The potentiodynamic polarization curves of coatings obtained using DC; dual and triple current pulses are shown in Fig. 5.15.

The corrosion protection efficacy of the multilayer (Fe-Ni)$_{2.0/4.0/6.0/triple}$ coatings can be related to the barrier effect of the alloys having alternate configuration, i.e. (Fe-Ni)$_{2.0}$, (Fe-Ni)$_{4.0}$ and (Fe-Ni)$_{6.0}$. Electrochemical impedance signals showed that the substantial decrease of corrosion rate is due to decreased capacitance and increased dielectric barrier at the interface.
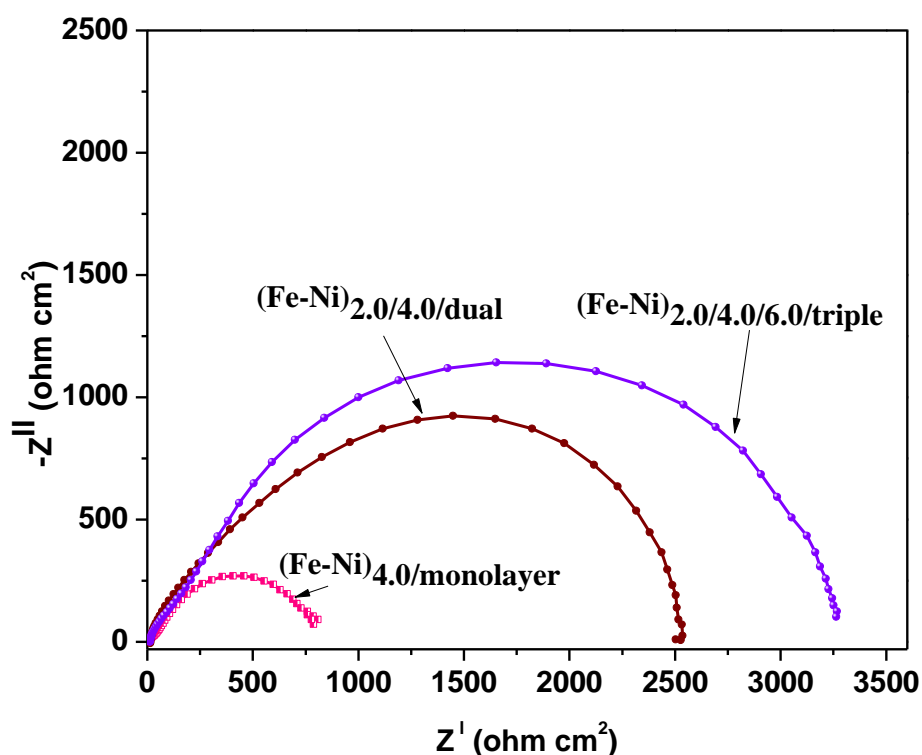
Fig. 5.16. Comparison of Nyquist responses for monolayer (Fe-Ni)$_{4.0}$ and multilayer (Fe-Ni) coatings developed using different cathode pulses, from the optimized bath at 303K

The behavior of Nyquist plots showed that the value of R_P was increased greatly when coating is changed from monolayer to multilayer type as shown in Fig. 5.16. The high corrosion resistance of multilayer coatings can be envisaged due to formation of pores, crevices occurring in one layer is blocked or neutralized by the successively

deposited coating layers, and thus the corrosion agent's path is delayed, or blocked. The improved corrosion resistance afforded by multilayer coatings can be also explained in terms of the formation of alternate layers of alloys with low and high wt. % of Ni as discussed in Section 5. 1.

The corrosion protection efficacy of multilayer Fe-Ni alloy coatings developed using dual and triple current pulses in relation to that of monolayer Fe-Ni alloy (all under optimal conditions) in 1M HCl solution is shown in Fig. 5.17. It was found that corrosion protection of coatings developed using triple current pulse, having $(Fe-Ni)_{2.0/4.0/6.0/300/triple}$ configuration is ~57 times better (0.13 mm y^{-1}) than that of monolayer $(Fe-Ni)_{4.0/monolayer}$ alloy (7.40 mm y^{-1}). Coatings with dual current pulse $(Fe-Ni)_{2.0/4.0/300/dual}$ exhibit ~23 times better corrosion resistance compared to corresponding monolayer alloy.
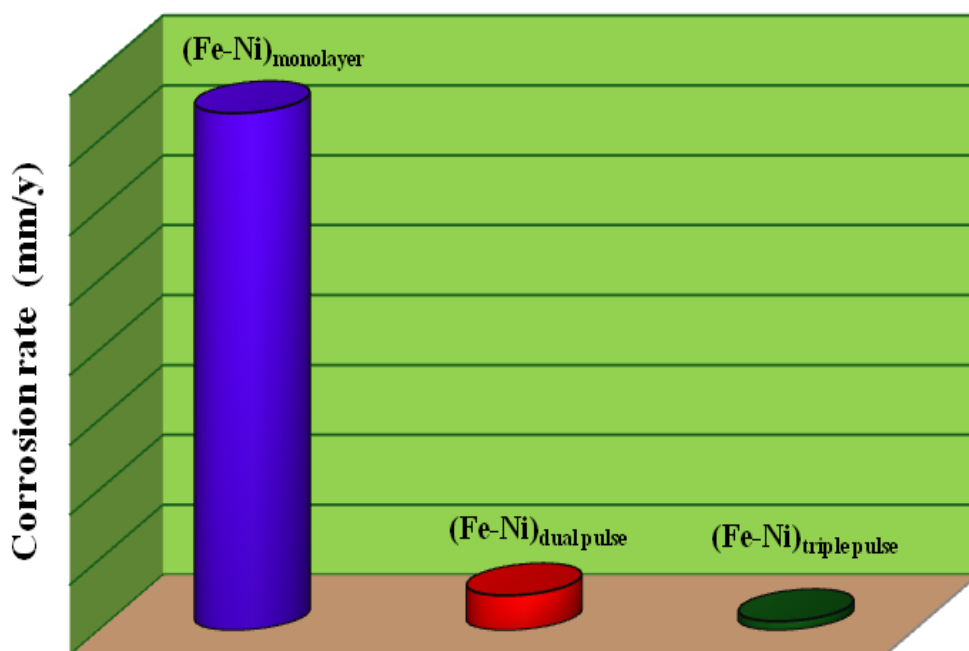
Fig. 5.17. Comparison of corrosion rates of monolayer and multilayer Fe-Ni coatings developed using dual and triple current pulses from optimized bath at 303 K

5.3.2 Conclusions

1. The corrosion rate decreased drastically when multilayer Fe-Ni coating was accomplished using both dual and triple current pulses. The CMMA (Fe-Ni) coatings developed using dual and triple current pulses were found to be, respectively about 23 and about 57 times more corrosion resistant than $(Fe-Ni)_{4.0/mono}$ alloy coating.

2. Almost same corrosion rates were observed in case of multilayer coatings using dual and triple current pulses. However, little higher corrosion resistance in triple current pulse is may be due to more compositional modulation.

3. In both dual and triple pulses, the decrease of corrosion rate was found only up to a certain optimal level, i.e. up to 300 layers and then decreased. At a higher degree of layering, the multilayer coating tends to become a monolayer.

4. The amplitude of the composition modulation is going to be diminished rapidly if layer thicknesses below certain limit (~ 1000 A°).

5. The improved corrosion resistance at different sets CCCD's in both current pulses reveal that the unique structural modulation of the layers is not the essential requirement for improved property of coatings.

ELECTRODEPOSITION OF MONOLAYER Co-Ni ALLOY AND THEIR CHARACTERIZATION

6.1 INTRODUCTION

Alloys of Fe-group metals are used in variety of applications such as aerospace, energy generation and corrosion protection and for an environment where materials have to withstand high temperatures and oxidizing conditions (Smith, 1993). Among these, Co-Ni alloy has been gaining popularity because of its improved functional properties, like magnetic, electro catalysis (in hydrometallurgy) and corrosion resistance (Landolt and Marlot 2003, Fenineche et al. 2003). Since electrodeposition allows the production of thin layer of metallic alloys at less cost, they are the obvious alternative for expensive physical vapor deposition (PVC) and chemical vapor deposition (CVD) (Petersson and Ahlberg 2000). For protective coatings, the electrodeposition approach has additional advantages involving enhanced control of alloy composition and coating thickness. Moreover, unlike vapor phase-produced coatings which are often porous, electrodeposition can be used for production of more compact coatings for better corrosion resistance (Heusler 1997). Therefore Co-Ni alloys, having broad variation in composition can be easily produced from aqueous electrolyte by electrodeposition. These alloys commonly consist of different phase structures including compounds of inter-metallic components, and they exhibit unique properties. The electrodeposited face centered cubic (fcc) Co-Ni alloys were found to be used as recorder head materials in computer hard drives, and in surface finishing industries for items such as printed circuit boards, wear resistant coating, corrosion resistance layers, electroformed laser mirrors and decorative coating etc (Bagotzky 1993).

Thus substantial amount of work have already been carried out while studying the effect of plating parameters on the composition and morphology of Co-Ni alloys (Dulal

et al. 2004, Correia and Machado 2003) as well as their catalytic behavior (Burzynska and Rudnik, 2000) and magnetic properties (Fenineche et al. 2003). Investigation on Co-Ni alloys having different composition and microstructure showed that their physical and electrochemical properties strongly depend on Co-content of the alloy. The maximum micro-hardness of the Co-Ni alloy appears at about 45 % Co content (Yang et al. 2010). The magnetic properties of the Co-Ni alloys have demonstrated to be sensitive to the composition and microstructure of the coatings. Therefore, control over the composition and structure of the coatings is the key factor in deciding their wide applications. The characteristic anomalous codeposition observed in Co-Ni alloys was explained by a mathematical model, via mass transfer process. Generally, current density (c.d.) greatly affects the properties of coatings in terms of their Co content. Further, the investigation on electrodeposited Co-Ni alloys have proved that their microstructure and properties depend strongly on their Co content (Correia and Machado 2000, Golodnitsky et al. 2002). The composition of Co-Ni alloy deposited from the given bath depends on the deposition conditions such as c.d., temperature, pH, and other bath constituents. Thus the composition of Co-Ni alloys, and hence its properties such as brightness, magnetic property, corrosion resistance etc can be regulated appropriately by choosing the bath composition and parameters of electrolysis.

The present chapter discusses the results of laboratory research centered on the deposition of Co-Ni alloys using sulfate solution. The objective of the work is to investigate how the composition and macroscopic properties of deposits are determined by the concentration of cobalt and nickel ions in the bath/deposit, c.d. and presence of additives. The main focus is to optimize the operating parameters and bath composition for deposition of bright, uniform Co-Ni alloy. Attempts have been made to relate the effect of deposition c.d. on composition, phase structure, corrosion and magnetic behavior of the coatings.

6.2 OPTIMIZATION OF Co-Ni ALLOY BATH

A wide variety of Co-Ni alloys having varying composition formed on Hull cell panel showed that c.d. plays an important role on properties of the electrodeposit. The practical difficulty of instability of the bath was overcome by adding ascorbic acid (AA), an antioxidant. The binary magnetic Co-Ni alloy film was developed on copper using procedure discussed in Section 4.2. Optimal bath composition and operating parameters have been arrived by Hull cell method. The deposit was found to be very bright and adherent over wide range of 1-8 A dm^{-2}. The bath constituents and operating parameters proposed for deposition of Co-Ni alloy is given in Table 6.1. Following to this, Co-Ni alloys having different compositions were developed from the optimal bath at different current densities, keeping anode and cathode parallel to each other (4 cm apart). The effect of c.d. on wt. % of Ni, surface morphology, phase structure, hardness, and crystallite grain size, corrosion and magnetic properties of the coatings are discussed in the following sections.

Table 6.1. Composition and operating parameter of the optimized bath for electrodeposition of bright Co-Ni alloy on copper

Bath constituents	Concentration (g L^{-1})	Operating parameters
NiSO$_4$. 6H$_2$O	131.0	c. d., 1.0-8.0 A dm^{-2}
CoSO$_4$. 7H$_2$O	14.0	pH: 3.5
Boric acid, H$_3$BO$_3$	30.0	Temperature: 303K
L-Ascorbic acid	8.0	Anode: Pure nickel
Sulphanilic acid	1.0	Cathode: copper

Electroplating was carried out galvanostatically at different c.d.'s, viz. 1.0, 2.0, 3.0, 4.0, 5.0, 6.0, 7.0 and 8.0 A dm^{-2} using DC power source. The experimental procedure adopted for production and characterization of Co-Ni alloy is same as discussed in Chapter 4.

6.3 RESULTS AND DISCUSSION

6.3.1 Effect of current density

i) Wt. % of Ni in the deposit

Electroplating of Co-Ni alloys has been recognized as an anomalous codeposition, i.e., nickel content (wt. %) in the deposited films was found to be less than that in its electrolyte. The dependency of Ni content in the codeposited Co-Ni alloy with c.d. is shown in Fig. 6.1. It should be noted that wt. % of Ni and Co, corresponding to the proposed Co-Ni alloy bath given in Table 6.1 is 91 and 9, respectively. There are two schools of thoughts to explain the anomalous codeposition. One is called, two-step adsorption mechanism, and other one is hydroxide suppression mechanism as detailed in Chapter 2.
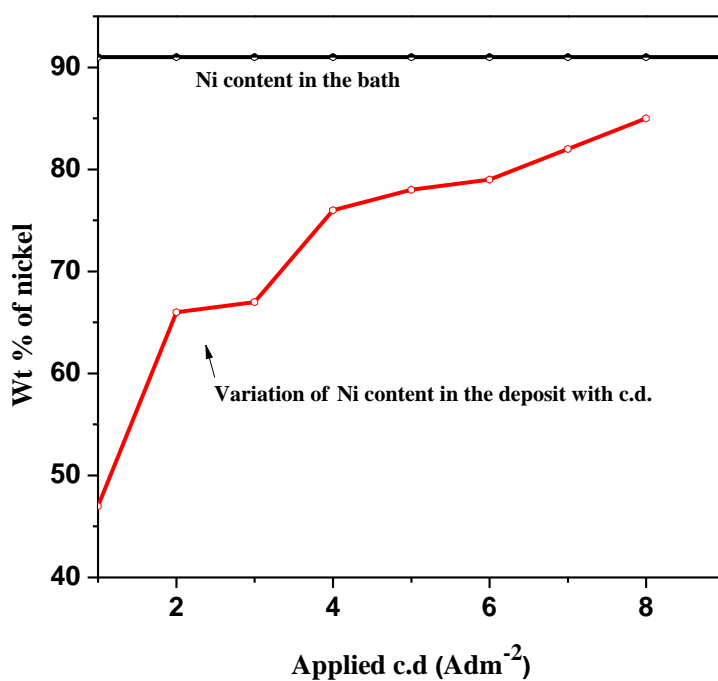
Fig. 6.1. Variation of Ni content in the deposit with applied c.d. at pH= 3.5 and 303 K, for optimal Co-Ni bath

It was observed that at c.d. greater than 2.0 A dm^{-2}, the wt. % of Ni in the deposit was found to increase with c.d. At 4.0 A dm^{-2}, the bath produced a sound and bright deposit having ~76 wt. % of Ni. This increase of Ni content with c.d. (Fig. 6.1) indicates that the deposition process is tending towards normal type. This is in compliance with the anomalous deposition of Co-Ni alloy, envisaged by Brenner (1963). i.e., low wt. % of noble metal at low c.d. and elevated temperature are characteristic of mutual alloys of Fe-group metals linked with significant mass transport process during deposition.

ii) *Partial current density and cathode current efficiency*

The partial current densities for deposition of individual metals, like Fe and Ni at various applied c.d.'s are shown in Fig.6.2. The partial c.d. for deposition of cobalt is lesser than that for nickel and hydrogen discharge over the entire c.d. range employed for the production of alloy.
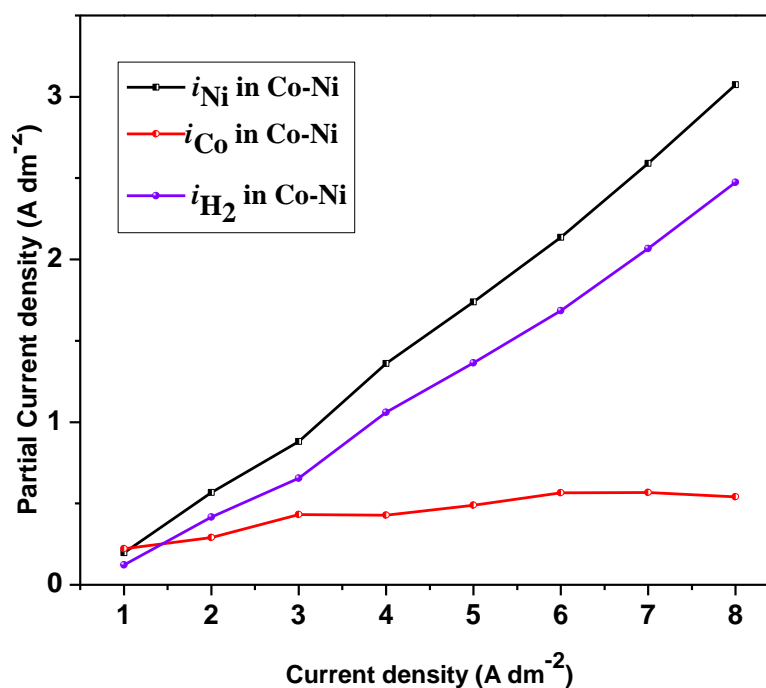
Fig. 6.2. The variation in partial current densities for deposition of Co, Ni and H$_2$ at different applied c.d. at pH= 3.5 and 303 K, for optimal Co-Ni bath

143

This is in compliance with the observed anomalous codeposition, and less cathodic current efficiency (CCE) as reported in Table. 6.2. The increased partial current densities for deposition of Ni and hydrogen liberation at higher c.d. range once again attributes to suppression of cathode current efficiencies with an increase in applied c.d.

iii) Thickness of the deposit

The applied c.d. is found to show direct dependency on thickness of deposit, evidenced by data given in Table 6.2. The observed increase of thickness of the coatings at high c.d. range is obvious due to two reasons: a) increased amount of the coatings governed by Faradays law, and b) possibility of adsorbed metal hydroxide caused by local alkalinity due to increased evolution of hydrogen gas.

Table 6.2. Effect of c.d. on deposit characters of monolayer Co-Ni alloy deposited at 303K at pH=3.5

Applied c. d. $(A\ dm^{-2})$	CCE (%)	Thickness (μm)
1.0	84	1.72
2.0	86	3.52
3.0	87	5.39
4.0	89	7.34
6.0	90	11.08
8.0	90	14.83

iv) Adhesion

The electroplated Co-Ni alloy was found to be very bright, uniform, hard and adherent. The adherence of the coatings developed at different c.d. was tested. It was found that all coatings except at very high c.d., the coatings were found be hard and adherent with completely smooth cut edges on adhesion testing. None of the squares of

the deposit was detached from the substrate indicating that coating at the optimal condition has exceptionally good adhesion.

v) Effect of pH

The pH of the bath was varied from 2.0 to 5.0. The appearance of the bath was found to unchange with pH up to 3.5. Above pH = 3.5, the bath was observed to be unstable.

6.3.2 Surface morphology

The effect of c.d. on surface morphology of the Co-Ni coatings was studied by SEM. The microstructure of the coatings at different c.d.'s is shown in Fig. 6.3.

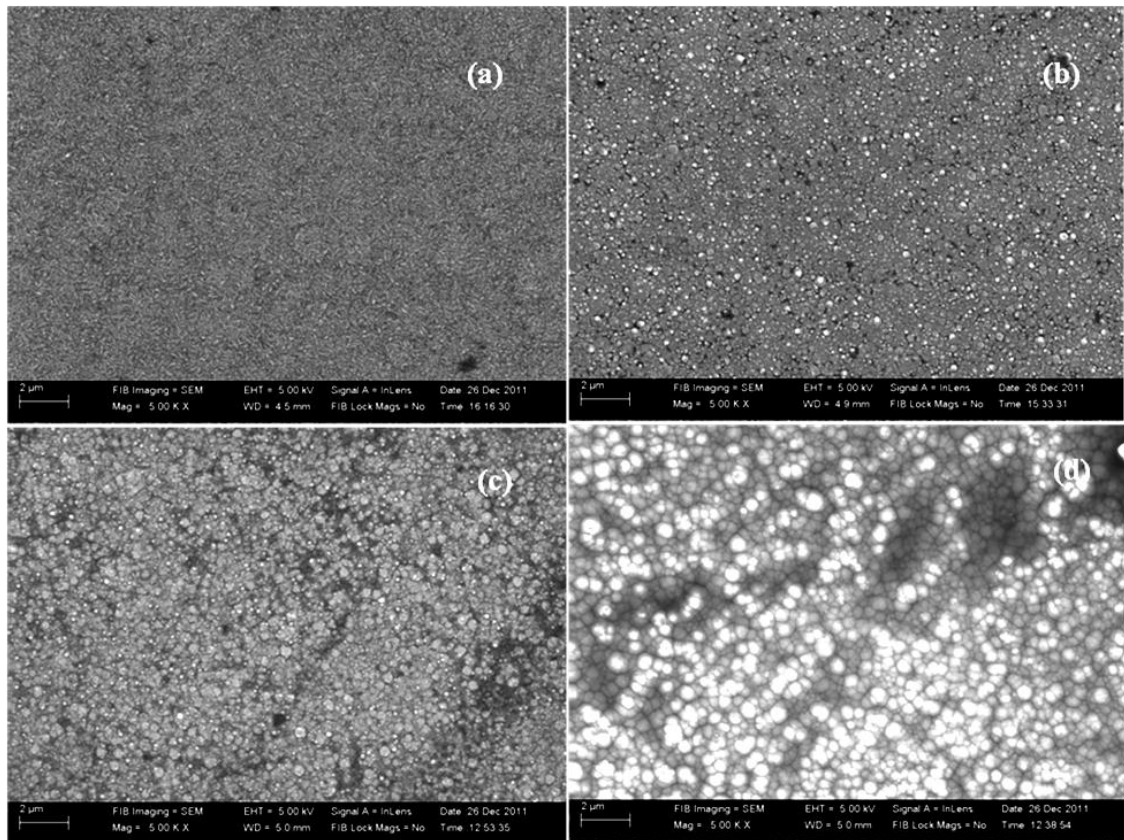Fig. 6.3. SEM micrographs Co-Ni coatings deposited at (a) 2.0 A dm^{-2} (b) 4.0 A dm^{-2} (c) 6.0A dm^{-2} (d) 8.0 A dm^{-2}, from optimal bath

It should be noted that the surface morphology of electroplated Co-Ni coating is greatly influenced by c.d. employed. At low c.d., the coating with acicular structure was observed with high wt % of cobalt, shown in Fig. 6.3(a). At very high c.d., the coating became rough and displayed a granular structure due to increased nickel content as shown in Fig. 6.3(c) and Fig. 6.3(d). This is due to significant effect of c.d. on surface morphology of the coatings (Chung and Chang, 2009, Karpuz et al. 2011). A smooth, bright and uniform coating of Co-Ni alloy was found at 4.0 A dm^{-2} as shown in Fig. 6.3(b).

6.3.3 Phase structure

The crystal orientation of Co-Ni alloys electrodeposited at different c.d.'s, having different compositions were characterized by XRD analysis. The identification of the phase structure of the deposits was obtained from the peak profiles of the X-ray reflection plotted as a function of 2θ is shown in Fig. 6.4. The phase structure of binary Co-Ni indicated that the XRD patterns consist of a substitutional solid solution of Ni and Co alloy with a preferential fcc phase structure. The XRD signals of Co-Ni coating at 2.0 A dm^{-2} showed predominant hcp phase related to Co crystal structure. At this c.d., a pronounced hcp (002) texture, characteristic of nanocrystalline cobalt was observed. As the wt. % of Ni in the deposit increased with applied c.d. an increase in fcc phase structure corresponding to Ni was found as shown in Fig. 6.4. Accordingly the cobalt content in the deposit decreased, indicated by increased intensity of (200) orientation. At optimal c.d. (4.0 A dm^{-2}) the Co-Ni alloy with a mixed phase structure was found as shown in Fig. 6.4.

Thus it may be concluded that at 4.0 A dm^{-2}, the coatings composed of mixed structure with peritectic phase has formed. The peritectic phase is a combination of fcc and hcp cellular system with (112) and (311) reflections. Further, increase in wt % of cobalt content at low c.d. is due to the onset of formation of fibrous structure as observed in the surface morphology of the coatings (Fig. 6.3(a)). This may be attributed to the predominance of the hcp phase compared to the Co-Ni alloy at higher c.d..

146
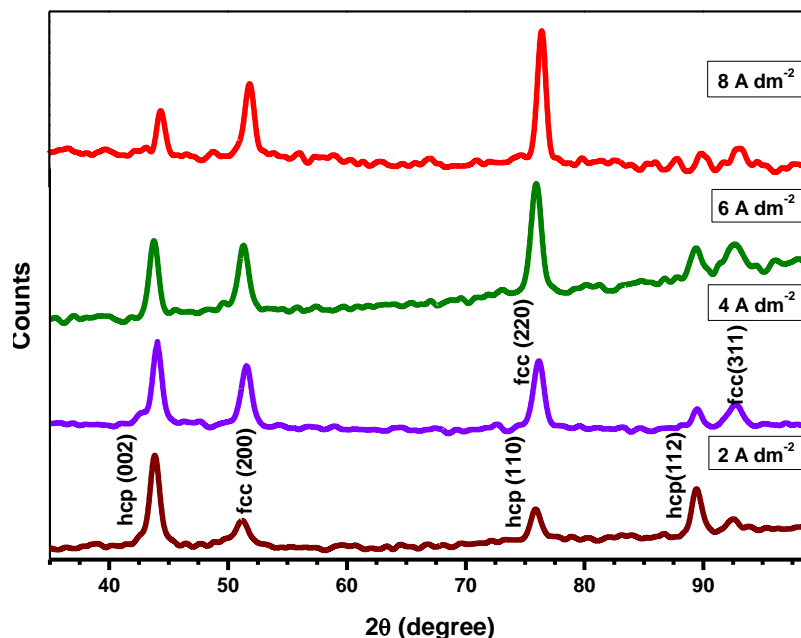
Fig. 6.4. XRD patterns of Co-Ni alloys electrodeposited at different c.d.'s from optimized bath at 303K

The XRD studies have demonstrated that the crystal structure corresponding to optimal c.d. is a combination of fcc and hcp, showing (002), (110), (112), (200) and (220) reflections.

6.3.4 Micro hardness

The micro-hardness of Co-Ni alloy coatings was found to increase with the c.d. employed for its deposition. Micro hardness is the property associated with the composition, crystallinity and surface morphology. Fig. 6.5 shows how the Vickers micro hardness of the Co-Ni alloy varies as function of applied c.d. A gradual decrease in hardness of the deposit with increasing applied c.d. was found due to decreased Co content of the alloy. Further, increased deposition rate with increased c.d. resulted in larger grain size as seen in SEM image shown in Fig.6.3(c) and Fig 6.3(d). These coatings with larger grain size are responsible for reduced micro-hardness of the coating, explained through Hall-Petch effect. (Zimmerman et al. 2002).
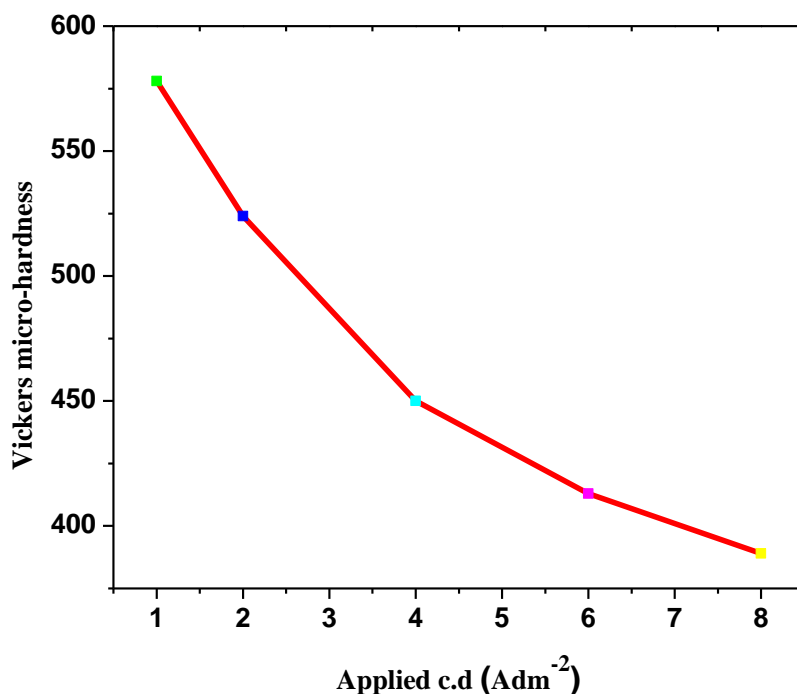
Fig.6.5. Variation of micro-hardness of Co-Ni coatings with applied c.d., deposited from the optimal bath at 303K

6.3.5 Magnetic property

The magnetic properties of electrodeposited Co-Ni coatings, deposited at different cathode current densities were measured, and corresponding hysteresis loops are shown in Fig.6.6. The behavior of hysteresis loops for Co-Ni coatings, deposited at different c.d. are shown in Fig. 6.6. The saturation magnetization, M_s and coercivity, H_c data corresponding to the coatings at different c.d.'s are given in Table 6.3. The variation of crystalline grain size and coercivity of electrodeposited Co-Ni alloy over range of applied c.d. is shown in Fig. 6.7.

The experimental observation may be explained as follows: It is well known that increased Co content of the deposit resulting in gradual increase of M_s value since M_s value of bulk Co (142.0 emu g^{-1}) which is higher than that of bulk Ni (55 emu g^{-1}) (Jiles, 1996). In other words, the increase of magnetic moment per volume depends on Co content. This is due to the fact that the dipole moment of Co is more than that of Ni. Therefore, it may be concluded that the value of M_s depends more on Co: Ni ratio in the coatings. Similarly, the decrease of M_s on increase of c.d., due to increased Ni content is

justified. Further, the coercivity value H_c is found to decrease constantly with applied c.d. as reported in Table 6.3.
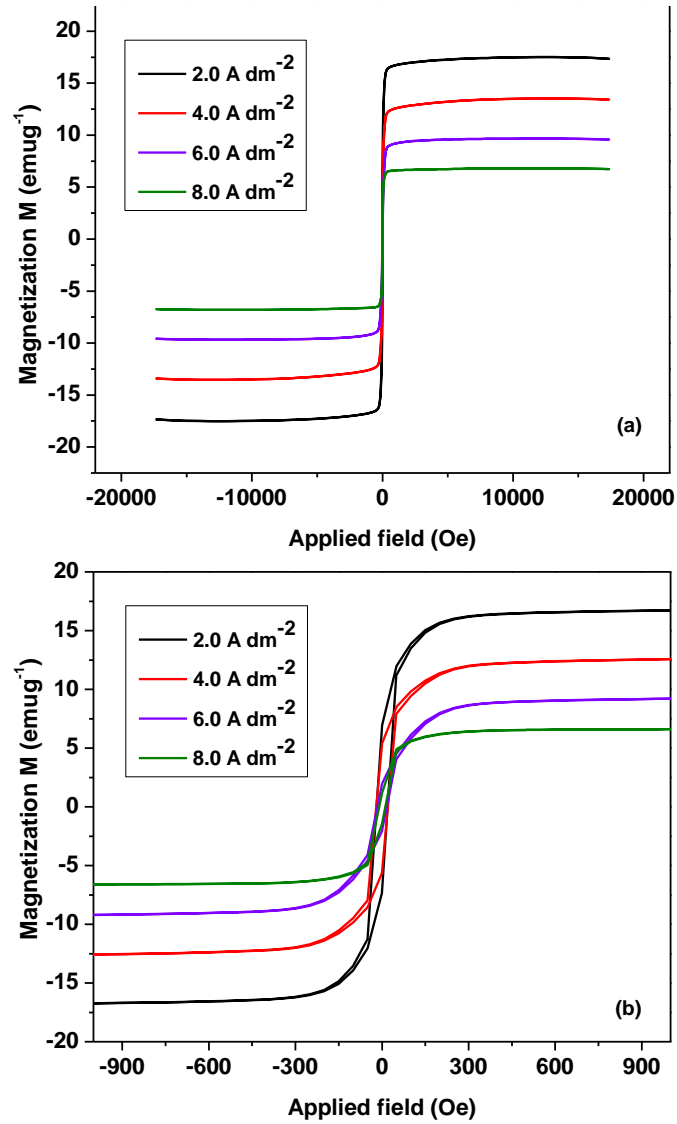
Fig. 6.6. (a) Magnetization curve of Co-Ni coatings deposited at different applied c.d.'s, and (b) enlarged view at close proximity of applied magnetic field

Table 6.3. Variation of saturation magnetization, M_s and coercivity, H_c of electrodeposited Co-Ni alloy with applied c.d.

Applied c.d. ($A \, dm^{-2}$)	M_s (emu g^{-1})	$H_{c,}$ (Oe)
2.0	17.19	19.70
4.0	13.16	18.90
6.0	9.57	16.80
8.0	6.0	11.10
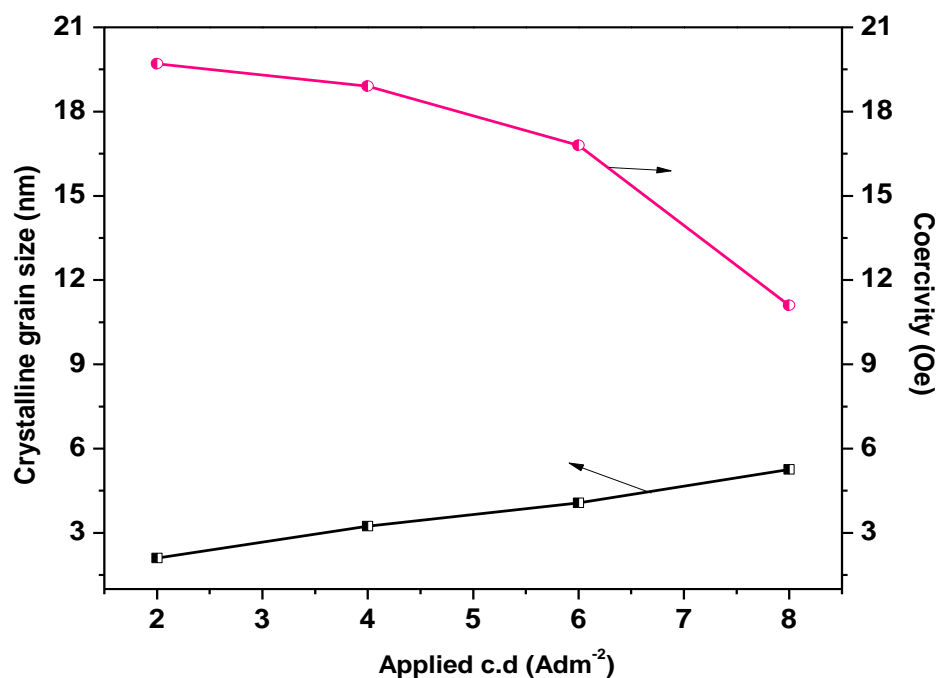
Fig. 6.7. Variation of crystalline grain size and coercivity of electrodeposited Co-Ni alloy over range of applied c.d.

Generally, the grain size and crystal structure has strong influence on the magnetic parameters. The variation of average grain size and coercivity of the coatings, with applied c. d., is shown in Fig. 6.7. The smaller grain size at low c.d. led into the

increased coercivity of the deposited Co-Ni coatings. This is due to the presence of preferential hcp phase having acicular surface structure.

6.3.6 Potentiodynamic polarization study

The corrosion behaviors of electrodeposited Co-Ni alloys have been evaluated by potentiodynamic polarization method, and corresponding diagram is shown in Fig. 6.8. The corrosion rates (CR) were calculated by Tafel's extrapolation method. The corrosion performance of the coatings deposited at different c.d., like 2.0, 3.0, 4.0, 6.0 and 8.0 A dm^{-2} have been evaluated by Tafel's extrapolation method and corresponding corrosion data are reported in Table 6.4. It should be noted that the CR of Co-Ni coatings are not greatly influenced by c.d. unlike in Fe-Co alloy coatings (to be discussed in Chapter 8). This is due to small increase in the Co content of alloy. However, Co-Ni coating at 4.0 A dm^{-2} exhibits least CR (17.64 mm y^{-1}) due to its unique phase structure, having intermediate transitional phase of hcp and fcc, shown in Fig. 6.4. The coexistence of hcp
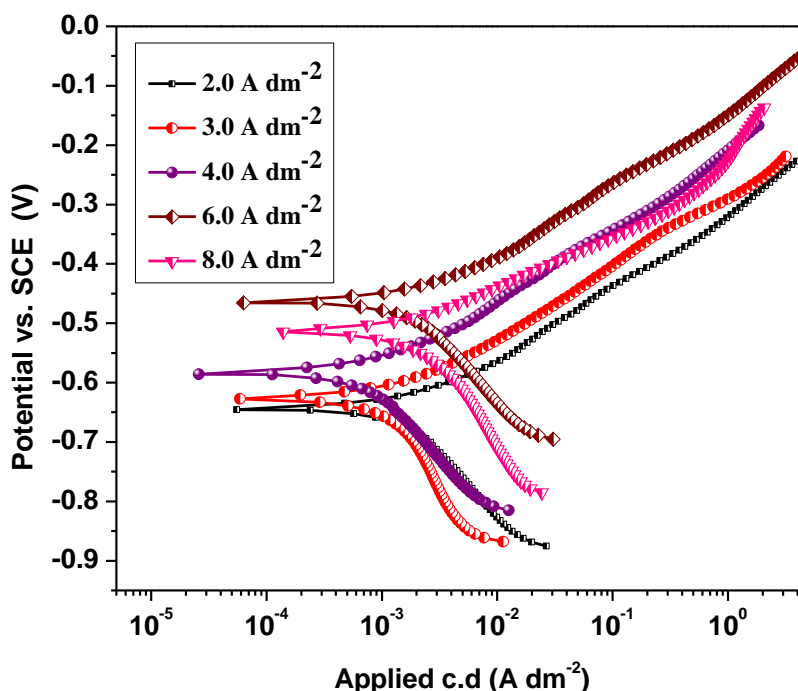
Fig. 6.8. Potentiodynamic polarization behavior of Co-Ni coatings deposited from the optimal bath at different c.d.'s

and fcc phases with smaller grain size is responsible for decreased CR. During this transition, the Co content tends to decrease and Ni tends to increase. Ni being nobler compared to Co, the decrease of CR was observed. But, further increase of c.d. resulted in decrease of CR, and is attributed to high porosity and changed phase structure of the coatings.

Table 6.4. Corrosion parameters of Co-Ni alloy coatings at different c.d.'s, from optimized bath at 303 K

c.d. $(A\ dm^{-2})$	$-E_{corr}$ vs SCE (V)	i_{corr} $(\mu A\ cm^{-2})$	CR $(mm\ y^{-1})$
1. 0	0.675	2297.8	25.56
2. 0	0.644	1974.9	21.97
3. 0	0.625	1816.3	20.20
4.0	0.583	1586.1	17.64
5.0	0.513	1770.8	19.70
6.0	0.463	1843.5	20.50
7.0	0.443	1986.7	22.10
8.0	0.512	2178.9	24.23

6.3.7 Electrochemical impedance spectroscopy

The study for electrodeposited Co-Ni alloy coatings developed at different c.d.'s were subjected to EIS study, instead of depressed semicircle impedance response characteristic of metal/coating interface, the Co-Ni alloy coatings showed pear shaped impedance response at all c.d.'s as shown in Fig. 6.9. i.e., impedance responses were found to be dominated by inductance. The polarization resistance, R_p corresponding to the coating at optimal c.d. i.e. at 4.0 A dm^{-2} is maximum (obtained from intercept of the curve corresponding to the highest value on real axis) and found to be most corrosion

resistant. However the solution resistance, Rs remained to be nearly identical in all cases as the same bath chemistry and cell configuration was used. The inductive loop observed at lower frequency limit of the impedance spectra of all Co-Ni alloys indicates that electrofabricated films exhibit high electrical conductivity.
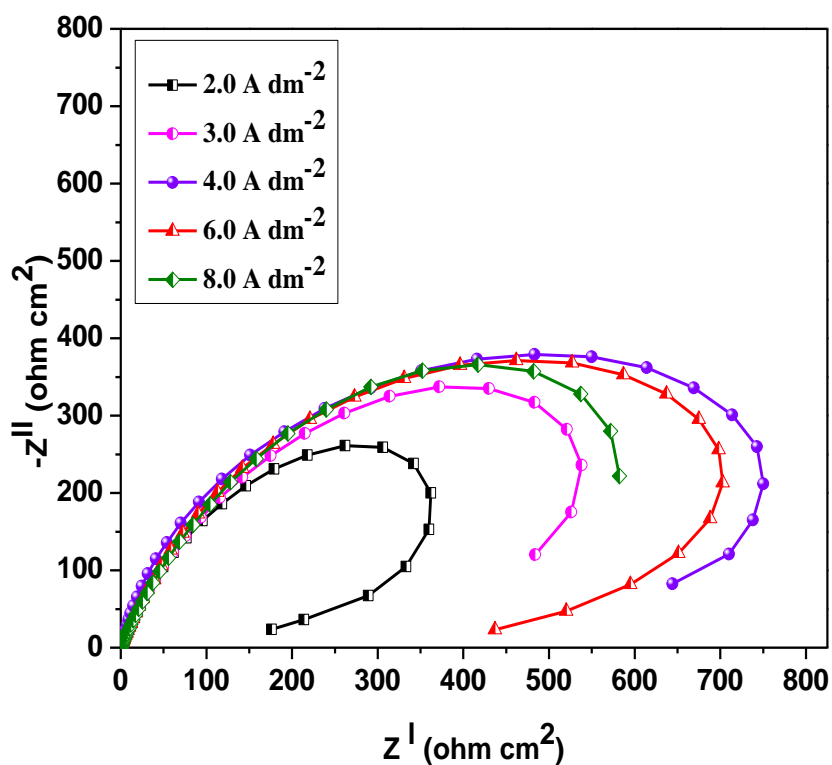
Fig. 6.9. Nyquist response of monolayer Co-Ni coatings developed at different c.d.'s from optimized bath at 303 K

6.4 CONCLUSIONS

The electrodeposition of bright Co-Ni alloy on copper was accomplished using a new sulphate bath and following conclusions were drawn:

1. The bath exhibited anomalous type of deposition over entire range of c.d. studied.

2. The SEM images of Co-Ni alloy deposited at different c.d. verified the structure-property relation of the coatings.

3. The XRD study of binary Co-Ni alloy indicated the structure consists of a substitutional solid solution phase.

4. Corrosion study demonstrated that Co-Ni alloy deposited at 4.0 A dm^{-2}, having ~76 % of Ni is the most corrosion resistant (CR = 17.64 mm y^{-1}). The highest corrosion resistance of the coatings attributed by the coexistence of hcp and fcc phases with smaller grain size.

<div align="right">**CHAPTER-7**</div>

<div align="center">

ELECTRODEPOSITION AND CHARACTERIZATION OF

MULTILAYER Co-Ni COATINGS

</div>

The development of multilayer materials is a subject of increasing interest in the protection, prevention and controlling of corrosion. One of the emerging areas in nano-structured materials research is electrodeposition of metals/alloys with a spatially periodic composition in one dimension, and are called composition modulated multilayer alloy (CMMA) coatings (Rangakrishnan et al. 2002). These coatings with thin layers of pure metals/alloys show wide range of applications owing to their unique technological properties, different from pure metals, or homogenous alloys. Due to increased effect of surface or interface arising from the exceptional thinness of the layers, there can be large deviations from bulk properties and gives new properties to the coatings. The composition and thickness of each individual layer can be manipulated to tailor the desired property of the coating. The overall property of the deposit is then a function of the individual components, the modulation thickness, as well as the structure of the interface. There are many reports pertaining to the improved mechanical strength, wear, elasticity, ductility, electrical, optical and corrosion properties of CMMA materials (Leisner et al. 1996). In so-called single bath technique (SBT) the composition modulation can be achieved with modulation in either current, or potential. The bath compositions applied are usually very similar to those developed for monolayer alloy coatings using direct current (DC). The modulation in composition can also be effected using different types of power patterns, depending on type of gradation required (Roy 2009).

Nanostructured coating by electroplating is a novel aspect of materials science and technology, which allows variation of the grain size in the crystal lattice. Many chemical and physical properties of the coatings can be improved by proper setting up of deposition conditions. Hence, it is possible to tune, and hopefully improve certain

<div align="center">156</div>

physical properties of one and the same material. The production of such "tailor-made" nanomaterials by electrochemical procedures is advantageous because of the two crucial steps of nanocrystal formation– nucleation and growth of nuclei can be controlled by physical (current, voltage, time, temperature), and chemical (grain refiners, complex formers) parameters during the deposition process. Such nanocrystalline materials exhibit considerably different properties than conventional coarse-grained polycrystalline materials. CMMA materials in which successive layers of alloys with alternating composition are created by bringing modulation in deposition process itself, usually by a complex pulse sequence (Kanani 2006).

The multilayer coating that comprises multiple nano/micro scale layers that periodically vary in electrodeposited species, and electrodeposited microstructures show the enhanced corrosion protection. A series of two or more non-identical layers can be repeatedly applied over an underlying surface, and multilayer coatings of desired thickness can be achieved by proper setting up of the power sources. The series of non-identical layers can include a simple alternating pattern of two or more non-identical layers. More complex alternating patters can involve two, three, or more layers arranged in constant or varying sequences. The thickness of individual layers in CMMA coatings can be controlled by, among other parameters the application of current in the electrodeposition process. This technique involves the application of current to the substrate to cause the formation of the coatings on the substrate. The current can be applied continuously or, more preferably, according to a pre-determined pattern such as a waveform. In particular, the waver form (e.g. sine waves, square waves, saw-tooth, or triangle waves) can be applied intermittently to promote the electrodeposition process to increase or decrease the rate of deposition, to alter the composition of the material being deposited.

The state of the art literature reveals that no work with regard to the optimization of deposition condition of multilayer Co-Ni alloy for best corrosion protection has been reported. Hence this chapter details the development of multilayer Co-Ni alloy coating on

copper from SBT using current having dual and triple pulses. The main objective of this chapter is to optimize the deposition condition for development of CMMA Co-Ni using different power pulses and to compare their corrosion performance with that of monolayer coatings. The chapter reports the experimental investigation on CMMA Co-Ni coatings, developed using dual and triple current pulses, in first two sections, followed by comparisons in last section.

SECTION - 7.1: Development and characterization of multilayer Co-Ni coatings using dual current pulse

7.1.1 Development of monolayer and multilayer Co-Ni alloy coating

Monolayer coatings of Co-Ni alloy has been developed on copper, using DC as detailed in Chapter 6. The effect of c.d. on deposit characters were studied in terms of their composition and phase structure. It was found that monolayer Co-Ni alloy, having about 76 % Ni at 4.0 A dm^{-2} was found to show the peak corrosion resistance, compared to at other c.d. Hence, it has been treated as its optimal coating configuration, represented as $(Co-Ni)_{4.0/monolayer}$, showing less corrosion rate (17.64 mm y^{-1}). The corrosion resistance of monolayer Co-Ni coating was tried to improve by multilayer coating technique using dual current pulse. Multilayer Co-Ni coatings were developed on copper by making the cathodic current to change suddenly from one c.d. to another after a definite time by setting suitably the power source. Multilayer coatings, having alternate layers of alloys with different composition were developed using current with dual pulses as shown in Fig. 3.1. The current pulses so generated led to the development of layered coatings with distinct interfaces. All monolayer and multilayer coatings were developed for 10 minutes for comparison purpose using same electrolytic bath.

7.1.2 Optimization of CCCD's

Electrofabrication of multilayer coatings were accomplished at different set of c.d.'s for best possible structural modulation for best corrosion resistance. Multilayer coatings having first layer of one composition and second layer of another composition were developed alternatively to the required thickness, of course up to total 600 s duration. As followed in Section 5.1.2, few sets of CCCD's have been arbitrarily selected (based on appearance and composition of the monolayer alloy), and CMMA coatings have been developed. By fixing the layers to some minimum number (say, 10 layers) to examine the effect of c.d. on corrosion behavior, the multilayer coatings with different configuration were developed and their corrosion rates were evaluated.

Among the various combinations tried, the less corrosion rate was measured in the coatings produced at difference of 2.0 and 4.0 A dm^{-2} (between CCCD's), as shown in Table 7.1. This indicated that at these sets of CCCD's, the coating configuration is the most optimal for better corrosion protection of the substrate. Hence, CMMA coatings having more number of layers have been developed with difference of 2.0 and 4.0 A dm^{-2} between CCCD's as described in the proceeding sections.

Table 7.1. Corrosion rates of multilayer (Co-Ni) coatings at different sets of CCCD's (having 10 layers), developed from optimized bath at 303K

CCCD's (A dm^{-2})	$-E_{corr}$ vs SCE (V)	i_{corr} (μA cm^{-2})	CR (mm y^{-1})
CMMA Co-Ni coatings at difference of 2.0 A dm^{-2} between CCCD's			
(Co-Ni)$_{2.0/4.0}$	0.642	144.27	1.60
(Co-Ni)$_{4.0/6.0}$	0.614	181.32	2.01
(Co-Ni)$_{6.0/8.0}$	0.632	206.75	2.30
(Co-Ni)$_{3.0/5.0}$	0.605	234.55	2.60
CMMA Co-Ni coatings at difference of 4.0 A dm^{-2} between CCCD's			
(Co-Ni)$_{2.0/6.0}$	0.687	158.35	1.76
(Co-Ni)$_{4.0/8.0}$	0.632	202.83	2.25
(Co-Ni)$_{3.0/7.0}$	0.611	297.50	3.30
(Co-Ni)$_{4.0/monolayer}$	0.583	1586.1	17.64

7.1.3 Optimization of total number of layers

Generally during electrodeposition of alloys from their aqueous solution, the c.d. has a complex effect on the composition, structure and properties of the deposit. An increase of c.d. usually causes an increase in the relative amount of the less noble metal

in the plated alloy. Consequently a periodic change in the c.d. brings periodic change in the composition of alloy in individual layers. Thus development of multilayer coating by electroplating technique offers promising route for synthesis of new materials showing novel properties (Cohen et al. 1983). Therefore at optimal CCCD's, multilayer coatings having 20, 60, and 75 layers including 10 layers were developed. The corrosion performance of these coatings was evaluated by potentiodynamic polarization method, and experimental data are reported in Table 7.2. It may be observed that the CR decreased drastically as the number of layers increased. The progressive decrease of CR was found only up to 60 layers, and then increased. Further, it may be noted that decrease of CR were observed in both sets of CCCD's as shown in Table 7.2.

The decrease of CR's in both sets of CCCD's, indicate that the CR is not specific of only the composition of individual layers, but also numbers of interfaces. At optimal configuration there will be appreciable increase of volume fraction of interface or grain boundary regions (analogously to the surface region of nanoparticles), due to layering. Thus the specific surface area has increased enormously on layering. In other words the monolayer coating is dominated by interfaces due to layering. This observation is in support of principles of nano/microstructure multilayer coatings of metals/alloys exhibiting variety of improved functional properties (Gurrappa and Binder 2008).

Out of two CCCD's tried, at 2.0-4.0 A dm^{-2} the multilayer coating with 60 layers, represented as $(Co-Ni)_{2.0/4.0/60/dual}$ showed minimum CR (0.2 mm y^{-1}) relative to monolayer $(Co-Ni)_{4.0}$ alloy coating (17.64 mm y^{-1}). Hence, multilayer coating having $(Co-Ni)_{2.0/4.0/60/dual}$ configuration is taken as optimal. From the total measured thickness (about 15μm), the average thickness of each layer in $(Co-Ni)_{2.0/4.0}$ coating can be calculated. The average thickness of each layer in $(Co-Ni)_{2.0/4.0/60/dual}$ was found to be ~ 250 nm as shown in Table 7.2.

However, an attempt to increase the corrosion resistance further by increasing number of layers has failed. i.e. increase of number of layers beyond 60 has resulted in decrease of CR, as shown by the data in Table 7.2. The increase of CR at high degree of

layering, viz. 75 layers may be ascribed by the less relaxation time for redistribution of solutes in the diffusion layer during plating, as discussed in Chapter 5. The early saturation of layering (beyond which no improvement in corrosion rate was found), i.e. 60 layers may be due to inherent property of Co-Ni alloy coating.

Table 7.2. Decrease of corrosion rate of multilayer Co-Ni coatings with increase in number of layers deposited from optimized bath at 303K in comparison with monolayer coating

CCCD's $(A\ dm^{-2})$	No. of layers	Deposition time for each layer (sec)	Average thickness of layer (nm)	$-E_{corr}$ vs SCE (V)	i_{corr} $(\mu A\ cm^{-2})$	CR $(mm\ y^{-1})$
$(Co-Ni)_{2.0/4.0}$	10	60	1500	0.64	144.2	1.60
	20	30	750	0.65	59.7	0.66
	60	10	250	0.64	18.8	0.20
	75	8	200	0.65	36.5	0.40
$(Co-Ni)_{2.0/6.0}$	10	60	1500	0.68	158.3	1.76
	20	30	750	0.69	69.7	0.77
	60	10	250	0.65	29.6	0.33
	75	8	200	0.68	53.2	0.59
$(Co-Ni)_{4.0/mono}$	monolayer	600	15000	0.583	1586.1	17.64

7.1.4 Corrosion study

i) Potentiodynamic polarization study

The polarization behavior of multilayer $(Co-Ni)_{2.0/4.0}$ coatings, developed using dual current pulses with different number of layers are shown in Fig. 7.1. It was found that the corrosion current (i_{corr}) values have decreased with increase in number of layers up to 60 layers. The progressive decrease of i_{corr} with number of layers indicates that improved corrosion resistances are due to layers of alloys having distinct properties. As discussed before the decrease of CR at higher degree of layering may be attributed to the

less relaxation time for redistribution of metal ions (Co^{2+} and Ni^{2+}) at the diffusion layer, during deposition. At higher degree of layering, the deposition time for each layer is very small. With the result, the metal ions could not relax (against the influence of applied c.d.), and get deposit on cathode with changed composition (Kanani 2006). In other words at higher degree of layering the deposit is tends to become monolayer. i.e. due to exceptional thinning of layers.
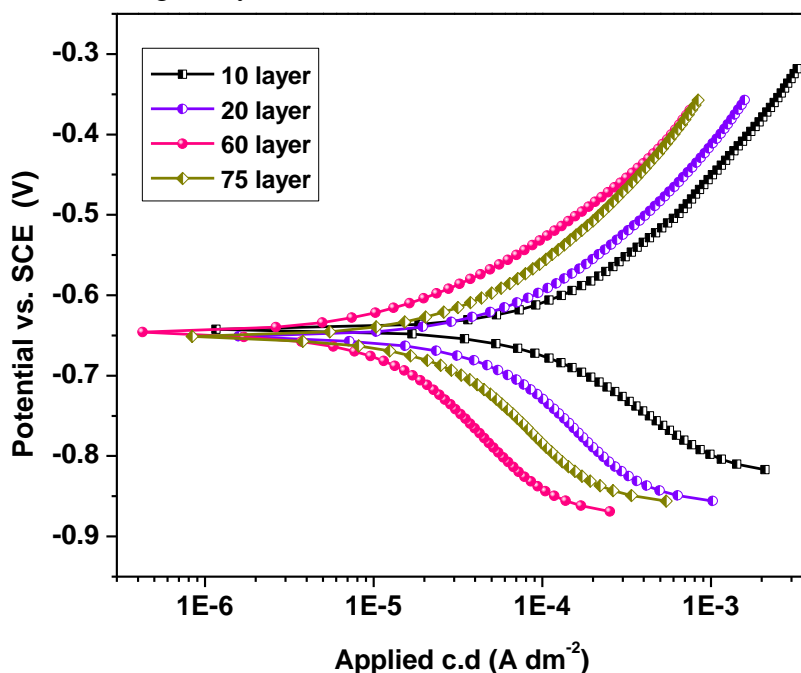
Fig. 7.1. Potentiodynamic polarization curves of multilayer (Co-Ni)$_{2.0/4.0}$ coatings having different number of layers developed using dual current pulses from the optimal bath at 303K

From the corrosion data reported in Table 7.2, it may be observed that (Co-Ni)$_{2.0/4.0/60}$ coating shows ~ 88 times better corrosion resistance than (Co-Ni)$_{4.0/monolayer}$ alloy coatings. Further, the shape of the polarization curves corresponding to the coatings having different number of layers, shown in Fig. 7.1 indicates that the enhanced corrosion protection of Co-Ni multilayer coatings is both anodic and cathodic controlled.

ii) Electrochemical impedance study

Nyquist behaviors of $(Co-Ni)_{2.0/4.0}$ coatings having different number of layers were studied, and are shown in Fig. 7.2. Electrochemical impedance signals clearly indicate that the capacitive reactance increases progressively with number of layers. The electrochemical impedance study is in support of the view that the coating having 60 layers, represented as multilayer $(Co-Ni)_{2.0/4.0/60}$ exhibits the highest corrosion resistance. The decrease of impedance, due to both capacitive reactance and real resistance at lower frequency limit suggests that the electrical conductivity of the coating decreases at all degree of layering, characteristic of Co-Ni alloys. The inductive loop observed at lower frequency limit of the impedance spectra of all multilayer Co-Ni alloys indicate that electrofabricated films exhibit high electrical conductivity.
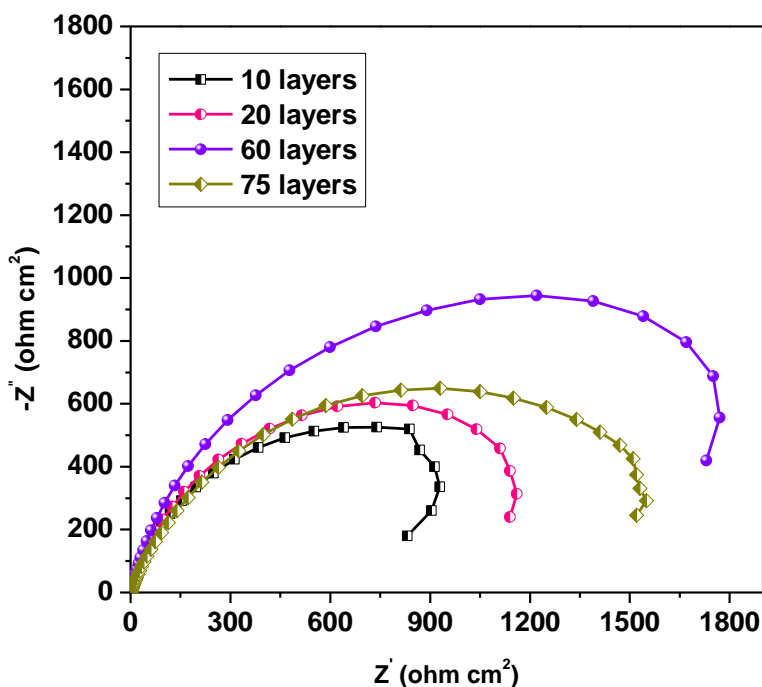
Fig. 7.2. Real versus imaginary resistance values of multilayer $(Co-Ni)_{2.0/4.0}$ coatings with different number of layers measured as function of frequency, developed using dual current pulses from the optimal at 303 K

7.1.5 Dielectric study

The improved corrosion resistance of multilayer coating can also be explained in terms changed dielectric property of the coating due to layering. The equation for the relative permittivity ε_r is given by,

$$\varepsilon_r = \frac{Z_I}{\omega C_0 \left(Z_R^2 + Z_I^2 \right)} \tag{7.1}$$

Where C_0 is the electrical capacitance (given by relation, $C_0 = \varepsilon_0 A/t$) and ε_0 is the permittivity of free space, A is the electrolyte-electrode contact area and t is the thickness of the dielectric medium and $\omega = 2\pi f$, where f is the frequency in Hz. Where, Z_R and Z_I are the real and imaginary parts of complex impedance spectra, Z^* given by $Z^* = Z_R + jZ_I$, where j is complex number. The ε_r being the measure of stored electrical energy associated with C_0, its variation with number layers can be studied. The plot of the relative permittivity, ε_r of multilayer (Co-Ni)$_{2.0/4.0}$ coatings having different number of layers vs. frequency is shown in Fig. 7.3.
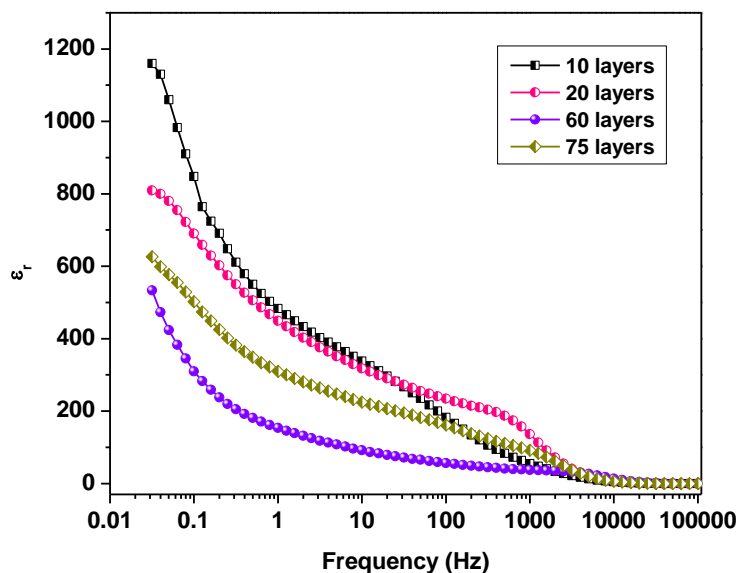
Fig. 7.3. Variation of dielectric constant of multilayer (Co-Ni)$_{2.0/4.0}$ coatings having different number of layers as function of frequency, developed from the optimal bath at 303 K

It may be noted that at low frequency limit, the dielectric constant decreases with increase in number of layers, and at higher frequency limit, it reaches a constant value. The variation in dielectric constant with frequency is due to the Maxwell–Wagner type of interfacial polarization and is in agreement with Koop's phenomenological theory (Aarti et al. 2010, Koops 1951, Maxwell 1973, Ravinder and Latha 1999). This behavior can be explained by assuming the mechanism of dielectric polarization, which is similar to that of conduction mechanism explained by Heikes and Johnston (1957). Thus the peak corrosion resistance of multilayer $(Co-Ni)_{2.0/4.0/60}$ coating is attributed to the decreased relative permittivity of the coating at the interface of substrate and corroding medium.

7.1.6 SEM Study

The surface morphology of $(Co-Ni)_{2.0/4.0/60}$ coating marked as (a) in Fig. 7.4 displays crack-free surface before subjecting to undergo corrosion. The successive layers of alloys, formed during deposition were confirmed by SEM analysis. The cross-sectional view of multilayer (Co-Ni) coating having 60 layers is shown in Fig. 7.4(b).

Fig. 7.4. SEM images of multilayer (Co-Ni) coating: (a) surface morphology of (Co-Ni)$_{2.0/4.0/60}$ coatings, and (b) cross-sectional view of (Co-Ni)$_{2.0/4.0/60}$ coating having 60 layers (diffused part is due to silver paste used for polishing the edge)

167

SECTION - 7.2: Development and characterization of multilayer Co-Ni coating using triple current pulse
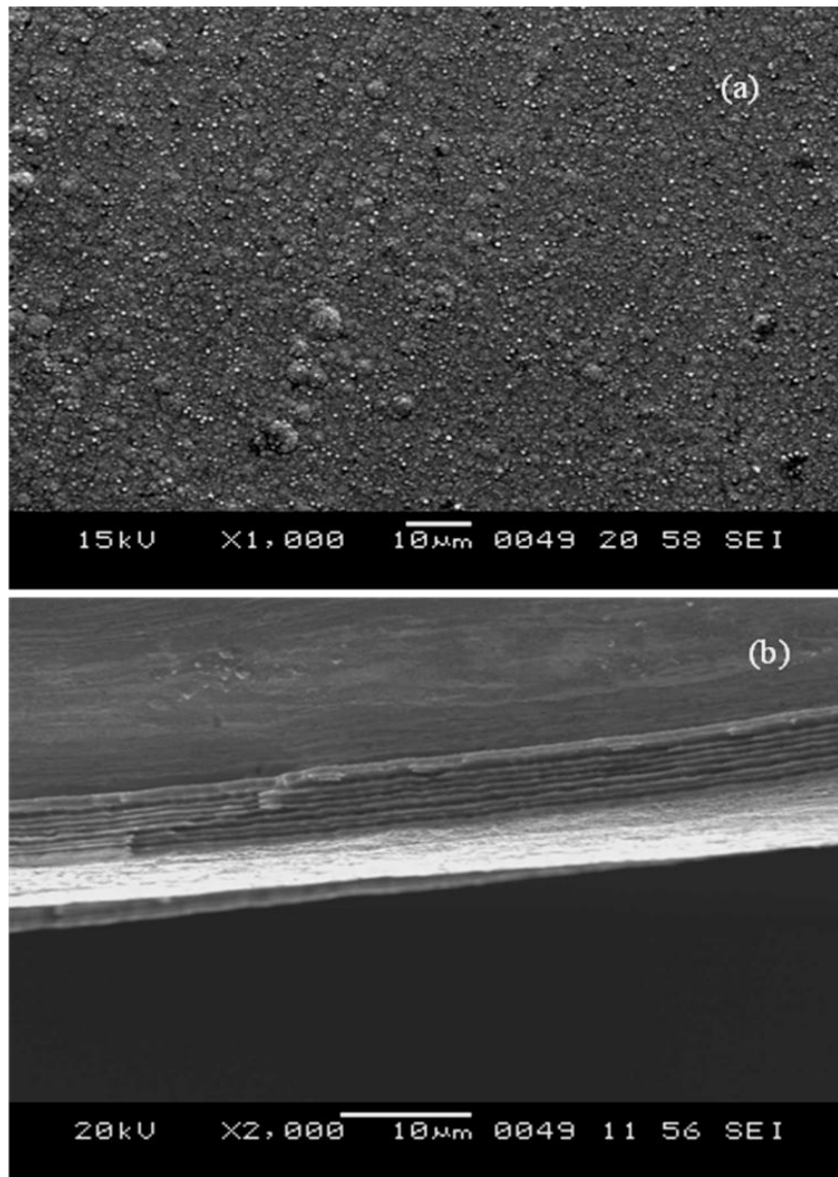
The term nanomaterial includes materials consisting of, or containing individual nanoparticles, nanorods, nanowires or nanoplatelets (for instance as composites), materials in the form of thin layers or coatings, and compact polycrystalline materials with grain sizes below 100 nm size. Magnetic and mechanical properties are examples of properties which, even for coarse-grained materials depend on grain boundaries and volume fraction. Therefore, bulk nanomaterials with large volume fraction exhibit pronounced nano-effects, which is the basis for the academic and industrial interest of nanostructured materials. Hence CMMA coating consisting of periodically changing layers of two different compositions are of crucial importance for imparting the better material properties (Despic and Jovic 1989). With this incentive multilayer coatings of Co-Ni alloy have been tried with triple current pulses. Co-Ni alloy deposited at 4.0 A dm^{-2}, represented as $(Co-Ni)_{4.0/monolayer}$, from the proposed bath (Section 6.2.1) is found to be 17.64 mm y^{-1}. This section details the experimental investigation on production and characterization of multilayer coatings of Co-Ni alloy using same optimal bath. The experimental procedure followed for optimization of deposition conditions for production of multilayer Co-Ni alloys is same as in Section 6.2.

7.2.1 Optimization of CCCD's

To achieve the most optimal configuration for best corrosion protection, the multilayer coatings have been carried out using triple current pulses at different sets of CCCD's as shown in Table 7.3. The experimental observation revealed that Co-Ni alloy at 2.0/4.0/6.0 and 2.0/5.0/8.0 A dm^{-2}, having 10 layers are the most corrosion resistant, and same sets have been selected for studying the effect of layering.

7.2.2 Optimization of total number of layers

Based on the corrosion performance of multilayer coatings, developed using triple current pulses at two sets of CCCD's namely, 2.0/4.0/6.0 and 2.0/5.0/8.0 A dm^{-2}, they

have been selected for further layering. Multilayer Co-Ni coatings with 20, 60 and 75 layers were developed and their corrosion data are reported in Table 7.4. It may be observed that the CR of coatings decreased with number of layers in both sets of CCCD's as shown in Table 7.4. However, at 2.0/4.0/6.0 A dm^{-2}, the coating with 60 layers showed minimum CR (0.11 mm y^{-1}), relative to 17.64 mm y^{-1} for monolayer Co-Ni alloy coating.

Table 7.3. Corrosion rate (CR) of Co-Ni multilayer coatings, developed from the optimized bath at different set of CCCD's (with 10 layers)

CCCD's (A dm^{-2})	$-E_{corr}$ vs SCE (V)	i_{corr} ($\mu A\ cm^{-2}$)	CR (mm y^{-1})
CMMA Co-Ni coatings developed at difference of 2.0 A dm^{-2} between CCCD's			
(Co-Ni)$_{2/4/6}$	0.625	62.9	0.70
(Co-Ni)$_{1/3/5}$	0.620	95.7	1.03
(Co-Ni)$_{3/5/7}$	0.644	118.1	1.27
(Co-Ni)$_{4/6/8}$	0.647	137.3	1.48
CMMA Co-Ni coatings developed at difference of 3.0 A dm^{-2} between CCCD's			
(Co-Ni)$_{2/5/8}$	0.644	85.36	0.92
(Co-Ni)$_{1/4/7}$	0.636	152.08	1.64

It may be noted that decrease in of CR were observed with increased number of layers in both CCCD's. This is due to the fact that property of nano-structure materials are affected by both composition and number of interfaces as discussed in Section 7.1. Though there is substantial decrease of CR with layering even at 2.0/4.0/6.0 A dm^{-2} as shown in Table 7.4, the result pertaining to 2.0/4.0/6.0 A dm^{-2} is more encouraging.

Hence, (Co-Ni)$_{2.0/4.0/6.0/60}$ has been proposed as the optimal configuration for development of multilayer coating from the proposed bath, and can be represented as (Co-Ni)$_{2.0/4.0/6.0/60/triple}$.

Table 7.4. Decrease of corrosion rate (CR) of multilayer Co-Ni coatings, developed from the optimized bath with increase in number of layers in comparison with monolayer coating

CCCD's (A dm^{-2})	No. of layers	Deposition time for each layer (sec)	Average thickness of layer (nm)	$-E_{corr}$ vs SCE (V)	i_{corr} (μA cm^{-2})	CR (mm y^{-1})
	10	60	1500	0.625	62.9	0.70
(Co-Ni)$_{2.0/4.0/6.0}$	20	30	750	0.629	34.9	0.38
	60	10	250	0.633	10.0	0.11
	75	8	200	0.624	29.6	0.33
	10	60	1500	0.644	85.3	0.92
(Co-Ni)$_{2.0/5.0/8.0}$	20	30	750	0.649	81.7	0.88
	60	10	250	0.662	42.3	0.45
	75	8	200	0.668	73.4	0.79
(Co-Ni)$_{4.0/mono}$	monolayer	600	15000	0.583	1586.1	17.64

7.2.3 Corrosion study

i) Tafel's polarization study

The corrosion behavior of (Co-Ni)$_{2.0/4.0/6.0/triple}$ coatings having different degree of layering is shown in Fig. 7.5. It may be observed that the corrosion current (i_{corr}) values decreased with increase in number of layers. Significant decrease in i_{corr} value was observed, when number of layers was increased, as reported in Table 7.3. However, at higher degree of layering no improvement in corrosion resistance was found, explained

by the reasons discussed in Section 7.1.2. The shape of Tafel plots shown in Fig. 7.5 demonstrates that Co-Ni alloys developed using even triple current pulses are also exhibit anodic and cathodic controlled corrosion protection. Further, the constancy of $E_{corr,}$ regardless of number of layers indicate that extended protection of multilayer coatings is due to only layering, not due to exterior surface of the coating.
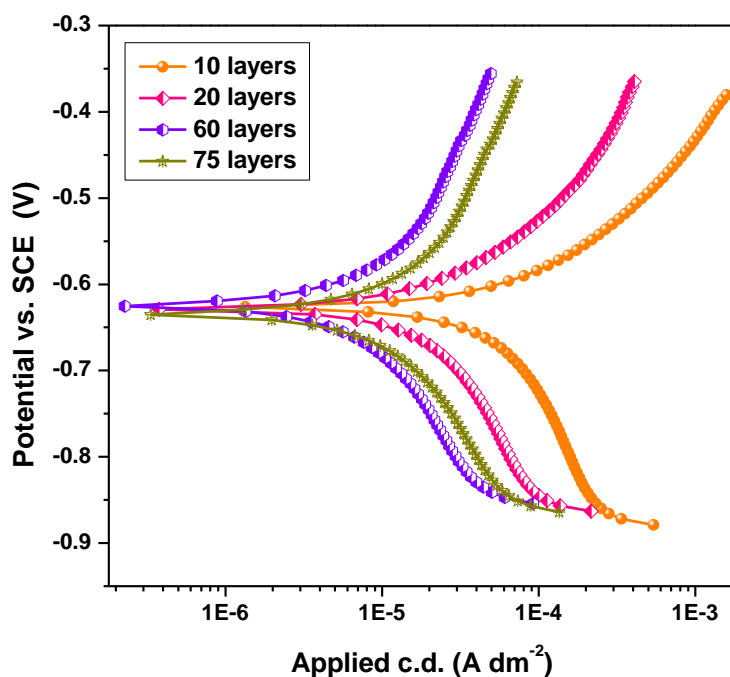
Fig. 7.5. Potentiodynamic polarization curves of $(Co-Ni)_{2.0/4.0/6.0/triple}$ coatings with different number of layers, developed from optimized bath at 303 K

ii) Electrochemical impedance study

EIS is a useful technique for ranking coatings, assessing interfacial reactions, quantifying coating breakdown, and predicting the lifetime of coating/metal systems. Advantages of this technique over DC technique include the absence of any significant perturbation to the system, its applicability to the assessment of low conductivity media, and the existence of a frequency component that may provide mechanistic information. The Nyquist response of multilayer $(Co-Ni)_{2.0/4.0/6.0}$ coatings with different number of layers is shown in Fig. 7.6. The inductive loop observed at lower frequency limit of the

impedance spectra for all (Co-Ni)$_{2.0/4.0/6.0}$ coatings indicate that electrofabricated films exhibit better conductivity as seen in Section 7.1.
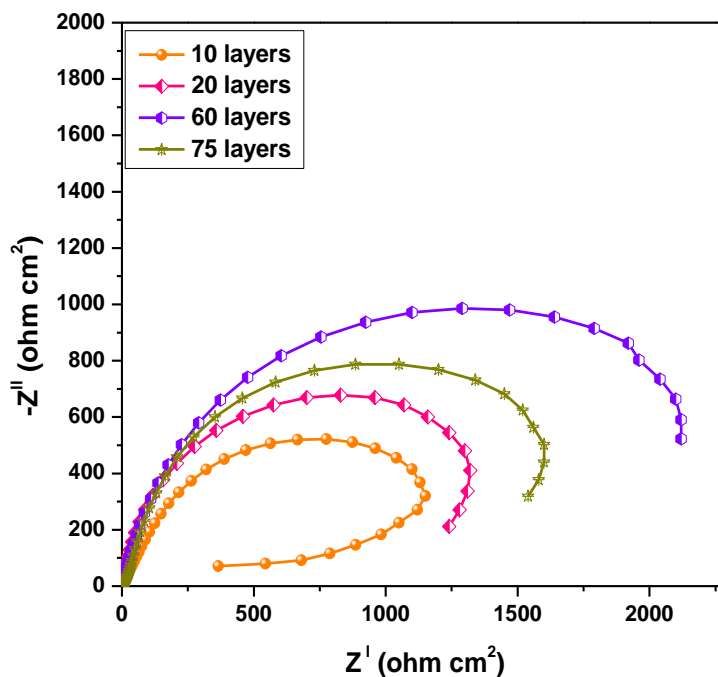
Fig. 7.6. Real versus imaginary resistance values of (Co-Ni)$_{2.0/4.0/6.0}$ coatings having different number of layers measured as function of frequency, developed from optimized bath at 303 K

At high frequency limit, all electroplates exhibited R$_{real}$ = 0, indicating that the solution resistance (Rs) is same for all analysis. Increase in the radius of the semicircle with increase in number of layers showed that the capacitive reactance of the double layer, responsible for improved corrosion resistance increased with layering. The high corrosion resistance at optimal layers (60 layers) is evidenced by bigger semicircle (incomplete), caused by large capacitive reactance. Nyquist plots with incomplete semi circles at low frequency limit indicated that the corrosion behavior of the coatings is not controlled only by charge transfer resistance, R$_{ct}$ but also by capacitive reactance.

7.2.4 Dielectric barrier of CMMA coatings

Fig. 7.7 shows the variation of relative permittivity, ε_r versus frequency of the coatings having different number of layers. It was observed that the value of ε_r for all coatings is high at low frequency which are diminished as the frequency is increased. At low frequency side, the decrease of ε_r with increase in number of layers indicate that the dielectric barrier of coating has increased with layering. This attributes to the increased interfacial polarization effect, caused by the heterogeneous media consisting of phases with different dielectric permittivity (Kouloumbi et al. 1996).
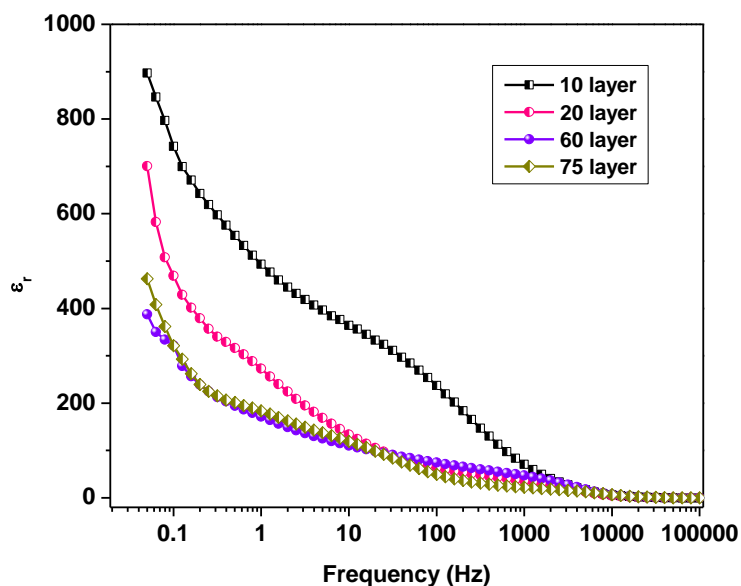
Fig. 7.7. Variation of dielectric constant of $(Co-Ni)_{2.0/4.0/6.0}$ coatings having different number of layers as function of frequency, developed from the optimal bath at 303 K

There are many causes for heterogeneity in materials, but concerning the multilayer coatings in the present work, is related to interfaces created by electron charge density. Thus the peak corrosion resistance of multilayer coating is due to the decreased ε_r of the coating.

7.2.5 SEM study

The SEM image displaying the cross sectional view and decayed surface (after corrosion test) of $(Co-Ni)_{2.0/4.0/6.0/20/triple}$ coating is shown in Fig. 7.8. This confirms the

173

formation of 20 layers in micrometric level, responsible for delayed decay of the coatings. The microscopic appearance of the surface after corrosion test is shown in Fig. 7.8(b).
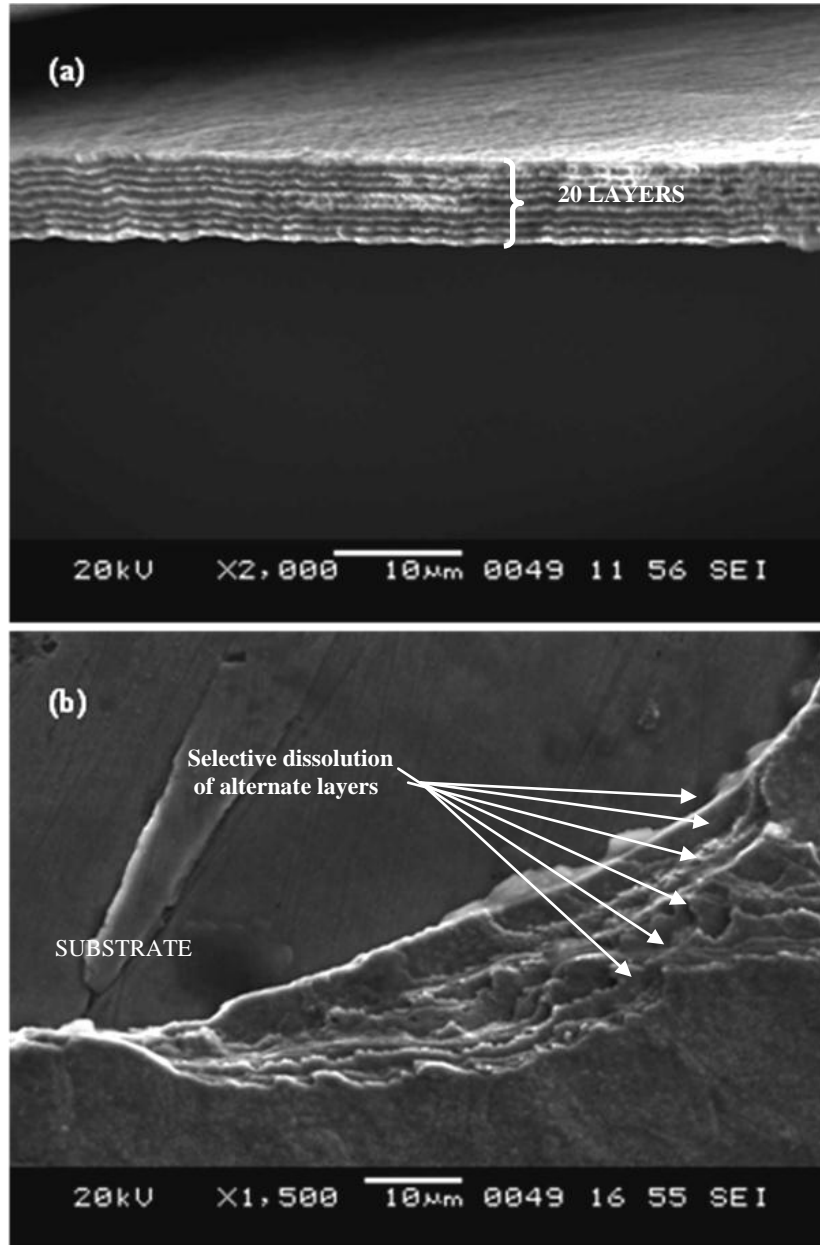
Fig. 7.8. SEM images of multilayer (Co-Ni) coatings: (a) Cross-sectional view of alloy having 20 layers and (b) multilayer (Co-Ni)$_{2.0/4.0/6.0}$ after corrosion test.

The selective dissolution of layers having alternatively different composition, shown by arrow marks may be seen. The possibility of high corrosion prevention of CMMA coatings can be explained as follows: Different degree of failures, like pores and crevices due to different wt. % of Co in alternate layers which are put down in the deposition process may be neutralized by the successively deposited coating layers (Dobrzanski et al. 2005). Due to layered coating the corrosive agent needs more time to penetrate through coating than in monolayer coating. In other words, the corrosive agent path is extended or blocked.
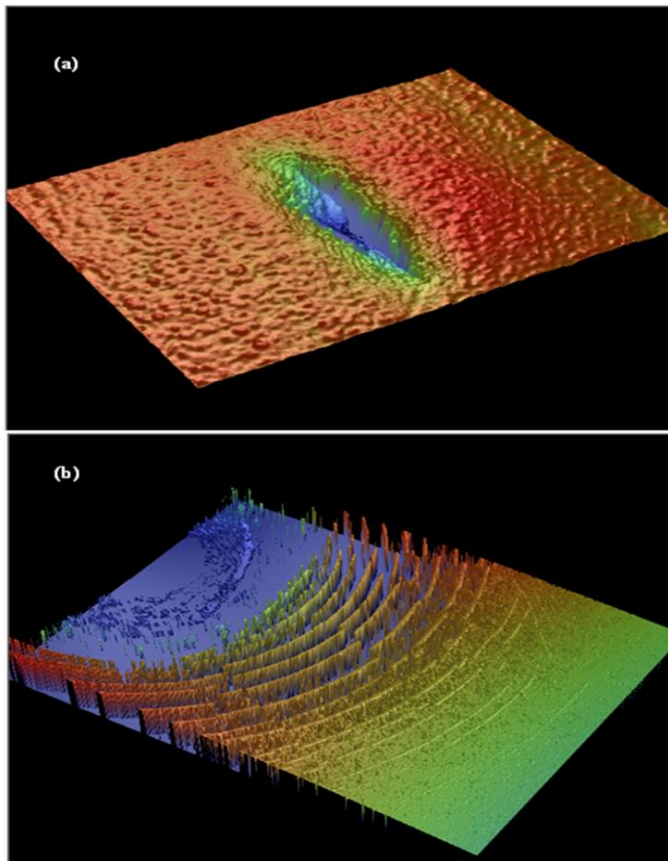
Fig. 7.9. Three dimensional (3-D) image of (a) monolayer $(Co-Ni)_{4.0}$ and (b) multilayer $(Co-Ni)_{2.0/4.0/6.0/60/triple}$, after corrosion test

As a whole, the protection efficacy of (Co-Ni)$_{2.0/4.0/60/triple}$ coatings may be explained by the barrier effect of Co-Ni layers having varied Ni content. A small change in wt. % of noble metal in the alloys layer is good enough to bring large change in the phase structure of the individual layers (Ganeshan et al. 2007).

A comparison of three dimensional (3–D) optical profilograms of monolayer (Co-Ni)$_{4.0}$ and (Co-Ni)$_{2.0/4.0/6.0/60/triple}$ coatings after corrosion test is shown in Fig. 7.9. It may be noted that the deformation of monolayer and multilayer coatings occurs in uniform and graded manner as shown in Fig. 7.9(a) and Fig. 7.9(b), respectively. This supports the selective breaching of layers having alternatively changing compositions, responsible for better corrosion protection of the coatings.

SECTION - 7.3: Comparison of corrosion performance of monolayer, and multilayer Co-Ni coatings developed using dual and triple current pulses

To identify the effect of current pulses on corrosion performance of CMMA Co-Ni alloy coatings, the depositions were carried out using dual and triple current pulses, and experimental results were reported in Sections 7.1 and 7.2. The corrosion performance of CMMA coatings were showed with that of monolayer Co-Ni alloy coating, represented as $(Co-Ni)_{4.0/monolayer.}$ A comparative account of corrosion data of multilayer coatings developed using dual and triple current pulses with $(Co-Ni)_{4.0/monolayer}$ developed using same electrolytic bath for same time is given in Table 7.5. The corrosion data reveals that multilayer coating systems are more corrosion resistant than corresponding monolayer alloy coating.

Table 7.5. Comparison of corrosion rates of monolayer $(Co-Ni)_{4.0}$, multilayer $(Co-Ni)_{2.0/4.0/dual}$ and $(Co-Ni)_{2.0/4.0/6.0/triple}$ coatings developed using dual and triple current pulses under optimal conditions, for same time.

Coating configuration	$-E_{corr}$ vs SCE (V)	i_{corr} (μA cm^{-2})	CR (mm y^{-1})
$(Co-Ni)_{2.0/4.0/60/dual}$	0.644	18.8	0.20
$(Co-Ni)_{2.0/4.0/6.0/60/triple}$	0.633	10.0	0.11
$(Co-Ni)_{4.0/monolayer}$	0.583	1586.1	17.64

The polarization behaviors of $(Co-Ni)_{4.0}$, $(Co-Ni)_{2.0/4.0/60/dual}$, and $(Co-Ni)_{2.0/4.0/6.0/60/triple}$ coatings (all under optimal conditions) are shown in Fig. 7.10. The corrosion current, i_{corr} decreased drastically when coating process is changed from monolayer to multilayer type. It may be observed that the corrosion protection of $(Co-Ni)_{2.0/4.0/60/dual}$ coating is ~88 times better (0.2 mm y^{-1}) than that of monolayer $(Co-Ni)_{4.0}$

alloy (17.64 mm y^{-1}), deposited for same length of time. Further, the coating having (Co-Ni)$_{2.0/4.0/6.0/60/triple}$ (0.11 mm y^{-1}) configurations exhibit ~160 times better corrosion resistance compared to (Co-Ni)$_{4.0}$ alloy. The observed high corrosion resistance of the multilayer coatings is attributed to the increased number of interfaces due to layering. It may be noted that there is no significant difference the corrosion performance of CMMA coatings developed using double and triple current pulses.

This indicates that improved corrosion protection is more a function of number of interfaces, than the composition of individual layers. The protection efficacy of the multilayer (Co-Ni) coatings can be related to the barrier effect of the alloys in alternate layers. Relative impedance response of (Co-Ni)$_{4.0/monolayer}$, multilayer (Co-Ni)$_{2.0/4.0/60/dual}$ and (Co-Ni)$_{2.0/4.0/6.0/60/triple}$ alloy coating systems are given in the Fig. 7.11.
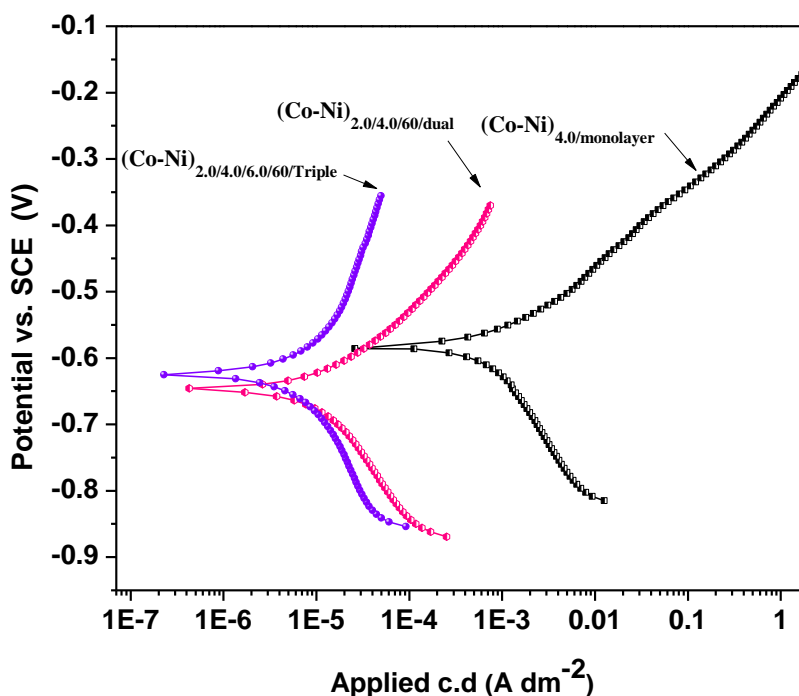
Fig. 7.10. Potentiodynamic polarization behaviors of (Co-Ni)$_{4.0/monolayer}$, (Co-Ni)$_{2.0/4.0/60/dual}$ and (Co-Ni)$_{2.0/4.0/6.0/60/triple}$ coatings developed from same bath

178

The impedance signals showed that the substantial decrease of corrosion rate is due to decreased capacitance and increased dielectric barrier of the coatings. Among different current pulses used, the coatings developed using triple current pulses exhibited highest corrosion resistance, may be due to more modulation caused by three current pulses.
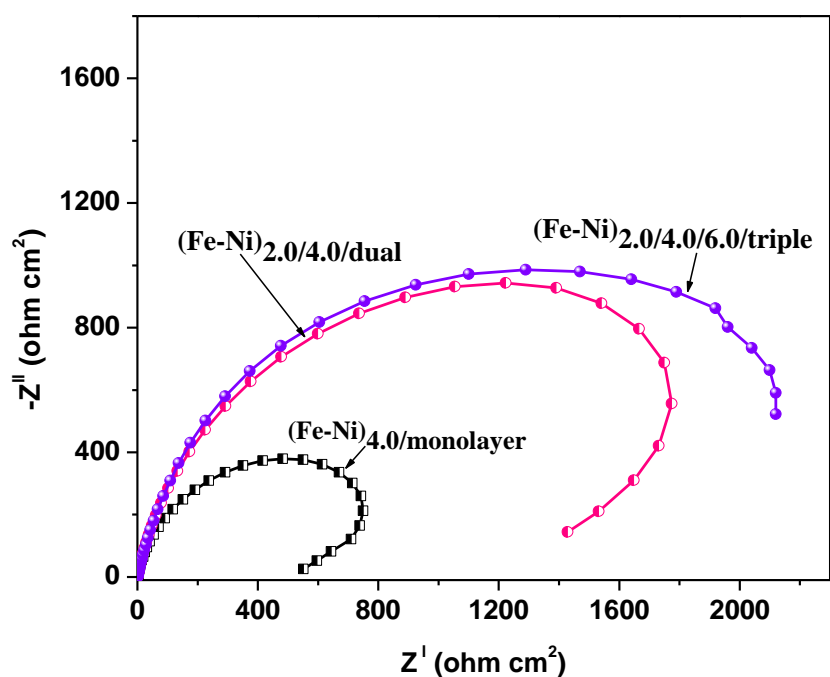
Fig. 7.11. Relative response (Nyquist) of (Co-Ni)$_{4.0/monolayer}$, (Co-Ni)$_{2.0/4.0/60/dual}$ and (Co-Ni)$_{2.0/4.0/6.0/60/triple}$ coatings deposited from the same bath at 303 K (under optimal conditions)
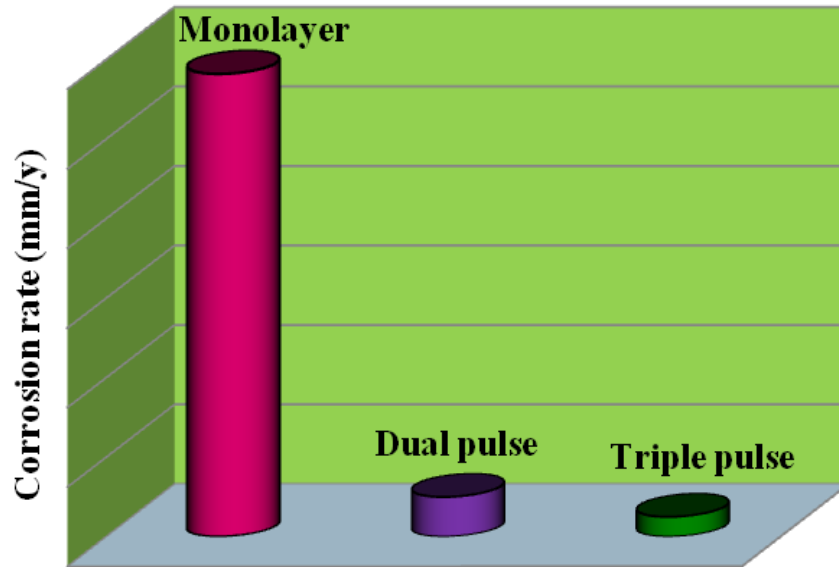
Fig. 7.12. Comparative account of corrosion rates of $(Co\text{-}Ni)_{4.0/monolayer}$, $(Co\text{-}Ni)_{2.0/4.0/60/dual}$ and $(Co\text{-}Ni)_{2.0/4.0/6.0/60/triple}$ coatings in 1 M HCl solution, developed from same bath at 303 K

A comparative account of corrosion rates of multilayer Co-Ni coatings developed using dual and triple current pulse, in comparison with that of monolayer alloy deposited from same bath in 1 M HCl solution is shown in Fig. 7.12. It may be concluded that the multilayer Co-Ni coatings are more corrosion resistant than monolayer Co-Ni coatings developed from same bath.

7.3.1 Conclusions

A multilayer coating having nano/micro scale sublayers have been developed on copper substrate using dual and triple current pulses and following conclusions were drawn.

1. The multilayer Co-Ni coatings developed using dual current pulses were shown to be more corrosion resistant (about 88 times) than monolayer Co-Ni coatings developed from same bath.

2. Even a small difference in the wt. % of Co in consecutive layers was sufficient to change significantly the corrosion resistance. The corrosion resistances were found to increase with number of layers only up to 60 layers and then decreased.

3. Under optimal conditions, CMMA (Co-Ni) coatings developed using dual and triple current pulses were found to be respectively, about 88 and 160 times more corrosion resistant than $(Co-Ni)_{4.0/mono}$ alloy coating, deposited from same bath for same time.

4. The corrosion resistance of multilayer coatings produced by SBT was shown to be higher than that of the monolayer coatings, developed from the same bath. i.e. multilayer $(Co-Ni)_{2.0/4.0/6.0/60/triple}$ showed ~160 times better corrosion resistance compared to $(Co-Ni)_{4.0/monolayer}$ alloy obtained from same bath.

<div align="right">

CHAPTER 8

</div>

<div align="center">

**ELECTRODEPOSITION OF MONOLAYER Fe-Co ALLOY COATINGS
AND THEIR CHARACTERIZATION**

</div>

8.1 INTRODUCTION

In last few decades a decisive advance has been made in the field of development of soft magnetic films for industrial use. This is due to the fact that they exhibit low coercive field, low hysteresis loss, low eddy current loss, high electric permeability and high saturation magnetization (Shao et al 2003). Among ferromagnetic materials, Fe-Co alloys have the highest saturation magnetization value (2.4 T) and hence find applications in computer memories. The coercivity of Fe-Co alloys is relatively high, and studies have been carried out to decrease coercivity of these alloys. Recent advances in the area of nanocrystalline materials have shown that grain size reduction in ferromagnetic materials can bring significant reduction in coercivity value with no effect on their saturation magnetization. The electrodeposition technique is one of the best routes for production of such nanocrystalline coatings.

The growth mechanism, morphology and microstructural properties of the electrodeposited films depend on electrodeposition conditions such as electrolyte composition, electrolyte pH and deposition current/potential etc. The electrolyte pH and concentration of both Co^{2+} and Fe^{2+} were observed to change significantly the magnetic and corrosion behaviors of the deposit (Osaka 2000). The results embodied in this chapter are pertaining to optimization of a new Fe-Co bath for production of the coating showing maximum susceptibility against corrosion. The bath chemistry and deposition conditions were optimized, combined with analyzing their structure, magnetic properties and corrosion protection ability. The effect of c.d. on composition, phase structure and morphology of the deposits were studied. The monolayer Fe-Co alloy coatings have been

accomplished using direct current (DC) with no modulation in current, and hence in the structure of alloy.

8.2 OPTIMIZATION OF Fe-Co ALLOY BATH

The optimization of a new Fe-Co alloy bath has been done by conventional Hull cell method. A wide spectrum of Fe-Co alloys (having varying composition) formed on Hull cell panel showed that c.d. plays an important role in deciding the structure and properties of deposits. The ascorbic acid (AA) was used at constant concentration to give stability to the bath. The AA being an antioxidant prevented the possible oxidation of Fe^{2+} into Fe^{3+}. The procedure discussed in Section 4.2 was followed for optimization of the bath. The optimal bath constituents and operating parameters, after Hull cell experiment is given in Table 8.1. The deposit over the full range of Hull cell panel was found to be bright, i.e. in the range of 1.0-8.0 A dm^{-2}. Hence Fe-Co alloy having varied compositions were developed at different current densities, keeping anode and cathode parallel to each other from the bath shown in Table 8.1. The effect of c.d. on wt. % of Fe, surface morphology, phase structure, hardness, and crystallite grain size of the coatings are discussed in the following sections.

Table 8.1. Composition and operating parameters of the proposed bath for electrodeposition of bright Fe-Co alloy on copper

Bath ingredients	Composition (g L^{-1})	Operating parameters
$CoSO_4. 7H_2O$	152.0	c.d. : 1.0-8.0 A dm^{-2}
$FeSO_4. 7H_2O$	16.0	pH : 3.5
Boric acid, H_3BO_3	30.0	Temperature: 303K
L-Ascorbic acid, AA	8.0	Anode: Stainless steel
Sulphanilic acid, SA	1.0	Cathode: Copper

Electroplating was carried out at different c.d.'s, viz. 1.0, 2.0, 3.0, 4.0, 5.0, 6.0, 7.0 and 8.0 A dm^{-2} using constant current source (N 6705A, Agilent Technologies, USA).

The experimental procedure adopted for production and characterization of Fe-Co alloy is same as discussed in Chapter 4.

8.3 RESULTS AND DISCUSSION

8.3.1 Effect of current density

i) Wt. % of Co in the deposit

It was found that the wt. % of more readily depositable metal, i.e. Fe in the deposit decreased (or Co content increased) with increase of c.d. as shown in Fig. 8.1 and Table 8.2. This behavior is in compliance with anomalous codeposition, characteristic of mutual alloys of Fe-group metals. It should be noted that in present Fe-Co alloy coating, the wt. % of Co and Fe in the bath is found to be 90.83 % and 9.17 %, respectively.
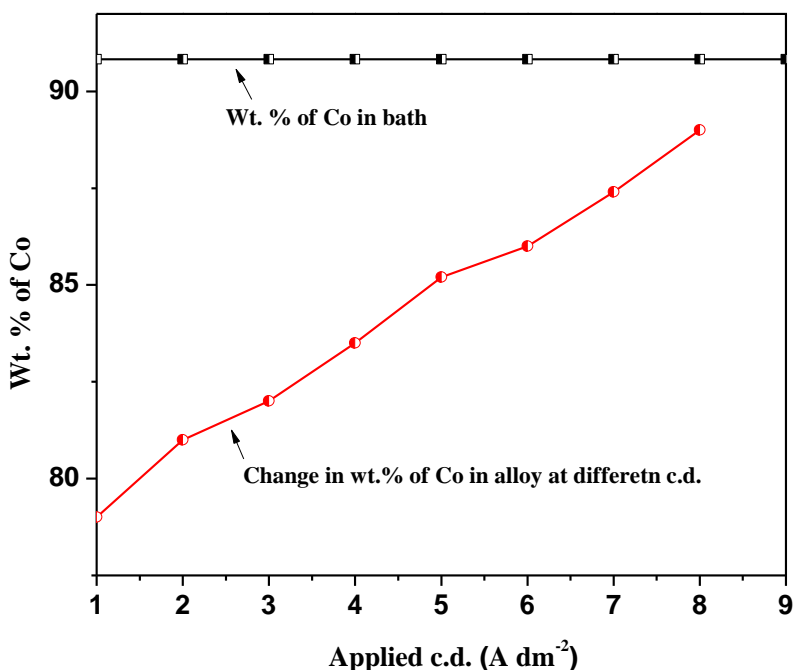
Fig. 8.1. Change in wt. % of Co in the deposit with applied c.d., deposited from optimal Fe-Co bath at 303 K (horizontal line represents wt. % Co in bath)

Further, it was observed that at c.d. more than 2.0 Adm^{-2}, the wt. % of Co in the deposit was found to increase with c.d. At 4.0 Adm^{-2}, the bath produced a bright and sound deposit having ~ 83 wt. % of Co. This increase in Co content with c.d. (Fig. 8.1)

indicates that the deposition process is tending towards normal type. It may be explained by the fact that at high c.d., more readily depositable metal, i.e. Fe is depleted at the cathode film leading to increased wt. of Co in the alloy (Brenner 1963). However, at low c.d., the wt. % of Fe in the deposit was found to be more due to pronounced effect of anomalous codeposition. It may be explained through less evolution of H_2, consequent to decreased rate of deposition. This leads to less alkalinization at the close vicinity of the cathode film, to prevent diffusion of noble metal ions (Co^{2+}) and their deposition on cathode. This is generally known as hydroxide suppression mechanism. It should also to be noted that under no conditions of c.d. studied, the wt. % of Co in the deposit was more than that in the bath. In other words, the bath followed anomalous codeposition at all c.d's. studied.

ii) Partial current density and cathode current efficiency

Fig. 8.2 shows the dependence of partial current densities of single metals, i.e. Fe and Co at various applied current densities. Partial current densities of individual metals were found to increase with applied c.d.
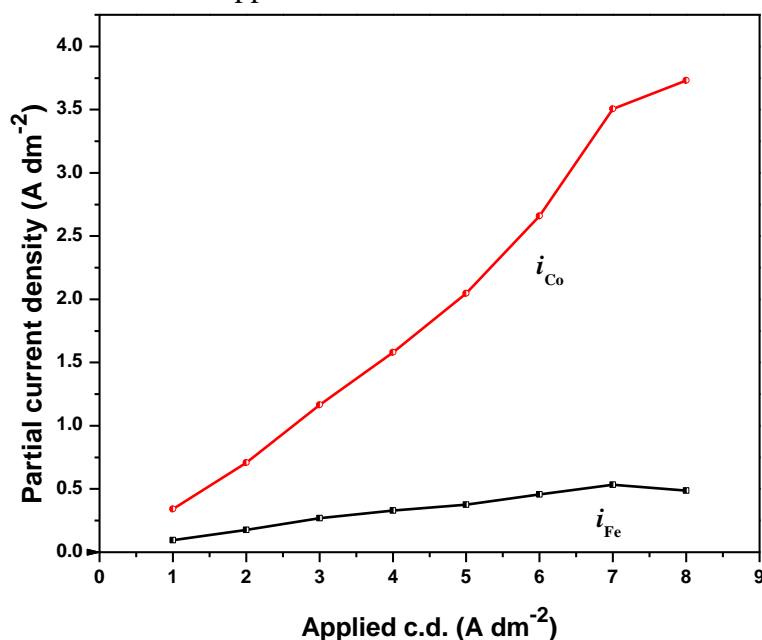
Fig. 8.2. The variation of partial current densities of iron (i_{Fe}) and cobalt (i_{Co}) with applied c.d., deposited from optimized bath at 303 K and pH=3.5.

However, the partial c.d. for deposition of Co (i_{Co}) is more sensitive of applied cathode c.d. In other words, i_{Co} increases drastically at higher c.d. This implies that the Fe-Co bath under study tend to exhibit normal codepositon at high c.d. as envisaged by Brenner A. (1963). This implies over the entire c.d. employed for production of alloy with low cobalt content. Further, the cathode current efficiency (CCE) of deposition process was found to increase with c.d. as shown in Table 8.2. The drastic increase of i_{Co} with applied c.d., in relation to i_{Fe} is indicative of the tendency for normal codeposition.

iii) Thickness of the deposit

The applied c.d. was found to show direct dependency on thickness of the deposit due to increased rate of deposition, evidenced by data given in Table 8.2. The increased thickness of the deposit with c.d. can also be substantiated by the adsorbed metal hydroxide, caused by the steady increase in pH, due to increased evolution of hydrogen.

Table 8.2. Effect of current density (c.d.) on deposit characters of monolayer Fe-Co alloy deposited from optimized bath at 303K

c.d. (A dm^{-2})	CCE (%)	Thickness (μm)
1.0	87	1.78
2.0	88	3.59
3.0	95	5.84
4.0	95	7.79
6.0	97	11.98
8.0	98	16.18

iv) Adhesion

The adherence of coatings deposited at different c.d.'s were tested. It was found that all coatings are hard adherent with completely smooth cut edges and none of the squares of the deposit is detached from the substrate indicating that coating at the optimal

condition has excellent adhesion. The hard adherent Fe-Co alloy coating, characteristic of mutual alloys of Fe-group metals was developed over entire Hull cell panel with no visual distinction by appearance.

v) Effect of pH

The pH of the bath was varied from 2.0 to 5.0. The bath was stable up to pH = 3.5. But at pH > 4.0, the bath was unstable due to hydroxide precipitation.

8.3.2 Surface morphology

The variation in the surface morphology of the coatings with c.d.'s is shown in Fig. 8.3. It was observed that at low c.d., the deposit is uniform with smooth surface, as shown in Fig. 8.3 (a).
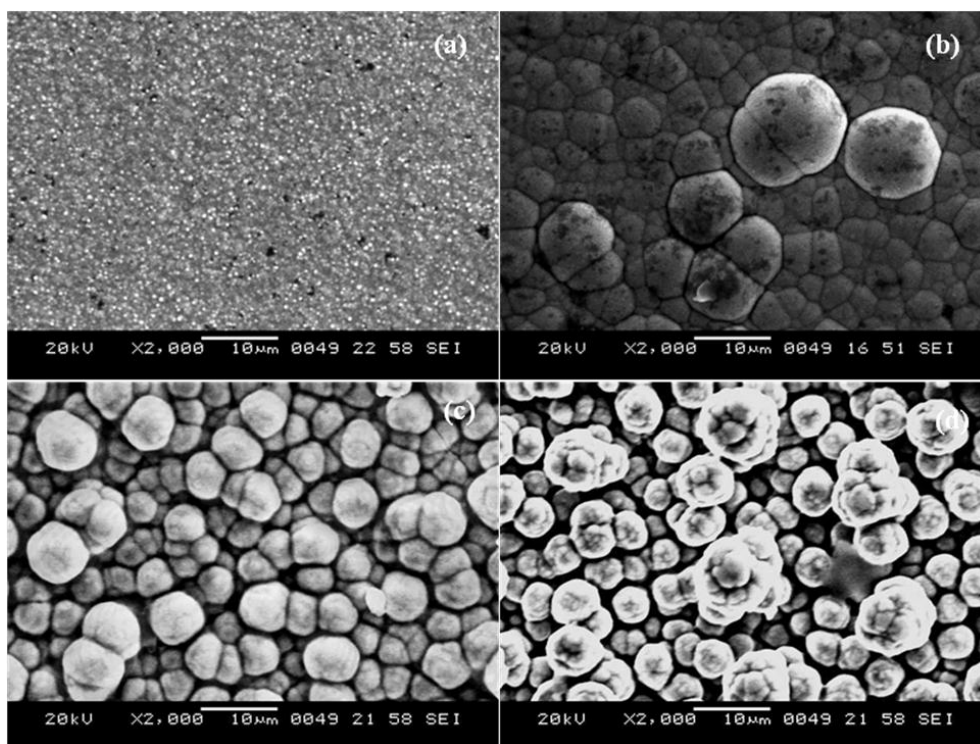
Fig. 8.3. SEM micrographs of Fe-Co coatings deposited at (a) 2.0 A dm^{-2} (b) 4.0 A dm^{-2} (c) 6.0 A dm^{-2} and (d) 8.0 A dm^{-2}, from optimized bath at 303 K

The surface morphology at high c.d. reveals that the initial growth of fresh nuclei randomly distributed over the copper surface. At 4.0 A dm^{-2} one can observe incomplete granule formation. Coatings at higher c.d. exhibit irregular granule shapes and formation of clusters. These granules are made up of a number of small crystallite spherical clusters, as shown in Fig. 8.3(d). Hence, the brightness and surface structure of the coatings were determined mainly by deposition c.d. as a function of its Co content, and hence the phase structure of the coatings.

8.3.3 Phase structure

The crystal orientation of Fe-Co alloys having different metal contents have been characterized by XRD technique. The phase structures have been identified from the peak profiles of X-ray reflection plotted as a function of 2θ as shown in Fig. 8.4. The XRD peaks of Fe-Co alloy indicates that the structure consists of a substitutional solid solution phase of Fe and Co. The formation of non-equilibrium the solid solution phases were observed. These are common in electrodepositions where there is no sufficient time for ordering of Co and Fe atoms on specific lattice positions to form Fe-Co alloy. Over the entire range of c.d. used for deposition, the Fe-Co coating showed mainly two phases; those are of bcc phase corresponding to iron crystal structure at low c.d. and of fcc phase corresponding to Fe-Co alloy crystal orientation. However, the tendency to form fcc phase structure has increased with applied c.d., with increase in cobalt content of the alloy.
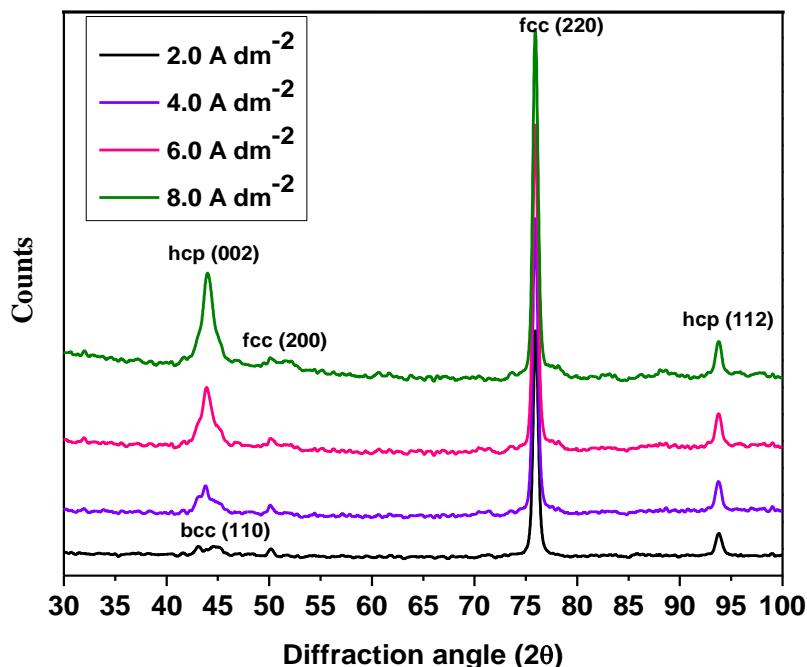
Fig. 8.4. X-ray diffraction patterns of Fe-Co alloys deposited at different c.d.'s showing the structural difference responsible for varied coating character

8.3.4 Micro hardness

The micro hardness of the coatings was measured, and was found to be dictated by the composition and phase structure of the deposit. Fig. 8.5 shows the variation of Vickers micro-hardness as a function of deposition c.d. The slight decrease in hardness with increase of applied c.d. may be attributed to decrease in wt % of Fe in the deposit. The maximum hardness observed at low c.d. is probably due to the presence of dual phases (fcc + bcc) as seen from XRD peaks. Another important factor which affects the micro hardness is the grain size observed in nanocrystalline Fe-Co alloy. The refinement in the grain size was observed as wt % of Co in the deposit is more, as evidenced by surface morphology in Fig. 8.3. The hardness of the deposit decreased for larger grain size, consequently low wt % of iron in the deposit. On the other hand an experimental a study revealed that the increase in hardness is due to the solid solution hardening with more wt. % of iron (Li and Ebrahimi 2003).
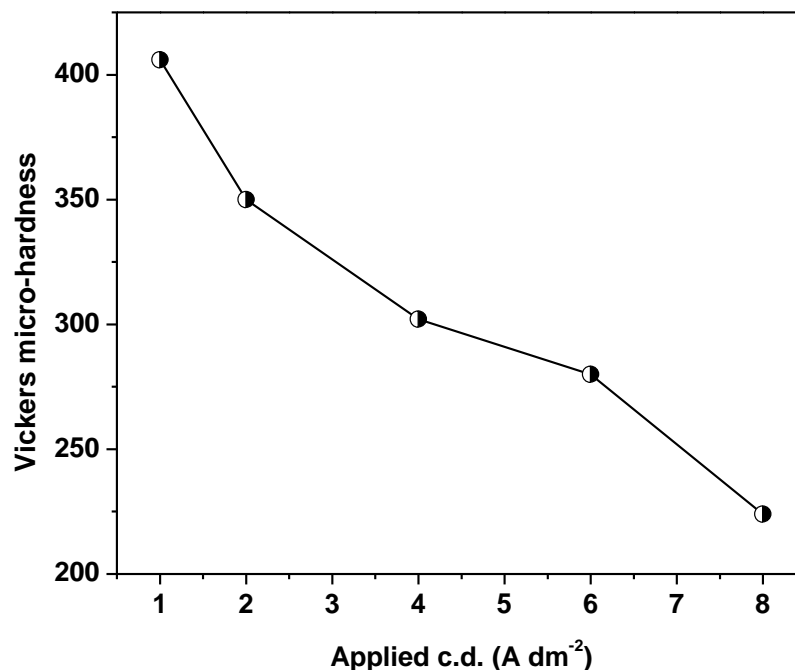
Fig. 8.5. Variation of micro-hardness of Fe-Co coatings at different applied c.d.,

deposited from optimal bath at 303K

8.3.5 Magnetic property of Fe-Co coatings

The magnetic properties of Fe-Co alloy films were measured under normal temperature, and corresponding hysteresis curve is shown in Fig. 8.6.

The saturation magnetization (M_s) and coercivity (H_c) values at different deposition c.d.'s are given in Table 8.3. The observed inverse and linear dependency of M_s and H_c, respectively with deposition c.d. may be explained as the magnetic properties of the materials depend on the chemical composition and grain size (Suryanarayana 1995).

Bulk iron and bulk cobalt are known to be ferromagnetic with M_s value equal to 220 emu g^{-1} and 142.0 emu g^{-1} respectively. At low c.d. increase of magnetic moment per volume is caused by the increase in wt % of iron in the coatings, since iron has higher magnetic dipole moment than cobalt (Myung and Nobe 2001). Hence, high M_s value of the coatings at low c.d. is attributed to high iron content of the coatings. This is further supported by coexistence of bcc phase of Fe and fcc phase of Fe-Co alloy (Liu et al.

191
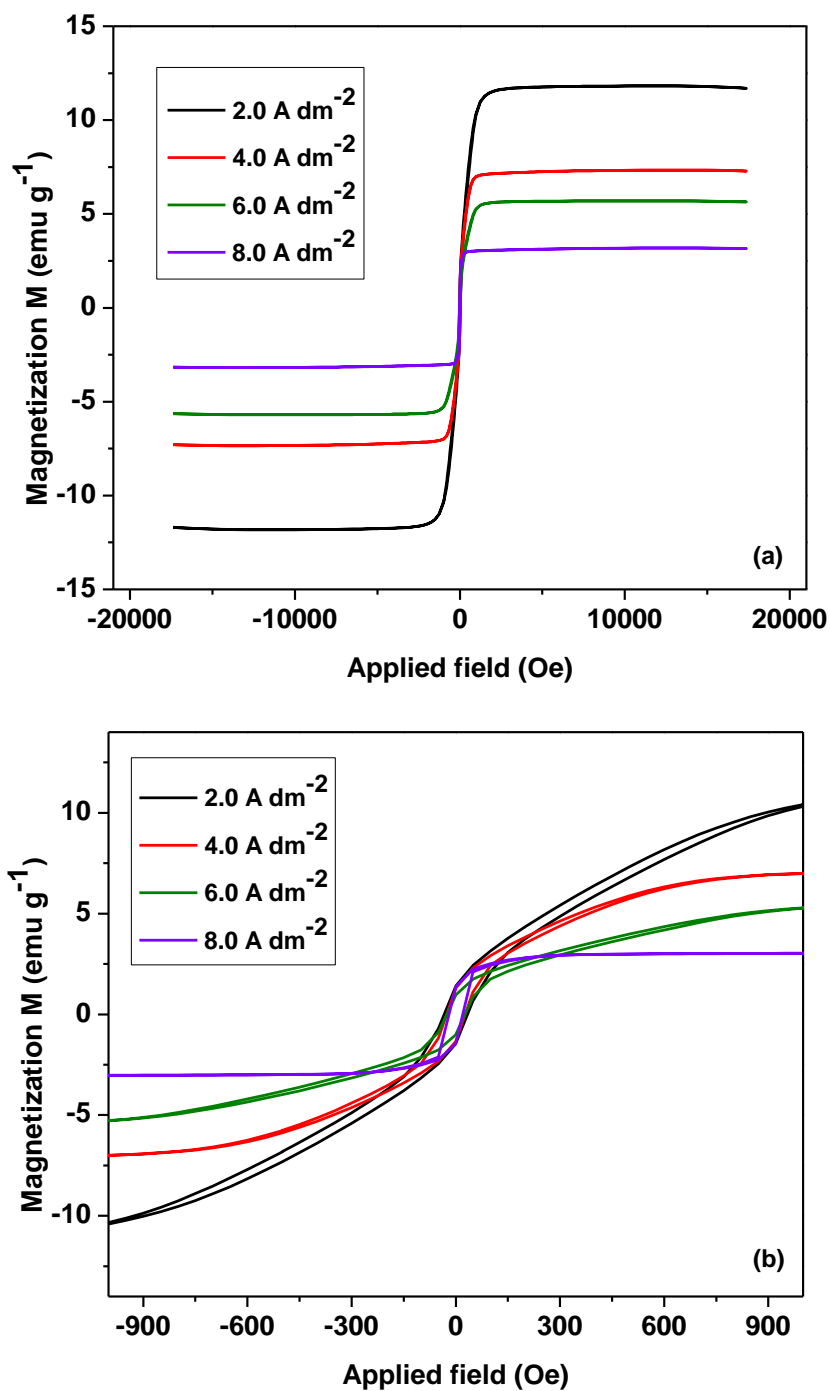
Fig. 8.6. (a) Magnetization behavior of Fe-Co coatings at different deposition c.d.'s and
(b) enlarged view in close proximity of applied magnetic field

2000). Further, the coercivity value was found to decrease constantly with deposition
c.d., shown in Table 8.3. This is due to the fact that microstructural parameters such as

average grain size and crystal structure can greatly influence the magnetic parameters, like Hc.

Table 8.3. Change in saturation magnetization, M_s and coercivity, H_c of Fe-Co films at different c.d.'s, deposited from optimized bath at 303K

Applied c.d. (A dm^{-2})	M_s (emu g^{-1})	H_c (Oe)
2.0	11.72	34.50
4.0	7.20	26.15
6.0	5.62	25.00
8.0	3.02	19.50

Fig.8.7 illustrates how the average grain size (determined by Scherrer's formula) and coercivity varies with the deposition c.d. of the coatings. It was observed that smaller the grain size, greater will be coercivity, as seen in Fig. 8.7 (Liu et al. 2006).
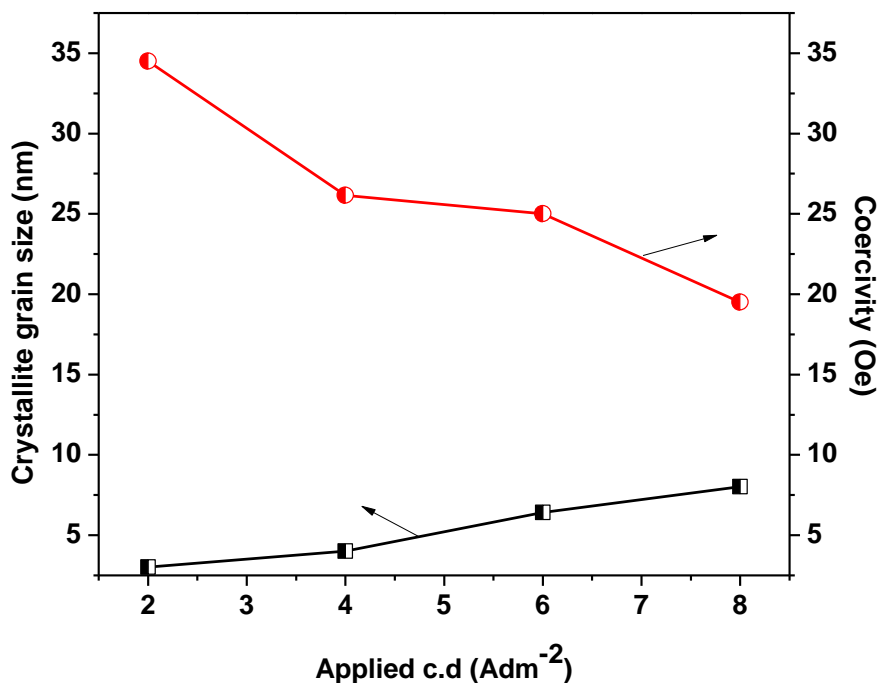
Fig. 8.7. Variation of crystallite grain size and coercivity of Fe-Co coatings at different c.d., from optimized bath at 303 K

193
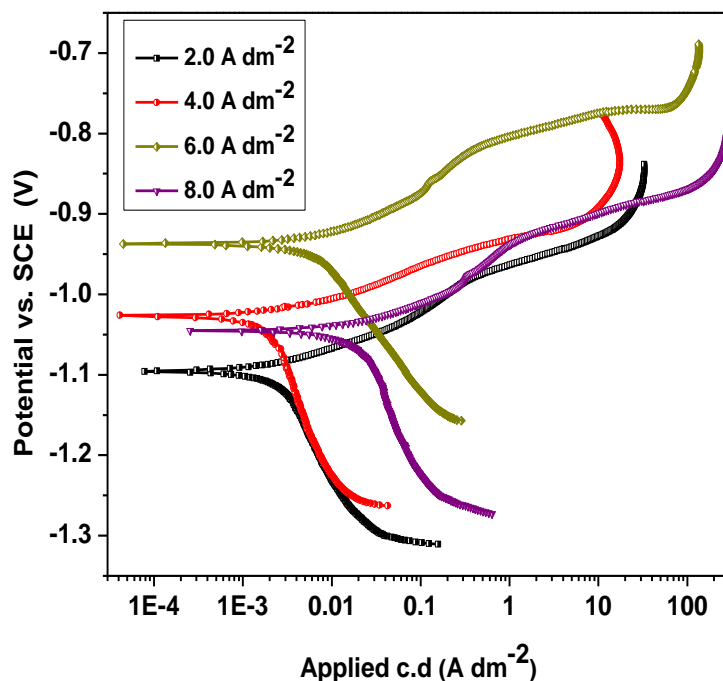
Fig. 8.8. Potentiodynamic polarization behavior of Fe-Co coatings at different c.d.'s, deposited from optimal bath at 303K

The high coercivity of the coatings observed at low c.d. is due to dominating bcc phase structure, in support of work reported by Tabakovic et al. (2000)

8.3.6 Potentiodynamic polarization study

The corrosion behaviors of electrodeposited Fe-Co alloys have been evaluated by potentiodynamic polarization method. The corrosion rates (CR) were calculated through Tafel's extrapolation method. Tafel's behavior of Fe-Co alloy coatings at different c.d., like 2.0, 3.0, 4.0, 6.0 and 8.0 A dm^{-2} have been studied, and corresponding data are reported in Table 8.4.

The CR decreased with increase of c.d. as function of changed phase structure of the deposits. It is observed that Fe-Co coating, at 4.0 A dm^{-2} exhibits least CR (27.81mm y^{-1}) due to characteristic phase structure of the deposit at that c.d. It may be noted that the CR decreased with c.d. up to 4.0 A dm^{-2} and then increased. However, at high c.d. the CR decreased drastically.

194

Table 8.4. Corrosion data of Fe-Co alloy coatings deposited at different cathode c.d., from the optimized bath at 303 K

c.d. (A dm^{-2})	-E$_{corr}$ vs SCE (V)	i$_{corr}$ (μA cm^{-2})	CR (mm y^{-1})
1.0	1.068	3521.3	39.64
2.0	1.095	3267.5	36.70
3.0	0.971	2956.3	33.21
4.0	1.026	2475.8	27.81
5.0	0.951	3352.5	37.66
6.0	0.937	3610.3	40.56
7.0	1.038	4092.7	45.98
8.0	1.044	4601.0	51.69

The peak corrosion performance of Fe-Co alloy corresponding to 4.0 A dm^{-2} is due to its unique phase structure, characterized by the coexistence of hcp and fcc phases as observed in Fig. 8.4. At this c.d. the coating was found to be nobler with more wt % of Co, and hence less wt. % of Fe. However, the increased CR at very high c.d.'s, viz 5.0, 6.0, 7.0, and 8.0 A dm^{-2} is attributed by the increased porosity of the coatings supported by the surface morphology shown in Fig. 8.3.

8.3.7 Electrochemical impedance spectroscopy

Though potentiodynamic polarization technique is used to study the kinetics of an electrode reaction, the result is often corrupted by side effects such as the charging currents of the double layer observed on a time-scale of the order of a millisecond, or by the ohmic drop associated to the experimental setup (Hubert and Girault 2004). The response of reversible electrochemical systems studied in the presence of an ohmic drop unfortunately resembled the response of kinetically slow systems. The best way of

differentiating the kinetics of an electrode reaction from experimental side effects is to use an excitation function covering a large time domain. Hence, EIS technique can be used to evaluate the barrier properties of the electrical double layer capacitance and to determine the charge-transfer resistance, R_{ct} (Yuan et al. 2010). The values are calculated from the difference in impedance at lower and higher frequencies. To obtain the double layer capacitance (C_{dl}) the frequency at which the imaginary component of the impedance is maximal ($-Z_{max}$) was found as represented in equation,

$$C_{dl} = \frac{1}{\omega R_{ct}} \qquad \text{Where } \omega = 2\pi f_{max} \quad \text{......... (8.1)}$$

The shape of the impedance response indicated that the corrosion resistance of coating is due to double layer capacitance (C_{dl}). It was found that the radii of the depressed semicircles depend on the deposition c.d. Maximum diameter of the capacitive loop at optimal c.d., i.e. at 4.0 A dm^{-2} showed that the corresponding deposit is the most corrosion resistant.
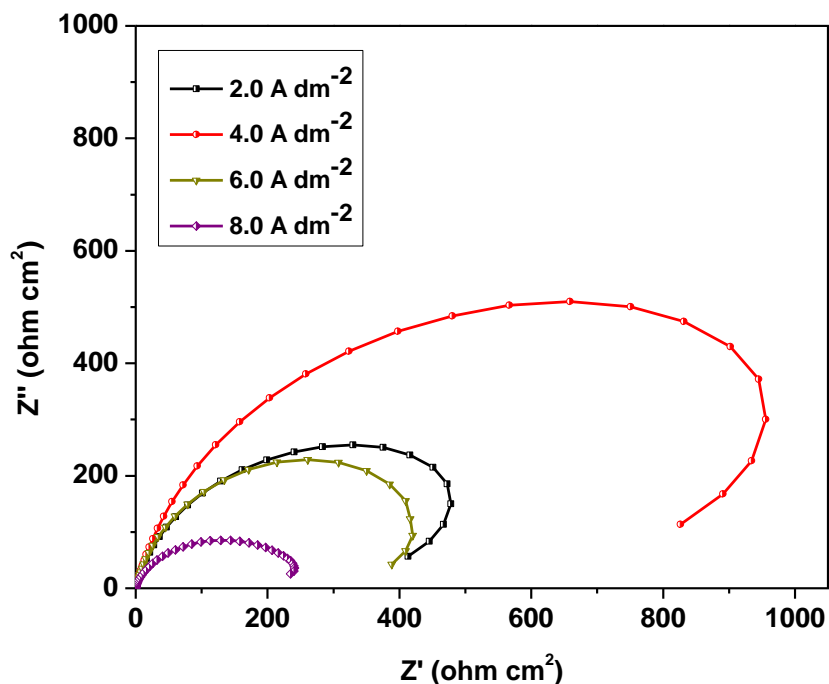
Fig. 8.9. Nyquist response of monolayer Fe-Co alloy coatings at different c.d.'s as function of frequency, deposited from optimal bath at 303K

Lastly, the impedance response of all the coatings showed an inductive loop at low frequency limit, indicating the high conductivity of the Fe-Co coatings. The inductive loop at lower frequency limit of Co-based alloys of Fe-group metals indicates that they exhibit high electrical conductivity.

8.4 CONCLUSIONS

A new sulphate bath has been proposed for galvanostatic deposition of bright Fe-Co alloy and following observations are made as conclusion:

1. Electrolytic bath exhibited anomalous type deposition at all c.d.'s studied, and cathode c.d. is found to be the deciding factor for composition and phase structure of the deposit.

2. The SEM images of Fe-Co alloy deposited at different c.d.'s verified the structure-property relations of the coatings.

3. At higher c.d., increased grain size of the Fe-Co alloy was observed. The micro-hardness of the deposit was found to decrease with c.d. as a matter of change in phase structures.

4. Saturation magnetization, M_s and coercivity, H_c of Fe-Co coatings show inverse dependency with each other over entire c.d. range studied, and are attributed to the crystallite grain size and phase structure of the coatings.

5. Corrosion study demonstrated that at 4.0 Adm^{-2}, the bath produced the least corrosive coatings (CR = 27.81 mm y^{-1}), having about 83 % of Co compared to at other c.d.'s.

ELECTRODEPOSITION AND CHARACTERIZATION OF MULTILAYER Fe-Co COATINGS

The electrochemical deposition of nanostructured metallic coatings is increasingly used for a wide range of applications in functional engineering coatings for corrosion resistivity and tribological applications, current collector coatings in batteries, fuel cell and supercapacitors, or anti-reflective coatings in solar cell and smart windows. Nanostructured coatings can typically demonstrate surface and coating properties more superior than non-nanostructured such as macro-structured or polycrystalline coatings. For example, wear and corrosion resistance of nanocrystalline nickel coating (grain size in the range of 1 to 100 nm) may perform better than a polycrystalline nickel (>500 nm grain size).

Hence CMMA coatings composed of alternate layers of metals/alloys with different composition, called CMMA coatings received more attention in the field of surface engineering. They often exhibit novel phenomenon such as improved mechanical strength, magnetic properties and corrosion resistance in comparison with simple monolayer coatings. By applying so called multilayer electrochemical deposition, it is possible to fabricate layered coatings in nano/micrometric dimension using sensitive power sources. This technique ensures the real benefits of advanced material properties upon other available techniques such as physical vapor deposition (PVD) and chemical vapor deposition (CVD) etc. Though CMMA can be produced by different techniques, the single bath technique (SBT) is commonly used due to its simplicity. The CMMA coatings consist of several layers of alloys with alternate composition. It can be developed by depositing alloys of two compositions successively by changing the c.d.

The repeating length of time is responsible for the structural modulation of the coating. The applied c.d.'s, called CCCD's., and repeating length of time are responsible for composition and thickness of the individual layers, respectively. Thus the development of multilayer coating by electrolytic means allows an easy route for tailoring the structure and properties of the materials.

Substantial amount of work have already been reported to support the improved corrosion resistance of CMMA coatings of Zn-M (where M = Fe, Co and Ni) alloy using SBT. Recently, development of multilayered Zn-Ni alloy coatings, using square current pulses for improved corrosion resistance have been reported (Venkatakrishna and Hegde 2010). But no work is reported with regard to development of corrosion resistant multilayer Fe-Co coatings using dual and triple current pulses. In this chapter, an effort has been made to optimize deposition conditions for development of multilayer coating Fe-Co alloy on copper, using the electrolytic bath optimized in Chapter 8. Multilayer coatings have been developed through different structural modulation, i.e. using dual and triple current pulses. The coating configurations have been optimized in terms of number and thickness of each layer using dual and triple current pulses in Section 9.1 and Section 9.2 respectively. A comparative account of coatings developed using dual and triple current pulses are presented in Section 9.3.

SECTION - 9.1: Development and characterization of multilayer Fe-Co coatings using dual current pulse

9.1.1 Development of monolayer and multilayer Fe-Co alloy coating

The experimental studies in Chapter 8 has shown that the c.d. plays an important role on deposit characters such as composition, thickness, hardness and corrosion resistance of the Fe-Co alloy coatings. The corrosion data of monolayer Fe-Co coating corresponding to 4.0 A dm^{-2}, reported as (Fe-Co)$_{4.0/mono}$ revealed that it is the most corrosion resistant (CR = 27.81 mm y^{-1}) compared to the coatings at other c.d.'s. Hence (Fe-Co)$_{4.0/mono}$ has been taken as the optimal configuration of the alloy deposited, from the bath proposed in Chapter 8. In the similar line as detailed for earlier in Chapters 5 and 7, multilayer coatings of Fe-Co alloy have been developed on copper, and their characterizations were made. Multilayer coatings having different configurations were developed using dual current pulse (square) as shown in Fig. 3.1. A sharp change in c.d. leads to the deposition of alloy with sharp change in composition. i.e., with distinct interface between layers.

9.1.2 Optimization of CCCD's

After deposition of monolayer Fe-Co alloy using D.C., the layered coatings of Fe-Co alloy were deposited at different sets of c.d.'s, called CCCD's. Pulse deposition techniques are known to improve the corrosion resistance of numerous elemental and alloy systems. Hence, multilayer coatings having alternate layers with different compositions were developed. The corrosion behaviors of monolayered and multilayered (Fe-Co) alloy coatings, having different configurations were characterized by potentiodynamic polarization and electrochemical impedance spectroscopy (EIS) methods. The corrosion data of multilayer alloys (having arbitrarily chosen 10 layers) deposited at different sets of CCCD's are shown in Table 9.1.

It may be noted that the CR of multilayer coating decreased drastically (compare to monolayer) in all sets of CCCD's as shown in Table 9.1. In other words, the CMMA Fe-Co coatings developed with difference of 2.0 A dm^{-2} and 4.0 A dm^{-2} between CCCD's

showed improved corrosion resistance on layering. Hence, it may be inferred that the improved corrosion resistance of multilayer coatings is not merely due to the structural modulation in individual layers. Even though the improvement in corrosion resistance was found in many sets of CCCD's, the most pronounced one was with difference 2.0 A dm^{-2} between CCCD's.

Table 9.1. Corrosion rate (CR) of multilayer (Fe-Co) coatings at different sets of CCCD's (with 10 layers), developed from the optimized bath at 303K

CCCD's (A dm^{-2})	$-E_{corr}$ vs SCE (V)	i_{corr} (μA cm^{-2})	CR (mm y^{-1})
CMMA Fe-Co coatings with difference of 2.0 A dm^{-2} between CCCD's			
(Fe-Co)$_{2.0/4.0}$	0.977	1032.5	11.60
(Fe-Co)$_{4.0/6.0}$	0.976	1337.0	15.02
(Fe-Co)$_{6.0/8.0}$	0.971	1743.2	19.58
(Fe-Co)$_{3.0/5.0}$	0.934	2037.6	22.89
CMMA Fe-Co coatings with difference of 4.0 A dm^{-2} between CCCD's			
(Fe-Co)$_{2.0/6.0}$	0.957	2218.5	24.92
(Fe-Co)$_{4.0/8.0}$	0.972	2308.9	25.93
(Fe-Co)$_{3.0/7.0}$	0.963	2378.8	26.72
(Fe-Co)$_{4.0/monolayer}$	1.026	2475.8	27.81

9.1.3 Optimization of total number of layers

To achieve a well-defined demarcation between Fe-Co alloy layers, CMMA coatings have been developed at 2.0/4.0 A dm^{-2} and 2.0/6.0 A dm^{-2}. The coatings having 20, 60, 120, and 200 layers, including 10 layers were developed and their corrosion

characters were evaluated by Tafel's extrapolation method. It was observed that the corrosion rates were decreased as the layering is continued up to 120 layers and then increased, in both sets of CCCD's as shown in Table 9.2.

Table 9.2. Decrease of corrosion rate (CR) of multilayer Fe-Co coatings with increase in number of layers, deposited from optimized bath at 303K

CCCD's $(A\ dm^{-2})$	No. of layers	Deposition time for each layer (sec)	Average thickness of layer (nm)	$-E_{corr}$ vs SCE (V)	i_{corr} $(\mu A\ cm^{-2})$	CR $(mm\ y^{-1})$
	10	60	1400.0	0.977	103.25	11.6
	20	30	700.0	0.979	707.52	7.94
$(Fe-Co)_{2.0/4.0}$	60	10	233.3	0.986	268.12	3.01
	120	5	116.6	0.981	88.62	0.99
	200	3	46.6	0.987	139.59	1.56
	10	60	1400.0	0.957	221.85	24.92
	20	30	700.0	0.958	181.38	20.37
$(Fe-Co)_{2.0/6.0}$	60	10	233.3	0.960	153.79	17.27
	120	5	116.6	0.970	147.92	16.61
	200	3	46.6	0.969	188.40	21.16
$(Fe-Co)_{4.0/mono}$	monolayer	600	14000	1.027	2475.8	27.81

At 2.0/4.0 A dm^{-2}, the corrosion rate reached saturation (beyond which no decrease of corrosion rate with layering was observed) value at 120 layers with corrosion rate (0.99 mm y^{-1}), relative to 27.81mm y^{-1} of monolayer alloy. But no substantial decrease of corrosion rate was found at 2.0/6.0 A dm^{-2} as shown in Table 9.2. This may be due to unfavorable condition for structural modulations, caused by large difference between CCCD's. An effort to increase the corrosion resistance of the CMMA coatings

by further layering, i.e. with 200 layers has resulted in increase of CR as shown in Table 9.2.

The increased corrosion rate at high degree of layering is attributed to less relaxation time for redistribution of ions (Co^{2+} and Fe^{2+}) in the diffusion layer, as explained in Chapter 5. As the number of layers increased the time for deposition of each layer is small, as the total time for deposition remains same. At higher degree of layering, there is no sufficient time for metal ions to relax (against diffusion under given c.d.) and to get deposit on cathode with changed composition. As a result at high degree of layering modulation in composition is not likely to take place. In other words, CMMA deposit is tending to become monolayer. Finally, $(Fe-Co)_{2.0/4.0/120}$ has been proposed as the optimal configuration of CMMA coating with individual layer thickness ~ 50 nm.

9.1.4 Corrosion study
i) Potentiodynamic polarization study

The corrosion behaviors of monolayer and multilayer Fe-Co alloy coatings are characterized by potentiodynamic polarization method and experimental results are reported in Table 9.2. A progressive decrease of corrosion current, i_{corr} and hence, the CR was observed on layering up to 120 layers as shown in Fig. 9.1. After which it increased drastically as shown in Table 9.2.

The shape of potentiodynamic polarization curves demonstrated that the decreased corrosion resistance is due to the combined effect of anodic and cathodic controlled reactions of corrosion process, i.e. corrosion protection is due to inhibition of both anodic and cathodic reactions caused by layered coating.
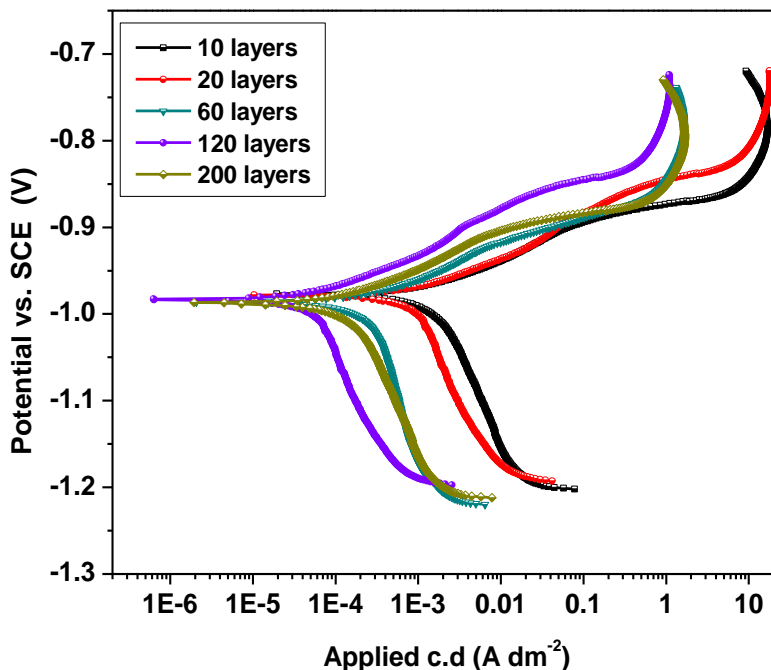
Fig. 9.1. Potentiodynamic polarization curves of multilayered (Fe-Co)$_{2.0/4.0}$ coatings having different number of layers developed using dual current pulses, from optimized bath at 303K

ii) Electrochemical impedance spectroscopy study

EIS is very useful approach for characterizing the electrical properties of coatings. The technique can be used to investigate the dynamics of bound or mobile charge in the bulk or interfacial regions of any kind of solid or liquid material: ionic, semiconducting, mixed electronic–ionic, and even insulators (dielectrics) (Barsoukov and Macdonald 2005). Accordingly, the information about interaction of coatings with corrosion medium can be obtained from Nyquist plots. The electrochemical impedance responses of CMMA (Fe-Co)$_{2.0/4.0}$ coating system, shown in Fig. 9.2 evidences that the diameter of the semi-circle increased with number of layers up to 120 layers and then decreased.
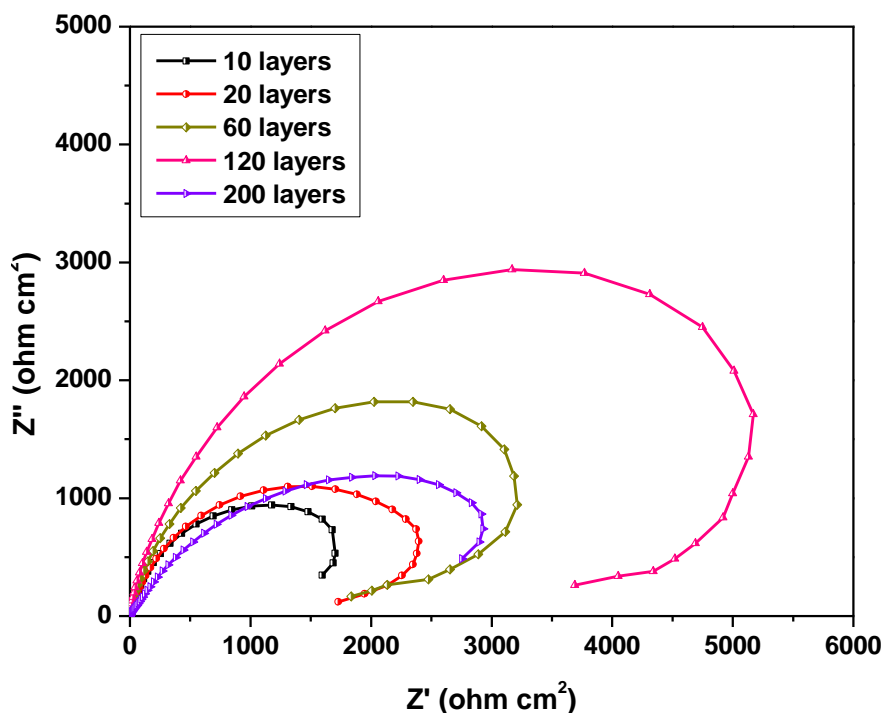
Fig. 9.2. Electrochemical impedance response of CMMA (Fe-Co)$_{2.0/4.0}$ coatings having different number of layers measured as function of frequency, deposited from optimal bath at 303K

It should be noted that the solution resistance R_s is nearly identical in all cases, as the same bath chemistry and cell configuration were used. But polarization resistance, R_P increased as the number of layers increased. But, for deposit with 200 layers the diameter of the semi-circle decreased substantially suggesting its poor corrosion resistance as shown in Fig. 9.2. The pear shaped impedance response, common for all Co-based alloys of Fe-group metals was observed. This behavior was attributed high conductivity of Co-based mutual alloys of Fe-group metals.

9.1.5 Dielectrics study

The change in relative dielectric constant, ε_r of CMMA Fe-Co coatings having different number of layers is shown in Fig. 9.3. At low frequency limit the frequency response of the capacitor was found to be dependent on ε_r. This is due to the fact that at

low frequency the AC becomes equal to DC, and is more sensitive to ε_r. But at high frequency limit, ε_r is found to be independent of number of layers. It may be analyzed as at very high frequency there is no charging of the capacitor, and thus capacitor is effectively like an open circuit (vacuum). Therefore, ε_r is almost same for all coatings, regardless of the number of layers involved.
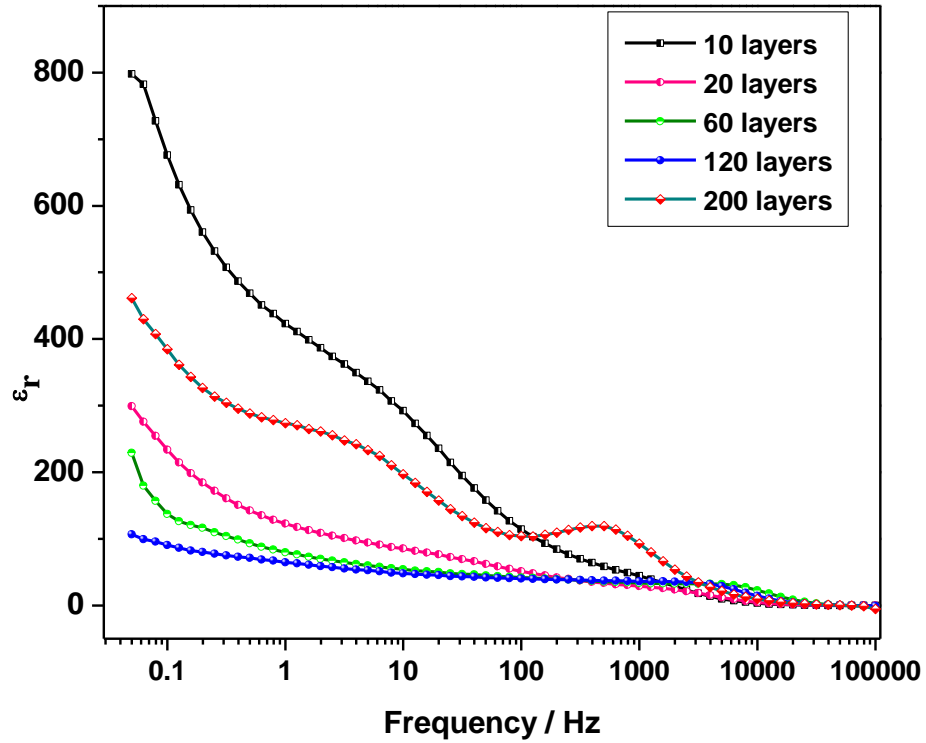
Fig. 9.3. Frequency response of relative permittivity, ε_r of CMMA (Fe-Co)$_{2.0/4.0}$ coatings having different number of layers, deposited from the optimized bath at 303 K

Hence, decrease of ε_r with number of layers indicated that the polarizing ability of the Electrical Double Layer (EDL) capacitor decreases with layering (Ravinder and Latha 1999). Therefore less ε_r of CMMA (Fe-Co)$_{2.0/4.0/120}$ compared to other coating systems, indicated that improved corrosion resistance is due to increased reactance, or less conductivity of the coatings. In other words, the coating behaves as a good dielectric barrier (insulator) for passage of current, causing less corrosion.

9.1.6 SEM Study

Cross-sectional view of CMMA (Fe-Co)$_{2.0/4.0/dual}$ coating was examined under SEM, and is shown in Fig. 9.4(a). Limited by the lower magnification of SEM machine used, the CMMA coating having only 60 layers were examined. Formation of layers during deposition was further confirmed by examining the corroded sample after corrosion, as explained in Section 5.1.10. The inspection of the acid treated surface under SEM confirmed the selective breaching of layers of alloys having different composition as shown in Fig. 9.4(b). This confirms the dissolution of multilayer coating layers after layer, responsible for delayed corrosion.

The extended protection of multilayer coatings is due to formation of layers with alternatively changing composition. The one layer with more wt. % of noble metal content acts cathodic with respect to the next one with less wt. % of noble metal, which is anodic. Thus enhanced corrosion protection of multilayer coating is due to cathodic protection of one layer and sacrificial protection of next layer, and may be interpreted as follows: The failures like pores, crevices or columnar structure occurring in case of the single layer put down in the deposition process may be neutralized by the successively deposited coating layers and thus the corrosion agents path is longer or blocked. Accordingly, the Fe-Co alloy layer, with less wt. % of Co beneath the high wt. % of Co top layer dissolves through the pores and micro-cracks existing in the CMMA coatings existing during corrosion (Fei et al. 2006). As a whole, the protection efficacy of CMMA (Fe-Co)$_{2.0/4.0/120}$ coatings may be explained by the barrier effect of Fe-Co layer, with high wt. % of Co and the sacrificial effect of Fe-Co layer, with less wt. % of Co (16.5). Small change in wt. % of noble metal in the alloys layer is good enough to bring large change in the phase structure, and hence their properties (Ganesan et al. 2007).
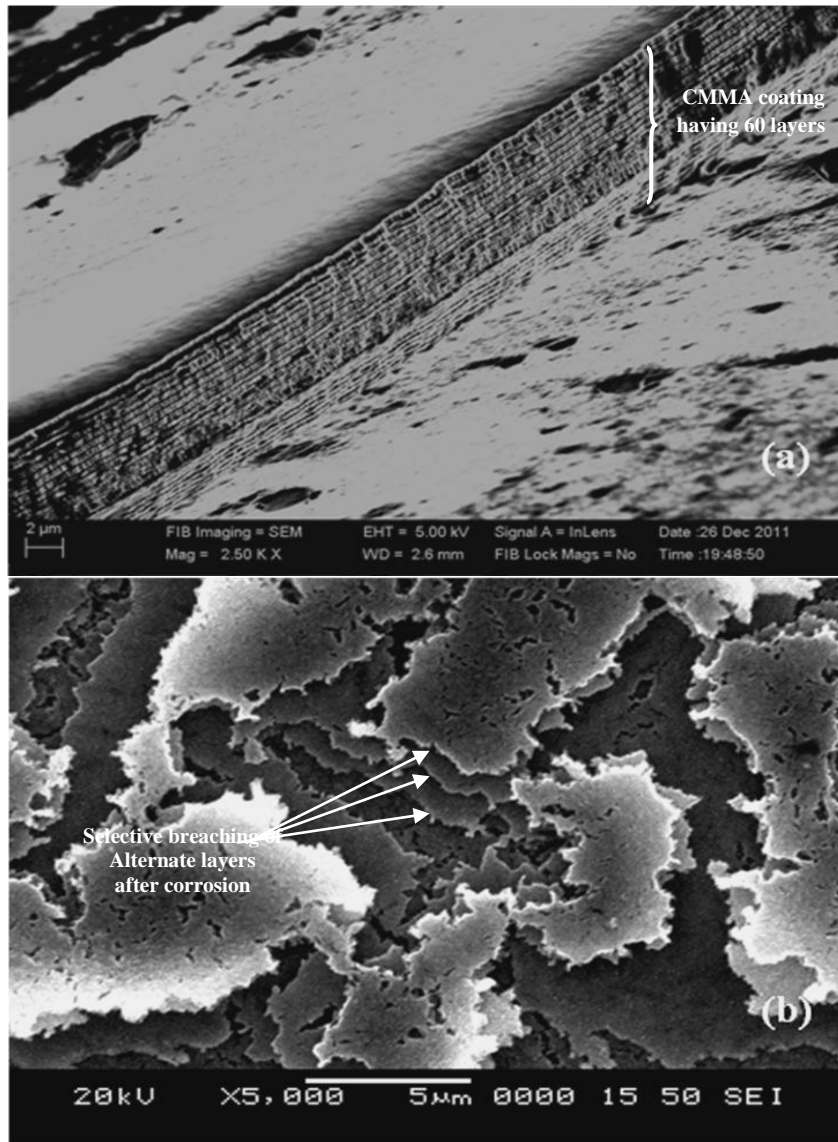
Fig. 9.4. SEM image of CMMA (Fe-Co) coatings: (a) cross-sectional view displaying 60 layers and (b) Surface structure of $(Fe-Co)_{2.0/4.0/10}$ after acid test demonstrating selective breaching of alternate layers after corrosion

SECTION - 9.2: Development and characterization of multilayer Fe-Co coating using triple current pulse

9.2.1 Development of multilayered Fe-Co coatings

Fe-Co alloy deposited at 4.0 A dm^{-2}, represented as (Fe-Co)$_{4.0/monolayer}$ from the bath proposed in Section 8.2.1 was found to exhibit the CR = 27.81 mm y^{-1}. In an effort to increase the corrosion resistance by multilayered technique using triple current pulses the following studies were made and results are presented in proceeding sections.

9.2.2 Optimization of CCCD's

It is well known that on exceptional thinning of layers, the CMMA coatings are going to acquire improved properties compared to non-nanostructure (bulk) materials (Despic and Jovic 1989). In this section, CMMA Fe-Co coatings have been developed using triple current pulses, i.e. current with three steps. In order to optimize the compositional conditions, called modulation, the deposition was accomplished at different CCCD's (having 10 layers), and their corrosion behaviors were studied, and are reported in Table 9.3.

Table 9.3. Corrosion rate (CR) of Fe-Co multilayer coatings, developed from the optimized bath at different set of CCCD's (with 10 layers)

CCCD's (A dm^{-2})	$-E_{corr}$ vs SCE (V)	i_{corr} (μA cm^{-2})	CR (mm y^{-1})
CMMA Fe-Co coatings with difference of 2.0 A dm^{-2} between CCCD's			
(Fe-Co)$_{2.0/4.0/6.0}$	0.935	130.32	1.46
(Fe-Co)$_{1.0/3.0/5.0}$	0.968	179.86	2.02
(Fe-Co)$_{3.0/5.0/7.0}$	0.955	318.51	3.57
(Fe-Co)$_{4.0/6.0/8.0}$	0.941	725.30	8.14
CMMA Fe-Co coatings with difference of 3.0 A dm^{-2} between CCCD's			
(Fe-Co)$_{2.0/5.0/8.0}$	0.977	226.22	2.54
(Fe-Co)$_{1.0/4.0/7.0}$	0.951	587.53	6.60

The improvement in corrosion performance was found at different CCCD's even in case of triple current pulses, revealing once again that the structural modulation is not the critical component for improved behavior. However, out of many sets of CCCD's tried, the coatings with $(Fe-Co)_{2.0/4.0/6.0}$ and $(Co-Ni)_{2.0/5.0/8.0}$ configurations have been selected for studying the effect of further layering.

9.2.3 Optimization of total number of layers

The corrosion resistance of CMMA coatings may often be increased substantially by increasing the number of layers, usually, up to an optimal limit without sacrificing the demarcation between each layer.

Table 9.4. Decrease of corrosion rate (CR) of multilayer Fe-Co coatings, developed from the optimized bath with increase in number of layers

CCCD's (A dm^{-2})	No. of layers	Deposition time for each layer (sec)	Average thickness of layer (nm)	-E$_{corr}$ vs SCE (V)	i$_{corr}$ (μA cm^{-2})	CR (mm y^{-1})
	10	60	1400.0	0.935	130.32	1.46
$(Fe-Co)_{2.0/4.0/6.0}$	20	30	700.0	0.946	61.08	0.68
	60	10	233.3	0.959	52.27	0.58
	120	8	116.6	0.967	10.12	0.16
	200	3	46.6	0.958	13.55	0.18
	10	60	1400.0	0.977	226.22	2.54
$(Fe-Co)_{2.0/5.0/8.0}$	20	30	700.0	0.978	170.72	1.91
	60	10	233.3	0.979	115.59	1.29
	120	8	116.6	0.977	71.17	0.80
	200	3	46.6	0.968	89.18	1.00
$(Fe-Co)_{4.0/mono}$	monolayer	600	14000	1.027	2475.8	27.81

As mentioned earlier, at 2.0/4.0/6.0 A dm^{-2} and 2.0/5.0/8.0 A dm^{-2} further layering was carried out. The coatings having 10, 20, 60, 120 and 200 layers were developed and their corrosion rates were measured. It was observed that in both sets of CCCD's the corrosion rates decreased as the number of layers increased up to 120 layers, and then increased (Table 9.4).

At 2.0/4.0/6.0 A dm^{-2}, the corrosion protection ability of the coating reached its maximum at 120 layers with minimum CR = 0.16 mm y^{-1}, in relation to mono-layer alloy (27.81 mm y^{-1}). The effort of increasing the corrosion resistance further, by increasing number of layers (i.e. 200 layers) in both sets of CCCD's resulted in increase of CR, as reported in Table 9.4. On exceptional thinning of layers, or at higher number of layers the modulation in composition is not likely to take place. In other words, CMMA deposit is tending to become monolayer. Based on the appearance and corrosion data, the CMMA (Fe-Co)$_{2.0/4.0/6.0/120}$ coating, having individual layers of ~50 nm thickness has been proposed as the optimal configuration for peak performance against corrosion

9.2.4 Corrosion study

i) Tafel's polarization study

The corrosion behaviors of multilayer (Fe-Co)$_{2.0/4.0/6.0}$ coatings having different degree of layering is shown i006E Fig. 9.5. It may be observed that the corrosion current (i_{corr}) values decreased with increase in numbers of layers. The progressive decrease of i_{corr} with number of layers indicated that improved corrosion resistance is due to the layering effect. A significant decrease in i_{corr} value was observed, when number of layers has increased from 10 to 120. However, at higher degree of layering no improvement in corrosion resistance was found (Table 9.4). This is attributed to less relaxation time for redistribution of metal ions in diffusion layer. i.e., no distinct interfaces were formed between the layers at very short cyclic time, to impart the novel properties to the coatings.
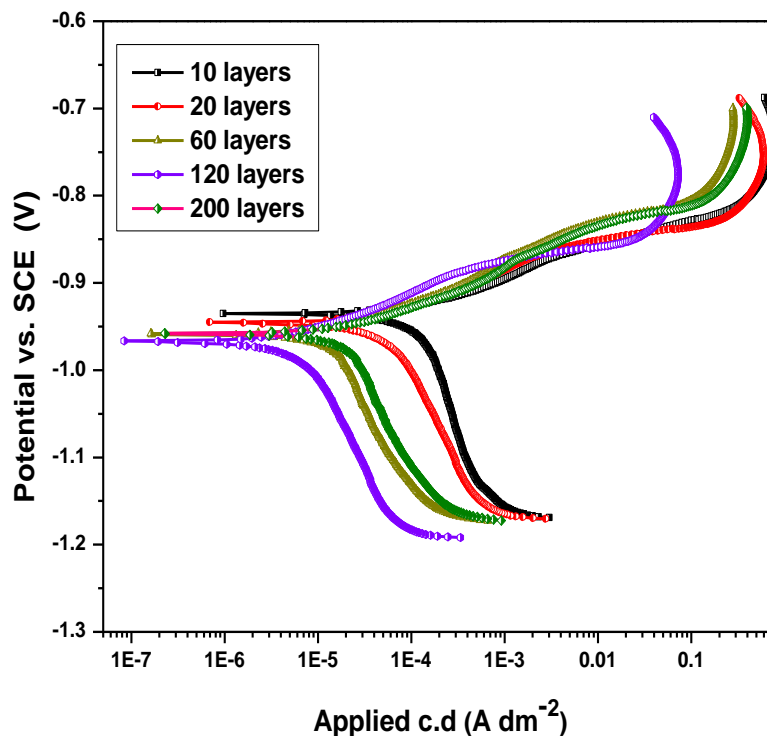
Fig. 9.5. Potentiodynamic polarization behaviors of multilayer (Fe-Co)$_{2.0/4.0/6.0}$ coatings with different number of layers, developed from the optimized bath at 303 K

ii) Electrochemical impedance study

The Nyquist response of multilayer (Fe-Co)$_{2.0/4.0/6.0}$ coatings with different number of layers is shown in Fig. 9.6.

At high frequency limit, all electroplates exhibited $R_{real} = 0$, indicating that the solution resistance (Rs) is same for all analysis. Increase in the diameter of the semicircle with increase in number of layers showed that the capacitive reactance of the double layer, responsible for improved corrosion resistance increased with layering. The high corrosion resistance at optimal layers (120 layers) is evidenced by bigger incomplete semicircle, caused by large capacitive reactance. Nyquist plots with incomplete semi circles at low frequency limit indicated that the corrosion behavior of the coatings is not only controlled by charge transfer resistance, R_{ct} but also by the capacitive reactance also.

The inductive loop observed at low frequency side, irrespective of the number of layers signifies the high electrical conductivity of the coatings. The pear shaped impedance response characteristics of Co-based alloys of Fe-group metals were observed as shown in Fig. 9.6.
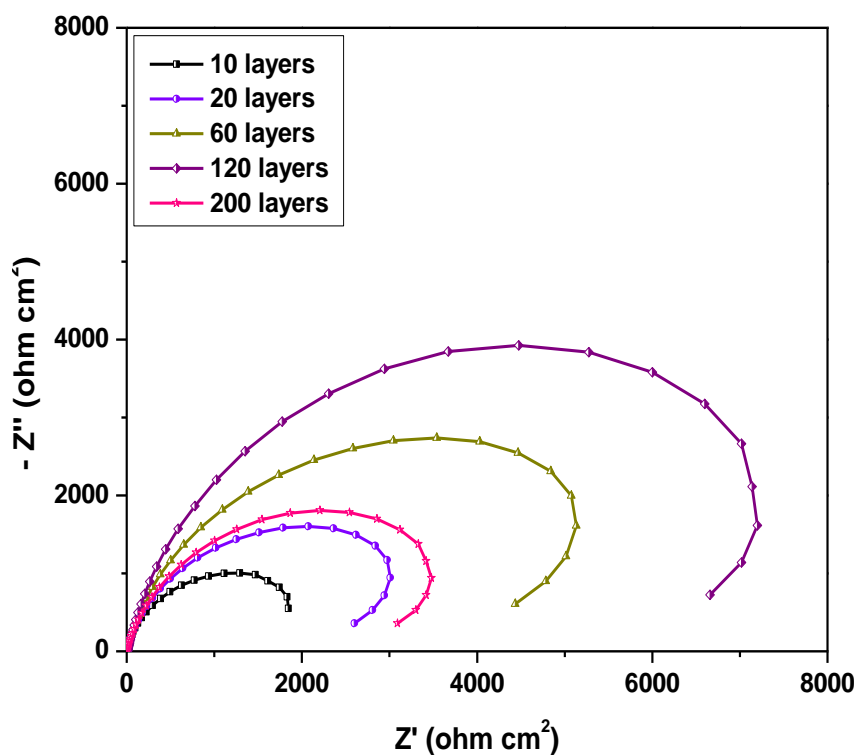
Fig. 9.6. Real versus imaginary resistance values of multilayer (Fe-Co)$_{2.0/4.0/6.0}$ coatings having different number of layers measured as function of frequency, developed from optimized bath at 303 K

9.2.5 Dielectrics study

The variation in relative permittivity, ε_r of CMMA Fe-Co coatings having varied number of layers are shown in Fig. 9.7. At low frequency side, the frequency response of the capacitor was found to be a function of ε_r. At high frequency limit, it may be observed that ε_r is found to be independent of the number of layers. It is due to the fact that at high

frequency, there is no charging and discharging of the capacitor and the capacitor is effectively like an open circuit (vacuum). Therefore, ε_r is almost same for all coatings, irrespective of the number of layers. Hence, decrease of ε_r with number of layers suggests that the polarizing ability of the Electrical Double Layer (EDL) capacitor decreases with layering (Ravinder and Latha, 1999). Therefore less ε_r of CMMA (Fe-Co)$_{2.0/4.0/6.0/120}$ compared to other coating systems, is responsible for improved corrosion resistance. In other words, the coating with more number of layers behaves a good dielectric barrier (insulator) for passage of current.
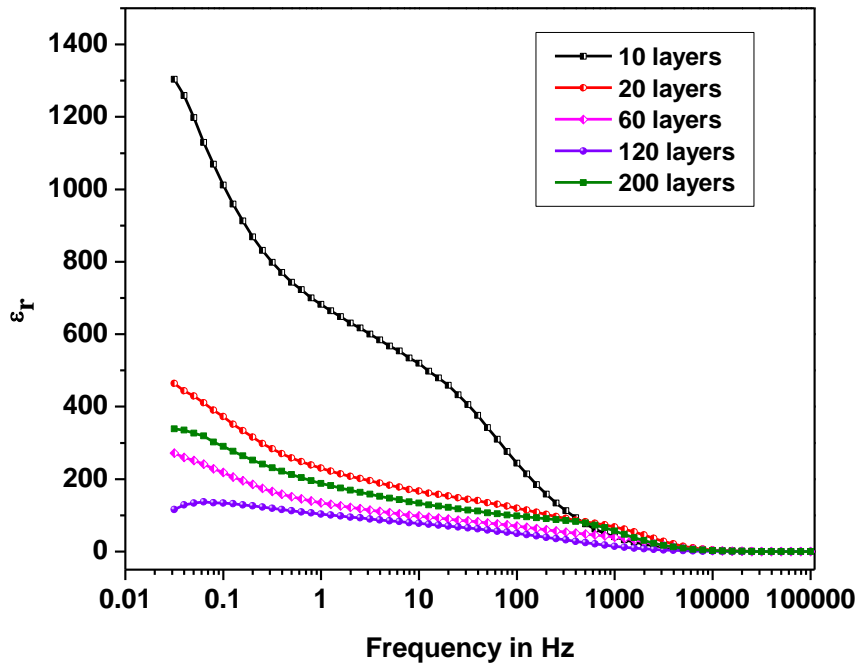
Fig. 9.7. Frequency response of relative dielectric constant of CMMA (Fe-Co)$_{2.0/4.0/6.0}$ coatings, deposited from the optimized bath with different number of layers

9.2.6 SEM Study

The formation of discrete layers with alternatively changing composition, during deposition was confirmed by SEM analysis. The cross sectional view of $(Fe-Co)_{2.0/4.0/6.0/10}$ coating, shown in Fig. 9.8 displays the formation of coatings having laminar structures. The mechanism of corrosion degradation was once again confirmed by acid test. The CMMA $(Fe-Co)_{2.0/4.0/6.0/10}$ coating was treated with a drop of dilute HCl for 10 seconds, and then washed with water and then dried.

The inspection of the microscopic appearance of the surface after acid test allows in understanding the mechanism of corrosion. The high corrosion prevention is due to fact that one layer of alloy having one type of failures (like pores, crevices or columnar structure, due to deposition at one current density) will be covered successively by the another layer of alloy, having another type of failures (due to deposition at some other current density). That is why, when multilayer coatings is exposed to a corrosive medium, the corrosive process needs more time to penetrate through layered structures than in monolayer coating. Consequently, the corrosion agent's path will be longer, or blocked.

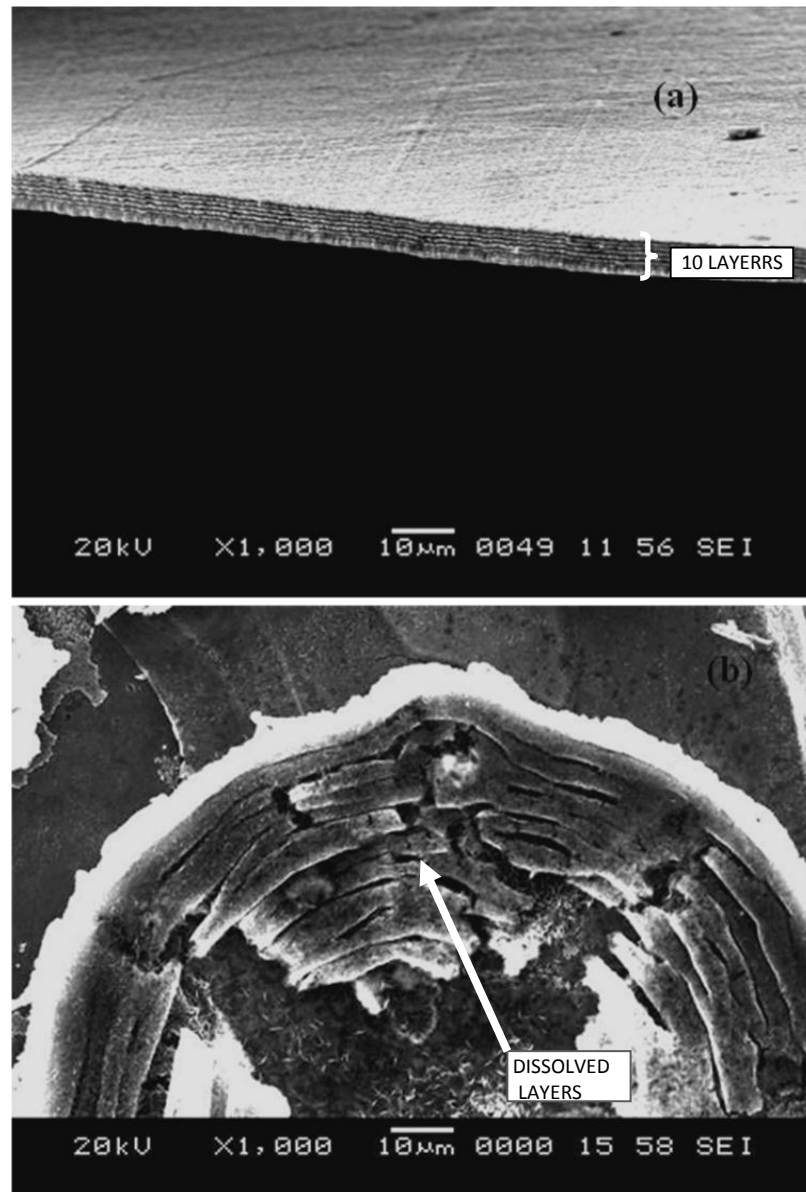Fig. 9.8. SEM image of multilayer coatings: (a) Cross sectional view of CMMA (Fe-Co)$_{2.0/4.0/6.0/10}$ and (b) surface after acid test displaying layered degradation

SECTION - 9.3 Comparison of corrosion rates of monolayer and multilayer Fe-Co alloy coatings developed using dual and triple current pulses

To identify the effect of compositional modulation in individual layers, the CMMA Fe-Co alloy coating was accomplished using dual and triple current pulses, and their corrosion behaviors were studied, and compared with that of monolayer $(Fe-Co)_{4.0}$ coatings. The multilayer alloy coating systems, under optimal configurations are more corrosion resistant than monolayer alloy coatings as discussed in Sections 9.1 & 9.2. The corrosion data of monolayer and multilayer coatings of Fe-Co alloy (all under optimal conditions) is reported in Table 9.5. It may be noted that a drastic decrease of CR was observed when monolayer coating method is changed to multilayer type. Further, the CMMA coating developed using triple current pulse is relatively more corrosion resistant than one developed using dual current pulse, may be due to increased modulation caused by three current pulses, instead of two.

Table 9.5. Comparison of corrosion rates of monolayer $(Fe-Co)_{4.0}$, multilayer $(Fe-Co)_{2.0/4.0/dual}$ and $(Fe-Co)_{2.0/4.0/6.0/triple}$ coatings developed using dual and triple current pulses under optimal conditions for same time.

Coating configuration	$-E_{corr}$ vs SCE (V)	i_{corr} (μA cm^{-2})	CR (mm y^{-1})
$(Fe-Co)_{4.0/monolayer}$	1.027	2475.8	27.81
$(Fe-Co)_{2.0/4.0/120/dual}$	0.981	88.62	0.99
$(Fe-Co)_{2.0/4.0/6.0/120/triple}$	0.967	10.12	0.16

The potentiodynamic polarization behavior of $(Fe-Co)_{2.0/4.0/120/dual}$ and $(Fe-Co)_{2.0/4.0/6.0/120/triple}$ in comparison with that of monolayer $(Fe-Co)_{4.0}$ coatings (all under optimal conditions) is shown in Fig. 9.9. A substantial decrease of corrosion rate was
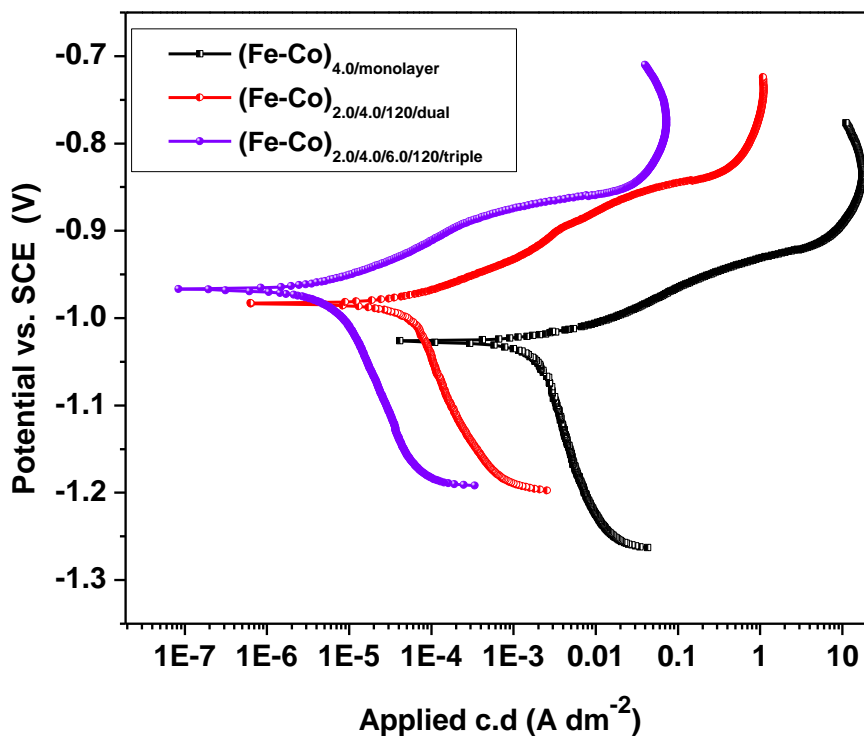
Fig. 9.9. Potentiodynamic polarization behavior of (Fe-Co)$_{4.0}$, (Fe-Co)$_{2.0/4.0/60/dual}$ and (Fe-Co)$_{2.0/4.0/6.0/60/triple}$ coatings developed from same bath at 303 K

observed when coating was carried out by multilayer method. It may be noted from the corrosion data reported in Table 9.5, that the corrosion protection of (Fe-Co)$_{2.0/4.0/120/triple}$ coating system is ~170 times better (0.16 mm y^{-1}) than that of monolayer (Fe-Co)$_{4.0}$ alloy (27.81 mm y^{-1}). Further, (Fe-Co)$_{2.0/4.0/120/dual}$ coatings exhibit ~27 times better corrosion resistant than (Fe-Co)$_{4.0/monolayer}$. The observed better corrosion resistance of multilayer coatings is due to the combined effect of structural modulation and increased number of interfaces due to layering.
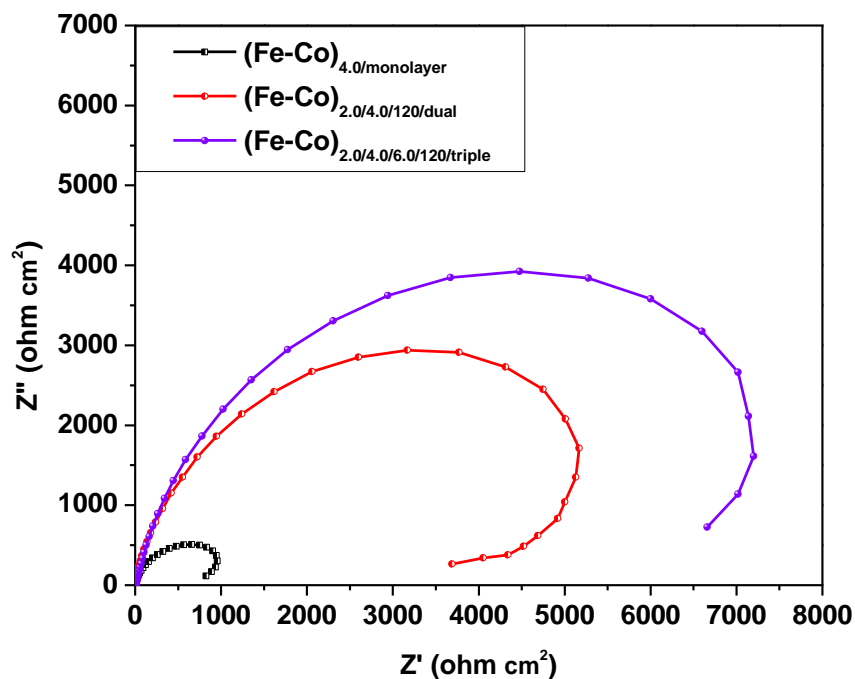
Fig. 9.10. Relative impedance response of (Fe-Co)$_{4.0/monolayer}$, (Fe-Co)$_{2.0/4.0/60/dual}$ and (Fe-Co)$_{2.0/4.0/6.0/60/triple}$ coatings developed from same bath at 303 K

Relative impedance response of (Fe-Co)$_{2.0/4.0/120/dual}$ and (Fe-Co)$_{2.0/4.0/6.0/120/triple}$ and monolayer (Fe-Co)$_{4.0/monolayer}$ coatings is shown in Fig. 9.10. The significant decrease in corrosion rates of CMMA coatings, in relation to a monolayer alloy coating is due to a large reactance of an electrical double layer capacitor at the interface of base metal (copper) and the medium. The experimental investigations have demonstrated that the multilayer coatings are more corrosion resistant than monolayer one.
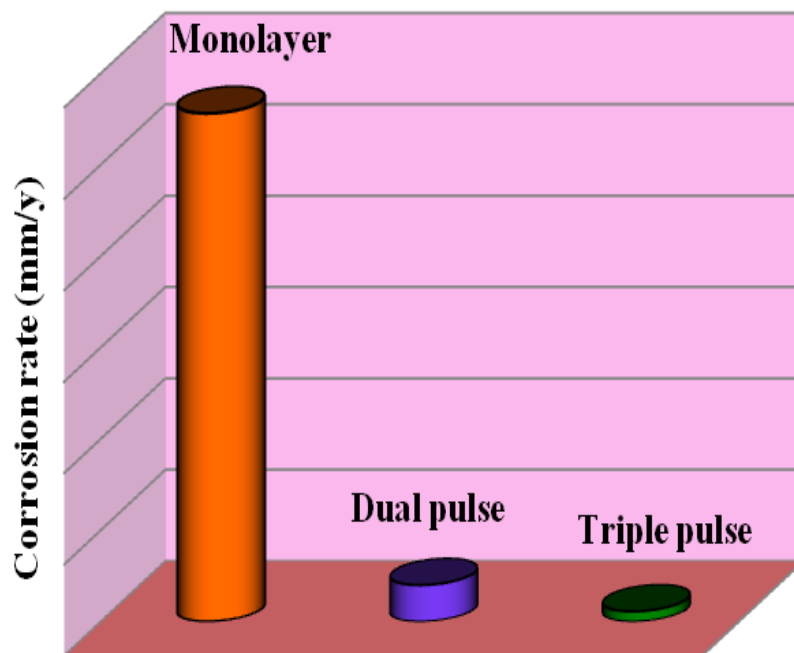
Fig. 9.11. Comparative account of corrosion rates of (Fe-Co) monolayer and CMMA (Fe-Co)dual and CMMA (Fe-Co)triple alloy coatings developed from same bath for same time (10 minutes)

No significant variation in the corrosion rates were observed when current is changed from dual pulse to triple pulse. A comparison of corrosion protection efficacy of CMMA coatings in 1M HCl solution, developed using dual and triple current pulses in comparison with that of monolayer alloy is shown in histogram in Fig. 9.11. All coatings have been carried out using same bath for same duration of deposition at 303 K.

9.3.1 Conclusions

1. The corrosion protection efficacy of the CMMA Fe-Co coating increases with number of layers substantially only up to certain optimal degree of layering, and then decreased in both dual and triple current pulses.

2. No significant difference in the corrosion performance of CMMA Co-Ni coatings was found, when current is changed from dual pulse to triple pulse.

3. The decreased CR of multilayer coatings is due to increased number of interfaces with large specific surface area of the materials. The increased corrosion resistance is attributed to the combined effect of compositional modulation and increased numbers of layers (interfaces).

4. The coatings developed using triple current pulse exhibits more corrosion resistance than one by dual current pulse may be due to more modulation caused by three current pulses.

SUMMARY AND CONCLUSIONS

The mutual alloys of Fe-group metals such as Fe-Ni, Co-Ni and Fe-Co alloys have been widely used as important engineering materials because of their high strength, good corrosion resistance, heat-conductive, and electrocatalytic activity. Among the various fabrication methods available for their synthesis, electrodeposition is proved to be the simple and most economic method to produce such coatings without high temperature and pressure. Moreover, microstructures and properties of the coatings can be easily tuned by changing the electrodeposition parameters, such as deposition current/voltage, bath composition, temperature and agitation etc. These alloys are of commercial reality and are good substitute for widely used anticorrosive coatings of Zn-M (where M = Fe, Ni, Co and less commonly Mn) alloys. The corrosion resistance of monolayer alloys of Fe-group metals, namely Fe-Ni, Co-Ni and Fe-Co can be improved to many fold of its magnitude by multilayer technique. Hence with that incentive, the electrofabrication of multilayer coatings of few alloys of Fe-group metals have been accomplished on copper for better protection of the coatings against corrosion. The corrosion stability of multilayer alloy coatings were compared with that of monolayer coatings, and results are discussed while understanding the possible reasons for extended protection by multilayer coatings.

10.1. SUMMARY

A systematic study on development monolayer coatings of Fe-Ni, Co-Ni and Fe-Co, denoted as (Fe-Ni)$_{mono}$, (Co-Ni)$_{mono}$ and (Fe-Co)$_{mono}$; and their multilayer coatings have been developed using dual and triple current pulses represented, respectively as (Fe-Ni)$_{dual}$, (Co-Ni)$_{dual}$ and (Fe-Co)$_{dual}$ and (Fe-Ni)$_{triple}$, (Co-Ni)$_{triple}$ and (Fe-Co)$_{triple}$. All depositions were carried out galvanostatically on copper substrate from the respective baths (optimized for best corrosion protection by changing the bath chemistry and

operating parameters) for 10 minutes (for comparison purpose). The power pattern used for production of monolayer and multilayer alloy coatings are shown in Fig 3.1.Three new baths, namely Fe-Ni, Co-Ni and Fe-Co have been proposed for development bright and uniform coatings of respective alloy on copper. The sulphanilic acid (SA), boric Acid (BA) and ascorbic Acid (AA) were used as common additives. The corrosion behaviors of electroplated coatings (both monolayer and multilayer) were evaluated in 1 M HCl solution (as representative medium for severe corrosion) by potentiodynamic polarization and EIS methods.

As an effort to increase the corrosion resistance of monolayer (bulk) binary alloy coatings of mutual alloys of Fe-group metals, the multilayer or alternatively composition modulated multilayer alloy (CMMA) coatings have been synthesized electrolytically using dual and triple current pulses. Multilayer coatings having different coating configurations have been developed by single bath technique (SBT) i.e. by consecutive deposition of alloys at different current densities, called cyclic cathode current densities (CCCD's) from the single bath having both metal ions. CMMA coatings having different configurations, in terms of number and thickness of individual layers have been developed, and coating conditions have been optimized for peak performance against corrosion. The operating parameters such as c.d., pH and bath variables such as metal salts and additives for each binary alloy baths have been optimized by standard Hull cell method.

The effect of metal salt, SA, BA and AA on deposit characters were studied.The coating characters in terms of appearance, thickness, hardness, composition, cathode current efficiency (CCE), magnetic property and corrosion rates (CR) were evaluated. All depositions, both monolayer and multilayer coatings were accomplished galvanostatically for 10 minutes for comparison purpose. The proposed composition and operating parameters of three new electrolytic baths, i.e. Fe-Ni, Co-Ni and Fe-Co baths have been given in Table 10.1.

Table 10.1. Bath composition and operating parameters of optimal baths for deposition of bright monolayer coatings of mutual alloys of Fe-group metals on copper substrate

Bath constituents (g L^{-1})	Fe-Ni	Co-Ni	Fe-Co
Nickel sulphate ($NiSO_4. 6H_2O$)	100	131	-
Cobalt sulphate ($CoSO_4. 7H_2O$)	-	14	152
Ferrous sulphate ($FeSO_4.7H_2O$)	16	-	16
Boric Acid, BA	30	30	30
Ascorbic Acid, AA	8	8	8
Sulphanilic Acid, SA	1	1	1
pH	3.5	3.5	3.5
Temperature (K)	303	303	303
Current density (A dm^{-2})	4.0	4.0	4.0

The process and product of electrolysis in each bath have been studied by different instrumental methods. Corrosion performances of each monolayer alloy coating, electroplated from respective bath (optimized) using direct current (D.C.) are summarized in Table 10.2. As part of an effort to increase the corrosion resistance of monolayer alloy coatings, multilayer coatings have been developed galvanostatically using respective binary alloy baths by bringing modulation in current pulse. The structural or compositional modulation in layers was effected using dual and triple current pulses.

To increase the corrosion performance of monolayer (bulk) binary alloys of Fe-group metals, the CMMA coatings, represented as CMMA (Fe-Ni), CMMA (Co-Ni) and CMMA (Fe-Co) have been developed with different configuration. The effect of CCCD's and number of layers on the corrosion resistance character of the coatings has been studied. The progressive decrease of CR was found in all sets of CCCD's tried. This

indicated that the observed decrease of CR is not specific of the composition of individual layer alone but also on number of interfaces involved. As the number of layers (or interfaces) increased, the monolayer coating is going to be dominated by number of interfaces. Consequently, there will be appreciable increase in specific surface area of materials, or at grain boundary regions (analogously to the surface region of nanoparticles). This observation is in support of principles of nano/microstructure multilayer coatings of metals/alloys exhibiting variety of improved functional properties (Gurrappa and Binder 2008).

Table 10.2.comparative account of corrosion rate (CR) and coating characters of binary alloys (monolayer) of Fe-group metals developed from optimized baths, corresponding to Table 10.1

Operating parameters	Monolayer Fe-group alloy coatings		
	Fe-Ni	Co-Ni	Fe-Co
Optimal c.d. (A dm^{-2})	4.0	4.0	4.0
pH	3.5	3.5	3.5
Bath temperature (K)	303	303	303
CCE (%)	82.0	89.0	95.0
Total thickness (μm)	6.76	7.34	7.79
Vickers Hardness (V$_{100}$)	359	450	302
Magnetic saturation (emug^{-1})	6.16	13.16	7.20
Coercivity (Oe)	15.95	18.90	26.15
CorrosionRate (CR)	7.4	17.64	27.81
Nature of deposit	Bright	Bright	Bright

The corrosion performance of CMMA coatings developed using both types of current pulses (dual and triple) were found to be increased with number of layers up to an optimal level, and then decreased. No significant difference in the corrosion performance was found, when dual current pulse is changed from dual to triple current pulse type. Further, it was observed that in each mode of current pulse used, the improvement in corrosion performance with layering was not restricted to only one set of CCCD's. These observations indicated that improved property of the coatings depends not only on modulation in composition but also on number of interfaces, developed due to layering. However, between dual and triple current pulses the coatings developed using triple current pulses exhibited more corrosion resistance due to more modulation caused by three current pulses.

The corrosion stability of the coatings increased with number of layers only up to certain optimal level, and then decreased. The decrease of CR at high degree of layering was attributed to the less relaxation time for redistribution of metal ions at the diffusion layer during deposition. At high degree of layering, the deposition time for each layer being very small, the metal ions could not relax (against the influence of applied c.d.), and get deposit on cathode with changed composition (Kanani, 2006). In other words at high degree of layering the deposit is tends to become monolayer, or non-nanostructured due to exceptional thinning of layers.The decrease of corrosion resistance at high degree of layering is thus attributed to interlayer diffusion. The optimal configuration, in terms of CCCD's and numbers of layers for development of the most corrosion resistant multilayer coatings, developed using dual and triple current pulses are summarized in Table 10.3.The average thickness of the layer and other operating conditions corresponding to each CMMA coatings is given in Table 10.3. Experimental investigation revealed that corrosion resistances of all electrodeposited coatings of mutual alloys of Fe-group metals are found to be more corrosion resistant than corresponding monolayer alloys, deposited from same bath for same duration.

Further, among the Fe-group mutual alloys, the monolayer $(Fe-Ni)_{4.0}$ alloy was found to be more corrosion resistant than monolayer $(Co-Ni)_{4.0}$ and $(Fe-Co)_{4.0}$ coatings as shown in Table 10.3.

Table 10.3. The optimal CCCD's and number of layers with corrosion rates of CMMA coatings of mutual alloys of Fe-group metals on copper substrate developed using dual and triple current pulses (in comparison with that of monolayer alloy coating)

Optimal parameters	Fe-Ni	Co-Ni	Fe-Co
CMMA coatings of mutual alloys of Fe-group metals using dual pulse			
CCCD's (A dm^{-2})	2.0/4.0	2.0/4.0	2.0/4.0
pH	3.5	3.5	3.5
Temperature, K	303	303	303
No. of layers	300	60	120
Average thickness of each layer, nm	50	83	67
Corrosion rate, CR (mm y^{-1})	0.32	0.20	0.99
Max. number of layerspossible	300	60	120
CMMA coatings of mutual alloys of Fe-group metals using triple pulse			
CCCD's (A dm^{-2})	2.0/4.0/6.0	2.0/4.0/6.0	2.0/4.0/6.0
pH	3.5	3.5	3.5
Temperature, K	303	303	303
No. of layers	300	60	120
Average thickness of each layer, nm	50	83	67
Corrosionrate, CR (mm y^{-1})	0.13	0.11	0.16
Max. number of layerspossible	300	60	120
Monolayer coatings of mutual alloys of Fe-group metals using D.C.			
Corrosionrate, CR (mm y^{-1})	7.40	17.64	27.81

It was observed that among all CMMA coatings of Fe-group metals, (Co-Ni)$_{2.0/4.0/6.0/60/triple}$ was found to be the most corrosion resistant than other multilayer coatings. It is due to the fact that both constituent metals, namely Co and Ni are noble when compared to Fe.

Table 10.4.Comparison of corrosion rates of multilayer iron-group alloy coatings developed, using both dual and triple current pulses with that of respective monolayer alloys (all under optimal conditions)

Coating configuration	$-E_{corr}$ vs SCE (V)	i_{corr} ($\mu A\ cm^{-2}$)	CR (mm y^{-1})
Monolayer (Fe-Ni)$_{4.0}$	0.913	650.38	7.40
CMA (Fe-Ni)$_{2.0/4.0/300/dual}$	0.924	28.7	0.32
CMA (Fe-Ni)$_{2.0/4.0/6.0/300/triple}$	0.920	12.0	0.13
Monolayer (Co-Ni)$_{4.0}$	0.583	1586.1	17.64
CMA (Co-Ni)$_{2.0/4.0/60/dual}$	0.644	18.8	0.2
CMA (Co-Ni)$_{2.0/4.0/6.0/60/triple}$	0.633	10.0	0.11
Monolayer (Fe-Co)$_{4.0}$	1.027	2475.8	27.81
CMA (Fe-Co)$_{2.0/4.0/120/dual}$	0.981	88.62	0.99
CMA (Fe-Co)$_{2.0/4.0/6.0/120/triple}$	0.967	10.12	0.16

Thus it may be summarized that all optimized CMMA coatings of mutual alloys of Fe-group metals are more corrosion resistant than corresponding monolayer binary alloy coatings. Monolayer alloys are less corrosion resistant than multilayer alloy coatings. i.e. corrosion tendency of monolayer (Fe-Ni, Co-Ni, Fe-Co) alloy is greater than multilayered (Fe-Ni), (Co-Ni) and (Fe-Co) alloy coatings developed using dual current

pulse which is greater than multilayered multilayered (Fe-Ni), (Co-Ni) and (Fe-Co) alloys developed using triple current pulse. Comparison of corrosion rates of multilayer coatings of mutual alloys of Fe-group metals developed using dual and triple current pulses with that of respective monolayer alloys (all under optimal conditions) is shown in Table 10.4. The relative corrosion performance of monolayer, multilayer coatings of mutual alloys of Fe-group metals developed using dual and triple current pulses in 1M HCl solution is depicted by histogram given in Fig.10.1.
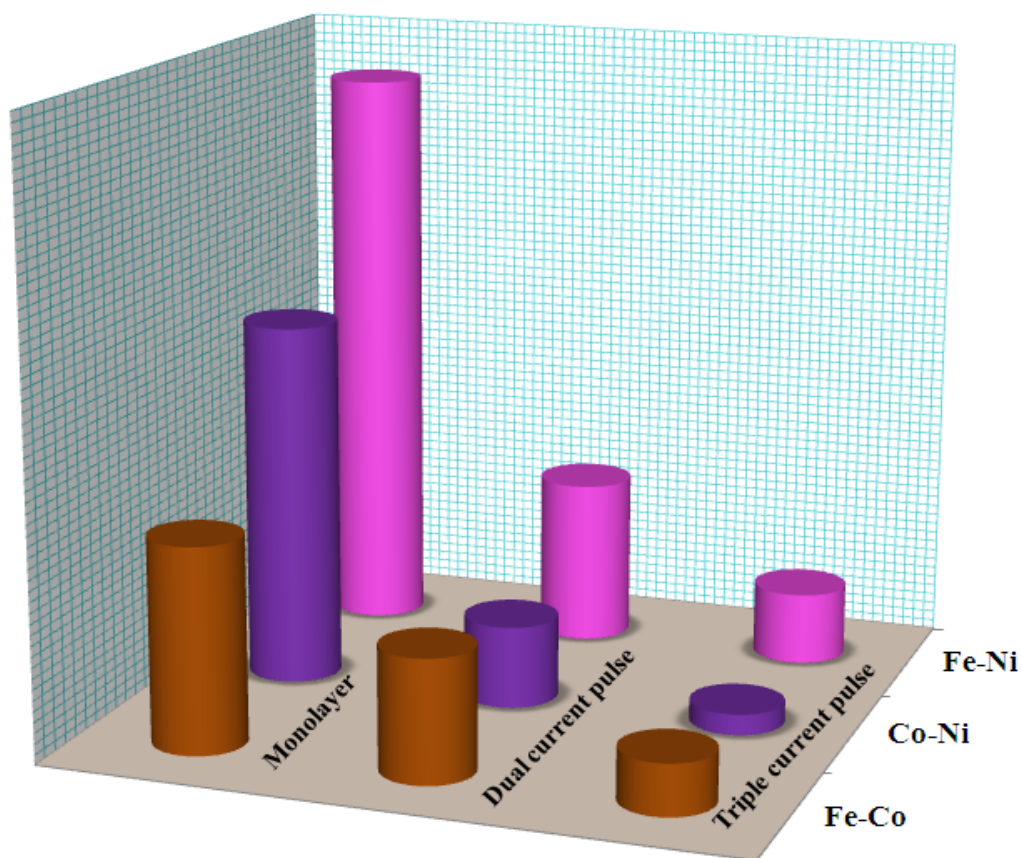

Fig. 10.1. The histogram showing relative rates of corrosion of monolayer and multilayer coatings of mutual alloys of Fe-group metals developed using D.C. and pulsed current (dual and triple), respectively from same bath for same time

In summary, the present research work concentrates on the deposition of monolayer and multilayer iron-group mutual alloys and their characterization. Each chapter is briefly summarized with mechanism and the conclusions drawn are given below:

Chapter 1 gives an overview of basic concepts of electroplating, including importance of alloy plating with a brief introduction to corrosion and corrosion measurement techniques. The various types of alloy deposition, the role of common variables on alloy deposition were explained, with special emphasis on electrodeposition of Fe-Ni, Co-Ni and Fe-Co alloys. A general introduction to different terms used in the thesis, and basic principles of experimental techniques employed in the thesis are detailed.

Chapter 2 is devoted for literature review on electrodeposition of Fe-Ni, Co-Ni and Fe-Co alloys developed using DC and modulated current pulses, followed by scope and objectives.

Chapter 3 explains the general methodology and experimental procedure adopted in the present research work.

Chapter 4 details the optimization of Fe-Ni alloy bath by standard Hull cell method for production of bright monolayer coatings using DC. The magnetic property and corrosion behaviors of the coatings were studied, and results were discussed. XRD study revealed that volume fraction of bcc structure is higher than that of fcc at low c.d.; and fcc phase becomes predominant over the bcc phase as c.d. is increased. The crystallite grain size and phase structure of the coatings has a positive effect on M_s and H_c of Fe-Ni coatings. Corrosion performance of Fe-Ni coatings at 4.0 Adm^{-2} (having ~ 81.5 % of Ni) were compared with those deposited at other c.d.'s, and results were discussed.

Chapter 5 outlines the detailed investigation on development of multilayer Fe-Ni alloy coatings, developed using dual and triple current pulse. The corrosion degradation behaviors have been studied in comparison with that of monolayer coating developed using the same bath. It was observed that even a small change in the wt. % of Ni in the layer is sufficient to bring large change in the corrosion resistance of the coatings due to intrinsic change in phase structure of the alloys in successive layers. The corrosion

232

protection efficacy of the multilayer Fe-Ni coatings was related to the *sacrificial* and *barrier* effect of the individual layers. The formation of multilayer and reasons responsible for better protection were explained using scanning electron microscopy (SEM) analysis.

Chapter 6 deals the optimization of a stable electrolytic bath for deposition of bright monolayer Co-Ni alloy on copper using DC. The structure and magnetic property of Co-Ni alloy films are tuned by adjusting the deposition c.d. The XRD study of electrodeposited binary Co-Ni alloy indicated the structure consists of a substitutional solid solution phase. An increase of grain size of Co-Ni alloy was observed at high c.d. The micro-hardness of the coatings was found to increase with c.d. as function of its phase structure. Corrosion study demonstrated that Co-Ni alloy deposited at 4.0 A dm^{-2}, having ~76 % of Ni is the most corrosion resistant (CR = 17.64 mm y^{-1}). The highest corrosion resistance was attributed to the coexistence of hcp and fcc phases with smaller grain size.

Chapter 7 deals with CMMA Co-Ni coatings developed using different power patterns viz. dual and triple current pulse, and their optimization. The reasons responsible for better corrosion resistance were analyzed, and discussed in the light of effect of nano-laminar coatings. The early saturation in corrosion resistance with less number of layers in case of multilayered Co-Ni alloy was found, and reasons were discussed. The corrosion resistances were found to increase with number of layers only up to 60 layers and then decreased. In other words, multilayer coating tends to become monolayer, showing the bulk property of the material.

Chapter 8 provides the galvanostatic deposition of bright Fe-Co alloy on copper substrate using a new sulphate bath. At higher c.d., increased grain size was observed. The micro-hardness of the deposits was found to decrease with c.d. as a function of phase structures. Saturation magnetization, M$_s$ and coercivity, H$_c$ of Fe-Co coatings show inverse dependency with each other over entire c.d. range studied, and were attributed to crystallite grain size and phase structure of the deposit. Both polarization and impedance

study of the coated samples revealed that Fe-Co alloy coating deposited at optimal condition, i.e. at 4.0 A dm^{-2} shows highest corrosion resistance.

Chapter 9 presents the development of nanostructured Fe-Co alloy coatings, demonstrating their superior corrosion resistance compared to non-nanostructured (monolayer) coatings. The thickness of individual layers of CMMA coatings, play important role in imparting the better corrosion protection. The corrosion rate decreased with number of layers only up to certain (optimal) number layers, and then increased. The increase of corrosion rate at high degree of layering was attributed to less relaxation time for redistribution of metal ions (Co^{2+} and Fe^{2+} ions) in the diffusion layer during plating. The impedance responses of Fe-Co alloy coatings developed using dual and triple current pulses are dominated by inductive loop. This suggests all Co-based alloys of Fe-group metals are more electrically conductive.

10.2. MECHANISM OF CORROSION PROTECTION BY CMMA COATINGS

A better functional property of any nanostructured materials is generally due to increased surface area, or number of interfaces. Accordingly, the better corrosion resistance of CMMA coatings of mutual alloys of Fe-group metals is attributed to increased number of layers. The probable mechanism of corrosion observed in all CMMA coatings, the regardless of the type of current pulses used may be illustrated schematically by Fig. 10.2.
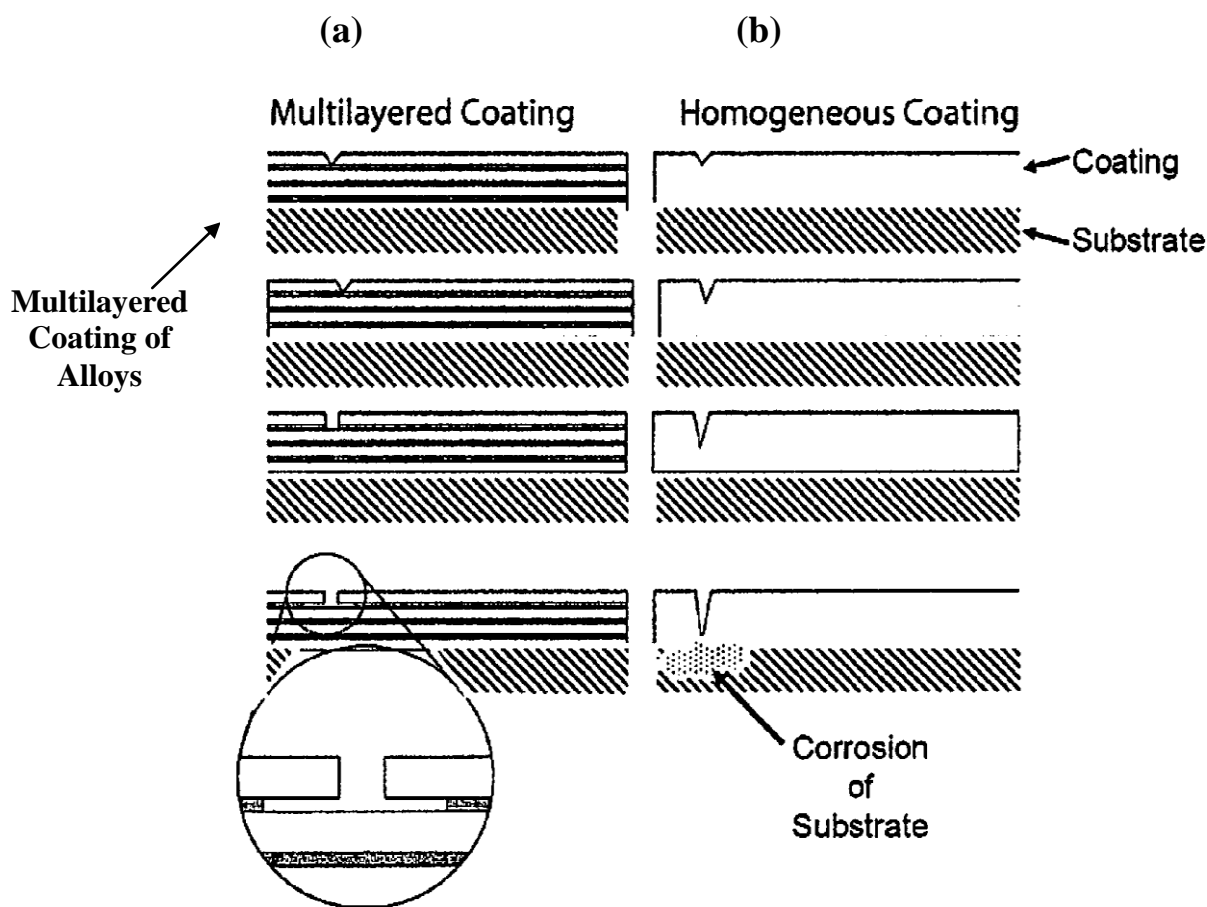
(a)   **(b)**

Fig. 10.2. Schematic of probable corrosion mechanism in CMMA coatings (a) 4 layers of alloys with composition 'x' alternated by 4 layers of alloys with composition 'y' and(b) monolayer alloy of metals M_1 and M_2,

         The Fig.10.2(a) represents a layers of alloys having compositions x and y., i.e. alloys of two compositions alternatively applied 4 times to provide a total of 8 layers with 4 periodic layers of a first type alternated with 4 layers of a second type, wherein the first and the second type of layers are not identical. Initially, the $(M_1-M_2)_X$ top layer (where x represents the composition of one alloy constituted by metals M_1 and M_2)having high wt.% noble metal corrode slowly, then it passes through beneath layer, $(M_1-M_2)_Y$ (where y represents the composition of another alloy) having less wt.% noble metal which corrode fast.

This process goes on layers after layers. As the number of layers increased, the corrosive agent needs more time to penetrate through coating defects into the substrate material. But in case of monolayer, or homogeneous/bulk coating, shown in Fig. 10.2(b) the corrosion takes place unabatedly, and reaches the substrate very fast. Thus corrosion protection efficacy of multilayer coatings is thus due to barrier effect of layers with high wt. % noble metal, and sacrificial effect of layers with less wt. % noble metal (Fei and Wilcox 2006). It can also be interpreted in terms of alternate layers having different composition, and hence different phase structures (Ganesan et al. 2007).

10.3. CONCLUSIONS

Based on the experimental research carried out on binary alloys of Fe-group metals, i.e. Fe-Ni, Co-Ni and Fe-Co and results obtained, the following conclusions were drawn.

1. Three new binary Fe-group metal alloy baths have been optimized by exploiting the synergistic effect of additives for improving performance of the coatings. Micro-hardness, saturation magnetization, Ms and coercivity, Hc of electrodeposited monolayer Fe-group metal alloys varies as a function of crystalline grain size and phase structure of the alloys.

2. At optimal conditions, $(Fe-Ni)_{4.0/mono}$ alloy coating exhibited less corrosion rate compared to $(Co-Ni)_{4.0/mono}$ and $(Fe-Co)_{4.0/mono}$ alloys, may be due to their distinct phase structures.

3. Multilayer coatings of Fe-group metals developed using both dual and triple current pulses are found to be more corrosion resistant compared to corresponding monolayer alloys developed using DC for same time, due to phase difference in alternate layers, consequent to difference in noble metal content.

4. Corrosion resistance of CMMA coatings of mutual alloys of Fe-group metals can be increased by increasing the number of layers. This is true only up to certain critical number of layers, and beyond which it decreases, due to less time for redistribution of metal ions in the diffusion layer during plating.

5. No significant difference in the corrosion performance of CMMA coatings was found, when current is changed from dual pulse to triple pulse. Which indicates the corrosion performance of CMMA coatings depends mainly on number of distinct interfaces but not only on composition modulation.

10.4. SCOPE FOR FUTURE WORK

In the present study monolayer and multilayer coatings of binary alloys of Fe-group metals have been studied using, respectively DC and pulsed DC. i.e. dual and triple square current pulses for better corrosion protection. As the present investigation established that the multilayer coatings offer better corrosion protection to copper substrate, the investigation will be tried using triangular and saw-tooth current pulses (for gradual and sharp-gradual change in composition) for better property of the coatings. The incredible claims of multilayer coating technique can be effectively used for optimization of deposition conditions. The coating configuration will be modulated by setting up of proper CCCD's and number of layers for better properties of the coatings, including corrosion, magnetic and their electrocatalytic behaviors.

REFERENCES

Aarti, S.B., Krishna, B.D. and Santosh, M.S. (2010). "Electrical and magnetic properties of chitosan-magnetite nanocomposites." *Physica B*., 405, 2078-2082.

Afshar, A., Dolati, A.G. and Ghorbani, M. (2002). "Electrochemical characterization of the Ni-Fe alloy electrodeposition from chloride-citrate-glycolic acid solutions." *Mater. Chem. Phy.,* 77, 352-358.

Aggen, G. (1990). *Properties and selection: irons, steels, and high-performance alloys,* Volume 1, ASM International, Portland.

Alper, M., Schwarzacher, W. and Lane, S.J. (1997). "The effect of pH changes on the giant magnetoresistance of electrodeposited superlattices." *J. Electrochem. Soc.,* 7, 2346-2352.

Amelinckx, S., Dyck, V.D., Landuyt, V.J. and Tendeloo, V.G. (1996). *Handbook of Microscopy - Applications in Materials Science, Solid-state Physics and Chemistry,* vol 3, Wiley-VCH, Weinheim.

Andricacos, P.C. and Romankiw, L.T. (1994). *Advances in electrochemical science and engineering,* Vol. 3, Wiley- VCH, New York.

ASM *Handbook, Surface Engineering,*(1994). vol. 5, Publisher: ASM International Handbook Committee.

ASTM B 374. (1996). "Standard terminology relating to electroplating." *American Society for Testing and Materials,* Pennsylvania.

Bagotzky, V.S. (1993). *Fundamentals of Electrochemistry*, Edition. 1, Plenum Press, New York.

Bai, A. and Hu, C.C. (2003). "Iron-cobalt and iron-cobalt-nickel nanowires deposited by means of cyclic voltametry and pulse reverse electroplating." *Electrochem. Commun.,* 5, 78-82.

Barker, H. (1992). *ASM handbook,* (ed.), ASM International, Ohio.

Barsoukov, E. and Macdonald, J.R. (2005). *Impedance Spectroscopy,* Second Edition, John Wiley & Sons, Inc.

Bento, R.F. and Mascaro, L.H. (2002). "Analysis of the initial stages of electrocrystallization of Fe, Co, and Fe–Co alloys in chloride solutions." *J. Braz. Chem. Soc.,* 13, 502–509.

Bockris, J.O.M., Reddy, A.K.N. and Aldeco, M.G. (2000). *Modern Electrochemistry,* Kluwer Academic, Plenum Publishers.

Brenner, A. (1963). *Electrodeposition of alloys-Principles and Practice.* Vol. 1 & 2. Academic Press, New York.

Budevski, E., Staikov, G. and Lorenz, W.J. (1996). "Electrochemical phase formation and growth." *VCH*, Weinheim.

Bull, S.J. and Jones, A.M. (1996). "Multilayer coatings for improved performance." *Surf. Coat. Technol.,* 78, 173-184.

Burzynska, L. and Rudnik, E. (2000). "The influence of electrolysis parameters on the composition and morphology of Co-Ni alloys." *Hydrometallurgy,* 54, 133–149.

Ch, F. and Piront, D.L. (1996) "Study of anomalous nickel-cobalt electrodeposition with different electrolytes and current densities." *Electrochim. Act*a*.,* 41, 1713-1719.

Chawa, G., Wilcox, G.D. and Gabe, D.R. (1998). "Compositionally modulated zinc alloy coatings for corrosion protection." *Trans. Inst. Met. Finish.,* 76, 117-120.

Cheung, C., Djuanda, F., Erb, U. and Palumbo, G. (1995). "Electrodeposition of nanocrystalline Ni-Fe alloys." *Nanostruct. Mater.*, 5, 513-523.

Chung, C.K. and Chang, W.T., (2009). "Effect of pulse frequency and current density on anomalous composition and nanomechanical property of electrodeposited Ni–Co films." *Thin Solid Films,* 517, 4800–4804.

Cohen, U., Koch, F.B. and Sard, R. (1983). "Electroplating of cyclic multilayered alloy (CMA) coatings." *J. Electrochem. Soc.,* 130, 1987-1995.

Conway, B.E. (1999). *Electrochemical Supercapacitors, Scientific Fundamentals and Technological Applications,* Kluwer Academic/Plenum Press, New York.

Correia, A.N. and Machado, S. A.S. (2000). "Electrodeposition and characterization of thin layers of Ni-Co alloys obtained from dilute chloride baths." *Electrochim. Acta.,* 45, 1733-1740.

Correia, A.N. and Machado, S.A.S. (2003). "Anodic linear sweep voltammetric analysis of Ni-Co alloys electrodeposited from dilute sulfate baths." *J. Appl. Electrochem.,* 33, 367-372.

Czerwinski, F. (1996). "Grain size-internal stress relationship in iron-nickel alloy electrodeposits." *J. Electrochem. Soc.,* 143, 3327-3332.

Czerwinski, F. (1998). "The synthesis of Fe-Ni nanocrystalline alloys from additive-free electrolytes." *Nanostruct. Mater.,*10, 1363-1369.

Dahms, H. and Croll, I.M. (1965). "The anomalous co-deposition of iron-nickel alloys." *J. Electrochem. Soc.*, 112, 771-775.

Despic, A.R. and Jovic, V.D. (1987). "Electrochemical formation of laminar deposits of controlled structure and composition using single current pulse galvanostatic technique." *J. Electrochem. Soc.,* 134, 3004-3011.

Despic, A.R. and Jovic, V.D. (1989). "Electrochemical formation of laminar deposits of controlled structure and composition using dual current pulse galvanostatic technique." *J. Electrochem. Soc.,* 136, 1651-1657.

Despic, A.R., Jovic, V.D., White, R.E. and J.O'M Bockris, B.E. (1995). *Modern Aspects of Electrochemistry*, Plenum Press, New York.

Dini, J.W. (1993). "Electrodeposition: the materials science of coatings and substrates." Noyes Publications, New Jersey.

Dobrzanski, L.A., Lukaszkowicz, K., Zarychta, A. and Cunha, L. (2005). "Corrosion resistance of multilayer coatings deposited by PVD techniques onto the brass substrate." *J. Mater. Process. Technol.,* 164, 816–821.

Dulal, S.M.S.I., Charles, E.A. and Roy, S. (2004). "Characterisation of Co-Ni(Cu)/Cu multilayers deposited from a citrate electrolyte in a flow channel cell." *Electrochim. Acta.,* 49, 2041-2049.

Ebrahim, F. and Li, H.Q. (2003). "Structure and properties of electrodeposited nanocrystalline FCC Ni–Fe alloy." *Rev. Adv. Mater. Sci.,* 5, 134–138.

Eliaz, N., Gileadi, E., Vayenas, C.G. and White, R.E. (2008). "Modern aspects of electrochemistry." *Springer,* Gamboa-AldecoME (eds), New York, 42, 191–301,

Fei, J.Y., Liang, G.Z., Xin, W.L. and Wang, W.K. (2006). "Surface modification with zinc and Zn-Ni alloy compositionally modulated multilayer coatings." *J. Iron. Steel Res. Int.*, 13, 61-67.

Fei. J.Y. and Wilcox, G.D. (2005). "Electrodeposition of Zn-Co alloys with pulse containing reverse current." *Electrochim. Acta.,* 50, 2693-2698.

Fenineche, N.E., Hamzaoui, R. and Kedim, O.E. (2003). "Structure and magnetic properties of nanocrystalline Co–Ni and Co–Fe mechanically alloyed." *Mater. Lett.,* 57, 4165– 4169.

Fontana, M.G. (1987). *Corrosion engineering,* McGraw Hill Book Co., New York, Third edition.

Fratesi, R. and Roventi, G. (1996). "Corrosion resistance of Zn-Ni alloy coatings in industrial production." *Surf. Coat. Technol*., 82, 158-164.

Fricoteaux, P. and Rousse, C. (2008). "Influence of substrate, pH and magnetic field onto composition and current efficiency of electrodeposited Ni–Fe alloys." *J. Electroanal. Chem.,* 612, 9-14.

Gabe, D.R. and Green, W.A. (1998). "The mathematical modelling of CMA multilayered coatings." *Surf. Coat. Technol.*, 105, 195-201.

Ganesan, P., Kumaraguru, S.P. and Popov, B.N. (2007). "Development of compositionally modulated Zn-Ni multilayer deposits as replacement for cadmium." *Surf. Coat. Technol.,* 201, 7896-7904.

Gellings, P.J. and Bouwmeester, H.J.M. (1997). *Handbook of Solid State Electrochemistry,* CRC Press, Netherlands.

Glasstone, S. (1960). *The Fundamentals of Electrochemistry and Electrodeposition.* Franklin Publising Company Inc., Palisade, New Jersey.

Golodnitsky, D., Rosenberg, Y. and Ulus, A., (2002). "The role of anion additives in the electrodeposition of Nickel-Cobalt alloys from sulfamate electrolyte." *Electrochim. Acta.,* 47, 2707-2714.

Gomez, E., Pane, S. and Valles, E. (2005). "Electrodeposition of Co–Ni and Co–Ni–Cu systems in sulphate-citrate medium," *Electrochim. Acta.,* 51, 146-153.

Grimmett, D. L., Schwartz, M. and Nobe, K. (1988). "Electrodeposition of iron-nickel (INVAR) alloys." *Plat. Surf. Finish.,* 75, 94-98.

Grimmett, D.L., Schwariz, M. and Nobe, K. (1993). "A comparison of DC and pulsed Fe-Ni alloy deposits." *J. Electrochem. Soc.,* 140, 973-977

Grimmett, D.L., Schwartz, M. and Nobe, K. (1990). "Pulsed electrodeposition of iron-nickel alloys." *J. Electrochem. Soc.,* 137, 3414.

Gurrappa, I. and Binder, L. (2008). "Electrodeposition of nanostructured coatings and their characterization-a Review." *Sci. Technol. Adv. Mater.,* 9, 043001

Haseeb, A., Celis, J. and Roos, J. (1992). "Electrodeposition of Cu/Ni compositionally modulated multilayers by the dual-plating bath technique." *Trans. Inst. Met. Finish.,* 70, 123.

Hegde, A.C., Venkatakrishna, K. and Eliaz, N. (2010). "Electrodeposition of Zn-Ni, Zn-Fe and Zn-Ni-Fe alloys." *Surf. Coat. Technol.*, 205, 2031-2041.

Heikes, R.R. and Johnston, W.D. (1957). "Mechanism of conduction in Li-substituted transition metal oxides." *J. Chem. Phys*., 26, 582-587.

Heusler, K.E. (1997). "Fundamental aspects of the corrosion of alloys." *Corros. Sci.,* 39, 1177-1191.

Huang, Q., Young, D.P., Chan, J.Y., Jiang, J. and Podlaha, E.J. (2002). "Electrodeposition of FeCoNiCu/Cu compositionally modulated multilayers". *J. Electrochem. Soc.,* 149, 349-354.

Hubert and Girault, H. (2004). *Analytical and Physical Electrochemistry,* First edition, EPFL Press Swiss publishing company distributed by Marcel Dekker, Inc.

Ivanov, I., Valkova, T. and Kirilova, I. (2002), "Corrosion resistance of compositionally modulated Zn-Ni multilayers electrodeposited from dual bath." *J. Appl. Electrochem.*, 32, 85-89.

Jartych, E., Jalochowski, M. and Budzynski, M. (2002). "Influence of the electrodeposition parameters on surface morphology and local magnetic properties of thin iron layers." *Appl. Surf. Sci.,* 193, 210–216.

Jensen, J.D., Crichlow, G.W. and Gabe, D.R. (1998). "A study on Zn-Fe alloy electrodeposition from chloride electrolyte." *Trans. Inst. Met. Finish.*, 76, 187-191.

Jensen, J.D., Gabe, D.R. and Wilcox, G.D. (1998). "The practical realization of zinc-iron CMA coatings." *Surf. Coat.Technol*., 105, 240-250.

Jiles, D. (1996). *Introduction to Magnetism and Magnetic Materials,* Chapman and Hall, London,

Jones, D.A. (1996). *Principles and prevention of corrosion,* Prentice Hall, New York.

Kakuno, E.M., Mosca, D.H., Mazzaro, I., Mattoso, N., Schreiner, W.H., Gomes, M.A.B. and Cantao, M.P. (1997). "Structure, composition, and morphology of electrodeposited Co_xFe_{1-x} alloys." *J. Electrochem. Soc.,* 144, 3222–3226

Kalantary, M.R., Wilcox, G.D. and Gabe, D.R. (1998). "Alternate layers of zinc and nickel electrodeposited to protect steel." *Br. Corros. J.,* 33, 197-201.

Kanani, N. (2006). *Electroplating: Basic Principles, Processes and Practice.* Elsevier Ltd, Berlin, Germany.

Karpuz, A., Kockar, H. and Alper, M. (2011). "The effect of different chemical compositions caused by the variation of deposition potential on properties of Ni–Co films." *Appl. Surf. Sci.,* 257, 3632–3635.

Kim, D., Park, D.Y., Yoo, B.Y., Sumodjo, P.T.A. and Myung, N.V. (2003). "Magnetic properties of nanocrystalline iron group thin film alloys electrodeposited from sulfate and chloride baths." *Electrochim. Acta.,* 48, 819- 830.

Koops, C.G. (1951). "On the dispersion of resistivity and dielectric constant of some semiconductors at audio frequencies." *Phys. Rev.,* 83, 121-124.

Kouloumbi, N., Tsangaris, G.M., Skordos, A. and Kyvelidis, S. (1996). "Evaluation of the behaviour of particulate polymeric coatings in a corrosive environment: Influence of the concentration of metal particles." *Prog. Org. Coat.*, 28, 117-124.

Lallemand, F., Ricq, L., Deschaseaux, E., Vettor, D.L. and Bercot, P. (2005). "Electrodeposition of cobalt-iron alloys in pulsed current from electrolytes containing organic additives." *Surf. Coat. Technol.,* 197, 10-17.

Lallemand, F., Ricq, L., Wery, M., Berçot, P. and Pagetti, J. (2004). "The influence of organic additives on the electrodeposition of iron-group metals and binary alloy from sulfate electrolyte." *Appl. Surf. Sci.,* 228, 326-333

Landolt, D. (2002). "Electrodeposition Science and Technology in the Last Quarter of the Twentieth Century." *J. Electrochem. Soc.*, 149, S9-S20.

Landolt, D. and Marlot, A. (2003). "Microstructure and composition of pulse-plated metals and alloys." *Surf. Coat. Technol.,* 169, 8-13.

Leisner, P., Nielsen, C.B., Tang, P.T., Dorge, T.C. and Moller, P. (1996). "Methods for electrodeposting compostion-modulated alloys." *J. Mater. Process. Technol.,* 58, 39-44.

Leith, S.D., Ramli, S. and Schwartz, D.T. (1999). "Characterization of Ni_xFe_{1-x} (0.10 < x < 0.95) electrodeposition from a family of sulfamate-chloride electrolytes." *J. Electrochem. Soc.,* 146, 1431–1435.

Li, H.Q. and Ebrahimi, F. (2003). "An investigation of thermal stability andmicrohardness of electrodeposited nanocrystalline nickel- 21% iron alloys." *Acta Mater.,* 51, 3905-3913.

Li, H.Q. and Ebrahimi, F. (2003). "Synthesis and characterization of electrodeposited nanocrystalline nickel-iron alloys." *Mater. Sci. Eng. A,* 347, 93–101.

Liew, H.F., Low, S.C. and Lew, W.S. (2011). "Fabrication of constricted compositionally-modulated Ni_xFe_{1-x} nanowires." *J. Phys. Conf. Ser.,* 266**,** 1-5.

Liu, X., Evans, P. and Zangari, G. (2000). "Electrodeposited Co-Fe and Co-Fe-Ni alloy films for magnetic recording write heads." *IEEE Trans. Magn.* 36, 3479-3481.

Liu, Y., Qin, X.Y. and Qiu, T. (2006). "Magnetic properties of nanostructural γ-Ni–28Fe alloy." *Trans. Nonferrous Met. Soc. China,* 16, 1370–1373.

Marcus, P. and Olefjord, I. (1986). "The dissolution and passivation of a single-crystal $Ni_{50}Fe_{50}$ alloy and the influence of sulfur studied by electron spectroscopy for chemical analysis." *Corros.,* 42, 91-98.

Matlosz, M. (1993). "Competitive adsorption effects in the electrodeposition of iron-nickel alloys." *J. Electrochem. Soc.,* 140, 2272-2279.

Maxwell, J.C. (1973). *A Treatise on Electricity and Magnetism,* Oxford Press, 1, 828, London.

McCrea, J.L., Palumbo, G., Hibbard, G.D. and Erb, U. (2003). "Properties and applications for electrodeposited nanocrystalline Ni–Fe alloys." *Rev. Adv. Mater. Sci.* 5, 252–258.

Myung, N.V. and Nobe, K. (2001). "Electrodeposited iron group thin-film alloys, structure-property relationships." *J. Electrochem. Soc.,* 148, 136–144.

Nabiyouni, G., Schwarzacher, W., Rolik, Z. and Bakonyi, I. (2002). "Giant magnetoresistance and magnetic properties of electrodeposited Ni–Co–Cu/Cu multilayers." *J. Magn. Magn. Mater.,* 253, 77-85.

Oniciu, L. and Muresan, L. (1991). "Some fundamental aspects of leveling and brightening in metal electrodeposition." *J. Appl. Electrochem.,* 21, 565–74.

Osaka, T. (2000). "Electrodeposition of highly functional thin films for magnetic recording devices of the next century." *Electrochim. Acta.,* 45, 3311-3321.

Parthasaradhy, N.V. (1989). *Practical Electroplating Handbook.* Simon and Schuster Englewood Cliffs, New Jersey.

Paunovic, M. and Schlesinger, M. (2006). *Fundamentals of electrochemical deposition,* John Wiley & Sons, Inc., Hoboken, New York.

Petersson and Ahlberg. (2000). "Kinetics of the electrodeposition of Pb-Sn alloys: Part I. At glassy carbon electrodes." *J. Electroanal. Chem.,* 485, 166-177.

Petrovic, J.J. (2001). "Mechanical properties of meteorites and their constituents." *J. Mater. Sci.,* 36, 1579-1583.

Pushpavanam. and Michaee, S.M. (2004). "Multilayered Zn-Ni and Zn-Co alloys-corrosion resistance under simulated conditions and field exposure." *Trans. Inst. Met. Finish.,* 82, 175.

Ramazan, S. and Gulfeza, K. (2007). "Hydrogen evolution and corrosion performance of Ni Zn coatings." *Energy Convers. Manage.*, 48, 583-591.

Rangakrishnan, K.S., Srinivasan, K. and Mohan, S. (2002). "Electrodeposition of compositionally modulated alloys- An overview." *Trans. Inst. Met. Finish.*, 80, 46-48.

Raub, E. and Muller, K. (1967). "Fundamentals of metal deposition." *Elsevier Publishing Company*, Amsterdam.

Ravinder, D. and Latha, K. (1999). "Dielectric behaviour of mixed Mg–Zn ferrites at low frequencies." *Mater. Lett.,* 41, 247-253.

Ray, E.F. (2005). *Physical Principles of Electron Microscopy- An Introduction to TEM, SEM, and AEM,* Springer Science, Inc., USA.

Rheem, Y., Yoo, B., Koo, B.K. and Myung, N.V. (2007). "Electrochemical synthesis of compositionally modulated NiFe nanowires." *Phys. Status Solidi A,* 204, 4021–4024.

Ricq, L., Lallemand, F., Gigandet, M.P. and Pagetti, J. (2001). "Influence of sodium saccharin on the electrodeposition and characterization of CoFe magnetic film." *Surf. Coat. Technol.,* 138, 278–283.

Roventi, G., Fratesi, R., Guardia, D.R.A. and Barucca, G. (2000). "Normal and anomalous codeposition of Zn–Ni alloys from chloride bath." *J. Appl. Electrochem.,* 30, 173-179.

Roy, S. (2009). *Electrochemistry at the Nanoscale,* Springer, Netherlands,.

Russell, G.J. and Mann, K. (1990). *Introductory Alternating Current Circuit Theory,* UNSW Press.

Saanaty-Zadeh, A., Raessi, K. and Saidi, A. (2009). "Properties of nanocrystalline iron–nickel alloys fabricated by galvanostatic electrodeposition." *J. Alloys Compd.*, 485, 402–407.

Safranek, W.H. (1973). *The Properties of Electrodeposited Metals and Alloys,* Elsevier, Amsterdam.

Schlesinger, M. and Paunovic, M. (2000). *Modern electroplating,* 4th edn, Wiley-Interscience, New York.

Schlesinger, M., Bird, K.D., Snyder, D.D. and Paunovic, M. (1995). "Electrochemically deposited thin films II Proceedings.", *J. Electrochem. Soc.* Pennington, Vol. 94–31, 97-102.

Shacham-Diamand, Y. and Paunovic, M. (1995). "Electrochemically deposited thin films II Proceedings." Vol. 94–31*, J. Electrochem. Soc.,* Pennington, 293-299.

Shao, I., Vereecken, P.M, Chien, C.L., Cammarata, RC. And Searson, PC. (2003). "Electrochemical deposition of FeCo and FeCoV alloys." *J. Electrochem. Soc.,* 150, 184-188.

Short, N.R. and Dennis, J.K. (1997). "Characterization of black chromate -conversion coating on the electrodeposited zinc-iron alloy." *Appl. Surf. Sci.*, 75, 47-53.

Short, N.R., Abibsi, A. and Dennis, J.K. (1984). "Corrosion resistance of electroplated zinc alloy coatings." *Trans. Inst. Met. Fin.*, 67, 73-77.

Simunovich, D., Schlesinger, M. and Snyder, D.D. (1994). "Electrochemically layered copper-nickel nanocomposites with enhanced hardness." *J. Electrochem. Soc.,* 141, L10.

Smith, W.F. (1993). *Foundations of Material Science and Engineering,* 2nd ed., McGraw-Hill, Inc., New York.

Soares, M.E., Souza, C.A.C. and Kuri, S.E. (2006). "Corrosion resistance of a Zn–Ni electrodeposited alloy obtained with a controlled electrolyte flow and gelatin additive." *Surf. Coat. Technol.,* 201, 2953-2959.

Sohi, H.M. and Jalali, M. (2003). "Study of the corrosion properties of zinc–nickel alloy electrodeposits before and after chromating." *J. Mater. Process. Technol.,* 138, 63-66.

Srivastava, M., Selvi, E.V., Grips, W.V.K. and Rajam, K.S. (2006). "Corrosion resistance and microstructure of electrodeposited nickel–cobalt alloy coatings." *Surf. Coat. Technol.,* 201, 3051–3060.

Stefec, R. (1973). "Magnetic properties of electrodeposited iron–nickel alloy." *Czech. J. Phys.,* 23, 1249–1260.

Suryanarayana, C. (1995). "Nanocrystalline materials." *Int. Mater. Rev.,* 40, 41–64.

Tabakovic, I., Riemer, S., Inturi, V., Jallen, P. and Thayer, A. (2000). "Organic additives in the electrochemical preparation of soft magnetic CoNiFe films." *J. Electrochem. Soc.,* 147, 219–226.

Ting, C.H., Paunovic, M. and Chiu, G. (1987). "The electrochemical society extended abstracts." Vol. 86-1, Philadelphia. 239- 343.

Trudeau, M.L. (1999). "Nanocrystalline Fe and Fe-riceied Fe-Ni through electrodeposition." *Nanostruct. Mater.*, 12, 55-60.

Turgut, Z., Fingers, R.T., Piehler, H.R. and McHenry, M.E. (2000). "Microstructural and magnetic observations of compacted FeCoV nanoparticles." *IEEE Trans. Magn.,* 36, 3024-3025.

Tury, B., Lakatos-Varasanyi, M., and Roy, S. (2006). "Ni-Co alloys plated by pulse currents". *Surf. Coat. Technol.,* 200, 6713-6717.

Uhlig, H.H. (1974). *Corrosion and Corrosion Control,* 2nd edn., C. E. Tuttle, Tokyo.

Venkatakrishna, K. and Hegde, A.C. (2010). "Electrolytic preparation of cyclic multilayer Zn-Ni alloy coating using switching cathode current densities." *J. Appl. Electrochem.,* 40, 2051-2059.

Wang, L., Gao, Y., Xue, Q., Liu, H. and Xu, T. (2005). "Microstructure and tribological properties of electrodeposited Ni–Co alloy deposits." *Appl. Surf. Sci.,* 242, 326–332.

Watanabe, T. (2004). *Nano-Plating, Microstructure Control Theory of Plated Film and Data Base of Plated Film*. Elsevier Ltd, Japan.

Wu, S.H. and Chen, D.H. (2003). "Synthesis and characterization of nickel nanoparticles by hydrazine reduction in ethylene glycol." *J. Colloid Interface Sci.,* 259, 282–286.

Yang, X., Li, Q., Zhang, S., Gao, H., Luo, F. and Dai, Y. (2010). "Electrochemical corrosion behaviors and corrosion protection properties of Ni–Co alloy coating prepared on sintered NdFeB permanent magnet." *J. Solid State Electrochem.*, 14, 1601–1608.

Yogesha, S., Udupa, K.R. and Hegde, A.C. (2012). "Surface modification by multilayered Zn-Co alloy coatings" *Surf. Eng.*, 28, 49-56.

Yuan, X., Song, C., Wang, H. and Zhang, J. (2010). *Electrochemical Impedance Spectroscopy in PEM Fuel Cells - Fundamentals and Applications,* Springer Publications, London.

Zadeh, A.S., Raessi, K. and Saidi, A. (2009) "Properties of nanocrystalline iron–nickel alloys fabricated by galvanostatic electrodeposition." *J. Alloys Compd.*, 485, 402–407.

Zhou, J.C., Li, W.J. and Zhu, J.B. (2008). "Theoretical study of Ni-Al nanoalloy clusters using particle swarm optimization algorithm." *Mater. Sci. Technol.,* 24, 870–874.

Zimmerman, A.F., Palumbo, G., Aust, K.T. and Erb, U. (2002). "Mechanical properties of nickel silicon carbide nanocomposites." *Mater. Sci. Eng. A,* 328, 137-146.